frontiers | Research Topics

# Longevity of T cell and antibody response to infection and vaccination

**Edited by**
Eui Ho Kim, Jin-Hwan Han, Sejin Im, Jieun Oh and Kihyuck Kwak

**Published in**
Frontiers in Immunology

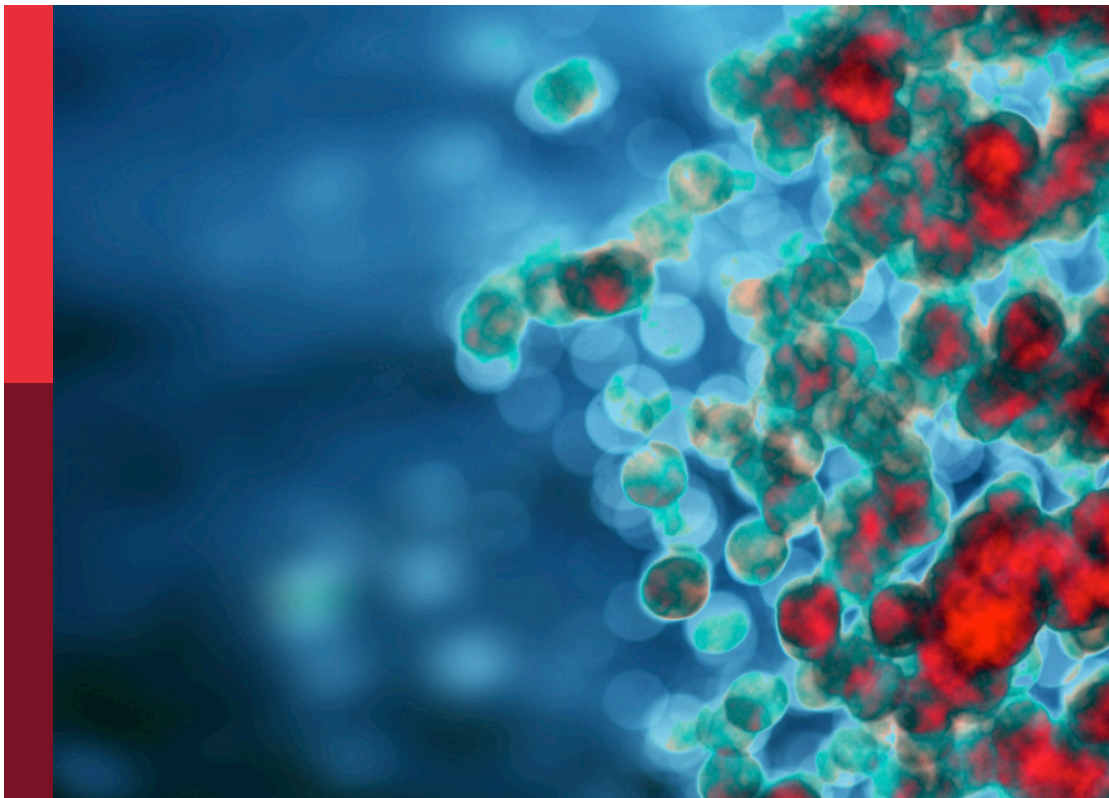

ISSN 1664-8714
ISBN 978-2-83251-718-5
DOI 10.3389/978-2-83251-718-5

## About Frontiers

Frontiers is more than just an open access publisher of scholarly articles: it is a pioneering approach to the world of academia, radically improving the way scholarly research is managed. The grand vision of Frontiers is a world where all people have an equal opportunity to seek, share and generate knowledge. Frontiers provides immediate and permanent online open access to all its publications, but this alone is not enough to realize our grand goals.

## Frontiers journal series

The Frontiers journal series is a multi-tier and interdisciplinary set of open-access, online journals, promising a paradigm shift from the current review, selection and dissemination processes in academic publishing. All Frontiers journals are driven by researchers for researchers; therefore, they constitute a service to the scholarly community. At the same time, the *Frontiers journal series* operates on a revolutionary invention, the tiered publishing system, initially addressing specific communities of scholars, and gradually climbing up to broader public understanding, thus serving the interests of the lay society, too.

## Dedication to quality

Each Frontiers article is a landmark of the highest quality, thanks to genuinely collaborative interactions between authors and review editors, who include some of the world's best academicians. Research must be certified by peers before entering a stream of knowledge that may eventually reach the public - and shape society; therefore, Frontiers only applies the most rigorous and unbiased reviews. Frontiers revolutionizes research publishing by freely delivering the most outstanding research, evaluated with no bias from both the academic and social point of view. By applying the most advanced information technologies, Frontiers is catapulting scholarly publishing into a new generation.

## What are Frontiers Research Topics?

Frontiers Research Topics are very popular trademarks of the *Frontiers journals series*: they are collections of at least ten articles, all centered on a particular subject. With their unique mix of varied contributions from Original Research to Review Articles, Frontiers Research Topics unify the most influential researchers, the latest key findings and historical advances in a hot research area.

Find out more on how to host your own Frontiers Research Topic or contribute to one as an author by contacting the Frontiers editorial office: frontiersin.org/about/contact

# Longevity of T cell and antibody response to infection and vaccination

**Topic editors**

Eui Ho Kim — Institut Pasteur Korea, Republic of Korea
Jin-Hwan Han — Merck, United States
Sejin Im — Sungkyunkwan University, Republic of Korea
Jieun Oh — Korea Advanced Institute of Science and Technology (KAIST), Republic of Korea
Kihyuck Kwak — Yonsei University, Republic of Korea

**Citation**

Kim, E. H., Han, J.-H., Im, S., Oh, J., Kwak, K., eds. (2023). *Longevity of T cell and antibody response to infection and vaccination*. Lausanne: Frontiers Media SA.
doi: 10.3389/978-2-83251-718-5

# Table of contents

frontiers in Immunology

ORIGINAL RESEARCH
published: 17 December 2021
doi: 10.3389/fimmu.2021.797919

# Assessment of SARS-CoV-2 Immunity in Convalescent Children and Adolescents

*Hing Wai Tsang[1†], Gilbert T. Chua[1†], Kelvin K. W. To[2†], Joshua S. C. Wong[3], Wenwei Tu[1], Janette S. Y. Kwok[4], Wilfred H. S. Wong[1], Xiwei Wang[1], Yanmei Zhang[1], Jaime S. Rosa Duque[1], Godfrey C. F. Chan[1], Wai Kit Chu[5], CP Pang[5], Paul K. H. Tam[6,7], Yu Lung Lau[1], Ian C. K. Wong[8], WH Leung[1], Kwok-Yung Yuen[2], Mike Y. W. Kwan[3*] and Patrick Ip[1*]*

[1] Department of Paediatrics and Adolescent Medicine, Li Ka Shing Faculty of Medicine, The University of Hong Kong, Hong Kong, Hong Kong SAR, China, [2] State Key Laboratory for Emerging Infectious Diseases, Carol Yu Centre for Infection, Department of Microbiology, Li Ka Shing Faculty of Medicine, The University of Hong Kong, Hong Kong, Hong Kong SAR, China, [3] Department of Paediatrics and Adolescent Medicine, Prince Margaret Hospital, Hospital Authority, Hong Kong, Hong Kong SAR, China, [4] Department of Pathology, Queen Mary Hospital, Hospital Authority, Hong Kong, Hong Kong SAR, China, [5] Department of Ophthalmology and Visual Sciences, The Chinese University of Hong Kong, Hong Kong, Hong Kong SAR, China, [6] Department of Surgery and Dr. Li Dak Sam Research Centre, Li Ka Shing Faculty of Medicine, The University of Hong Kong, Hong Kong, Hong Kong SAR, China, [7] Faculty of Medicine, Macau University of Science and Technology, Macau, Macau SAR, China, [8] Department of Pharmacology and Pharmacy, Li Ka Shing Faculty of Medicine, The University of Hong Kong, Hong Kong, Hong Kong SAR, China

Persistence of protective immunity for SARS-CoV-2 is important against reinfection. Knowledge on SARS-CoV-2 immunity in pediatric patients is currently lacking. We opted to assess the SARS-CoV-2 adaptive immunity in recovered children and adolescents, addressing the pediatrics specific immunity towards COVID-19. Two independent assays were performed to investigate humoral and cellular immunological memory in pediatric convalescent COVID-19 patients. Specifically, RBD IgG, CD4+, and CD8+ T cell responses were identified and quantified in recovered children and adolescents. SARS-CoV-2-specific RBD IgG detected in recovered patients had a half-life of 121.6 days and estimated duration of 7.9 months compared with baseline levels in controls. The specific T cell response was shown to be independent of days after diagnosis. Both CD4+ and CD8+ T cells showed robust responses not only to spike (S) peptides (a main target of vaccine platforms) but were also similarly activated when stimulated by membrane (M) and nuclear (N) peptides. Importantly, we found the differences in the adaptive responses were correlated with the age of the recovered patients. The CD4+ T cell response to SARS-CoV-2 S peptide in children aged <12 years correlated with higher SARS-CoV-2 RBD IgG levels, suggesting

OPEN ACCESS

**Edited by:**
*Kihyuck Kwak,*
*Yonsei University, South Korea*

**Reviewed by:**
*Nico Marr,*
*Sidra Medicine, Qatar*
*Lucia Elena Alvarado-Arnez,*
*Franz Tamayo University, Bolivia*

***Correspondence:**
*Mike Y. W. Kwan*
*kwanyw1@ha.org.hk*
*Patrick Ip*
*patricip@hku.hk*

*†These authors have contributed equally to this work*

**Specialty section:**
*This article was submitted to Immunological Memory, a section of the journal Frontiers in Immunology*

**Received:** *19 October 2021*
**Accepted:** *02 December 2021*
**Published:** *17 December 2021*

**Citation:**
*Tsang HW, Chua GT, To KKW, Wong JSC, Tu W, Kwok JSY, Wong WHS, Wang X, Zhang Y, Rosa Duque JS, Chan GCF, Chu WK, Pang CP, Tam PKH, Lau YL, Wong ICK, Leung WH, Yuen K-Y, Kwan MYW and Ip P (2021) Assessment of SARS-CoV-2 Immunity in Convalescent Children and Adolescents. Front. Immunol. 12:797919. doi: 10.3389/fimmu.2021.797919*

the importance of a T cell-dependent humoral response in younger children under 12 years. Both cellular and humoral immunity against SARS-CoV-2 infections can be induced in pediatric patients. Our important findings provide fundamental knowledge on the immune memory responses to SARS-CoV-2 in recovered pediatric patients.

**Keywords: COVID-19, SARS-CoV-2, convalescence, children, adolescents, T cell response, SARS-CoV-2 RBD IgG**

## INTRODUCTION

At the end of 2019, a pneumonia outbreak with unknown etiology was reported in Wuhan, China (1, 2). The World Health Organization (WHO) officially named this disease Coronavirus Disease-2019 (COVID-19), which was later identified to be caused by the severe acute respiratory syndrome coronavirus 2 (SARS-CoV-2) (3). The worldwide pandemic has significantly impacted public health and the global economy (4). Preventive measures were enforced to increase social distancing, including limited gatherings, school closures, and restricted travel to reduce transmission (3, 5).

The clinical spectrum of COVID-19 ranges from asymptomatic to fatal disease. Unfavorable outcomes were associated with the age and comorbidities of patients (6, 7), particularly those older than 65 years and individuals with diabetes mellitus or renal disease (8–10). Children infected with SARS-CoV-2 generally have mild symptoms and a low mortality rate (11–13), with a lower likelihood of severe symptoms in children than in adults (14–16). The SARS-CoV-2 viral-host response plays an important role in the pathogenesis of the disease, including changes in the biological responses of peripheral immune cells and the levels of proinflammatory cytokines. Lymphopenia is a common clinical characteristic symptom observed in COVID-19 patients, especially in critical cases (2, 15–20), with up to 83.2% of patients showing lymphopenia during admission (21). Moreover, symptomatic children with COVID-19 were found to have higher viral load, lower total lymphocyte count, lower lymphocyte subsets, and elevated interleukin 6 (IL-6), IL-10, tumor necrosis factor-alpha (TNF-α), and interferon-gamma (IFN-γ) levels compared with asymptomatic patients (22, 23). The data collectively suggest that altered immune cell subsets could be a prognostic factor for COVID-19 (24), especially in critical cases (25). There are knowledge gaps in degree of host immune responses among patients in terms of age, which could help to identify beneficial factors associated with lower disease severity due to SARS-CoV-2 infections.

The long-term persistence of T cell memory is important in mediating both cellular and humoral immunity against SARS-CoV-2 reinfections (26, 27). Patients infected with SARS-CoV-2 virus show T cell memory along with neutralizing antibodies and polyfunctional T cell responses (26, 28). This T cell memory is capable of being reactivated in patients with mild symptoms up to 8 months after recovery (29, 30). Epitope identification studies of SARS-CoV-2 T cells have demonstrated that both CD4+ and CD8+ T cells respond to a broad spectrum of structural and non-structural proteins (NSP) of the SARS-CoV-2 virus. T cells showed immunodominant responses to spike (S), membrane (M), and nuclear (N) structural proteins, whereas B cells showed sub-dominant responses to ORF-1 ab-encoded NSPs (31, 32). However, current knowledge of SARS-CoV-2 immune responses specific to pediatric patients is still lacking, such as the immunodominance of SARS-CoV-2 epitopes and durability of antibodies after an infection.

Given the fundamental differences in the immunity of adults and children (33), we assessed the adaptive SARS-CoV-2-specific immune responses in children and adolescents recovered from COVID-19.

## MATERIALS AND METHODS

### Subject Recruitment

Children and adolescents under 18 years of age who had recovered from COVID-19 were recruited to the study during the clinical follow up visits. These subjects were admitted and managed in the Paediatric Infectious Disease Centre, Princess Margaret Hospital, Hong Kong, China. Patients were confirmed to have COVID-19 by a positive SARS-CoV-2 RT-PCR test of their nasopharyngeal swab (NPS). Patients were confirmed to have recovered from COVID-19 by either two consecutives negative NPS by SARS-CoV-2 RT-PCR or the seroconversion of SARS-CoV-2 anti-NP antibody response. Details of the admission and discharge criteria and the laboratory investigations have been previously described (5, 23). Briefly, all children and adolescents who were tested positive for SARS-CoV-2 PCR were hospitalized. They were either asymptomatic or had mild diseases (5). Details of the admission and discharge criteria and the laboratory investigations have been previously described (23). Their demographics, clinical symptoms during the infection, and time since recovery were retrieved.

Uninfected controls were recruited from pediatric patients admitted to the Queen Mary Hospital for follow up of other medical conditions unrelated to COVID-19 or from healthy individuals in the community (**Table S1**). Subjects below 18 years of age with no history of COVID-19 and a negative SARS-CoV-2 RT-PCR on the day of recruitment were invited to participate in the study. Exclusion criteria included participants with other acute infections 2 weeks before recruitment, having received any kind of COVID-19 vaccines, known underlying primary or acquired immunodeficiency, and autoimmune disease or other condition that required immunosuppressants.

### Isolation of Peripheral Blood Mononuclear Cells

Whole blood samples from recovered patients and controls were collected in heparin-coated blood tubes. Peripheral blood

mononuclear cells (PBMCs) were isolated by Ficoll density gradient centrifugation as previously described (34). Isolated PBMCs were cryo-preserved in storage medium containing 90% heat-inactivated fetal bovine serum (FBS; Gibco, Thermo Fisher Scientific, Inc., Waltham, MA) and 10% cell culture grade DMSO (Sigma Aldrich, Merck, Germany). Samples were stored in liquid nitrogen until batch recovery for the assays.

## T Cell Stimulation Assay and SARS-CoV-2 Peptide Pools

*In vitro* T cell stimulation assays were carried out with spike (S), membrane (M), and nuclear (N) structural proteins. Briefly, viable cell numbers were determined in the thawed PBMCs by staining with crystal violet and counting with a hemocytometer. For the assays, $10^6$ cells were resuspended in 100 µL RPMI 1640 medium (Gibco) supplemented with 10% heat-inactivated FBS and 1% penicillin/streptomycin. The SARS-CoV-2 peptide pools (Miltenyi Biotec, Germany) were prepared according to the manufacturer's recommendations. Next, 1 µg of peptide/mL (0.6 nmol) separately or in a mixture was introduced to the T cells. Along with the peptide pools, 0.1 µg/mL purified anti-human CD28 (Miltenyi Biotec, Clone: REA612) and 0.1 µg/mL purified anti-human CD49d (Miltenyi Biotec, Clone: MZ18-24A9) as coactivators of T cells were also added to the wells for the entire stimulation period. The T cells and peptide mixtures were incubated at 37°C in 5% $CO_2$ for 16 hours. Brefeldin A (Biolegend, San Diego, CA) at a concentration of 0.1 µg/mL was added to the culture medium in the last 4 hours to enhance intracellular cytokine staining signals. The negative control was 10% DMSO and the positive control was an activation cocktail (Biolegend) containing 8.1 nM phorbol-12-myristate (PMA) and 1.3 mM ionomycin.

## Flow Cytometry

Stimulated PBMCs were recovered from the culture plates and resuspended in 100 µL PBS. Cell viability was assessed by staining with Viobility™ Fixable Dyes (Miltenyi Biotec, Germany). Cells were washed, fixed, permeabilized, and then stained with an antibody cocktail containing Pacific Blue™ anti-human CD3 (Biolegend, clone: HIT3a), PE/Cyanine7 anti-human CD4 (Biolegend, clone:A161A1) and PerCP/Cyanine5.5 anti-human CD8 (Biolegend, clone: SK1) for T cell identification; APC anti-human CD69 (Biolegend, clone: FN50) and PE anti-human IFN-γ (Biolegend, clone:4S.B3) for the activation analysis; and FITC anti-human CD14 (Biolegend, clone:HCD14) and FITC anti-human CD20 (Biolegend, clone:2H7) for the exclusion of non-specific signals and B cells. Fifty thousand events were analyzed by a BD LSR-II flow cytometer. (BD Biosciences, San Jose, CA) The gates applied for the quantification of the stimulated T cells are illustrated in **Figure S1**.

## SARS-CoV-2 RBD ELISA

Serum was isolated from whole blood samples obtained from recovered patients and controls. The RBD IgG antibody level was measured using an Euroimmun anti-SARS-CoV-2 ELISA assay (Lubeck, Germany) according to manufacturer's protocol. Data were expressed as semi-quantitative IgG ratios.

## Quantification and Statistical Analysis

Data analyses were performed using FlowJo (version 10.1, BD Bioscience, Ashland, OR). Statistical analyses were performed using SPSS for Windows (version 26.0, SPSS Inc., Chicago, IL) and Prism for Windows (version 8.0.1, GraphPad Software, San Diego, CA). Data are expressed as mean ± standard deviation (SD), and statistical details are provided in the respective figure legends. Comparison analysis was carried out by two-tailed Student's t test with $p<0.05$ considered statistically significant. The antigenicity effect size of the different SARS-CoV-2 peptides on T cell activation was assessed by Cohen's d (35).

To examine SARS-CoV-2-specific T cell response in recovered patients, we measured the upregulation status of the early activation marker CD69 and expression of intracellular cytokine IFN-γ, a functional T cell marker for protective immunity and analyzed the double-positive status of CD69/IFN-γ in CD4+ and CD8+ T cells, normalized to DMSO control (36–38). To estimate the half-life of SARS-CoV-2 RBD IgG, we calculated $t_{1/2} = A_o/2k$, where $A_o$ is the initial amount of the antibody obtained from the y-intercept of the trendline and k is the slope of the trendline obtained from the scattered plot of RBD IgG ratio against days after diagnosis. The days after diagnosis is defined as the time between the date of the patient's clinical diagnosis to the date of the blood sample collections. To analyze the relationship between anti-RBD IgG level and T cells response, we performed Spearman's correlations and expressed as correlation coefficient (r).

## Ethics Approval

The study was approved by the Institutional Review Board of the University of Hong Kong/Hospital Authority Hong Kong West Cluster (Reference: UW 20-292 and UW 21-157) and the Kowloon West Cluster Research Ethics Committee [Reference: KW/FR-20-086(148-10)]. Written consent was obtained from parents or legal guardians of the subjects.

# RESULTS

## Subject Recruitment and Clinical Characteristics

Between 1st December 2020 to 31st March 2021, 31 patients who had recovered from COVID-19 were recruited from Princess Margret Hospital, Hong Kong SAR. Fourteen (45.2%) were boys and 17 (54.8%) were girls with a median age of 12 years (range 2.7-18 years). The age distribution of the recruited patients was shown in **Figure S2**. Twenty age-matched uninfected controls were also recruited from Queen Mary Hospital, Hong Kong SAR, China and from the community. Subject demographics and clinical characteristics are shown in **Table 1**. The majority of subjects were Chinese (80.6%). Among the COVID-19 cases, 83.9% were domestic cases, 32.3% were asymptomatic, and the remaining cases (67.7%) had mild disease. Blood samples were collected at 29 to 219 days after recovery.

**TABLE 1** | Demographics and clinical characteristics of recovered pediatric COVID-19 patients and uninfected controls.

| | Children Recovered From COVID-19 (N = 31) | Uninfected Controls (N = 20) |
|---|---|---|
| Median age in years | 12 | 14 |
| Age range | 2.7-18 | 8-15 |
| Sex (%) | | |
| Male | 45.2 (14/31) | 80.0 (16/20) |
| Female | 54.8 (17/31) | 20.0 (4/20) |
| Residence (%) | | |
| Hong Kong | 100 | 100 |
| Ethnicity (%) | | |
| Han Chinese | 80.6 (25/31) | 80.0 (16/20) |
| Others | 19.4 (6/31) | 20.0 (4/20) |
| Travel history (%) | | |
| Yes | 16.1 (5/31) | N/A |
| No | 83.9 (26/31) | N/A |
| Disease awareness (%) | | |
| Asymptomatic | 32.3 (10/31) | N/A |
| Symptomatic | 67.7 (21/31) | N/A |
| Signs/symptoms (%) | | |
| Fever | 61.9 (13/21) | N/A |
| Cough | 47.6 (10/21) | N/A |
| Runny nose | 28.6 (6/21) | N/A |
| Ageusia | 19.0 (4/21) | N/A |
| Vomit | 14.3 (3/21) | N/A |
| Anosmia | 9.5 (2/21) | N/A |
| Sputum | 4.9 (1/21) | N/A |
| Headache | 4.9 (1/21) | N/A |
| SARS-CoV-2 PCR positivity (%) | | |
| Positive | 100 (31/31) | N/A |
| Negative | 0 (0/31) | 100(20/20) |
| SARS-CoV-2 anti-NP IgG positivity (%) | 100 | N/A |
| Sample collection period | Dec 2020 - March 2021 | |
| Days After Diagnosis | 29-219 (Median=46.5) | N/A |

*N/A, Not Applicable.*

## Quantification of SARS-CoV-2 RBD IgG Level and Identification of SARS-CoV-2 Reactive T Cells in Recovered Children and Adolescents

We detected the presence of SARS-CoV-2 RBD IgG antibodies in 30/31 recovered COVID-19 patients compared with the 20 healthy unexposed cases ($p<0.001$), with 1 patient showed negative in the RBD IgG antibodies test (**Figure 1A**). Stimulation of CD4+ and CD8+ T cells with the mixed SARS-CoV-2 peptide pool (S + M + N peptides, representing the reactive epitopes of the SARS-CoV-2 virus) showed significantly higher numbers of CD69+, IFN-γ+, and double-positive CD69+/IFN-γ+ T cells in recovered patients compared with controls.(**Figure 1B**) Significantly higher numbers of CD4+ and CD8+ T cells responding to stimulations by mixed M, N and S peptide pools were observed, with the exception of CD8+CD69 +IFN-γ+ subsets that showed statistically marginal differences. (**Table 2**) Overall, 29/31 and 28/31 demonstrated CD4+ and CD8+ T-cell response respectively to SARS-CoV-2 mixed-peptide stimulations at a level above those of the controls. (**Figure 1C**)

Next, the reactivity of the CD4+ and CD8+ T cells towards individual M, N, and S peptide pools were analyzed in convalescent patients. (**Figure 2**) SARS-CoV-2 reactive CD4+ and CD8+ T cells were detectable towards each structural protein in most of the patients' samples (**Figure 2A**); 24/31 and 25/31 showed stronger CD4+ and CD8+ T cells response respectively to SARS-CoV-2 M peptide stimulation than control. Similar response levels were also observed in CD4+ T cells stimulated by SARS-CoV-2 S peptide and CD8+ T cells stimulated by SARS-CoV-2 N peptide with 27/31 showed higher response than control. However, relatively lower response was observed in both S peptide stimulated CD8+ T cells and N peptide stimulated CD4+ T cells with 11 patients showed similar response to control. Overall summation analysis on the T cells response towards SARS-CoV-2 peptides stimulation was demonstrated. (**Figure 2B**) The CD4+ T cells responded more strongly to stimulation by S peptide than to N (Cohen's d=0.53) or M peptides (Cohen's d=0.34). On the other hand, CD8+ T cells responded less strongly to stimulation by M peptides compared with N peptides (Cohen's d=-0.36) or S peptide (Cohen's d=-0.23), where the difference in CD8+ T cell responses between S and N peptides was small (Cohen's d=0.10).

## The Dynamics of Humoral and Cellular Immunity in Recovered Children and Adolescents

SARS-CoV-2 specific humoral immunity was found to decay over time, but not T cell immunity (**Figure 3**). Linear regression analysis showed that the level of SARS-CoV-2 RBD IgG was significantly associated with days after diagnosis ($p=6.31^{e-07}$, $R^2 = 0.5808$) (**Figure 3A**), but not with the specific CD4+ ($p=0.783$) or

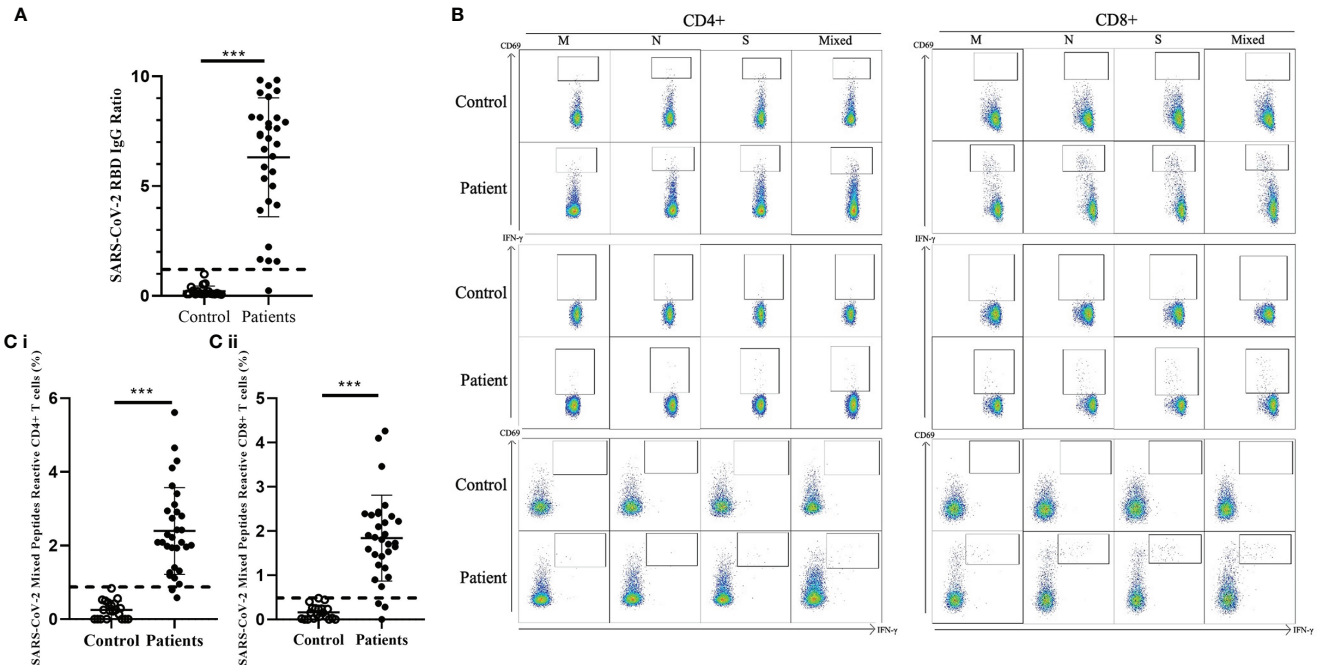


**FIGURE 1** | Comparison of SARS-CoV-2 RBD-specific antibodies and SARS-CoV-2-specific T cell response in healthy controls and recovered children and adolescents. **(A)** Serological responses to recombinant RBD protein in 31 recovered COVID-19 patients with median 46.5 recovery days and ranging 29-219 days and 20 uninfected controls. Dash line indicated the anti-RBD IgG ratio reference obtained from uninfected controls. **(B)** Representative data of the T cell response towards SARS-CoV-2 peptide pools in controls and recovered patients. **(C)** (i) CD4+ and (ii) CD8+ T cell responses to SARS-CoV-2 mixed peptides in the recovered COVID-19 patients and uninfected controls. Dash line indicated the measured T cell responses reference obtained from the uninfected controls. Data are presented as mean ± SD and analyzed using two-sided Student's t-test between control and patient groups. ***p < 0.001.

**TABLE 2** | Comparison of SARS-CoV-2 specific T cells subsets in controls and recovered children and adolescents.

| | | | M (Mean ± SD) | p-value | N (Mean ± SD) | p-value | S (Mean ± SD) | p-value | Mixed (Mean ± SD) | p-value |
|---|---|---|---|---|---|---|---|---|---|---|
| CD4 | CD69+ | Control | 0.183 ± 0.177 | <0.0001 | 0.193 ± 0.253 | <0.0001 | 0.238 ± 0.212 | <0.0001 | 0.241 ± 0.224 | <0.0001 |
| | | Patients | 1.039 ± 0.692 | *** | 0.933 ± 0.573 | *** | 1.295 ± 0.786 | *** | 1.957 ± 1.084 | *** |
| | IFN-γ+ | Control | 0.036 ± 0.068 | <0.0001 | 0.022 ± 0.038 | <0.0001 | 0.085 ± 0.140 | 0.0023 | 0.015 ± 0.039 | <0.0001 |
| | | Patients | 0.252 ± 0.191 | *** | 0.225 ± 0.183 | *** | 0.232 ± 0.186 | ** | 0.282 ± 0.217 | *** |
| | CD69+/IFN-γ+ | Control | 0.017 ± 0.027 | 0.0016 | 0.019 ± 0.029 | <0.0001 | 0.030 ± 0.036 | 0.0001 | 0.021 ± 0.023 | <0.0001 |
| | | Patients | 0.070 ± 0.080 | ** | 0.083 ± 0.058 | *** | 0.108 ± 0.093 | *** | 0.156 ± 0.136 | *** |
| CD8 | CD69+ | Control | 0.073 ± 0.085 | 0.0001 | 0.118 ± 0.204 | 0.0009 | 0.091 ± 0.132 | 0.0001 | 0.136 ± 0.182 | <0.0001 |
| | | Patients | 0.392 ± 0.395 | *** | 0.490 ± 0.523 | *** | 0.468 ± 0.459 | *** | 1.302 ± 0.775 | *** |
| | IFN-γ+ | Control | 0.046 ± 0.047 | <0.0001 | 0.083 ± 0.152 | 0.0001 | 0.073 ± 0.145 | 0.0004 | 0.053 ± 0.088 | <0.0001 |
| | | Patients | 0.259 ± 0.186 | *** | 0.341 ± 0.274 | *** | 0.275 ± 0.237 | *** | 0.378 ± 0.280 | *** |
| | CD69+/IFN-γ+ | Control | 0.012 ± 0.022 | 0.0050 | 0.012 ± 0.034 | 0.0263 | 0.028 ± 0.049 | 0.0517 | 0.011 ± 0.020 | 0.0060 |
| | | Patients | 0.049 ± 0.065 | ** | 0.097 ± 0.197 | * | 0.106 ± 0.209 | | 0.159 ± 0.279 | ** |

*Immunophenotyping of PBMCs for frequency of CD4+, CD8+, or CD69+ T cells, IFN-γ+ cells, and CD69+/IFN-γ+ double-positive cells from uninfected individuals (n=20) or convalescent children and adolescents (n=31). Data are presented as mean ± SD and analyzed using two-sided Student's t-test between control and patient groups. *p<0.05, **p<0.01, ***p<0.001*

CD8+ (p=0.915) T cell responses (**Figure 3B**). SARS-CoV-2 RBD IgG had a fast decay rate (-0.0377 anti-RBD IgG ratio/day) while CD4+ (-0.0022%/day) and CD8+ (-0.0001%/day) T cell responses persist over time, including the patient with the longest follow-up time at 219 days who had undetectable anti-RBD IgG but persistent SARS-CoV-2 specific CD4+ and CD8+ T-cell response. The average SARS-CoV-2 RBD IgG half-life ($t_{1/2}$) decay was 121.6 days, and the presence of antibodies was estimated to last for 237.7 days or 7.9 months. The same estimation was not applicable to CD4+ and CD8+ T cell responses because of the lack of association with time.

## Age Is a Factor Associated With the Measured RBD IgG Level and T Cell Activation Magnitudes in Recovered Children and Adolescents

Fifteen patients were younger than 12 years and 16 patients were 12 years or older. The results demonstrated differences in the

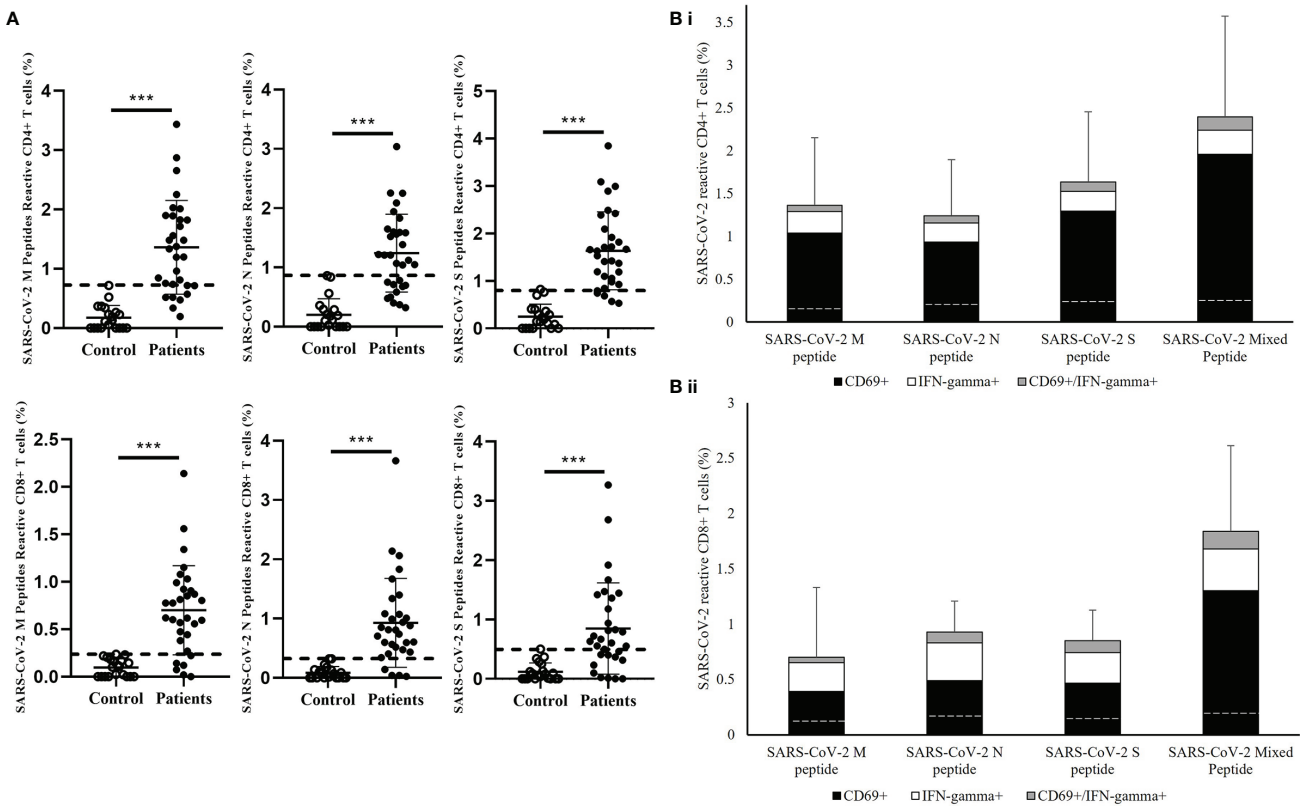


**FIGURE 2** | Measurement of SARS-CoV-2-specific T cell response in in healthy controls and recovered pediatrics patients. **(A)** Comparison of T cell responses stimulated by SARS-CoV-2 Membrane (M), Nuclear (N), Spike (S) peptides in the recovered COVID-19 patients and uninfected controls. Dash line indicated the measured T cell responses reference obtained from the uninfected controls. Data are presented as mean ± SD and analyzed using two-sided Student's t-test between control and patient groups. ***p < 0.001 **(B)** Total T cell responses towards SARS-CoV-2 M, N,S peptides and mixed peptide pools in stacked columns representing the summation of different measured immune subsets in (i) CD4+ and (ii) CD8+ T cells after 16 hours of incubation of PBMCs from recovered patient. Data are expressed as mean ± SD. Dash line in the stack columns indicated the corresponding reference CD4+ and CD8+ T cells response stimulated by different SARS-CoV-2 peptide in uninfected controls group.

immune responses to SARS-CoV-2 between older and younger children. In comparison to children older than 12 years, the younger patients had a significantly higher level of SARS-CoV-2 RBD IgG ratio (p=0.041) (**Figure 4A**). While the frequency of CD4+ T cells reactive to mixed M, N and S peptide pool was similar between the age groups (Cohen's d=0.071) [**Figure 4B** (i)], the frequency of S-peptide specific CD4+ T cells was higher in younger children (Cohen's d=0.3058) [**Figure 4B**(ii)]. Correlative analysis showed that the four patients with highest level of anti-RBD IgG and S-peptide specific CD4+ T cells were all from the younger age group [**Figure 4D**(i)]. In contrast, no difference was observed between the two age groups in SARS-CoV-2 S-reactive CD8+ T cells (Cohen's d=0.03164) [**Figures 4C, 4D**(ii)].

## DISCUSSION

This study characterizes SARS-CoV-2-specific humoral and cellular immunity in children recovered from COVID-19. There was acquired immunity observed in children with either symptomatic or asymptomatic infections. Both SARS-CoV-2-specific humoral and cellular immunity were detectable at different time points during the recovery period. Detection of SARS-CoV-2 RBD IgG and reactive CD4+ and CD8+ T cells against the various peptide pools suggests broad humoral and cellular immunity are present that can counter re-infections.

Our study showed that there were both CD4+ and CD8+ T cell responses to SARS-CoV-2 S, N, and M proteins. The observed up-regulated production of intracellular IFN-γ in our patients cohort was similar to previous published adults studies, suggesting the protective cellular immunity elicited by the T cell memory towards SARS-CoV-2 was also developed in children and adolescents (26, 30, 39). A larger-scale study will be needed to confirm our observations.

The persistence of humoral and cellular responses against the SARS-CoV-2 virus is key to understanding the risk of re-infections (40, 41). We observed a decline in humoral immunity associated with days after diagnosis. The SARS-CoV-2 RBD IgG antibody level lasted on average 7.9 months

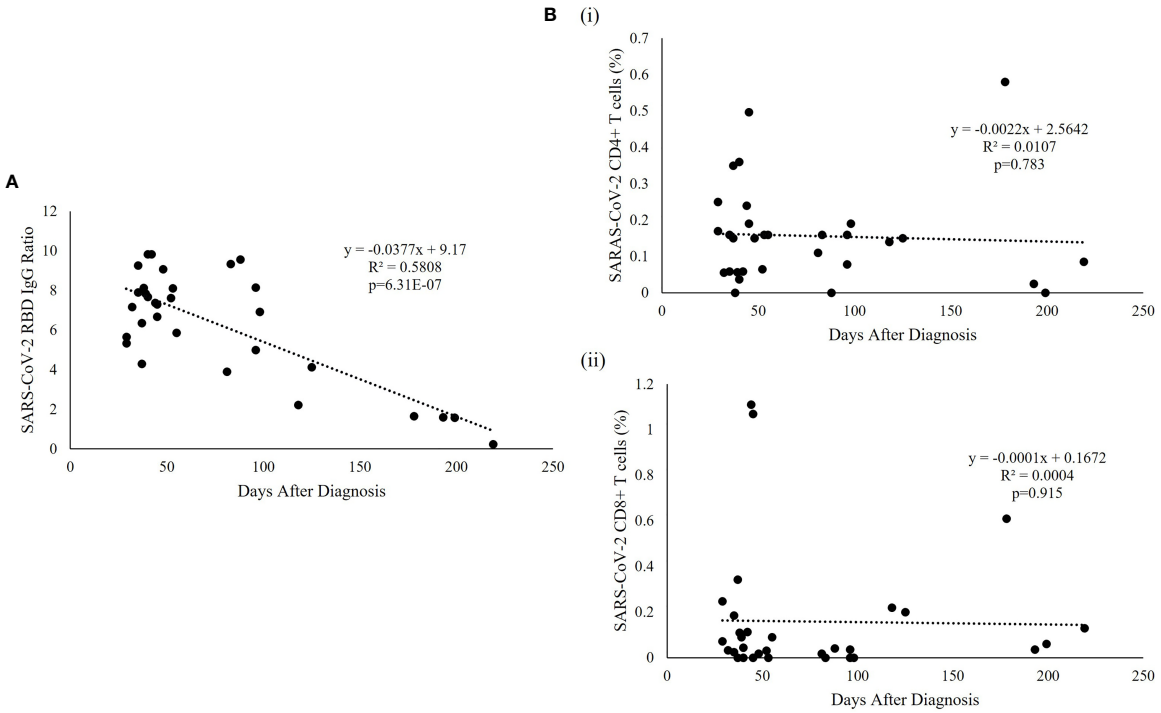


**FIGURE 3** | SARS-CoV-2-specific RBD and T cell responses over time. **(A)** Regression analysis of the measured RBD IgG ratio in convalescent serum was plotted against the days after diagnosis. The best fitting trendline is shown. The calculated $t_{1/2}$ was 121.6 days and the estimated duration of antibodies was 7.9 months compared with the average basal level obtained from uninfected individuals. **(B)** Representative T cell subset frequencies in PBMC of recovered patients were plotted against the post-infection period showing a flat slope for (i) CD4+ and (ii) CD8+, indicating a sustained T cell response to SARS-CoV-2 virus in recovered pediatric patients.

with a half-life of 121.6 days, which is similar to other studies across different age groups (42–47). There have only been a few studies demonstrating the longevity of SARS-CoV-2 T cell response in recovered pediatrics patients. Dan et al., demonstrated that approximately 92% and 50% of recovered patients had specific CD4+ and CD8+ responses, respectively, up to 8 months after the primary infection (30). Based on our finding and the above study, the humoral immunity against SARS-CoV-2 in recovered pediatrics patients can last up to 7-8 months after the primary infection, which seems shorter than cellular immunity.

Ding et al., demonstrated an age-specific variation in childhood CD4+ and CD8+ T cell subsets in healthy Chinese, suggesting differences in immune composition across pediatric age groups (48). Along with this finding, our data demonstrated that the age of the pediatric patients is an important factor influencing the level of SARS-CoV-2 RBD IgG and the magnitude of the T cell response to SARS-CoV-2. Recovered children younger than 12 years had higher SARS-CoV-2 RBD IgG levels. There was also age-dependent CD4+ T cell activity in the production of the RBD IgG antibody. Based on our data, we demonstrated an unreported observation of stronger SARS-CoV-2 S CD4+ T cells response correlated with higher level of anti-RBD IgG ratio in younger children. Our novel findings on the immune responses in convalescent pediatrics patients in younger age group underscored the importance of SARS-CoV-2 S specific CD4+ dependent humoral response in relations to the level of anti-RBD IgG against reinfections, which warrant further larger-scale studies to confirm the observations.

The study findings need to be interpreted with the following caveats. First, the number of patients and controls was relatively small. However, all the controls demonstrated negative immune memory responses with undetectable SARS-CoV-2 anti-RBD antibody titer, indicating immune protection against SARS-CoV-2 in unvaccinated and undiagnosed children were minimal. Second, the duration of follow-up was limited and unevenly distributed, it may affect the correlation analysis in determining the kinetics of SARS-CoV-2 anti-RBD decays in this study. Third, only SARS-CoV-2 anti-RBD, which targeted the S1 domain of the Spike protein, was investigated in this study. Other protective neutralizing antibodies targeted to other parts of SARS-CoV-2 spike protein, such as fusion peptide and heptad repeats located in S2 domain, were not evaluated. Last, the quantity of blood that can be obtained from younger children is limited, hence, other subsets of T cell responses to SARS-CoV-2 peptide pools were not evaluated in this study. Future investigations should include other T cell subsets such as regulatory T cells and T follicular helper cells (Tfh) to draw a more comprehensive picture of the T cell response against SARS-CoV-2 in children.

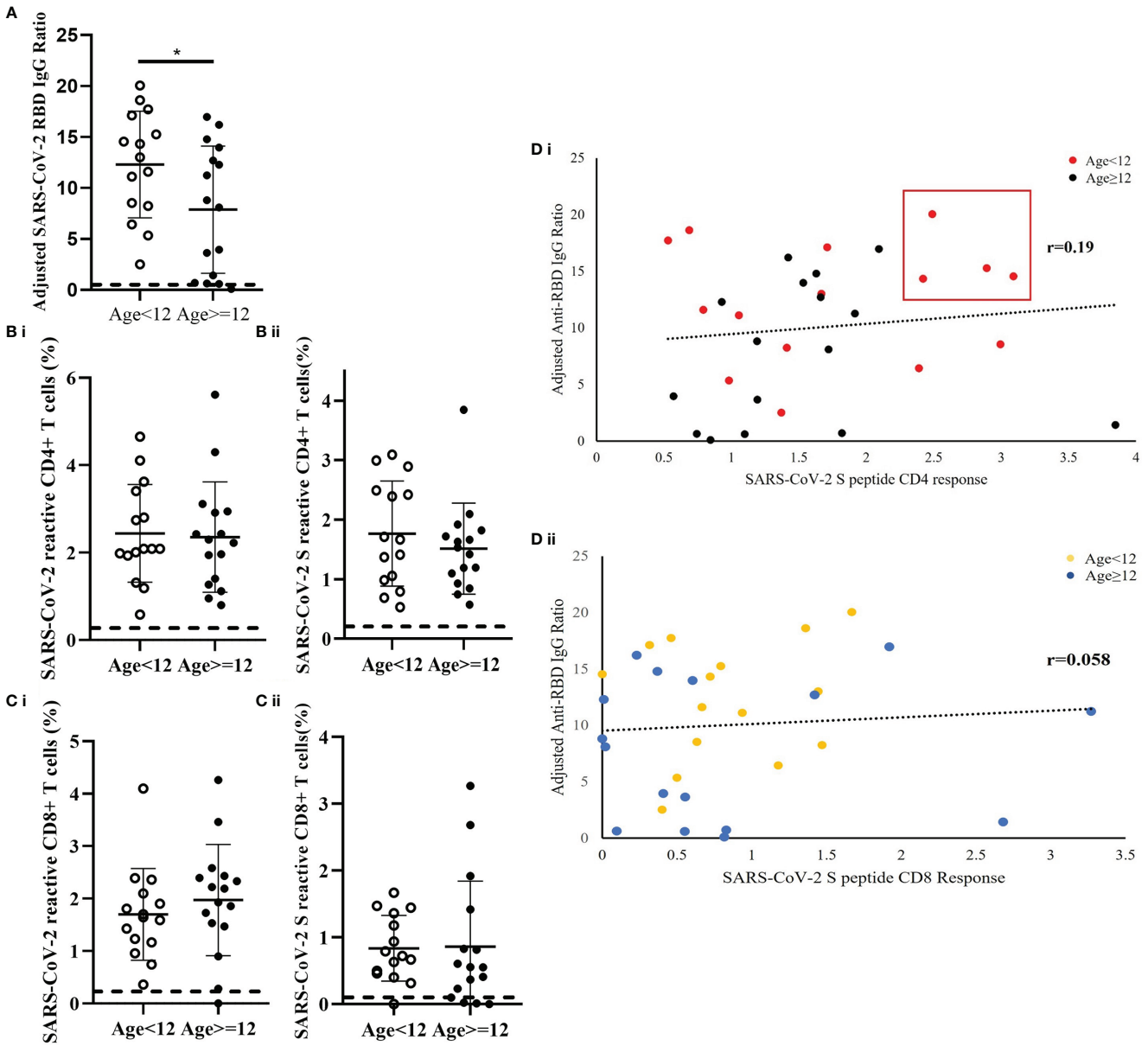


**FIGURE 4** | Age-dependent differences of SARS-CoV-2-specific S-RBD IgG level and SARS-CoV-2-specific T cell response in recovered children and adolescents. The corresponding reference anti-RBD IgG ratio and T cell response obtained from uninfected control was indicated as a dash line in the figures. **(A)** Serological analysis in 15 patients who were younger than 12 years and 16 patients who were 12 years or older. Data was adjusted by days after diagnosis and comparisons analyzed by two-sided Student's t-test *p<0.05. **(B)** Comparison analysis of the total measured CD4+ T cell responses to (i) mixed peptide pools and (ii) S peptide between younger children and older children. **(C)** Comparison analysis of the total measured CD8+ T cell responses to (i) mixed peptide pools and (ii) S peptide between younger children and older children. **(D)** Correlation analysis of anti-RBD IgG level against (i) CD4+ and (ii) CD8+ T cells response in the recovery patients. Data was plotted as age-subgroups with color-labelled dots in the scattered plots. A trendline indicated the correlations direction of the analysis parameters.

## CONCLUSION

SARS-CoV-2 infection induces immune memory in recovered pediatrics patients. The T cell reactivity upon stimulation by M, N, S peptide pools in recovered pediatric patients were similar. There were differences in the level of SARS-CoV-2 RBD IgG and the magnitude of T cell responses between younger and older children. Our findings pave the way for large-scale studies, which could help explain the differences in clinical findings between children and adults with COVID-19. Our findings also have important implications for the development of COVID-19 vaccines targeting younger children.

## DATA AVAILABILITY STATEMENT

The raw data supporting the conclusions of this article will be made available by the authors, without undue reservation.

## ETHICS STATEMENT

The studies involving human participants were reviewed and approved by Institutional Review Board of the University of Hong Kong/Hospital Authority Hong Kong West Cluster (Reference: UW 20-292 and UW 21-157) and the Kowloon West Cluster Research Ethics Committee [Reference: KW/FR-20-086(148-10)]. Written informed consent to participate in this study was provided by the participants' legal guardian/next of kin.

## AUTHOR CONTRIBUTIONS

PI is the Principal Investigator of the Collaborative Research Fund, the funding source of this study. PI, HWT, and GTC contributed to the study conception and research design. MK, KWT, WW, and WHL contributed to the data collection and analysis. PI, HWT, GTC, YLL, WWT, and JK contributed to the data interpretation. HWT, XW, and YZ contributed to the experimental sample preparation and processing. HWT and GTC drafted the manuscript and all co-authors commented and contributed to the revisions and final manuscript.

## FUNDING

This work was supported by the Hong Kong Collaborative Research Fund (CRF) 2020/21 and the CRF Coronavirus and Novel Infectious Diseases Research Exercises (Reference Number: C7149-20G), and the Health and Medical Research Fund (Reference number: COVID190106). The funding sources were not involved in the study design, data collection, analysis, and interpretation, writing of the manuscripts, and the decision to submit the manuscript for publication.

## SUPPLEMENTARY MATERIAL

The Supplementary Material for this article can be found online at: https://www.frontiersin.org/articles/10.3389/fimmu.2021.797919/full#supplementary-material

**Supplementary Table 1 |** Other medical conditions in the controls.

**Supplementary Figure 1 |** Representative gating analysis by flow cytometry. **(A)** Forward scatter height (FSC-H) versus forward scatter area (FSC-A) plot for single cell inclusion. **(B)** Live cells were gated based on live/dead discrimination dye staining. **(C)** Side scatter (SSC-A) versus Forward scatter area (FSC-A) plot for lymphocyte identification. **(D)** T cells were gated based on specific CD3 expression, excluding CD14 and CD20 expressing cells. **(E, F)** Subsets of T cells were gated based on the high expression of CD4 and CD8, and were used in further marker analysis. Floating gates on CD69, IFN-γ, and double-positive CD69/IFN-γ plots were based on the corresponding expressions of the positive control cells.

**Supplementary Figure 2 |** Age distribution of the recovered COVID-19 pediatrics patients.

## REFERENCES

1. Zhou P, Yang XL, Wang XG, Hu B, Zhang L, Zhang W, et al. Addendum: A Pneumonia Outbreak Associated With a New Coronavirus of Probable Bat Origin. *Nature* (2020) 588(7836):E6. doi: 10.1038/s41586-020-2951-z
2. Huang C, Wang Y, Li X, Ren L, Zhao J, Hu Y, et al. Clinical Features of Patients Infected With 2019 Novel Coronavirus in Wuhan, China. *Lancet* (2020) 395(10223):497–506. doi: 10.1016/S0140-6736(20)30183-5
3. Lai CC, Shih TP, Ko WC, Tang HJ, Hsueh PR. Severe Acute Respiratory Syndrome Coronavirus 2 (SARS-CoV-2) and Coronavirus Disease-2019 (COVID-19): The Epidemic and the Challenges. *Int J Antimicrob Agents* (2020) 55(3):105924. doi: 10.1016/j.ijantimicag.2020.105924
4. Dong E, Du H, Gardner L. An Interactive Web-Based Dashboard to Track COVID-19 in Real Time. *Lancet Infect Dis* (2020) 20(5):533–4. doi: 10.1016/S1473-3099(20)30120-1
5. Chua GT, Wong JSC, Lam I, Ho PPK, Chan WH, Yau FYS, et al. Clinical Characteristics and Transmission of COVID-19 in Children and Youths During 3 Waves of Outbreaks in Hong Kong. *JAMA Netw Open* (2021) 4(5):e218824. doi: 10.1001/jamanetworkopen.2021.8824
6. Liu Y, Mao B, Liang S, Yang JW, Lu HW, Chai YH, et al. Association Between Age and Clinical Characteristics and Outcomes of COVID-19. *Eur Respir J* (2020) 55(5):2001112–5. doi: 10.1183/13993003.01112-2020
7. Takagi H. Risk and Protective Factors of SARS-CoV-2 Infection. *J Med Virol* (2021) 93(2):649–51. doi: 10.1002/jmv.26427
8. Du RH, Liang LR, Yang CQ, Wang W, Cao TZ, Li M, et al. Predictors of Mortality for Patients With COVID-19 Pneumonia Caused by SARS-CoV-2: A Prospective Cohort Study. *Eur Respir J* (2020) 55(5):2000524–531. doi: 10.1183/13993003.00524-2020
9. Wu C, Chen X, Cai Y, Xia J, Zhou X, Xu S, et al. Risk Factors Associated With Acute Respiratory Distress Syndrome and Death in Patients With Coronavirus Disease 2019 Pneumonia in Wuhan, China. *JAMA Intern Med* (2020) 180(7):934–43. doi: 10.1001/jamainternmed.2020.0994
10. Palaiodimos L, Kokkinidis DG, Li W, Karamanis D, Ognibene J, Arora S, et al. Severe Obesity, Increasing Age and Male Sex Are Independently Associated With Worse in-Hospital Outcomes, and Higher in-Hospital Mortality, in a Cohort of Patients With COVID-19 in the Bronx, New York. *Metabolism* (2020) 108:154262. doi: 10.1016/j.metabol.2020.154262
11. Lu X, Zhang L, Du H, Zhang J, Li YY, Qu J, et al. SARS-CoV-2 Infection in Children. *N Engl J Med* (2020) 382(17):1663–5. doi: 10.1056/NEJMc2005073
12. Wu Z, McGoogan JM. Characteristics of and Important Lessons From the Coronavirus Disease 2019 (COVID-19) Outbreak in China: Summary of a Report of 72314 Cases From the Chinese Center for Disease Control and Prevention. *JAMA* (2020) 323(13):1239–42. doi: 10.1001/jama.2020.2648
13. Yasuhara J, Kuno T, Takagi H, Sumitomo N. Clinical Characteristics of COVID-19 in Children: A Systematic Review. *Pediatr Pulmonol* (2020) 55(10):2565–75. doi: 10.1002/ppul.24991
14. Gotzinger F, Santiago-Garcia B, Noguera-Julian A, Lanaspa M, Lancella L, Calo Carducci FI, et al. COVID-19 in Children and Adolescents in Europe: A Multinational, Multicentre Cohort Study. *Lancet Child Adolesc Health* (2020) 4(9):653–61. doi: 10.1016/S2352-4642(20)30177-2
15. Chua GT, Xiong X, Choi EH, Han MS, Chang SH, Jin BL, et al. COVID-19 in Children Across Three Asian Cosmopolitan Regions. *Emerg Microbes Infect* (2020) 9(1):2588–96. doi: 10.1080/22221751.2020.1846462
16. Xiong X, Chua GT, Chi S, Kwan MYW, Sang Wong WH, Zhou A, et al. A Comparison Between Chinese Children Infected With Coronavirus Disease-2019 and With Severe Acute Respiratory Syndrome 2003. *J Pediatr* (2020) 224:30–6. doi: 10.1016/j.jpeds.2020.06.041
17. Chen G, Wu D, Guo W, Cao Y, Huang D, Wang H, et al. Clinical and Immunological Features of Severe and Moderate Coronavirus Disease 2019. *J Clin Invest* (2020) 130(5):2620–9. doi: 10.1172/JCI137244

18. He R, Lu Z, Zhang L, Fan T, Xiong R, Shen X, et al. The Clinical Course and Its Correlated Immune Status in COVID-19 Pneumonia. *J Clin Virol* (2020) 127:104361. doi: 10.1016/j.jcv.2020.104361
19. Weiskopf D, Schmitz KS, Raadsen MP, Grifoni A, Okba NMA, Endeman H, et al. Phenotype and Kinetics of SARS-CoV-2-Specific T Cells in COVID-19 Patients With Acute Respiratory Distress Syndrome. *Sci Immunol* (2020) 5 (48). doi: 10.1126/sciimmunol.abd2071
20. Zheng M, Gao Y, Wang G, Song G, Liu S, Sun D, et al. Functional Exhaustion of Antiviral Lymphocytes in COVID-19 Patients. *Cell Mol Immunol* (2020) 17 (5):533–5. doi: 10.1038/s41423-020-0402-2
21. Guan WJ, Ni ZY, Hu Y, Liang WH, Ou CQ, He JX, et al. Clinical Characteristics of Coronavirus Disease 2019 in China. *N Engl J Med* (2020) 382(18):1708–20. doi: 10.1056/NEJMoa2002032
22. Xiong X, Chua GT, Chi S, Kwan MYW, Wong WHS, Zhou A, et al. Haematological and Immunological Data of Chinese Children Infected With Coronavirus Disease 2019. *Data Brief* (2020) 31:105953. doi: 10.1016/j.dib.2020.105953
23. Chua GT, Wong JSC, To KKW, Lam ICS, Yau FYS, Chan WH, et al. Saliva Viral Load Better Correlates With Clinical and Immunological Profiles in Children With Coronavirus Disease 2019. *Emerg Microbes Infect* (2021) 10 (1):235–41. doi: 10.1080/22221751.2021.1878937
24. Laing AG, Lorenc A, Del Molino Del Barrio I, Das A, Fish M, Monin L, et al. A Dynamic COVID-19 Immune Signature Includes Associations With Poor Prognosis. *Nat Med* (2020) 26(10):1623–35. doi: 10.1038/s41591-020-1038-6
25. Rydyznski Moderbacher C, Ramirez SI, Dan JM, Grifoni A, Hastie KM, Weiskopf D, et al. Antigen-Specific Adaptive Immunity to SARS-CoV-2 in Acute COVID-19 and Associations With Age and Disease Severity. *Cell* (2020) 183(4):996–1012.e19. doi: 10.1016/j.cell.2020.09.038
26. Grifoni A, Weiskopf D, Ramirez SI, Mateus J, Dan JM, Moderbacher CR, et al. Targets of T Cell Responses to SARS-CoV-2 Coronavirus in Humans With COVID-19 Disease and Unexposed Individuals. *Cell* (2020) 181(7):1489–1501 e15. doi: 10.1016/j.cell.2020.05.015
27. Suthar MS, Zimmerman M, Kauffman R, Mantus G, Linderman S, Vanderheiden A, et al. Rapid Generation of Neutralizing Antibody Responses in COVID-19 Patients. *medRxiv* (2020) 1(3):100040–50. doi: 10.1016/j.xcrm.2020.100040
28. Long QX, Liu BZ, Deng HJ, Wu GC, Deng K, Chen YK, et al. Antibody Responses to SARS-CoV-2 in Patients With COVID-19. *Nat Med* (2020) 26 (6):845–8. doi: 10.1038/s41591-020-0897-1
29. Rodda LB, Netland J, Shehata L, Pruner KB, Morawski PA, Thouvenel CD, et al. Functional SARS-CoV-2-Specific Immune Memory Persists After Mild COVID-19. *Cell* (2021) 184(1):169–83.e17. doi: 10.1016/j.cell.2020.11.029
30. Dan JM, Mateus J, Kato Y, Hastie KM, Yu ED, Faliti CE, et al. Immunological Memory to SARS-CoV-2 Assessed for Up to 8 Months After Infection. *Science* (2021) 371(6529). doi: 10.1126/science.abf4063
31. Oja AE, Saris A, Ghandour CA, Kragten NAM, Hogema BM, Nossent EJ, et al. Divergent SARS-CoV-2-Specific T- and B-Cell Responses in Severe But Not Mild COVID-19 Patients. *Eur J Immunol* (2020) 50(12):1998–2012. doi: 10.1002/eji.202048908
32. Thieme CJ, Anft M, Paniskaki K, Blazquez-Navarro A, Doevelaar A, Seibert FS, et al. Robust T Cell Response Toward Spike, Membrane, and Nucleocapsid SARS-CoV-2 Proteins Is Not Associated With Recovery in Critical COVID-19 Patients. *Cell Rep Med* (2020) 1(6):100092. doi: 10.1016/j.xcrm.2020.100092
33. Simon AK, Hollander GA, McMichael A. Evolution of the Immune System in Humans From Infancy to Old Age. *Proc Biol Sci* (2015) 282(1821):20143085. doi: 10.1098/rspb.2014.3085
34. Liu Y, Wu Y, Lam KT, Lee PP, Tu W, Lau YL. Dendritic and T Cell Response to Influenza Is Normal in the Patients With X-Linked Agammaglobulinemia. *J Clin Immunol* (2012) 32(3):421–9. doi: 10.1007/s10875-011-9639-y
35. Sullivan GM, Feinn R. Using Effect Size-Or Why the P Value Is Not Enough. *J Grad Med Educ* (2012) 4(3):279–82. doi: 10.4300/JGME-D-12-00156.1
36. Duvall MG, Precopio ML, Ambrozak DA, Jaye A, McMichael AJ, Whittle HC, et al. Polyfunctional T Cell Responses Are a Hallmark of HIV-2 Infection. *Eur J Immunol* (2008) 38(2):350–63. doi: 10.1002/eji.200737768
37. Prompetchara E, Ketloy C, Palaga T. Immune Responses in COVID-19 and Potential Vaccines: Lessons Learned From SARS and MERS Epidemic. *Asian Pac J Allergy Immunol* (2020) 38(1):1–9. doi: 10.12932/AP-200220-0772
38. Zhao J, Zhao J, Mangalam AK, Channappanavar R, Fett C, Meyerholz DK, et al. Airway Memory CD4(+) T Cells Mediate Protective Immunity Against Emerging Respiratory Coronaviruses. *Immunity* (2016) 44(6):1379–91. doi: 10.1016/j.immuni.2016.05.006
39. Nelde A, Bilich T, Heitmann JS, Maringer Y, Salih HR, Roerden M, et al. SARS-CoV-2-Derived Peptides Define Heterologous and COVID-19-Induced T Cell Recognition. *Nat Immunol* (2021) 22(1):74–85. doi: 10.1038/s41590-020-00808-x
40. Altmann DM, Boyton RJ. SARS-CoV-2 T Cell Immunity: Specificity, Function, Durability, and Role in Protection. *Sci Immunol* (2020) 5(49). doi: 10.1126/sciimmunol.abd6160
41. Carrillo J, Izquierdo-Useros N, Avila-Nieto C, Pradenas E, Clotet B, Blanco J. Humoral Immune Responses and Neutralizing Antibodies Against SARS-CoV-2; Implications in Pathogenesis and Protective Immunity. *Biochem Biophys Res Commun* (2021) 538:187–91. doi: 10.1016/j.bbrc.2020.10.108
42. Choe PG, Kim KH, Kang CK, Suh HJ, Kang E, Lee SY, et al. Antibody Responses 8 Months After Asymptomatic or Mild SARS-CoV-2 Infection. *Emerg Infect Dis* (2021) 27(3):928–31. doi: 10.3201/eid2703.204543
43. Gudbjartsson DF, Norddahl GL, Melsted P, Gunnarsdottir K, Holm H, Eythorsson E, et al. Humoral Immune Response to SARS-CoV-2 in Iceland. *N Engl J Med* (2020) 383(18):1724–34. doi: 10.1056/NEJMoa2026116
44. Ibarrondo FJ, Fulcher JA, Goodman-Meza D, Elliott J, Hofmann C, Hausner MA, et al. Rapid Decay of Anti-SARS-CoV-2 Antibodies in Persons With Mild Covid-19. *N Engl J Med* (2020) 383(11):1085–7. doi: 10.1056/NEJMc2025179
45. Iyer AS, Jones FK, Nodoushani A, Kelly M, Becker M, Slater D, et al. Persistence and Decay of Human Antibody Responses to the Receptor Binding Domain of SARS-CoV-2 Spike Protein in COVID-19 Patients. *Sci Immunol* (2020) 5(52). doi: 10.1126/sciimmunol.abe0367
46. Perreault J, Tremblay T, Fournier MJ, Drouin M, Beaudoin-Bussieres G, Prevost J, et al. Waning of SARS-CoV-2 RBD Antibodies in Longitudinal Convalescent Plasma Samples Within 4 Months After Symptom Onset. *Blood* (2020) 136(22):2588–91. doi: 10.1182/blood.2020008367
47. Tan Y, Liu F, Xu X, Ling Y, Huang W, Zhu Z, et al. Durability of Neutralizing Antibodies and T-Cell Response Post SARS-CoV-2 Infection. *Front Med* (2020) 14(6):746–51. doi: 10.1007/s11684-020-0822-5
48. Ding Y, Zhou L, Xia Y, Wang W, Wang Y, Li L, et al. Reference Values for Peripheral Blood Lymphocyte Subsets of Healthy Children in China. *J Allergy Clin Immunol* (2018) 142(3):970–3.e8. doi: 10.1016/j.jaci.2018.04.022


**Conflict of Interest:** The authors declare that the research was conducted in the absence of any commercial or financial relationships that could be construed as a potential conflict of interest.

frontiers in Immunology

ORIGINAL RESEARCH
published: 06 January 2022
doi: 10.3389/fimmu.2021.793142

# Comprehensive Flow Cytometry Profiling of the Immune System in COVID-19 Convalescent Individuals

*Sergio Gil-Manso[1], Iria Miguens Blanco[2], Rocío López-Esteban[1], Diego Carbonell[1,3], Luis Andrés López-Fernández[4], Lori West[5,6,7,8], Rafael Correa-Rocha[1] and Marjorie Pion[1]**

*[1] Laboratory of Immune-Regulation, Gregorio Marañón Health Research Institute (liSGM), Gregorio Marañón University General Hospital, Madrid, Spain, [2] Department of Emergency, Gregorio Marañón University General Hospital, Madrid, Spain, [3] Department of Hematology, Gregorio Marañón Health Research Institute (liSGM), Gregorio Marañón University General Hospital, Madrid, Spain, [4] Service of Pharmacy, Gregorio Marañón Health Research Institute (liSGM), Gregorio Marañón University General Hospital, Madrid, Spain, [5] Department of Pediatrics, Alberta Transplant Institute and Canadian Donation and Transplantation Research Program, University of Alberta, Edmonton, AB, Canada, [6] Department of Medical Microbiology & Immunology, Alberta Transplant Institute and Canadian Donation and Transplantation Research Program, University of Alberta, Edmonton, AB, Canada, [7] Department of Surgery, Alberta Transplant Institute and Canadian Donation and Transplantation Research Program, University of Alberta, Edmonton, AB, Canada, [8] Department of Laboratory Medicine & Pathology, Alberta Transplant Institute and Canadian Donation and Transplantation Research Program, University of Alberta, Edmonton, AB, Canada*

OPEN ACCESS

**Edited by:**
*Eui Ho Kim,*
*Institut Pasteur Korea, South Korea*

**Reviewed by:**
*Johan Van Weyenbergh,*
*KU Leuven, Belgium*
*Arpan Acharya,*
*University of Nebraska Medical Center, United States*

***Correspondence:**
*Marjorie Pion*
*marjorie.pion@iisgm.com*

**Specialty section:**
*This article was submitted to Immunological Memory, a section of the journal Frontiers in Immunology*

**Received:** *11 October 2021*
**Accepted:** *15 December 2021*
**Published:** *06 January 2022*

**Citation:**
*Gil-Manso S, Miguens Blanco I, López-Esteban R, Carbonell D, López-Fernández LA, West L, Correa-Rocha R and Pion M (2022) Comprehensive Flow Cytometry Profiling of the Immune System in COVID-19 Convalescent Individuals. Front. Immunol. 12:793142. doi: 10.3389/fimmu.2021.793142*

SARS-CoV-2 has infected more than 200 million people worldwide, with more than 4 million associated deaths. Although more than 80% of infected people develop asymptomatic or mild COVID-19, SARS-CoV-2 can induce a profound dysregulation of the immune system. Therefore, it is important to investigate whether clinically recovered individuals present immune sequelae. The potential presence of a long-term dysregulation of the immune system could constitute a risk factor for re-infection and the development of other pathologies. Here, we performed a deep analysis of the immune system in 35 COVID-19 recovered individuals previously infected with SARS-CoV-2 compared to 16 healthy donors, by flow cytometry. Samples from COVID-19 individuals were analysed from 12 days to 305 days post-infection. We observed that, 10 months post-infection, recovered COVID-19 patients presented alterations in the values of some T-cell, B-cell, and innate cell subsets compared to healthy controls. Moreover, we found in recovered COVID-19 individuals increased levels of circulating follicular helper type 1 (cTfh1), plasmablast/plasma cells, and follicular dendritic cells (foDC), which could indicate that the Tfh-B-foDC axis might be functional to produce specific immunoglobulins 10 months post-infection. The presence of this axis and the immune system alterations could constitute prognosis markers and could play an important role in potential re-infection or the presence of long-term symptoms in some individuals.

**Keywords: COVID-19, immune system, flow cytometry, unsupervised algorithms, immune dysregulation**

## INTRODUCTION

Up to now, the COVID-19 pandemic has affected more than 230 million people and has claimed the lives of more than 4.8 million people worldwide. COVID-19 is induced by the Severe acute respiratory syndrome coronavirus 2 (SARS-CoV-2). Infected individuals range from asymptomatic to presenting with severe symptoms, with a median fatality rate of 0.27% (1). After infection, the

immune system manages to control it successfully in most cases, generating an immunological memory. More than 80% of infected people are asymptomatic or develop mild symptoms (2). However, some of them suffer from long-term COVID-19-associated symptoms after the infection is resolved (3). In some cases, the virus triggers an exacerbated immune response that goes from protecting to attacking the infected individual. During the inflammatory response, an increase in pro-inflammatory cytokines, T cell activation, and T cell exhaustion was observed (4–6). At the same time, decreases in regulatory cells, T-cell cytotoxicity, and T cells' polyfunctionality were observed (5, 7–9). Even when deeper dysregulation is linked to severe disease, it was observed that COVID-19 individuals, even with mild symptoms, also present immune dysregulation (10).

Due to the interest in the possible acquisition of strong immune protection after natural infection, numerous studies have analysed the immune-specific response against SARS-CoV-2 in convalescent individuals. However, the impact of the infection on the whole immune system after recovery has not been studied. As a result of increasing evidence of long-term COVID-19 symptoms after viral clearance (11–13), there is growing interest in understanding whether immunologic dysregulation may persist among convalescent individuals versus uninfected healthy individuals. With more than 230 million COVID-19 cases documented worldwide, the long-term COVID-19 individual numbers are growing every day, and therefore, the health consequences of SARS-CoV-2 infection and their subsequent socioeconomic costs are far beyond those of active infection alone.

Therefore, a deep understanding of the state of the immune system after natural infection could give important information about the duration of immune dysregulation or the immune response to possible re-infection. Moreover, knowing the immune status after infection, even in individuals who no longer present symptoms, is necessary to determine the risks and the sequelae that may remain.

We performed a deep analysis of innate and adaptive immune cells in 35 COVID-19 convalescent individuals with previous asymptomatic/mild symptoms and 16 non-infected individuals. Our study revealed that various cellular subsets associated with innate or adaptive compartments were differentially expressed between the groups 10 months post-infection. More importantly, some of them could be pivotal to fight future re-infection. These results provide important insights into the potential immune consequences that can mark the future health of previously infected individuals.

# MATERIALS AND METHODS

## Patients and Blood Samples

Blood samples and data questionnaires of donor characteristics during COVID-19 from SARS-CoV-2 convalescent donors were collected from June to December 2020, and healthy controls were collected from January to February 2021, at the General University Hospital Gregorio Marañón, Spain. Informed consent was obtained under the Declaration of Helsinki protocol. The study was approved and performed according to local ethics committees (COV1-20-007). SARS-CoV-2 infection was confirmed by PCR test after nasopharyngeal swab. SARS-CoV-2 donor recruitment was conducted in healthcare workers in the General University Hospital Gregorio Marañón in Madrid, infected with SARS-CoV-2 between March and December 2020. Sample collection was performed at a single time point, between 12 days post-positive PCR (P-PCR+) and 305 days P-PCR+. Detailed healthy and recovered individuals' characteristics are provided in **Table 1**.

## Cell Surface Marker Staining

Whole blood was labelled for surface markers with the antibodies and their fluorochromes distributed in four flow cytometry panels named T-cell, B-cell, Tfh–Tγδ cell, and innate immune cell panels (**Table S1**). CD80 and CD86 are used with the same fluorochrome in the aim to detect the activated B cells. After surface labelling, red blood cells were lysed using RBC Lysis/Fixation Solution (Bio-Legend, San Diego, CA, USA). Surface markers were analysed by flow cytometry using a MACSQuant Analyser 16 cytometer (Miltenyi Biotec, Bergisch Gladbach, Germany). Whole blood was labelled within 2 h of the extraction.

## Detection of Cytokine Levels in Plasma

Cytokine levels were measured in plasma samples employing the automated immunoassay ELLA (Protein Simple, San Jose, CA, USA). We used two different simple plex panels to study the levels of IL-1 β, IL-6, IL-8, TNF- α, CCL2, IL-10, CXCL10, GM-CSF, and IFNγ. The determination of cytokine levels was done using Simple Plex Runner v. 3.7.2.0 software (San Jose, CA, USA). If any measurement was below or above the detection range, we set the minimum or maximum detection limit as value.

## Unsupervised Analysis of the Four Flow Cytometry Panels

In addition to doing traditional manual gating from cytometry data, as presented in the **Supplementary Materials**, we performed a high-dimensional flow cytometric analysis in the four flow cytometry panels using three different algorithms in Cytobank (www.cytobank.org): viSNE, FlowSOM, and CITRUS. viSNE (visualisation of t-distributed Stochastic Neighbour Embedding) is an algorithm that reduces high-parameter data down to two dimensions and allows for easy visualisation of all markers in each cytometry panel and detects visual differences in specific cell subsets. We used the following settings: 1,300,000 events were analysed under proportional sampling between the individuals from total events. Iteration: 7,000; perplexity: 30; theta: 0.5 with a random seed. Onto the viSNE reduced dimension, we ran FlowSOM clustering (Self-Organizing Map from Flow cytometry). FlowSOM is another algorithm to transform cell clusters into higher-order metaclusters. We selected this algorithm because it reveals cell subsets that could be overlooked when using classical manual gating. FlowSOM settings randomly selected 13 individuals in the COV group and the CT group, and the sampling was done with equal event numbers between individuals. Clustering method: hierarchical consensus; number of metaclusters: 15; number of clusters: 100; iterations: 100 with a

**TABLE 1** | Demographic and clinical characteristics and comorbidities in healthy and recovered individuals.

| Characteristics | Healthy control (n = 16) | Recovered COVID19 (n = 35) | p-value |
|---|---|---|---|
| **Age (years), median (range)** | 43,5 (23-59) | 40 (25-62) | 0.805 |
| **Gender, n (%)** | | | 0.753 |
| Male | 6 (37.5) | 11 (31.4) | – |
| Female | 10 (62.5) | 24 (68.6) | – |
| **Ethnicity, n (%)** | | | 0.543 |
| Caucasian | 16 (100) | 32 (91.43) | – |
| Latin American | 0 (0.0) | 3 (8.57) | – |
| **Comorbidities, n (%)** | | | |
| Current smoker/ex-smoker | 2 (12.5)/3 (18.75) | 3 (8.6)/4 (11.4) | 0.671 |
| Asthma | 1 (6.25) | 3 (8.6) | 1.000 |
| Obesity | 1 (6.25) | 1 (2.9) | 1.000 |
| Allergy | 1 (6.25) | 0 (0.0) | 0.314 |
| Heart disease | 0 (0.0) | 2 (5.7) | 0.561 |
| Hypertension | 0 (0.0) | 1 (2.9) | 1.000 |
| Epilepsy | 0 (0.0) | 1 (2.9) | 1.000 |
| Psoriasis | 0 (0.0) | 1 (2.9) | 1.000 |
| Sleep apnea | 0 (0.0) | 1 (2.9) | 1.000 |
| Fibromyalgia | 0 (0.0) | 1 (2.9) | 1.000 |
| Diabetes | 0 (0.0) | 0 (0.0) | – |
| Kidney disease | 0 (0.0) | 0 (0.0) | – |
| Liver disease | 0 (0.0) | 0 (0.0) | – |
| **Symptoms during COVID-19, n (%)** | | | |
| Fatigue | – | 19 (54.3) | |
| Myalgia | – | 19 (54.3) | |
| Anosmia | – | 16 (45.7) | |
| Fever (≥38) | – | 14 (40.0) | |
| Headache | – | 14 (40.0) | |
| Ageusia | – | 13 (37.1) | |
| Cough | – | 13 (37.1) | |
| Diarrhea | – | 10 (28.6) | |
| Dyspnea | – | 9 (25.7) | |
| Arthralgia | – | 5 (14.3) | |
| Nausea or vomiting | – | 5 (14.3) | |
| Fever (<38) | – | 3 (8.6) | |
| Pneumonia | – | 3 (8.6) | |
| Dizziness | – | 3 (8.6) | |
| Tachycardia | – | 3 (8.6) | |
| Sore throat | – | 2 (5.7) | |
| Conjunctivitis | – | 1 (2.9) | |
| Congestion | – | 1 (2.9) | |
| Skin rash | – | 1 (2.9) | |

*Characteristics of the healthy controls (n = 16) and recovered COVID-19 patients (COV, n = 35). The total number of individuals is indicated for all the characteristics and symptoms, except for age (years). A Mann–Whitney U test was performed to analyse age differences between groups. Fisher's exact test was performed to analyze the rest of the characteristics.*

random seed. CITRUS (cluster identification, characterisation, and regression) was the third algorithm used and is designed for fully automated discovery of statistically significant stratifying biological signatures.

As for the analysis of FlowSOM, we randomly selected 13 individuals from the COV group and the CT group, and the sampling was done with equal event numbers between individuals. We ran two predictive association models: (i) the Nearest Shrunken Centroid (PAMR) and (ii) the L1-Penalized Regression (LASSO *via* GLMNET). Cluster characterization: abundance, event sampling: equal; minimum cluster size: 1%; cross-validation Folds: 13; false discovery rate; 1%. For the T-cells panel, the unsupervised analyses were done on CD3+ T-cells. For the B-cells panel, the unsupervised analyses were done on CD19/CD20 gated B-cells. For the Tfh–Tγδ cells panel, the unsupervised analyses were done on CD3+ gated T-cells. For the innate immune cell panel, the unsupervised analyses were done on gated leukocytes.

## Titration for SARS-CoV-2 Antibodies Using Luminex Single-Antigen Beads

SARS-CoV-2 S1 (Abcam) and RBD (Sino Biological, Wayne, PA, US) proteins were conjugated to Luminex beads using standard coupling procedures (14). Coupling was confirmed using a rabbit IgG anti-SARS-CoV-2 Spike monoclonal antibody (Sino Biological) and PE-conjugated goat anti-rabbit IgG secondary antibody (Southern Biotech). To detect SARS-CoV-2 antibodies, sera (25-fold dilution) were incubated with Luminex beads for 30 min at room temperature, washed, and then incubated with a 50-fold dilution of secondary antibody for 30 min at room temperature. Samples were acquired using a FLEXMAP 3D® Luminex system (Toronto, Canada). Cut-off for SARS-CoV-2 S1 and RBD was 1000 MFI and 5000 MFI, respectively.

## Software and Statistical Analysis

Flow cytometry data was analysed using Kaluza version 2.1 and Cytobank algorithms (both from Beckman Coulter, Brea, CA, USA). Data from flow cytometry is displayed as the mean with standard error deviation (SEM). Data from the medians of fluorescent intensity (MFI) is displayed as the median with SEM. A description of the statistical tests used to evaluate the experiments is provided within the respective figure legends. Continuous data was tested for distribution, and individual groups were tested using the Mann–Whitney U test. Spearman's rho (r) was calculated for the correlation between continuous data. *P*-value significance levels were corrected using the Benjamini–Hochberg method for multiple testing. Adjusted *p*-values of <0.05 were considered statistically significant. Graphs were plotted using GraphPad Prism 7.0. Statistical analyses were conducted using GraphPad Prism 7.0 (GraphPad, San Diego, CA, USA) and SPSS (IBM, version 25, Armonk, NY, USA) software.

# RESULTS

## COVID-19 and Healthy Control Cohorts

We recruited 35 PCR-confirmed COVID-19 individuals; 4 were asymptomatic, 29 presented with mild symptoms, and 2 presented with moderate symptoms according to the WHO classification (15) (**Table 1**). They were healthcare workers at General University Hospital Gregorio Marañón in Madrid, infected by SARS-CoV-2 between March and December 2020. Recovered subjects (COV) provided a blood sample at a single time point, between 12 days post-PCR (P-PCR+) and 305 days P-PCR+. Ninety-four percent of subjects were never hospitalised for COVID-19; 6% were hospitalised ($n$ = 2), but none required intensive care unit (ICU) care. Sixteen healthy individuals were recruited and assessed as controls (CT). CT individuals never presented COVID-19 symptoms and were negative for anti-SARS-CoV-2 antibodies at the time of the sample extraction. No difference in comorbidities between the groups was observed (**Table 1**).

## Residual Plasmatic Inflammation Observed in Recovery Individuals

We measured a wide range of pro-inflammatory cytokines in plasma samples related to COVID-19 infection in the infected individuals at the time of the samples extraction. We did not find any differences in cytokines (IL-1β, IL-8, TNF-α, CCL2, IL-10, CXCL10, GM-CSF, and IFN-γ) between recovered and healthy individuals, except for IL-6 levels (**Figure 1A**). Recovered individuals showed slightly higher IL-6 mean levels than those of healthy controls (1.83 ± 0.203 pg/mL; 1.20 ± 0.19 pg/mL, respectively; $p$ = 0.012). Because samples from recovered patients

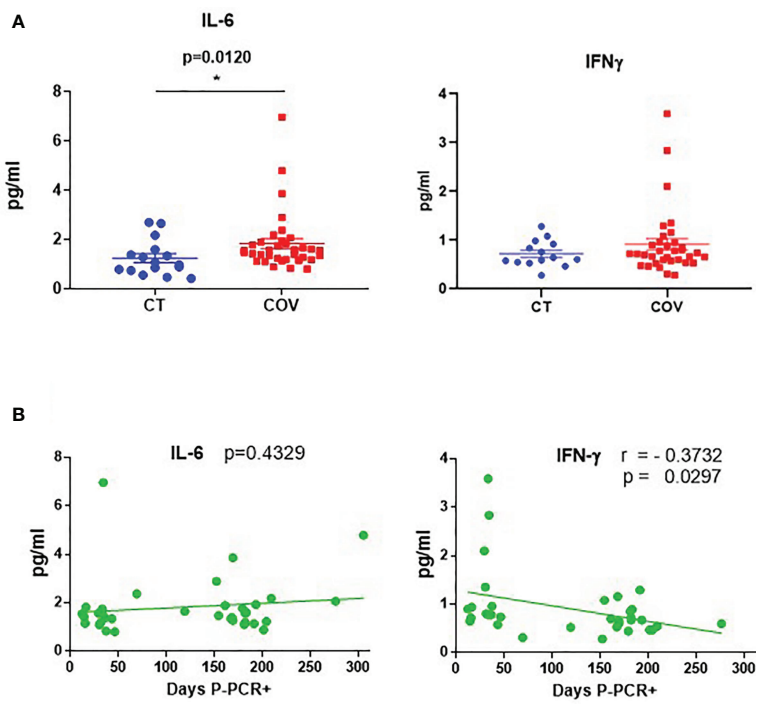


**FIGURE 1** | Cytokine levels in recovered COVID-19 and healthy individuals. **(A)** Cytokine levels of IL-6 and IFN-γ in healthy (CT) and recovered individuals (COV). Mean ± SEM. Pairwise comparisons were performed by a Mann–Whitney U-test corrected using the Benjamini–Hochberg method for multiple testing. **(B)** Correlation between days P-PCR+ and IL-6 and IFN-γ levels. A linear regression curve is represented in each graph. Correlations were done using Spearman's rank-order correlation test; r = Spearman's rank correlation coefficient. *P* = *p*-value, adjusted by the Benjamini–Hochberg adjustment method for multiple testing. *$p < 0.05$. Each symbol corresponds to an individual.

were analysed 12 to 305 days post-PCR+ (P-PCR+), we also investigated possible changes in cytokine levels as time passed. We observed no correlation between days P-PCR+ and IL-6 levels ($p = 0.4329$) and one negative correlation between days P-PCR+ and IFN-γ (r = –0.3732, $p = 0.0297$, **Figure 1B**). This negative correlation might indicate that, the longer ago the infection was, the less IFN-γ patients have in their plasma, reaching a basal non-inflammatory level of this cytokine (1 pg/mL).

## Activation of T-Cell Subsets in Recovered COVID-19 Individuals

We studied T-cell subsets, using traditional manual gating (**Figure S1**), and found that the absolute number of the activated CD4+ HLA-DR+ CD38+ T cells subset was significantly different between the groups (**Figure 2A** and **Figure S1**), being lower in the COV group than in the CT group (**Figure 2B**; CD4+ HLA-DR+ CD38+ T cells 4.38 ± 0.412 cells/μL and 6.82 ± 0.748 cells/μL, absolute number mean ± SEM, respectively, in the COV and CT groups).

Because the samples were extracted from 12 to 305 days P-PCR+, we investigated possible changes in subsets regarding the time P-PCR+. No significant correlation was observed in terms of the distribution of the absolute numbers of CD4+ HLA-DR+ CD38+ as time passed (**Figure 2C**). We also observed that, even if no difference was seen between the groups, the frequency of CD4 effector memory (EM) decreased significantly as time passed from infection (**Figure 2D**), indicating a diminution in the frequency of differentiated CD4+ T cells.

We then applied a high-dimensional flow cytometry analysis to explore lymphocyte activation and differentiation between recovered COVID-19 and healthy individuals. Using the unsupervised algorithms (viSNE), we detected only a few variations in the distribution of cellular populations between the CT and COV groups (data not shown). Using the viSNE results, we ran a Self-Organising Map from flow cytometry (FlowSOM), which permits clustering cells that can reveal how all markers are behaving in all cells. All 35 recovered COVID-19 individuals were analysed independently of the time post-infection. From the 15 metaclusters generated, one showed a significant difference in abundance between the groups (metacluster 12, **Figure 2E**), being more abundant in the CT group than in the COV group. Metacluster 12 was composed of 22 clusters (**Figure S2A**), but only one of them (cluster 67, **Figure S2B**) was significantly different between the COV and CT groups (**Figure S2C**). We observed that the phenotype of this metacluster was CD4+ CD45RAneg CCR4neg CCR10neg CD27+ CCR6neg CXCR3+ CD127+ (**Figure 2F** and **Figure S2D**), which corresponds to the effector Th1 central memory subset. This subset presented a significantly lower mean of fluorescence intensity for the CXCR3 marker in the COV group than in the CT group; as well as a trafficking marker that promotes Th1 response, and CCR10, a skin-homing marker (**Figure 2F**).

After the viSNE analysis, we ran the CITRUS algorithm (cluster identification, characterisation, and regression), which is designed for the automated discovery of statistically significant biological signatures within datasets (CT versus COV). Two clusters were discovered to have higher abundance in the CT than in the COV group (**Figure 2G**). Regarding the fluorescence intensity of each panel's markers, the first cluster (**Figure 2H**—cluster A, and **Figure S3**) was defined as CD8+ CD127+ CD27+ CCR10+ CD45RA+, which may correspond to the naïve CD8+ T cell subset. The second cluster (**Figure 2I**—cluster B) was defined as CD4+ CXCR3+ CCR6neg CCR4neg CD127+ CD27+ CCR10+ (**Figure S3**), related to the Th1 central memory, confirming the results obtained by the FlowSOM analysis. Surprisingly, both subsets expressed the CCR10 marker that is generally associated with skin or mucosal-resident T-cells (16, 17). This marker is generally not associated with Th1 or naïve CD8+ T cells.

In summary, recovered COVID-19 individuals presented sustained lower counts of activated CD4+ T cells than healthy controls. The unsupervised analyses permitted us to detect that CT group individuals presented a higher abundance of Th1 central memory and naïve CD8+ T cells, both expressing the mucosal homing receptor CCR10. This diminution is likely due to residual lymphopenia, but it cannot be ruled out that these cells expressing CCR10 could also be still present in tissues instead of recirculating in the periphery in convalescent individuals.

## The Type-1 T Follicular Helper Subset Is More Frequent in Recovered Than in Healthy Individuals

Functional T cells such as pro-inflammatory and senescent T cells were also analysed. Using the traditional manual gating strategy (**Figure S4A**), we observed that the frequency of the peripheral or circular T follicular helper type-1 subset (cTfh1 ICOS+ PD-1+) was significantly higher in the COV group than in the CT group (**Figures 3A, B**). Moreover, even if not significant, the frequency of the cTfh1 ICOS+ PD-1+ subset was higher in individuals with early infection than in individuals with a longer time post-infection (**Figure 3C**).

The FlowSOM algorithm was run on a viSNE analysis, and one metacluster (metacluster 6) was significantly more represented in the CT than in the COV group (**Figure S4B**), with a clear expression of CD4 and no expression of CD25 (**Figure S4C**). This metacluster comprises three clusters (clusters 13, 31, and 52, **Figure S5A**) and was significantly more abundant in the CT group than in the COV group (**Figure 3D**). Cluster 13 expressed CD4+ CD28+ CXCR3+ PD-1+, which could be related to a Th1 PD-1+ subset (**Figure 3E** and **Figure S5B**). Cluster 31 expressed CD4+ CD28+ CD45RAneg CD127+ CXCR3+, which could be related to the memory Th1 subset (**Figure 3F** and **Figure S5B**), and the cluster 52 expressing CD4+ CD28+ CD127+ CCR6+ CXCR3+ could be related to the memory Th1/Th17 subsets (**Figure 3G** and **Figure S5B**).

To confirm these results, we used the second clustering algorithm, CITRUS, which permitted us to discover statistically significant biological signatures between COV and CT. One cluster was significantly less represented in the COV group (**Figure 3H**, cluster C). Cluster C was related to the Th1 memory subset and the expression of CD4+ CD28+ CD127+ CXCR3+ (**Figure 3I** and **Figure S6**), confirming the previous

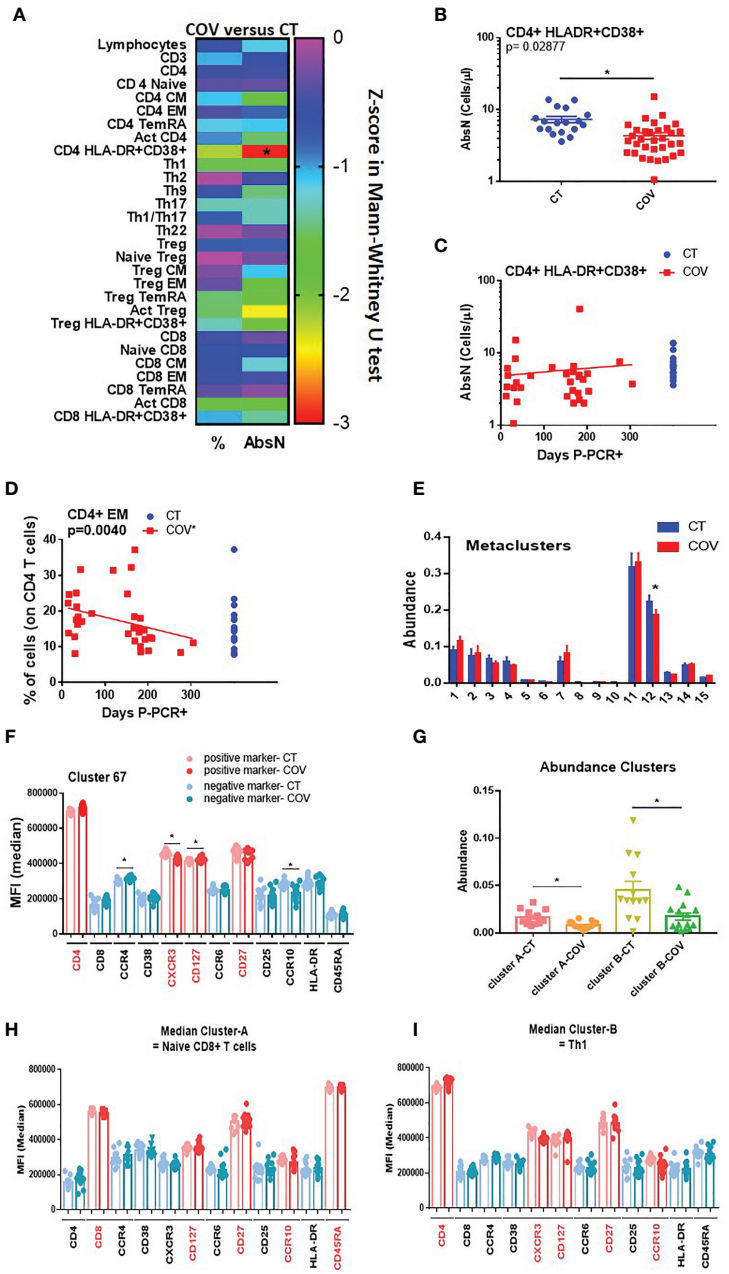


**FIGURE 2** | Manual gating and high-dimensional flow cytometry unsupervised analysis in T-cell panel. **(A)** Heat map of the pairwise comparison between recovered COVID-19 (COV) and healthy control (CT) individuals of results obtained by classical manual flow cytometry gating. Statistical analysis was performed with the Mann–Whitney U test. The colour scale represents the Z-score on the right Y-axis. Immune population names are represented on the left Y-axis. The left column represents the z-score from the pairwise comparison for the cellular population's percentage (%), and the right column represents the z-score from the pairwise comparison for the absolute numbers (cells/uL, AbsN). The *p*-value was corrected using the Benjamini–Hochberg method for multiple testing. **(B)** AbsN of CD4+ HLA-DR+ CD38+ in CT and COV individuals. Pairwise comparisons were performed using a Mann–Whitney U-test corrected using the Benjamini–Hochberg method for multiple testing; mean ± SEM. **(C)** Correlation between days P-PCR+ and CD4+ HLA-DR+ CD38+ AbsN. Spearman's rank-order correlation test with Benjamini–Hochberg adjustment for multiple testing. **(D)** Correlation between days P-PCR+ and frequency of CD4+ effector memory (EM). Spearman's rank-order correlation test with Benjamini–Hochberg adjustment for multiple testing. **(E)** The metaclusters' abundance was obtained through FlowSOM analysis. Two-way ANOVA with Benjamini–Hochberg adjustment for multiple testing. Median ± SEM. **(F)** The median of fluorescence (MFI) of cluster 67 was obtained through a FlowSOM analysis. One-way ANOVA with Benjamini–Hochberg adjustment for multiple testing. Median ± SEM. **(G)** The clusters' abundance was significantly different between COV and CT individuals obtained through CITRUS analysis. One-way ANOVA with Benjamini–Hochberg adjustment for multiple testing. Median ± SEM. **(H)** The median of fluorescence (MFI) of cluster A or cluster B **(I)** was obtained through CITRUS analysis. One-way ANOVA with Benjamini–Hochberg adjustment for multiple testing. Median ± SEM. $^*p < 0.05$.

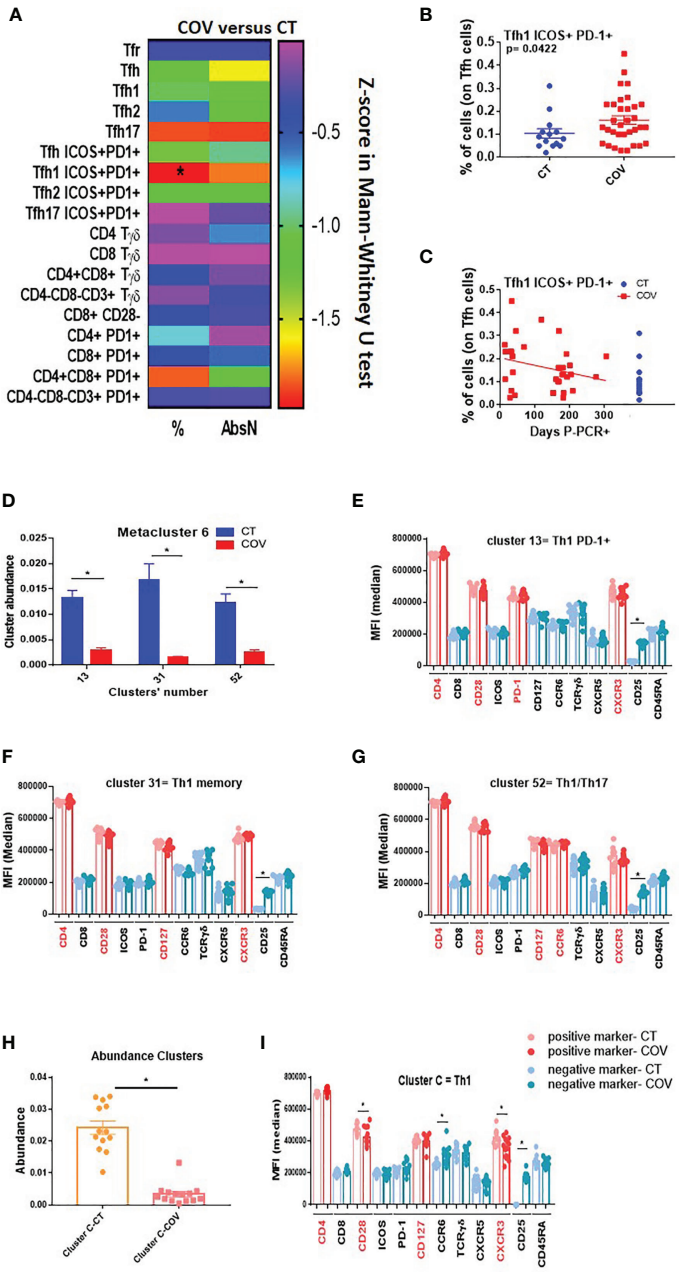


**FIGURE 3** | Manual gating and high-dimensional flow cytometry unsupervised analysis in Tfh–Tγδ cells panel. **(A)** Heat map of the pairwise comparison between recovered COVID-19 (COV) and healthy control (CT) individuals of cellular subsets obtained by classical manual flow cytometry gating. Analysis was performed with the Mann–Whitney U test. The colour scale represents Z-score on the right Y-axis. Immune population names are represented on the left Y-axis. The left column represents the z-score from the pairwise comparison for the cellular population's percentage (%), and the right column represents the z-score from the pairwise comparison for the absolute numbers (cells/uL, AbsN). p-value was adjusted by the Benjamini–Hochberg adjustment method for multiple testing, $^*p < 0.05$. **(B)** Frequency of Tfh1 ICOS+ PD-1+ in CT and COV individuals. Pairwise comparisons were performed using a Man–Whitney U-test with Benjamini–Hochberg adjustment for multiple testing. Mean ± SEM. **(C)** Correlation between days P-PCR+ and frequency of Tfh ICOS+ PD-1+. Spearman's rank-order correlation test with Benjamini–Hochberg adjustment for multiple testing. **(D)** The abundance of the three metaclusters was obtained through FlowSOM analysis. One-way ANOVA with Benjamini–Hochberg adjustment for multiple testing. Median ± SEM. **(E)** Medians of fluorescence (MFI) of clusters 13, 31 **(F)**, and 52 **(G)** were obtained through FlowSOM analysis. One-way ANOVA with Benjamini–Hochberg adjustment for multiple testing. Median ± SEM. **(H)** The abundance of the cluster was significantly different between CT and COV individuals, as obtained through CITRUS analysis. One-way ANOVA with Benjamini–Hochberg adjustment for multiple testing. Median ± SEM. **(I)** MFI of cluster C was obtained through CITRUS analysis. One-way ANOVA with Benjamini–Hochberg adjustment for multiple testing. Median ± SEM. $^*p < 0.05$.

discovery by FlowSOM analysis (**Figure 3F**). Moreover, the MFI of CD28 and CXCR3 were diminished in the COV group compared to the CT group (**Figure 3I**). Therefore, the difference between the groups was due, not only to the cell abundance, but also to the markers' expression intensity.

Summing up, we confirmed in this panel that Th1 and Th1/Th17 were differentially represented in both groups, with greater abundance in the CT than in the COV group, likely due to remnant lymphopenia. Furthermore, COV individuals presented higher frequencies of the activated cTfh1 subset (ICOS+ PD-1+) in the COV group than in the CT group, independent of the sampling time, which are implicated in the B-cell response during the infection.

## B Cell Activation in Recovered COVID-19 Individuals

cTfh1 is related to B cell response and immunoglobulin secretion; therefore, we analysed the B-cell differentiation and activation phenotypes using a classical gating strategy (**Figure S7**). A significant difference in the frequency and absolute numbers of activated B cells (CD80/CD86+, **Figure 4A**) was observed, with a higher frequency (**Figure 4B**) and AbsN (**Figure 4C**) in the COV group than in the CT group. However, the frequencies and AbsN of CD80+ CD86+ B cells (**Figure 4D**, right panel) were not correlated with the sampling time, showing that the higher frequencies and AbsN of activated B cells persist. In future studies, it will be essential to discriminate CD80+ and CD86+ B cells, and not only the combination of CD80/CD86 since CD80 and CD86 are not only activation markers, but they might also be differentially expressed on B cells. Therefore, CD80 and CD86 markers can represent B cells with different function.

The unsupervised FlowSOM analysis permitted us to detect one metacluster (metacluster 13) with a significantly higher abundance in the COV group than in the CT group, even if this cluster represented a minority subset (**Figure S8A**). Metacluster 13 was related to PD-1+-expressing plasmablasts since it presented CD19+ CD20+ CD80/CD86+ CD38+ markers (**Figure 4E** and **Figure S8B**). It was already described that pre-plasmablasts and plasmablasts could express CD80 and CD86 (18). Because of the intermediary expression of CD138 in these cells, one can assume that they were plasmablasts differentiating into plasma cells. Moreover, in the CITRUS algorithm applied to the two groups of individuals, only one cluster was defined as predictively different between CT and COV, with a higher abundance in COV than in the CT group (**Figure 4F**). This cluster was expressing CD80/CD86+ CD27+ CD38+ CD138+ PD-1+ in the surface of the cells —all markers that could be related to PD-1+ plasma cells (**Figure 4G** and **Figure S9**). Moreover, the CD138 MFI was significantly higher in the COV group than in the CT group (417,290 ± 11,410 and 382,224 ± 9505, MFI ± SEM, respectively, $p = 0.0479$). Therefore, from two different unsupervised analyses, we found that individuals in the COV group presented more PD-1+ plasmablasts and PD-1+ plasma cells than in the CT group, showing that immunoglobulin-producing cells were present in recovered individuals. Interestingly, the abundance of the PD-1+ plasma cell subset was found to be positively correlated with absolute counts of cTfh ICOS+ PD-1+ (p= 0.00508) in the COV group but not in the CT group (p= 0.7392, **Figure 4H**). In summary, COV group individuals presented a sustained activated B-cell compartment with higher abundance of PD-1+ plasma cells and plasmablast subsets than healthy controls, likely due to a remnant of the viral infection. Antigen-activated B cells interact with follicular helper T cells to produce strong anti-antigen-specific immunoglobulins, and the ability of B cells to produce anti-SARS-CoV-2 specific immunoglobulins is essential to fight viral infection. Indeed, we observed that the abundance of PD-1+ plasma cells was correlated with the numbers of ICOS+ PD-1+ Tfh, which could evidence that the COVID-19 recovered individuals still have a solid Tfh-B cell axis 10 months post-infection.

## Innate Immunity in Recovered COVID-19 Individuals

Innate immunity is also crucial for developing a solid immune response, and patients with mild symptoms also presented dysregulation of innate immunity (19). Using the traditional manual gating strategy (**Figure S10**), we detected a significant difference in frequencies and AbsN for several cellular subsets, such as eosinophils, neutrophils, and follicular DCs (foDCs) (**Figure 5A**), with an increased frequency of eosinophils and foDC in the COV group compared to the CT group (**Figures 5B, C**), but a decreased frequency of neutrophils in the COV group in comparison to the CT group (**Figure 5D**). At 10 months post-infection, there were no correlations between eosinophils and foDC frequencies and time P-PCR+ and both subsets showed sustained high frequencies as time passed post-infection (**Figures 5E, F**).

The CITRUS analysis detected three clusters that were significantly more abundant in the COV group than in the CT group (**Figure 5G**). Clusters E and F (**Figures 5H, I**) presented almost the same phenotype, CD14+ CD3+ CD62L+, representing an unconventional CD14+ CD3+ double-positive subset that was already associated with immune dysregulation (20) (**Figure S11**). We did not determine CD14+ CD3+ doublet since our analysis was done in the singlet gate, and therefore, we cannot conclude whether this double positive subset is a real subset expressing both markers or if it was composed by T-cell: monocyte complexes, as observed in the ref 20.

Cluster G expressed HLA-DRneg CD11cneg CD14neg CD62L+ CD16+ CD123+ CD1cint (**Figure 5J**). While CD16 and CD1c are markers for myeloid dendritic cells (CD1c+ mDC and CD16+ mDC), CD123 is a marker for plasmacytoid dendritic cells. More surprisingly, HLA-DR and CD11c were not expressed in this cluster. Both markers are generally used during the first step for the total DC gating strategy. Therefore, this cluster could also represent an atypical DC subset that has not been detected by manual gating.

In summary, this panel demonstrated that innate immune dysregulation was still observed 10 months post-infection with atypical DC subsets associated with recovered COVID-19 individuals.

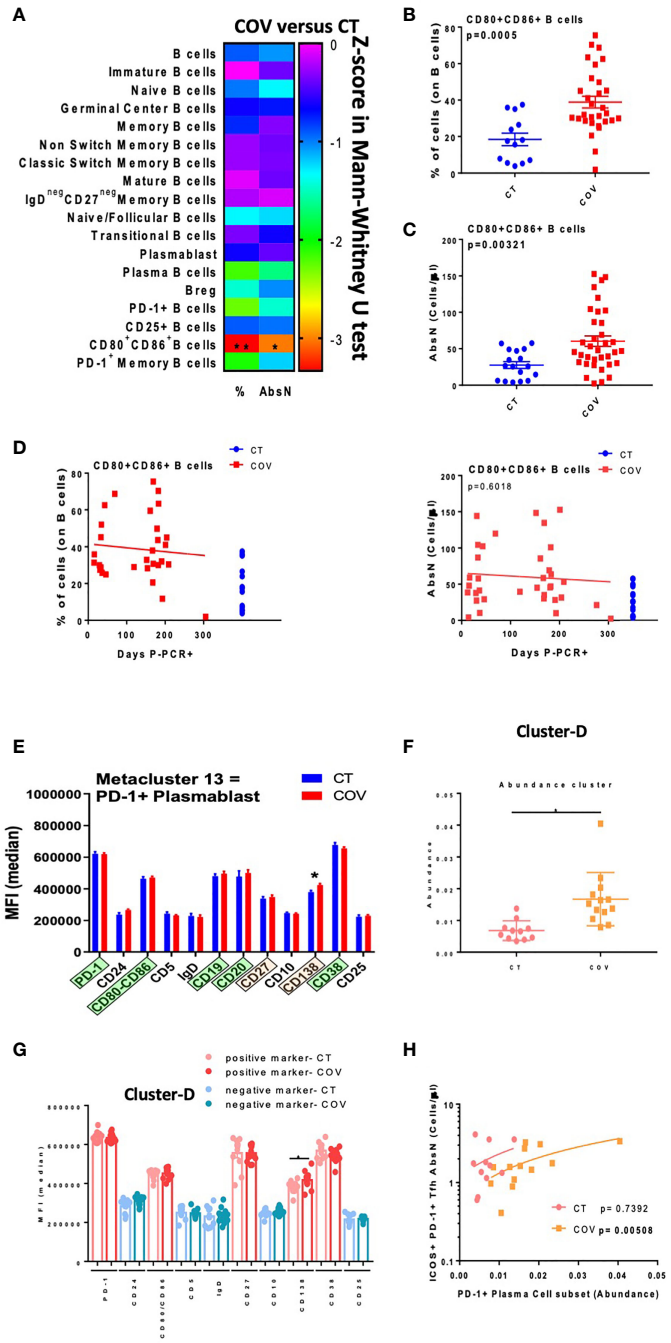


**FIGURE 4** | Manual gating and high-dimensional flow cytometry unsupervised analysis in B-cell panel. **(A)** Heat map of the pairwise comparison between recovered COVID-19 (COV) and healthy control (CT) individuals of cellular subsets obtained by classical flow cytometry analysis. Analysis was performed with the Mann–Whitney U test. The colour scale represents the Z-score on the right Y-axis. Immune population names are represented on the left Y-axis. The left column represents the z-score from the pairwise comparison of the cellular population's percentage (%), and the right column represents the z-score from the pairwise comparison of the absolute numbers (cells/uL, AbsN). The *p*-value was adjusted by the Benjamini–Hochberg adjustment method for multiple testing. **(B)** Frequency or AbsN **(C)** of CD80/CD86+ B-cells in CT and COV individuals. Pairwise comparisons were performed using a Mann–Whitney U-test with Benjamini–Hochberg adjustment for multiple testing. Mean ± SEM. **(D)** Correlation between days P-PCR+ and frequency of CD80/CD86+ (left panel) and AbsN of CD80/CD86+ B cells (right panel). Spearman's rank-order correlation test with Benjamini–Hochberg adjustment for multiple testing. **(E)** MFI of cluster 13 was obtained through FlowSOM analysis. One-way ANOVA with Benjamini–Hochberg adjustment for multiple testing. Median ± SEM. **(F)** The abundance of cluster D was significantly different between COV and CT individuals and was obtained through CITRUS analysis. One-way ANOVA with Benjamini–Hochberg adjustment for multiple testing. Median ± SEM. **(G)** MFI of cluster D obtained through CITRUS analysis. One-way ANOVA with Benjamini–Hochberg adjustment for multiple testing. Median ± SEM. **(H)** Correlation between AbsN of ICOS+ PD-1+ Tfh and the abundance of PD-1+ plasma cells. Spearman's rank-order correlation test with Benjamini–Hochberg adjustment for multiple testing. $^{*}p < 0.05$ and $^{**}p < 0.01$.

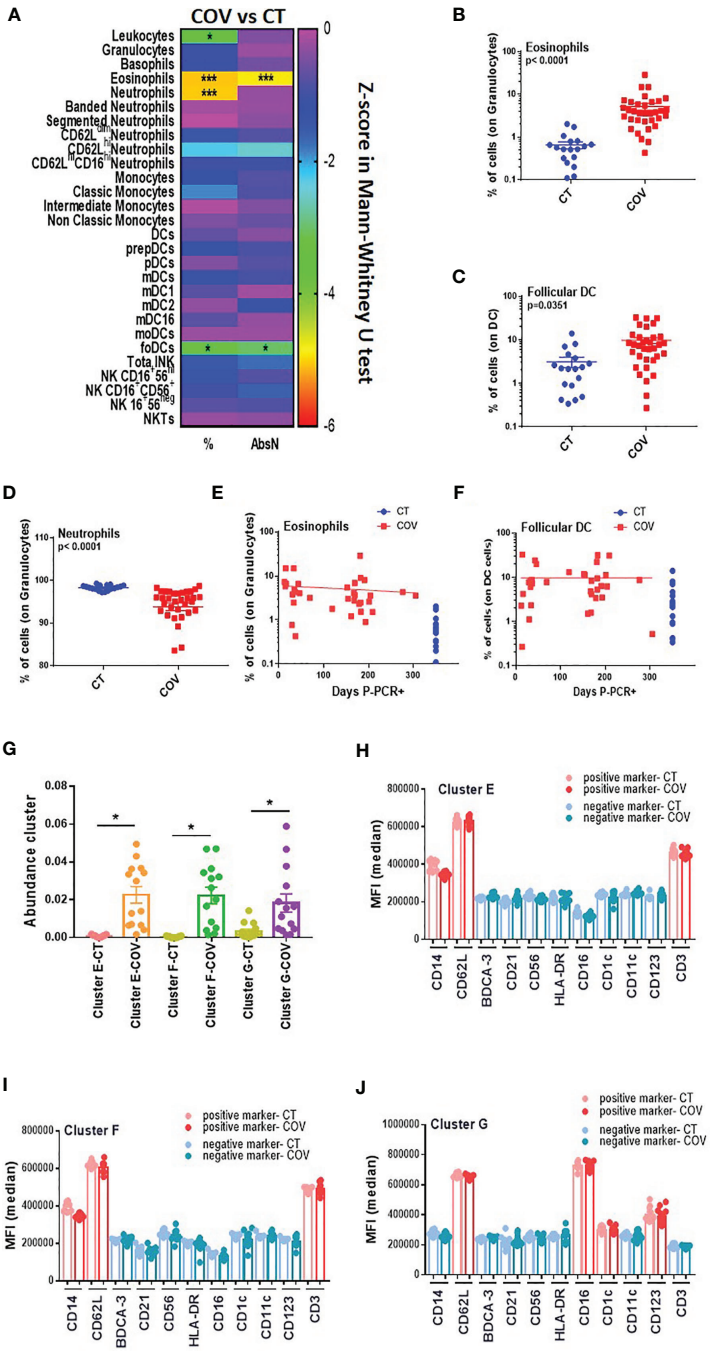


**FIGURE 5** | Manual gating and high-dimensional flow cytometry unsupervised analysis in innate cells panel. **(A)** Heat map of the pairwise comparison between recovered COVID-19 (COV) and healthy control (CT) individuals of cellular subsets obtained by classical flow cytometry analysis. The analysis was performed with the Mann–Whitney U test. The colour scale represents the Z-score on the right Y-axis. Immune population names are represented on the left Y-axis. The left column represents the z-score from the pairwise comparison of the cellular population's percentage (%), and the right column represents the z-score from the pairwise comparison of the absolute numbers (cells/uL, AbsN). The *p*-value was adjusted by the Benjamini–Hochberg adjustment method for multiple testing. $^{*}p < 0.05$, and $^{***}p < 0.001$. **(B)** Frequency of eosinophils and **(C)** follicular DC in CT and COV individuals. Pairwise comparisons were performed by Mann–Whitney U-test with Benjamini–Hochberg adjustment for multiple testing. Mean ± SEM. **(D)** Frequency of neutrophils in CT and COV individuals. Pairwise comparisons were performed using Mann–Whitney U-test with Benjamini–Hochberg adjustment for multiple testing. Mean ± SEM. **(E)** Correlation between days P-PCR+ and frequency of eosinophils or **(F)** follicular DC. Spearman's rank-order correlation test with Benjamini–Hochberg adjustment for multiple testing. **(G)** The abundance of clusters was significantly different between CT and COV individuals and was obtained through CITRUS analysis. One-way ANOVA with Benjamini–Hochberg adjustment for multiple testing. Median ± SEM. **(H)** MFI of cluster E, **(I)** cluster F, and **(J)** cluster G were obtained through CITRUS analysis. One-way ANOVA with Benjamini–Hochberg adjustment for multiple testing. Median ± SEM. $^{*}p < 0.05$.

The results of the four cytometry panels are recapitulated in **Figure 6**.

## DISCUSSION

The great majority of COVID-19 individuals present mild symptoms or are asymptomatic, but little is known about the status of the immune system in COVID-19 individuals after asymptomatic/mild disease. In this study, we performed comprehensive immune profiling in COVID-19 recovered patients using a traditional gating strategy and different unsupervised algorithms. We compared the results with healthy individuals with no SARS-CoV-2 antecedent to determine possible immune subsets dysregulated due to past infection. The detection and identification of these subsets could help us better understand the immune system after SARS-CoV-2 infection and determine which individuals could be prone to reinfection. In addition, this study can help us understand the long-term symptoms that some recovered COVID-19 individuals may suffer. The results are summarised in **Table 2** and **Figure 6**.

We found only a few dysregulated immune cell subsets in recovered patients compared to healthy controls. Some of them were atypical subsets that could be key to understanding the infection, such as the double-positive CD14+CD3+ subset observed within the 'live singlet' events gate, a T-cell/monocyte complex described in diseases where the immune system is disturbed (20). Indeed, Burel JG. et al. have also demonstrated that the T-cell/monocyte complexes are observed in the living singlet gate. These complexes are formed due to an increase of adhesion molecules at their surface leading to a higher constant of association between both T (cells) and monocyte subsets. These complexes were observed essentially during the acute phase of active tuberculosis or acute dengue fever infection (20). Acute tuberculosis and dengue fever present similarities with SARS-CoV-2-associated symptoms (21, 22) and the three pathogens were also able to increase peripheral cytokines' levels such as IFN-γ and thus, dysregulate the innate and adaptive immune system (23, 24). Even though we have not determined if the CD14+ CD3+ subset observed in our study is related to those complexes, there are associated with former COVID-19 individuals who presented immune system inflammation and

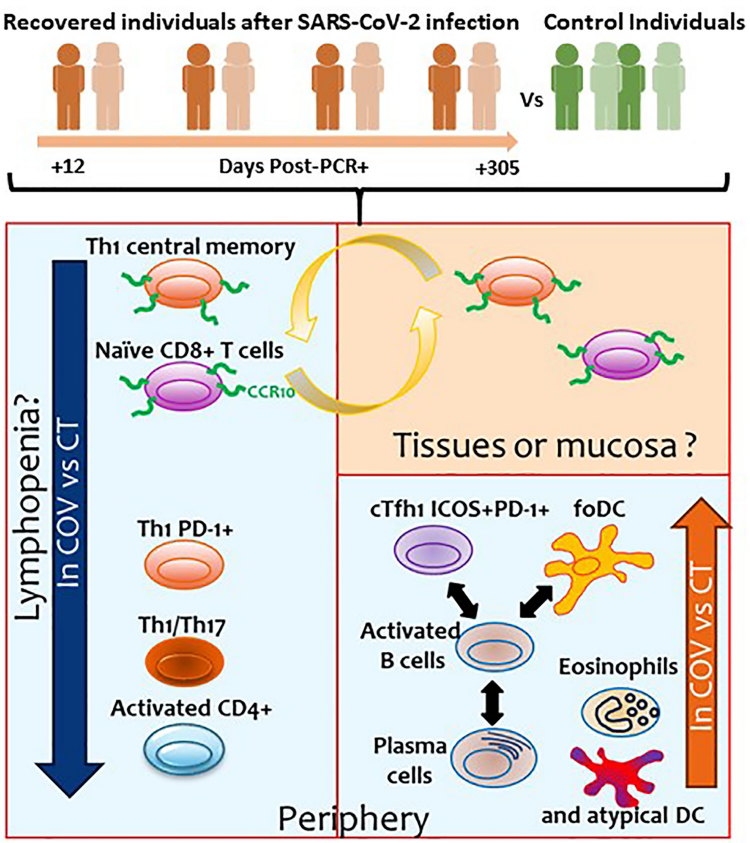


**FIGURE 6** | Summary of the results obtained in the present study. Orange and green individuals represent the recovered individuals after SARS-CoV-2 infection and controls, respectively. Numbers represents the days post-PCR+ when the samples of the former COVID-19 individuals were analysed. Blue squares represent the cellular subsets with altered levels observed in the periphery. Orange square represents the cellular subsets that could be potentially found in tissues or mucosa.

**TABLE 2 |** Summary of the principal cellular subsets significantly and differentially abundant between COV and CT group individuals.

| **Inferior in COV-Group compared to CT-group**<br>**Cellular subsets** | **Frequency/AbsN** |
|---|---|
| CD4+ HLADR+ CD38+ → **activated CD4+ T cells** | AbsN |
| CD4+ CD45RAneg CCR4neg CCR10neg CCR6neg CD27+ CXCR3+ CD127+ → **Th1 central memory** | Frequency |
| CD8+ CD127+ CD27+ CCR10+ CD45RA+ → **atypical naïve CD8** | Frequency |
| CD4+ CXCR3+ CD127+ CD27+ CCR10+ → **atypical Th1 central memory** | Frequency |
| CD4+ CD28+ CXCR3+ PD-1+ → **Tfh1 PD-1+** | Frequency |
| CD4+ CD28+ CD45RAneg CD127+ CXCR3+ → **memory Th1** | Frequency |
| CD4+ CD28+ CD45RAneg CD127+ CXCR3+ CCR6+ → **memory Th1/Th17** | Frequency |
| **Neutrophils** | Frequency |
| **Superior in COV-Group compared to CT-group**<br>**Cellular subsets** | **Frequency/AbsN** |
| **Tfh1** ICOS+ **PD-1+** → **cTfh1 ICOS+ PD-1+** | Frequency |
| CD80+/CD86+ B cells → **activated B cells** | Frequency/AbsN |
| CD80/CD86+ CD38+ CD27int CD138int B cells → **plasmablasts** | Frequency |
| CD80/CD86+ CD27+ CD138+ CD38+ PD-1+ B cells → **PD-1+ plasma cells** | Frequency |
| **Eosinophils** | Frequency/AbsN |
| **Follicular DC** | Frequency/AbsN |
| CD14+ CD3+ CD62L+ → **unconventional double positive** | Frequency |
| CD3neg CD14neg CD62L+ CD16+ CD123+ CD1c int → **atypical DC** | Frequency |

*At the top of the table are the cell subsets with a frequency or AbsN lower in the COV group compared to the CT group, while the bottom part of the table has the subsets with a frequency or AbsN greater in the COV group compared to the CT group. The left column gives the cellular subsets and their most representative markers. The right column indicates if a difference between groups was observed in terms of subsets' frequency or absolute numbers.*

dysregulation. Therefore, this CD14+ CD3+ subset could surge from the activation of the immune system during SARS-CoV-2 infection, but its role in the disease progression or viral clearance is not known and further studies will be needed to determine their possible implication in reinfection protection.

It was also observed an atypical DC subset characterised by the low HLA-DR and CD11c expression, intermediate expression of CD1c and high expression of CD16 and CD123. CD123 is a general marker for plasmacytoid DC, and CD1c or CD16 are markers for myeloid DC. Therefore, this subset presents some DC characteristics, but it has not yet been described to our knowledge. A rare DC subset named CD16+ slanDC presenting CD14neg CD1c+ with high CD16 expression and low expression of HLA-DR in their immature form has already been observed (25–27). However, we cannot determine if this subset could be related to immature CD16+ slanDC since the expression of CD123 on these cells was not described. Nevertheless, it was reported that precursor myeloid cells could express CD123 (28, 29). Therefore, one can hypothesise that the atypical DC subset determined in our study was related to a precursor or an immature state of CD16+ DC. This subset was depicted to be a pro-inflammatory DC subset (30) and could explain why they are found in recovered COVID-19 instead of healthy individuals.

The role of the CD3+ CD14+ and atypical DC subsets is unknown, and we cannot conclude that these subsets are a consequence of the inflammation after SARS-CoV-2 infection or if they could have helped during the viral clearance. Therefore, further studies will be needed to determine their possible implication in reinfection, protection or disease severity.

As expected, diminished frequencies and absolute counts of leukocytes, naïve, activated, and effector (Th1 or Th17) CD4+ T cells can be associated with a remnant of lymphopenia already observed in the majority of COVID-19 individuals (9, 10, 31) and recovered individuals (32). However, the lower abundance in the COV group compared to the CT group of the atypical Th1 memory and atypical naïve CD8 T-cells, both expressing CCR10, could have one other explanation. Indeed, CCR10 is a skin- and mucosal-homing marker (16, 17). Therefore, one can assume that these subsets can still be found in the airways, mucosa, and/or inflamed tissues in recovered individuals. Indeed, SARS-CoV-2 infects the epithelial airways, and local inflammation occurs. It was shown that SARS-CoV-2 ORF7 could induce the expression of CCL27, one of the CCR10 ligands (33). Moreover, CCL27 and CCL28 serum levels are high during SARS-CoV-2 infection (34–36) and were shown to be upregulated in the lungs during the late stages of SARS infection (37). COVID-19 individuals often have lung and other organ damage where high concentrations of the CCR10 ligands have been described (38, 39). Therefore, one can suppose that CCL27 and/or CCL28 could be expressed in the lung and that CCR10-expressing cells could be attracted to the inflammatory site, diminishing their frequency in the periphery.

Another key observation is that after 10 months post-infection, the frequency and absolute counts of activated B cells (CD80+/CD86+) were higher in convalescent individuals. CD80 and CD86 are two markers expressed on naïve B cells upon stimulation. In this study, these markers were labelled with the same fluorochrome to determine such activation. Therefore, it was not possible to distinguish between CD80+-B cells and CD86+-B cells. Further studies will be needed to distinguish both B-cell subsets into COVID-19 individuals since it was demonstrated that both could have differential functions in different pathologies (40–42). Indeed, CD80 was associated with pro-inflammatory cytokine stimulation, while CD86 could play a protective role mediated through anti-inflammatory cytokines in APC. More importantly, CD86 was highly

expressed after type-I-IFN stimulation in the marginal zone of the lymph node where they could promote autoimmune response and participate in the co-stimulation of CD4 T cells (43). Therefore, the level of CD80+- and CD86+-B cells in recovered COVID-19 should be studied to determine if those cells have a role in protecting the individuals from reinfection.

In the total B cell subset, PD-1+ plasmablasts and plasma cells were more abundant in recovered COVID-19 individuals than in healthy controls. Plasmablasts are the precursor subset of plasma cells. They are recognisable for their ability to secrete large numbers of antibodies. An increase in the number of atypical memory B cells and plasma cells had already been observed in COVID-19 individuals (44). In our work, the immunoglobulin-producing subsets expressed the immunomodulatory markers PD-1+ at high levels. PD-1 was described as a negative regulator of B-cell activation (45). Indeed, a diminution of anti-SARS-CoV-2 and neutralising antibodies had already been observed over time in convalescent individuals, even though a potential long-lasting humoral B-cell memory subset was detected (32, 46–48). Therefore, it is not clear if these PD-1+ plasmablasts/plasma cells could produce a sustained level of anti-SARS-CoV-2 immunoglobulins. Further studies are necessary to elucidate the protective role of PD-1+ plasma cells in in the long term.

FoDC are non-migratory DC subtypes and are generally found in the secondary lymph nodes. The formation of the functional GC requires an architecture composed of different sorts of leukocytes, especially foDC (49). FoDC intervenes in specific B-cell response generation after forming the germinal center (GC), where the B cells are differentiated into plasma cells to produce protective high-affinity antibodies (50). Circulating foDC have been described in patients with chronic hepatitis B virus infection (51), and their frequencies positively correlate with plasma cells; foDC could contribute to the efficient immune responses against the pathogen. In this work, we also found higher circulating foDC frequencies in the peripheral blood of recovered COVID-19 individuals compared to healthy controls. Tfh are also essential for germinal centre formation, as well as in regulation and B cell differentiation into plasma cell producers of high-affinity antibodies. The expression of ICOS and PD-1 points to activated cTfh cells and plays an essential role in regulating germinal centre formation, B-cell survival, and B-cell differentiation into long-lived plasma cells (52). It is already described that after SARS-CoV-2 infection, there is a production of S-specific antibodies, memory B cells and cTfh cells (53). Here, we show that the absolute numbers of cTfh ICOS+ PD-1+ are positively correlated with the abundance of the PD-1+ plasma subset, as already described (54, 55). ICOS and PD-1 expression in cTfh is reported to be increased in several immune-related diseases, such as ulcerative colitis (56) and multiple sclerosis (57), or associated with disease severity in such conditions as Primary Sjogren's Syndrome (58). Thus, the ICOS+PD-1+ cTfh subset presence in recovered individuals could be related to past inflammation during infection. Also, cTfh cells have been related to the production of neutralising antibody titers in COVID-19 convalescent individuals (59), which may indicate that the durability of the antibody titers is due to the cTfh cells, among others. It was already observed that anti-SARS-CoV-2-S IgG titers persist for 12 months (60, 61) along with cTfh cells for at least 6 months after SARS-CoV-2 infection (62). The fact that absolute numbers of this subset are correlated with the abundance of the PD-1+ plasma cell subset in recovered COVID-19 individuals, could indicate that the past-inflammation was related to a plasma B cell response in individuals who were presenting mild/moderate symptoms and thus raises hope for long-lasting COVID-19 immunity.

Therefore, besides PD-1+ plasma cells and activated B-cells, the presence of sustained high frequencies or absolute counts of cTfh1 ICOS+PD-1+ and circulating foDC could also be explained by the destructuring of the germinal centre in the lymphoid organs due to inflammation, as already observed during fatal COVID-19 (63, 64). In our work, we study individuals with asymptomatic/mild COVID-19; thus, it is unlikely that these individuals will present a deficiency in germinal centre organisation. Therefore, their presence is likely due to sustain residual activation of the immune system, which could be the hallmark of a solid foDC-Tfh-B cells axis at 10 months post-infection, which could effectively produce specific anti-SARS-CoV-2 antibodies after reactivation. Consequently, one can hypothesise that these patients would be protected from possible reinfection, as already proposed (65, 66).

It would be interesting to understand the function of these rare population (double-positive CD3+ CD14+, CCR10-Th1/CCR10-CD8+ T cells and atypical DC), and perform functional assays or deep sequencing to study their implication in convalescent individuals after SARS-CoV-2 infection. However, this is a limitation of this study since more than 95% of the health workers have been vaccinated, therefore the recruitment of the volunteers with or without previous infection is challenging. Indeed, we cannot affirm that these subsets have not been altered or are even present in those vaccinated individuals. Since most healthcare workers are vaccinated, another limitation of the study is the number of individuals analysed, and the difficulty to recruit more individuals to strengthen the findings of this work. Therefore, further studies are urgently needed to determine the exact role of circulating foDC and Tfh during and after SARS-CoV-2 infection, and the assessment of the presence of GC and foDC in lymphoid organs is highly desirable since GC formation is critical for long-lived memory or high-affinity B cells.

## DATA AVAILABILITY STATEMENT

The original contributions presented in the study are included in the article/**Supplementary Material**. Further inquiries can be directed to the corresponding author.

## ETHICS STATEMENT

The studies involving human participants were reviewed and approved by Gregorio Marañón ethics committee

(REF: COV1-20-007). The patients/participants provided their written informed consent to participate in this study.

## AUTHOR CONTRIBUTIONS

Conceptualisation: MP. Data curation: MP, SG-M, DC, and RL-E. Formal Analysis: MP and SG-M. Funding acquisition: MP and RC-R. Investigation: MP, SG-M, DC, and RL-E. Methodology: MP and SG-M. Project administration: MP. Resources: MP, IM-B, LL-F, and LW. Supervision: MP. Validation: MP, LW, SG-M, LL-F, and IM-B. Writing, original draft: MP and SG-M. Review and editing: LL-F, RC-R, IM-B, DC, and RL-E revised the manuscript. All the authors interpreted and discussed the data. All the authors read and approved the final manuscript.

## FUNDING

This work was partially financed by the Madrid Community grant B2017/BMD3727 and the IiSGM Intramural grant PI-MP-2018. This work was partially funded by a grant from "Fundación Familia Alonso" (FFA-FIBHGM-2019). SG-M was supported by the Youth Employment Program, co-financed by the Madrid community and FEDER Founds (PEJ-2020-AI/BMD-17954), and by the ACT4COVID consortium (CellNex funding). The funders had no role in study design, data collection and analysis, decision to publish, or manuscript preparation. This work was partially supported by grants from the Instituto de Salud Carlos III (ISCIII) (PI18/00506; COV20/00063), co-funded by ERDF (FEDER) Funds from the European Commission, "A way of making Europe".

## ACKNOWLEDGMENTS

The authors thank all the health workers who participated in this study. We acknowledge Dr. Bruce Motyka and Dr. Anne Halpin from Alberta Transplant Institute and Canadian Donation and Transplantation Research Program; University of Alberta, Edmonton, Alberta, Canada for their help in the quantification of the immunoglobulins anti-SARS-CoV-2. We acknowledge Dr. Maribel Clemente from the Cell Culture Unit and Dr. Laura Díaz from the Cytometry Unit of IiSGM. We acknowledge José Maria Bellón from the Statistical unit of IiSGM.

## SUPPLEMENTARY MATERIAL

The Supplementary Material for this article can be found online at: https://www.frontiersin.org/articles/10.3389/fimmu.2021.793142/full#supplementary-material

## REFERENCES

1. Ioannidis JPA. Infection Fatality Rate of COVID-19 Inferred From Seroprevalence Data. *Bull World Health Organ* (2021) 99(1):19–33F. doi: 10.2471/BLT.20.265892
2. Wang Y, Chen Y, Qin Q. Unique Epidemiological and Clinical Features of the Emerging 2019 Novel Coronavirus Pneumonia (COVID-19) Implicate Special Control Measures. *J Med Virol* (2020) 92(6):568–76. doi: 10.1002/jmv.25748
3. Akbarialiabad H, Taghrir MH, Abdollahi A, Ghahramani N, Kumar M, Paydar S, et al. Long COVID, A Comprehensive Systematic Scoping Review. *Infection* (2021) 49(6):1163–86. doi: 10.1007/s15010-021-01666-x
4. Zheng HY, Zhang M, Yang CX, Zhang N, Wang XC, Yang XP, et al. Elevated Exhaustion Levels and Reduced Functional Diversity of T Cells in Peripheral Blood may Predict Severe Progression in COVID-19 Patients. *Cell Mol Immunol* (2020) 17(5):541–3. doi: 10.1038/s41423-020-0401-3
5. Zheng M, Gao Y, Wang G, Song G, Liu S, Sun D, et al. Functional Exhaustion of Antiviral Lymphocytes in COVID-19 Patients. *Cell Mol Immunol* (2020) 17 (5):533–5. doi: 10.1038/s41423-020-0402-2
6. Thevarajan I, Nguyen THO, Koutsakos M, Druce J, Caly L, van de Sandt CE, et al. Breadth of Concomitant Immune Responses Prior to Patient Recovery: A Case Report of Non-Severe COVID-19. *Nat Med* (2020) 26(4):453–5. doi: 10.1038/s41591-020-0819-2
7. Qin C, Zhou L, Hu Z, Zhang S, Yang S, Tao Y, et al. Dysregulation of Immune Response in Patients With Coronavirus 2019 (COVID-19) in Wuhan, China. *Clin Infect Dis* (2020) 71(15):762–8. doi: 10.1093/cid/ciaa248
8. Laing AG, Lorenc A, Del Molino Del Barrio I, Das A, Fish M, Monin L, et al. A Dynamic COVID-19 Immune Signature Includes Associations With Poor Prognosis. *Nat Med* (2020) 26(10):1623–35. doi: 10.1038/s41591-020-1038-6
9. Chen G, Wu D, Guo W, Cao Y, Huang D, Wang H, et al. Clinical and Immunological Features of Severe and Moderate Coronavirus Disease 2019. *J Clin Invest* (2020) 130(5):2620–9. doi: 10.1172/JCI137244
10. Mathew D, Giles JR, Baxter AE, Oldridge DA, Greenplate AR, Wu JE, et al. Deep Immune Profiling of COVID-19 Patients Reveals Distinct Immunotypes With Therapeutic Implications. *Science* (2020) 369(6508):eabc8511. doi: 10.1126/science.abc8511
11. Logue JK, Franko NM, McCulloch DJ, McDonald D, Magedson A, Wolf CR, et al. Sequelae in Adults at 6 Months After COVID-19 Infection. *JAMA Netw Open* (2021) 4(2):e210830. doi: 10.1001/jamanetworkopen.2021.0830
12. Del Rio C, Collins LF, Malani P. Long-Term Health Consequences of COVID-19. *JAMA* (2020) 324(17):1723–4. doi: 10.1001/jama.2020.19719
13. Garrigues E, Janvier P, Kherabi Y, Le Bot A, Hamon A, Gouze H, et al. Post-Discharge Persistent Symptoms and Health-Related Quality of Life After Hospitalization for COVID-19. *J Infect* (2020) 81(6):e4–6. doi: 10.1016/j.jinf.2020.08.029
14. Stephen A, Shubhagata D, Sherry D, Valerie S, Sarah S. *XMAP Cookbook: A Collection of Methods and Protocols for Developing Multiplex Assays With xMAP Technolog*. Austin, editor. Austin: Corporation L. TX2018 (2014).
15. infection WWGotCCaMoC. A Minimal Common Outcome Measure Set for COVID-19 Clinical Research. *Lancet Infect Dis* (2020) 20(8):e192–e7. doi: 10.1016/S1473-3099(20)30483-7
16. Homey B, Wang W, Soto H, Buchanan ME, Wiesenborn A, Catron D, et al. Cutting Edge: The Orphan Chemokine Receptor G Protein-Coupled Receptor-2 (GPR-2, CCR10) Binds the Skin-Associated Chemokine CCL27 (CTACK/ALP/ILC). *J Immunol* (2000) 164(7):3465–70. doi: 10.4049/jimmunol.164.7.3465
17. Pan J, Kunkel EJ, Gosslar U, Lazarus N, Langdon P, Broadwell K, et al. A Novel Chemokine Ligand for CCR10 and CCR3 Expressed by Epithelial Cells in Mucosal Tissues. *J Immunol* (2000) 165(6):2943–9. doi: 10.4049/jimmunol.165.6.2943
18. Henn AD, Laski M, Yang H, Welle S, Qiu X, Miao H, et al. Functionally Distinct Subpopulations of CpG-Activated Memory B Cells. *Sci Rep* (2012) 2:345. doi: 10.1038/srep00345
19. Schultze JL, Aschenbrenner AC. COVID-19 and the Human Innate Immune System. *Cell* (2021) 184(7):1671–92. doi: 10.1016/j.cell.2021.02.029
20. Burel JG, Pomaznoy M, Lindestam Arlehamn CS, Weiskopf D, da Silva Antunes R, Jung Y, et al. Circulating T Cell-Monocyte Complexes are Markers of Immune Perturbations. *Elife* (2019) 8:e46045. doi: 10.7554/eLife.46045

21. Thein TL, Ang LW, Young BE, Chen MI, Leo YS, Lye DCB. Differentiating Coronavirus Disease 2019 (COVID-19) From Influenza and Dengue. *Sci Rep* (2021) 11(1):19713. doi: 10.1038/s41598-021-99027-z
22. Visca D, Ong CWM, Tiberi S, Centis R, D'Ambrosio L, Chen B, et al. Tuberculosis and COVID-19 Interaction: A Review of Biological, Clinical and Public Health Effects. *Pulmonology* (2021) 27(2):151–65. doi: 10.1016/j.pulmoe.2020.12.012
23. Cliff JM, Kaufmann SH, McShane H, van Helden P, O'Garra A. The Human Immune Response to Tuberculosis and Its Treatment: A View From the Blood. *Immunol Rev* (2015) 264(1):88–102. doi: 10.1111/imr.12269
24. Zheng W, Wu H, Liu C, Yan Q, Wang T, Wu P, et al. Identification of COVID-19 and Dengue Host Factor Interaction Networks Based on Integrative Bioinformatics Analyses. *Front Immunol* (2021) 12:707287. doi: 10.3389/fimmu.2021.707287
25. Rhodes JW, Tong O, Harman AN, Turville SG. Human Dendritic Cell Subsets, Ontogeny, and Impact on HIV Infection. *Front Immunol* (2019) 10:1088. doi: 10.3389/fimmu.2019.01088
26. van Leeuwen-Kerkhoff N, Lundberg K, Westers TM, Kordasti S, Bontkes HJ, de Gruijl TD, et al. Transcriptional Profiling Reveals Functional Dichotomy Between Human Slan. *J Leukoc Biol* (2017) 102(4):1055–68. doi: 10.1189/jlb.3MA0117-037R
27. Döbel T, Kunze A, Babatz J, Tränkner K, Ludwig A, Schmitz M, et al. Fcγriii (CD16) Equips Immature 6-Sulfo LacNAc-Expressing Dendritic Cells (slanDCs) With a Unique Capacity to Handle IgG-Complexed Antigens. *Blood* (2013) 121(18):3609–18. doi: 10.1182/blood-2012-08-447045
28. Villani AC, Satija R, Reynolds G, Sarkizova S, Shekhar K, Fletcher J, et al. Single-Cell RNA-Seq Reveals New Types of Human Blood Dendritic Cells, Monocytes, and Progenitors. *Science* (2017) 356(6335):eaah4573. doi: 10.1126/science.aah4573
29. Collin M, Bigley V. Human Dendritic Cell Subsets: An Update. *Immunology* (2018) 154(1):3–20. doi: 10.1111/imm.12888
30. Schäkel K, Kannagi R, Kniep B, Goto Y, Mitsuoka C, Zwirner J, et al. 6-Sulfo LacNAc, a Novel Carbohydrate Modification of PSGL-1, Defines an Inflammatory Type of Human Dendritic Cells. *Immunity* (2002) 17(3):289–301. doi: 10.1016/s1074-7613(02)00393-x
31. Gutiérrez-Bautista JF, Rodriguez-Nicolas A, Rosales-Castillo A, Jiménez P, Garrido F, Anderson P, et al. Negative Clinical Evolution in COVID-19 Patients Is Frequently Accompanied With an Increased Proportion of Undifferentiated Th Cells and a Strong Underrepresentation of the Th1 Subset. *Front Immunol* (2020) 11:596553. doi: 10.3389/fimmu.2020.596553
32. de Campos-Mata L, Tejedor Vaquero S, Tachó-Piñot R, Piñero J, Grasset EK, Arrieta Aldea I, et al. SARS-CoV-2 Sculpts the Immune System to Induce Sustained Virus-Specific Naïve-Like and Memory B-Cell Responses. *Clin Transl Immunol* (2021) 10(9):e1339. doi: 10.1002/cti2.1339
33. Su CM, Wang L, Yoo D. Activation of NF-κb and Induction of Proinflammatory Cytokine Expressions Mediated by ORF7a Protein of SARS-CoV-2. *Sci Rep* (2021) 11(1):13464. doi: 10.1038/s41598-021-92941-2
34. Khalil BA, Elemam NM, Maghazachi AA. Chemokines and Chemokine Receptors During COVID-19 Infection. *Comput Struct Biotechnol J* (2021) 19:976–88. doi: 10.1016/j.csbj.2021.01.034
35. Xu ZS, Shu T, Kang L, Wu D, Zhou X, Liao BW, et al. Temporal Profiling of Plasma Cytokines, Chemokines and Growth Factors From Mild, Severe and Fatal COVID-19 Patients. *Signal Transduct Target Ther* (2020) 5(1):100. doi: 10.1038/s41392-020-0211-1
36. Bouadma L, Wiedemann A, Patrier J, Surénaud M, Wicky PH, Foucat E, et al. Immune Alterations in a Patient With SARS-CoV-2-Related Acute Respiratory Distress Syndrome. *J Clin Immunol* (2020) 40(8):1082–92. doi: 10.1007/s10875-020-00839-x
37. Kong SL, Chui P, Lim B, Salto-Tellez M. Elucidating the Molecular Physiopathology of Acute Respiratory Distress Syndrome in Severe Acute Respiratory Syndrome Patients. *Virus Res* (2009) 145(2):260–9. doi: 10.1016/j.virusres.2009.07.014
38. Yan Y, Jiang X, Wang X, Liu B, Ding H, Jiang M, et al. CCL28 Mucosal Expression in SARS-CoV-2-Infected Patients With Diarrhea in Relation to Disease Severity. *J Infect* (2021) 82(1):e19–21. doi: 10.1016/j.jinf.2020.08.042
39. Wollina U, Karadağ AS, Rowland-Payne C, Chiriac A, Lotti T. Cutaneous Signs in COVID-19 Patients: A Review. *Dermatol Ther* (2020) 33(5):e13549. doi: 10.1111/dth.13549
40. Menezes SM, Decanine D, Brassat D, Khouri R, Schnitman SV, Kruschewsky R, et al. CD80+ and CD86+ B Cells as Biomarkers and Possible Therapeutic Targets in HTLV-1 Associated Myelopathy/Tropical Spastic Paraparesis and Multiple Sclerosis. *J Neuroinflamm* (2014) 11:18. doi: 10.1186/1742-2094-11-18
41. Huang Y, Wei B, Gao X, Deng Y, Wu W. Expression of CD80 and CD86 on B Cells During Coxsackievirus B3-Induced Acute Myocarditis. *Cent Eur J Immunol* (2019) 44(4):364–9. doi: 10.5114/ceji.2019.92786
42. Suvas S, Singh V, Sahdev S, Vohra H, Agrewala JN. Distinct Role of CD80 and CD86 in the Regulation of the Activation of B Cell and B Cell Lymphoma. *J Biol Chem* (2002) 277(10):7766–75. doi: 10.1074/jbc.M105902200
43. Wang JH, Wu Q, Yang P, Li H, Li J, Mountz JD, et al. Type I Interferon-Dependent CD86(high) Marginal Zone Precursor B Cells Are Potent T Cell Costimulators in Mice. *Arthritis Rheum* (2011) 63(4):1054–64. doi: 10.1002/art.30231
44. Wildner NH, Ahmadi P, Schulte S, Brauneck F, Kohsar M, Lütgehetmann M, et al. B Cell Analysis in SARS-CoV-2 Versus Malaria: Increased Frequencies of Plasmablasts and Atypical Memory B Cells in COVID-19. *J Leukoc Biol* (2021) 109(1):77–90. doi: 10.1002/JLB.5COVA0620-370RR
45. Thibult ML, Mamessier E, Gertner-Dardenne J, Pastor S, Just-Landi S, Xerri L, et al. PD-1 is a Novel Regulator of Human B-Cell Activation. *Int Immunol* (2013) 25(2):129–37. doi: 10.1093/intimm/dxs098
46. Beaudoin-Bussières G, Laumaea A, Anand SP, Prévost J, Gasser R, Goyette G, et al. Decline of Humoral Responses Against SARS-CoV-2 Spike in Convalescent Individuals. *mBio* (2020) 11(5):e02590–20. doi: 10.1128/mBio.02590-20
47. Long QX, Liu BZ, Deng HJ, Wu GC, Deng K, Chen YK, et al. Antibody Responses to SARS-CoV-2 in Patients With COVID-19. *Nat Med* (2020) 26(6):845–8. doi: 10.1038/s41591-020-0897-1
48. Ogega CO, Skinner NE, Blair PW, Park HS, Littlefield K, Ganesan A, et al. Durable SARS-CoV-2 B Cell Immunity After Mild or Severe Disease. *medRxiv* (2020) 10.28.20220996. doi: 10.1101/2020.10.28.20220996
49. Denton AE, Linterman MA. Stromal Networking: Cellular Connections in the Germinal Centre. *Curr Opin Immunol* (2017) 45:103–11. doi: 10.1016/j.coi.2017.03.001
50. Oropallo MA, Cerutti A. Germinal Center Reaction: Antigen Affinity and Presentation Explain it All. *Trends Immunol* (2014) 35(7):287–9. doi: 10.1016/j.it.2014.06.001
51. Li X, Zhang Q, Zhang W, Ye G, Ma Y, Wen C, et al. Expanded Circulating Follicular Dendritic Cells Facilitate Immune Responses in Chronic HBV Infection. *J Transl Med* (2020) 18(1):417. doi: 10.1186/s12967-020-02584-6
52. Good-Jacobson KL, Szumilas CG, Chen L, Sharpe AH, Tomayko MM, Shlomchik MJ. PD-1 Regulates Germinal Center B Cell Survival and the Formation and Affinity of Long-Lived Plasma Cells. *Nat Immunol* (2010) 11(6):535–42. doi: 10.1038/ni.1877
53. Juno JA, Tan HX, Lee WS, Reynaldi A, Kelly HG, Wragg K, et al. Humoral and Circulating Follicular Helper T Cell Responses in Recovered Patients With COVID-19. *Nat Med* (2020) 26(9):1428–34. doi: 10.1038/s41591-020-0995-0
54. Gong F, Dai Y, Zheng T, Cheng L, Zhao D, Wang H, et al. Peripheral CD4+ T Cell Subsets and Antibody Response in COVID-19 Convalescent Individuals. *J Clin Invest* (2020) 130(12):6588–99. doi: 10.1172/JCI141054
55. Ni L, Ye F, Cheng ML, Feng Y, Deng YQ, Zhao H, et al. Detection of SARS-CoV-2-Specific Humoral and Cellular Immunity in COVID-19 Convalescent Individuals. *Immunity* (2020) 52(6):971–7.e3. doi: 10.1016/j.immuni.2020.04.023
56. Long Y, Zhao X, Liu C, Xia C. Activated Inducible Co-Stimulator-Positive Programmed Cell Death 1-Positive Follicular Helper T Cells Indicate Disease Activity and Severity in Ulcerative Colitis Patients. *Clin Exp Immunol* (2020) 202(1):106–18. doi: 10.1111/cei.13485
57. Fan X, Jin T, Zhao S, Liu C, Han J, Jiang X, et al. Circulating CCR7+ICOS+ Memory T Follicular Helper Cells in Patients With Multiple Sclerosis. *PloS One* (2015) 10(7):e0134523. doi: 10.1371/journal.pone.0134523
58. Kim JW, Lee J, Hong SM, Cho ML, Park SH. Circulating CCR7loPD-1hi Follicular Helper T Cells Indicate Disease Activity and Glandular Inflammation in Patients With Primary Sjögren's Syndrome. *Immune Netw* (2019) 19(4):e26. doi: 10.4110/in.2019.19.e26

59. Zhang J, Wu Q, Liu Z, Wang Q, Wu J, Hu Y, et al. Spike-Specific Circulating T Follicular Helper Cell and Cross-Neutralizing Antibody Responses in COVID-19-Convalescent Individuals. *Nat Microbiol* (2021) 6(1):51–8. doi: 10.1038/s41564-020-00824-5
60. De Giorgi V, West KA, Henning AN, Chen LN, Holbrook MR, Gross R, et al. Naturally Acquired SARS-CoV-2 Immunity Persists for Up to 11 Months Following Infection. *J Infect Dis* (2021) 224(8):1294–304. doi: 10.1093/infdis/jiab295
61. Glöckner S, Hornung F, Baier M, Weis S, Pletz MW, Deinhardt-Emmer S, et al. Robust Neutralizing Antibody Levels Detected After Either SARS-CoV-2 Vaccination or One Year After Infection. *Viruses* (2021) 13(10):2003. doi: 10.3390/v13102003
62. Sakharkar M, Rappazzo CG, Wieland-Alter WF, Hsieh CL, Wrapp D, Esterman ES, et al. Prolonged Evolution of the Human B Cell Response to SARS-CoV-2 Infection. *Sci Immunol* (2021) 6(56):eabg6916. doi: 10.1126/sciimmunol.abg6916
63. Kaneko N, Kuo HH, Boucau J, Farmer JR, Allard-Chamard H, Mahajan VS, et al. Loss of Bcl-6-Expressing T Follicular Helper Cells and Germinal Centers in COVID-19. *Cell* (2020) 183(1):143–57.e13. doi: 10.1016/j.cell.2020.08.025
64. Duan YQ, Xia MH, Ren L, Zhang YF, Ao QL, Xu SP, et al. Deficiency of Tfh Cells and Germinal Center in Deceased COVID-19 Patients. *Curr Med Sci* (2020) 40(4):618–24. doi: 10.1007/s11596-020-2225-x
65. Gallais F, Gantner P, Bruel T, Velay A, Planas D, Wendling MJ, et al. Evolution of Antibody Responses Up to 13 Months After SARS-CoV-2 Infection and Risk of Reinfection. *EBioMedicine* (2021) 71:103561. doi: 10.1016/j.ebiom.2021.103561
66. Dobaño C, Ramírez-Morros A, Alonso S, Vidal-Alaball J, Ruiz-Olalla G, Vidal M, et al. Persistence and Baseline Determinants of Seropositivity and Reinfection Rates in Health Care Workers Up to 12.5 Months After COVID-19. *BMC Med* (2021) 19(1):155. doi: 10.1186/s12916-021-02032-2

**Conflict of Interest:** The authors declare that the research was conducted in the absence of any commercial or financial relationships that could be construed as a potential conflict of interest.

frontiers in Immunology

REVIEW
published: 12 January 2022
doi: 10.3389/fimmu.2021.825813

# Generation of High Quality Memory B Cells

*Takeshi Inoue*[1]*, *Ryo Shinnakasu*[1] and *Tomohiro Kurosaki*[1,2,3]*

[1] Laboratory of Lymphocyte Differentiation, WPI Immunology Frontier Research Center, Osaka University, Osaka, Japan, [2] Center for Infectious Diseases Education and Research, Osaka University, Osaka, Japan, [3] Laboratory for Lymphocyte Differentiation, RIKEN Center for Integrative Medical Sciences, Kanagawa, Japan

Protection against pathogen re-infection is mediated, in large part, by two humoral cellular compartments, namely, long-lived plasma cells and memory B cells. Recent data have reinforced the importance of memory B cells, particularly in response to re-infection of different viral subtypes or in response with viral escape mutants. In regard to memory B cell generation, considerable advancements have been made in recent years in elucidating its basic mechanism, which seems to well explain why the memory B cells pool can deal with variant viruses. Despite such progress, efforts to develop vaccines that induce broadly protective memory B cells to fight against rapidly mutating pathogens such as influenza virus and HIV have not yet been successful. Here, we discuss recent advances regarding the key signals and factors regulating germinal center-derived memory B cell development and activation and highlight the challenges for successful vaccine development.

**Keywords: memory B cell, germinal center, vaccine, broadly neutralizing antibody, BCR affinity**

OPEN ACCESS

***Edited by:***
*Jieun Oh,*
*Korea Advanced Institute of Science and Technology, South Korea*

***Reviewed by:***
*Kim Good-Jacobson,*
*Monash University, Australia*
*Masato Kubo,*
*Tokyo University of Science, Japan*

***Correspondence:**
*Takeshi Inoue*
*inoue@ifrec.osaka-u.ac.jp*
*Tomohiro Kurosaki*
*kurosaki@ifrec.osaka-u.ac.jp*

***Specialty section:***
*This article was submitted to Immunological Memory, a section of the journal Frontiers in Immunology*

***Received:*** *30 November 2021*
***Accepted:*** *23 December 2021*
***Published:*** *12 January 2022*

***Citation:***
*Inoue T, Shinnakasu R and Kurosaki T (2022) Generation of High Quality Memory B Cells. Front. Immunol. 12:825813. doi: 10.3389/fimmu.2021.825813*

## INTRODUCTION

Humoral immunological memory, the basis of antibody (Ab)-based vaccination, is critical for protection against pathogen re-infection, which is largely mediated by two cellular compartments, long-lived plasma cells and memory B cells. Early memory B cells emerge after the initial immunization are primarily composed of IgM-expressing B cells harboring a small number of somatic hypermutation (SHM), whereas subsequent memory B cell development occurs in the germinal center (GC), the primary site in which iterative rounds of SHM and subsequent selection of affinity-matured B cell clones take place (1–3).

Since long-lived plasma cells are producing highly-selected and high affinity Abs for the primary antigen, such pre-existing Abs act as a first line of defense against reinfection by homologous pathogens. On the other hand, selection for memory B cells is less stringent, therefore, it has been predicted that memory B cells rather participate in defense against challenge by related pathogens or variant pathogens that escape the long-lived plasma cell-mediated defense. Indeed, memory B cells have been found to be differentiated from lower affinity precursor GC B cells, in contrast to long lived plasma cells, which arise from highly selected and high affinity cells (4–7). This probably allows memory B cells to maintain flexibility in their responsiveness to variant and related antigens. Recently, the above prediction has been directly proven. First, studies using mouse infection models (West Nile and influenza viruses) have provided clear evidence for involvement of memory B cells

in heterosubtypic immunity, i.e., cross-protection to a different viral serotype than the ones in the primary infection (8, 9). Second, in the case of pandemic 2009 H1N1 influenza vaccination, individuals who had low levels of pre-existing Abs to this novel vaccine could generate broadly reactive Abs from memory B cells (10).

Given such importance of memory B cells, a vaccination strategy involving iterative exposure to cross-reactive viral antigens has been designed to elicit broadly reactive memory B cells capable of mediating heterosubtypic immunity against mutating pathogens. However, in the case of influenza vaccination, its potential efficacy seems to be limited by the inefficiency with which memory B cells enter the GC. For instance, in the case of homotypic re-challenge, the secondary GC response is largely derived from naïve, and not from memory B cells. This is likely one of the major reasons why vaccines against influenza viruses have not yet been highly successful. In this review, we first discuss recent advances in our understanding of how GC responses take place and generate memory B cells. Furthermore, mainly emphasizing the influenza system, we discuss how broadly protective memory B cells are generated, here particularly focusing on anti-stem Abs, why they cannot be efficiently induced by the current vaccination method, and the potential way to overcome these obstacles. Although we briefly touch upon pre-GC processes, more thorough reviews of these topics are available elsewhere (11, 12). Likewise, differentiation of GC B cells to plasma cells has been extensively reviewed in recent years (3, 13) and is beyond the scope of this article.

## GC RESPONSES

A major challenge in understanding humoral immunity is to decipher how affinity maturation takes place during responses to infections or vaccine antigens. While the emphasis on GC studies has long been to understand how they support maturation towards the highest affinity Abs, recent new findings have made us realize that these GC responses also maintain a diverse population of antigen-specific B cells. Thus, affinity maturation does not necessarily involve radical loss of diversity (2). This point is particularly important from the viewpoint of development of broadly protective memory B cells during the GC reaction. Hence, we first discuss positive selection of high-affinity GC B cells, clonal diversity in the GC and memory B cell differentiation mechanisms, mainly by using model antigens.

### Positive Selection of High-Affinity GC B Cells

Before entering the GC, activated B cells compete for follicular helper T (Tfh) cell help at the T-B border based on the amount of peptide-MHC class II (MHC-II) presented by the B cells to the Tfh cells. Hence, the success of B cells competing for early Tfh help depends on their frequency and their B cell receptor (BCR) affinity for antigens (14–17). Rare B cells, such as broadly neutralizing antibody (bnAb) precursor B cells with low affinity (18), may be excluded from entering the GC at this early Tfh cell checkpoint.

After the B cells join the GC reaction, inter-clonal (between clones with different V(D)J rearrangements harboring variable epitope specificities and affinities) as well as intra-clonal (between SHM variants originating from the same clone) competition begins to take place. Previous model hapten studies showed that hapten-driven GCs tend to become more clonally homogeneous over time and reflect only the intra-clonal competition; variable-sized expansions of particular SHM variants of the one particular B cell clone (2).

A fundamental characteristic of the GC reaction is that GC B cells constantly migrate between microanatomical compartments (**Figure 1**). The GC is classically defined as the

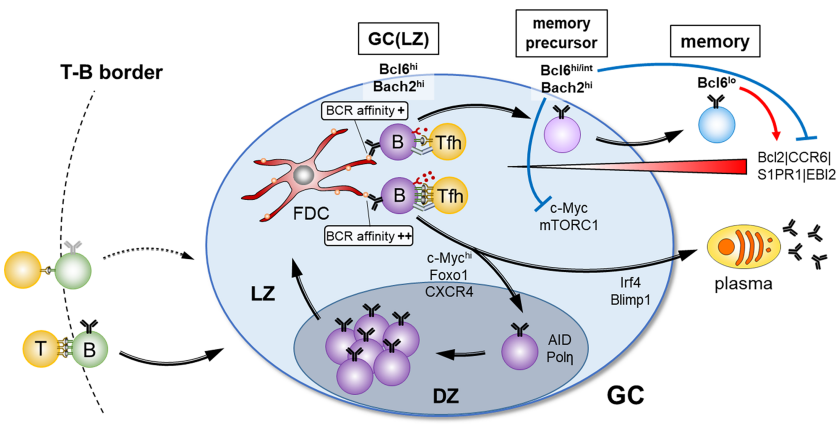


**FIGURE 1** | Overview of the GC selection and the factors for memory B cell fate. After antigen-activated B- and T cell contact at the T-B border in secondary lymphoid organs, B cells enter into GC reaction. Clonal expansion and BCR diversification occur in the DZ, and affinity selection for the fate decision of B cell differentiation through interaction with FDCs and Tfh cells takes place in the LZ. Strong T cell help due to high BCR affinity determines the plasma cell fate or the reentry to the DZ, whereas weak T cell help due to low BCR affinity favors memory B cell fate. Suppression of mTORC1 activity and c-Myc expression mediated by high Bach2 expression, and a provision of survival signals mediated by down-regulation of Bcl6 are the key drivers for GC B cells to adopt a memory B cell fate.

dark zone (DZ) and light zone (LZ). SHM and subsequent cellular selection occur in the DZ and the LZ, respectively. The DZ consists primarily of highly proliferating B cells, expressing high levels of AID and error-prone DNA polymerase η, while the LZ is composed of GC B cells, follicular dendritic cells (FDCs), and Tfh cells. Intravital photoactivation experiments revealed that although the LZ is constantly being repopulated by massive immigration from the DZ, at a rate of 50% of DZ cells transitioning to the LZ over a period of 4 hrs, less than 10% of LZ cells return to the DZ over a period of 6 hrs (19). Overall, in contrast to the DZ to LZ transition, the LZ to DZ transition is a highly selective process; only about 10% of B cells that arrive to the LZ are selected to re-enter the DZ. A small population of the LZ exits the GC as memory B cells and plasma cells, and the majority of the remaining cells die by apoptosis. Thus, how these re-entering cells are positively selected is one of the key points for affinity maturation. B cells with damaged BCRs undergo apoptosis in the DZ and cells failing to receive sufficient helper signals in the LZ are also thought to undergo cell death (discussed in detail below). The overall rate of cell death is such that up to half of all GC B cells die every 6 hrs, suggesting that GC B cells possess specific systems for provision of high proliferation together with high apoptotic capabilities (20). Of note, a recent study defined an additional group of proliferating DZ cells enriched for G2/M phases of the cell cycle as gray zone GC B cells (21).

In regard to antigen-based signals involved in affinity maturation, the LZ GC B cells are well-equipped with two sensing systems; one is through the BCR and the other is delivered by cognate interaction with Tfh cells. The BCR recognizes antigen, which is displayed on FDCs as antigen-Ab complexes, through their binding to FcγRII and complement receptor 2 on FDCs. The BCR recognizes the antigen on FDCs and acts as a signal-transducing receptor as well as an endocytic receptor. Therefore, GC B cells utilize the BCR to retrieve antigen in an affinity-dependent manner, and present processed peptides/MHC-II complexes to Tfh cells, thus providing a mechanism by which Tfh cells can indirectly sense BCR affinity (2). Then, Tfh cells provide T cell help, mainly CD40 and IL-4/IL-21 cytokine signals, to cognate GC B cells. Indeed, recent studies suggested that progressive differentiation of Tfh cells regulate the GC response through IL-4 and IL-21 secretion, and Tfh-derived IL-4 plays a critical role in the expansion of rare broadly neutralizing GC B cell clone (22, 23). Thus, the importance of Tfh cell help in GC B cell selection is clear, but it is not the only factor. GC B cells with MHC-II haplo-insufficiency compete equivalently to wild type cells under conditions of physiological antigen concentration (16). Thus, both BCR signaling and Tfh cell help signals appear to be integrated in GC B cells to determine survival and proliferation (24). Different from naïve B cells, in the case of GC B cells, CD40L-CD40 engagement triggers NF-κB, and BCR antigen signaling engages PI3K signaling (25).

Antigen-loaded B cells in the LZ begin to achieve clonal dominance through accelerated cell division and increased biomass accumulation, which are c-Myc and mTORC1-dependent, respectively (26). For cell division, the strength of the Tfh cell signal delivered in the LZ is directly proportional to the levels of c-Myc and this then dictates the number of cell divisions that occur in the DZ, supporting the previously proposed "timer model" to explain how many times DZ GC B cell could proliferate (27). In addition, a recent study has demonstrated that cyclin D3 plays a specialized role in the GC cell cycle transition from G1- to S-phase (28).

## Clonal Diversity in the GC

As described above, previous studies using hapten-immunization showed that the Ab responses are strongly focused on the hapten and heavily dominated by stereotypical V genes (2, 29, 30). Apart from this occasion, in the case of viral infection and vaccination, many clones with distinct V(D)J rearrangements participate initially and competition occurs among B cells derived from various clones, too.

Two studies aimed to circumvent this hapten-related issue by applying technologies that allow examination of the more diverse GC responses to un-haptenated protein antigens (31, 32). Although it was previously thought that only one or a few clones participate in one GC, as demonstrated by employing hapten conjugates, these new studies showed that tens-hundreds of clones participate in one GC at the early phase. Among several GCs formed after protein-immunization, rapid and massive expansion of specific higher-affinity SHM variants, as observed in the hapten model, leads to substantial loss of diversity in a subset of GCs, while other GCs in the same lymphoid tissue continue the affinity maturation process and still retain substantial clonal diversity. Since individual GCs are spatially separated, this model explains how GCs support a diversity of antigen-specific clones against complex protein antigens (20). Other mechanisms can be also envisaged. For instance, clonal diversity may be promoted by antibody-mediated feedback (33–35), as dominant GC clones with BCRs specific for a particular antigen epitope give rise to plasma cells that secrete Ab. This Ab then masks its own epitope, thereafter halting proliferation of the already expanded clone, while enhancing the selection of other clones that bind to different epitopes (**Figure 2**). Further investigation of the mechanisms allowing sustained diversity in GCs is important as they have wide implications, for example in the context of efforts to generate bnAb responses by iterative immunization.

## Differentiation of GC B Cells Into Memory B Cells

An early study in which transgenic overexpression of the anti-apoptotic factor Bcl2 resulted in a marked increase of low affinity B cells in both GC and memory compartments without impairing the selection of high affinity plasma cells (36), suggested that the differentiation of GC B cells to memory B cells is a default process. However, this notion has been challenged by recent studies employing mono-epitope hapten or HEL antigens, which provided evidence for the existence of instructive regulations in memory B cell selection from the GC

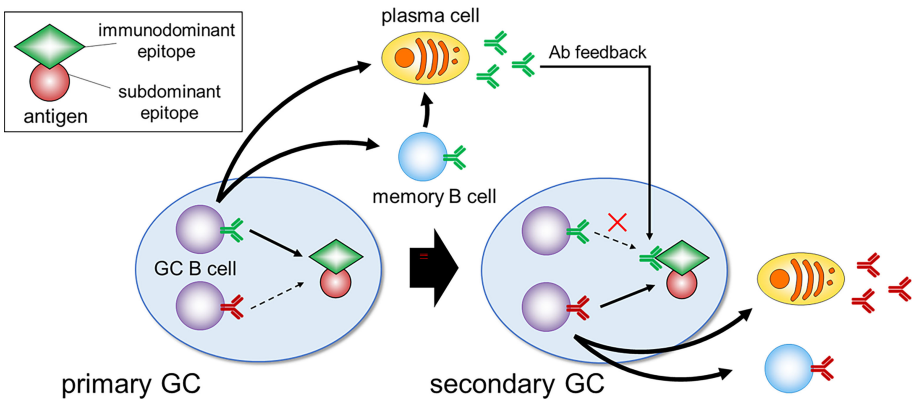


**FIGURE 2** | Immunodominance and Ab feedback. In the primary GC, B cell clones specific for the immunodominant epitopes dominate and give rise to plasma cells that secrete Ab. During the secondary GC response, this Ab masks its own epitope, which can suppress the expansion of immunodominant clones and enhance the selection of clones specific for less accessible subdominant epitopes.

compartment (4, 6). First, contemporaneous comparison of memory and GC B cells indicates that the memory B cell pool arises predominantly from the low affinity cells. Second, consistent with another study (5), the memory B cell pool is generated early during an immune response. Considering that affinity maturation in the GC is still continuing after stopping memory cell generation, this would also contribute to the observed accumulation of overall less SHM and the preponderance of low affinity B cells in the memory B cell compartment in the case of mono-epitope antigen. A recent study employing poly-epitope protein antigens has also reinforced these conclusions, except that in this case the memory B cells are generated throughout the immune response (7). A probable explanation for this difference is that, unlike mono-epitope systems, in the case of a poly-epitope system, some clones keep expanding in the late GC reaction, thereby also generating memory B cells at later time point. Furthermore, this study showed that, like in the case of flavivirus-specific memory B cell generation (37), B cells with low affinity germline BCRs are prone to be selected into memory B cells. Given that the germline BCR of bnAbs usually has very low affinity for the native antigens of influenza virus, this may be one of the reasons why broadly reactive clones against influenza virus can exist in the memory fraction (38).

The question then arises of what is the molecular nature of the above instruction program for memory B cell generation. In contrast to plasma cell precursors, memory B cell precursors within the GC are no longer cycling (6, 39, 40). In addition, these memory precursors reside at the edge of the LZ (41). Thus, at least, three inter-connected processes seem to be required for the transition from GC to memory B cells; i) stopping proliferation in the DZ; ii) returning to the LZ and being in the process of exiting the GC; iii) entering the quiescent (G0) stage with acquisition of survival signals.

As mentioned above, once positively selected GC B cells possessing high levels of c-Myc expression and mTORC1 activity reenter the DZ, they start proliferation, accompanied by a stepwise decline of the level of c-Myc and active mTORC1, depending upon their proliferation numbers. Trafficking back to the LZ requires decay of both mTORC1 activity and c-Myc expression. Since rapamycin treatment downregulates Foxo1 expression (26), decay of mTORC1 activity is likely to downregulate CXCR4, thereby promoting the return from the DZ to the LZ. After their return to the LZ, memory B cell precursors should maintain high Bach2 expression, because of receiving low T cell help, and dampen mTORC1 activity and c-Myc expression, which is thought to be one of the mandatory steps for transition to memory B cells (**Figure 1**). In support of this, Bach2-deficient GC B cells manifested constitutively active mTORC1 and c-Myc expression, thereby resulting in hyper-proliferation, and subsequent inability to generate memory B cells (40). Conversely, impairment of the interaction of c-Myc and MIZ1 skewed the system towards memory B cell generation (42). c-Myc and MIZ1 form a transcriptional repressor complex for MIZ1 target genes, such as cell cycle inhibitors. The absence of the c-Myc-MIZ1 interaction releases this repression, resulting in impaired cell cycle entry of positively selected GC B cells, supporting the notion that the inhibition of the c-Myc activity contributes to memory B cell generation.

The above anti-proliferative activity is required but appears not to be sufficient for development of memory B cells. Since low-affinity B cells receive low T cell help, it has been previously thought that these GC B cells undergo apoptosis. Therefore, the question arose of how such memory precursor cells with low affinity are prevented from dying and are able to differentiate into mature memory B cells. A recent detailed GC B cell analysis of Bcl2 transgenic mice provided us a hint to answer this question. In these mice, aberrant populations of seemingly quiescent cells arise that express markers of memory precursor cells ($CD38^+$ and $CCR6^+$) (43). Hence, we speculated that, in physiological settings, initiation of Bcl2 up-regulation might take place in these precursor cells, thereby giving them a survival advantage. This idea was directly tested, demonstrating that it is indeed the case (40). Then, in regard to how to initiate Bcl2 expression, we

considered that differentiation of GC B cells to memory B cells to a large extent involves reversion to the gene expression profile they possessed prior to differentiation into GC B cells. This includes re-expression of genes, *Ccr6*, *Gpr183* (EBI2), *S1pr1*, and *Bcl2*, each of which is known to be directly repressed by Bcl6 (44–46). Given that *Il21* knockout mice showed down-regulated Bcl6 in GC B cells (47), it is likely that memory precursor cells limit access to IL-21, which, in turn, begins the process of down-regulation of Bcl6. Consequently, Bcl2 is up-regulated, thereby providing survival signals. This Bcl6 down-regulation is further augmented by a recently identified transcription factor Hhex during the maturation processes in GC-mediated memory B cells (48). Hence, we would propose the existence of two key drivers for differentiation of GC B cells to memory cells; one is high expression of Bach2, antagonizing the c-Myc and mTORC1 pathways, and the second is down-regulation of Bcl6, releasing its repression of Bcl2 and providing survival signals. Importantly, this model seems to well explain why memory precursor cells, despite receiving low T cell help, acquire the survival signal (**Figure 1**).

## GENERATION OF BROADLY-NEUTRALIZING MEMORY B CELLS AND THEIR RECALL

Recent discoveries of bnAbs for HIV and influenza virus have provided new outlooks in the vaccine field and highlighted the need to understand how such bnAb precursors enter the GCs, thereafter, creating memory B cells expressing high quality bnAbs (18).

Abs against the influenza virus surface glycoprotein hemagglutinin (HA) are a key correlate of protection (49). HA is composed of head- and stem-regions; in contrast to the structural changes in the head-region by antigenic drift and shift, the stem-region is well conserved, thereby making it a good target for generating cross-reactive bnAbs. However, in normal immune settings, most Abs are generated against the HA head-region, because of its immune dominance, while the stem-region acts as an immune subdominant epitope. Three potential mechanisms are thought to explain the subdominance of the stem Ab response (18, 50, 51). First, most of the germline BCRs of the stem Abs have very low affinity for the native antigen. Second, overlapping with the first possibility, these Abs have limited access to the stem epitope due to a steric hindrance. Finally, many of the stem Abs are polyreactive towards dsDNA, LPS, and insulin, potentially having inherent self-reactivity (52).

Nevertheless, it was observed that, upon vaccination with a novel influenza virus, the 2009 pandemic H1N1, some, but not all individuals generated broadly reactive HA stem-binding Abs (10, 53). Considering that almost all the induced anti-stem plasmablasts were mutated, these data indicate that, prior to vaccination, anti-stem memory B cells existed in individuals already exposed to previous infection of other types of influenza viruses, and that these memory B cells got activated after novel pandemic H1N1 vaccination. The conclusions from human vaccination data are further strengthened by a mouse infection model (9). Infection of naïve mice with H1N1 Narita strain influenza virus generated anti-stem memory B cells, but very low levels of anti-stem Abs, reflecting the long-lived plasma cell compartment, indicating a relative enrichment of anti-stem clones in the memory B cell rather than long-lived plasma cell compartment. Then, upon secondary infection with a drifted virus (H1N1 PR8 strain), such anti-stem memory B cells were promptly activated and differentiated to plasmablasts, thereby contributing to protection against PR8 virus infection. Furthermore, single cell Ab analysis showed that these anti-stem memory B cells are generated through GC reactions during primary Narita virus infection, thereby manifesting affinity-maturation and breadth at least to some extent. Thus, it is important to understand how GC-experienced (mature mutated) anti-stem memory B cells can be generated in naïve and recall conditions.

### Generation of Anti-Stem Memory B Cells Under Naïve Conditions

In the naïve state, the key to generating mature influenza anti-stem bnAb memory B cells depend upon several aspects; recruitment of appropriate naïve precursors into the GC; positive selection of appropriate clones during the GC reaction; exiting from the GC as long-lived memory B cells. Considering that, during the GC processes, selection into memory B cells is less stringent than that for long-lived plasma cells, major hurdles seem to be the GC recruitment of rare anti-stem bnAb precursors and the duration of rare bnAb B cells in the GC.

In regard to the recruitment to the GCs, difficulties are due to; i) a very low affinity of the naïve anti-stem precursors for the native HA antigen; ii) the subsequent problem in receiving sufficient T cell help; iii) the possibly anergic state of these precursor B cells because of poly-reactivity (54). In regard to problem iii), studies using the model antigen HEL system provided significant insight into how we can awaken such anergic B cells (55, 56). The key to activating anergic B cells is applying particulate type immunogens decorated with high densities of a closely related foreign and higher affinity antigen. In regard to point i), in the HIV case, it was shown that the quantity and affinity of the precursor naïve B cells are important for their entry into the GC. In addition, multimerization of antigen increased GC recruitment of rare naïve precursors by 200- to 500-fold compared to the equivalent monomeric antigen (15). Hence, like the immunogen in the HIV case, designing immunogen variants with higher affinity for rare anti-stem precursor Ab and their multimerization is one way to overcome points i) and iii).

How can we tackle point ii)? Indeed, several HIV human cohort data indicated the positive association between Tfh cells and anti-HIV bnAbs; frequencies of PD-1$^{+}$CXCR3$^{-}$CXCR5$^{+}$, or PD-1$^{lo}$CXCR3$^{+}$CXCR5$^{+}$ CD4 T cells correlated with HIV neutralization breadth (57, 58). This raised the question of whether this is a simple correlation or a causal association.

This issue has been approached in the mouse by employing BCR (VRC01 germline version) knock-in B cells and transgenic TCR T cells (59). Since, in the case of influenza and HIV bnAb responses, immunodominance is one of the key issues, this study was particularly designed to address whether increasing accessibility to T cell help preferentially enhances the rare immune-subdominant bnAb precursor B cell responses. GC occupancy by rare bnAb precursor VRC01 B cells was improved by increasing the quantity of HIV Env-specific CD4 T cells, even in the presence of the endogenous immunodominant B cell precursors. Moreover, the action point of this T cell help seems to be on the recruitment of VRC01 B cells into GCs. Because this study utilized modified high affinity antigen for bnAb precursor B cells ($K_D$ value of ~ 0.1 μM), it was concluded that, as long as high affinity antigen for bnAb precursor B cells is used, a high quantity of T cell help can promote recruitment of these rare B cells into GCs. However, it remains to be addressed what increasing T cell help does in conditions of weaker affinity antigen for bnAb precursors. Insufficient T cell help is also likely to occur in the case of influenza anti-stem bnAb precursor B cell responses. In fact, in mice, when employing only the stem region as an antigen, recruitment of polyclonal anti-stem B cells into the GC was very rare, whereas conjugation of this antigen to KLH, which contains strong T cell epitopes, resulted in better recruitment into the GC (60). Thus, conjugation of appropriate T cell epitopes to a B cell antigen is worth considering. In addition to antigen, development of good adjuvants for inducing Tfh cells is also important. Indeed, lipid nanoparticles used for mRNA vaccines have recently been shown to facilitate Tfh cell generation, presumably through enhancing IL-6 production (37).

Given that it takes years for bnAbs to emerge during infection (61), generation of rare high quality bnAb-producing clones may require prolonged GC responses, which may simply reflect the need for many rounds of SHM (3). Alternatively, it is also possible that prolonged GCs include more clonally permissive B cells over time. As discussed above, limited Tfh cell help or epitope-masking by generated Abs may be redirected towards B cell clones that bind non-dominant epitopes. In addition, changing Tfh cell clones during GC responses also may contribute to such redirection towards different B cell clones. For maintaining GC responses, as proposed in the HIV vaccination system, slow continuous delivery of native antigen might be one approach (62). This delivery method directed the response away from non-neutralizing Abs, which were dominantly present on degraded HIV Env trimers, instead towards a neutralizing Ab response. This method, in addition to continuous provision of antigen, provides more of it in native conformational form, therefore causing the observed biological effects. In the case of influenza vaccination, recently developed oil-in-water adjuvant (AS03) might utilize similar mechanisms, thereby increasing cross-reactive anti-influenza Ab responses (52, 63). This oil-in-water adjuvant functions to emulsify viral antigens within the adjuvant, which may protect them from degradation and may allow for the delivery of native antigens to lymph nodes. Collectively, delivery of antigen in its native form seems to be one of the important factors for maintaining GC reactions.

## Behavior of Anti-Stem B Cells During Recall Responses

Between yearly vaccination and seasonal infection, individuals repeatedly mount an immune response against the influenza virus. Hence, it is important to understand how such immune history, formed by previous infection/vaccination, affects the *de novo* immune response induced by the current vaccine. Mouse studies traced the fate of HA-induced memory B cells after repeated immunization with the same antigen and demonstrated that more than 90% of B cells in the secondary GCs have no prior GC experience; many of them are likely derived from naïve B cells (64). Thus, memory B cell reentry into GCs is rare upon repeated vaccination with the same antigen.

Then, the question became, what is the outcome when a variant of the original antigen was used for the second immunization, a situation similar to what occurs with annual influenza vaccination. By using fine-needle aspiration for obtaining human immune cells from lymph nodes, GCs were analyzed from people immunized with the 2018-2019 influenza seasonal vaccine (65). This analysis revealed that some of the GC B cell repertoire was shared with that of the *de novo* generated plasmablasts. This suggests that memory B cells, formed in response to a different earlier influenza strain, proliferated in response to the 2018-2019 vaccine, probably corresponding to a new influenza strain to these individuals, and that the progeny cells became plasmablasts or entered the GCs. In contrast, the GC B cells that did not share the Ab repertoire with plasmablasts were likely derived from naïve B cells. Importantly, the BCR repertoire from the memory-derived GC cells was directed toward cross-reactive epitopes, whereas those from naïve-derived GC cells were strain-specific. Although it remains to be determined whether cross-reactive and/or strain-specific GC B cells joined the long-lived memory B cell compartment, these human data suggest the encouraging possibility that once memory B cells with bnAb are generated, they can be recruited to secondary GCs. These 2018-2019 vaccination data appear to be consistent with the aforementioned 2009 pandemic H1N1 vaccination cohort data indicating that pre-existing anti-stem memory B cells are activated by vaccination with a novel type of influenza virus (10). However, a previous longitudinal study after vaccination with a current influenza revealed no overall increase in SHM in memory B cells over time (66), suggesting either that, despite entering the GCs, the entry efficiency is low, or that the step from GC to memory B cells is limiting.

In regard to entering the GC, one key difference between mouse and human data described above is vaccination with the same or variant antigens, suggesting that the extent the second antigen differs from the first is one of the key factors that dictates which B cells are recalled by influenza vaccination and recruited into the secondary GCs. Below we will discuss the potential mechanisms.

It was previously thought that memory B cells have higher affinity and are present at higher frequencies than naïve B cells

specific for the same antigen. However, given the current view that memory B cells possess a more diverse range of affinities, it is possible that the numbers of memory B cells with higher affinities than naïve B cells might be smaller than expected. In addition, several functionally distinct memory B cell subsets are generated, among which the $CD80^{+}CD273^{+}$ subset is more prone to differentiate into plasmablasts rather than enter the GC (67–69). Thus, the actual numbers of memory B cells that are competent for entering the GC might be small. Such low numbers of competent memory B cells might be one of the reasons of why recruitment of memory B cells into secondary GCs is unexpectedly low. In this case, as discussed in section 2-1, affinity and multiplicity of the B cell antigen and T cell epitopes should be carefully considered.

One of the big differences in the immune state between naïve and memory cells is that due to already establishing long-lived plasma cells upon primary vaccination/infection, high titer and high affinity Abs for the primary antigen preexist prior to the secondary vaccination. Among many effector functions of Abs, the following three activities presumably affect subsequent recall humoral responses; 1) rapid antigen clearance, e.g., *via* macrophage Fc and complement receptors; 2) immune complex formation (70) and subsequent antigen presentation on FDCs; 3) epitope masking (71). Although the relative involvement and importance of these three mechanisms in recall responses have not been carefully addressed, epitope masking is likely to occur, evidenced by recent data employing malaria vaccination (72). Abs against *Plasmodium falciparum* circumsporozoite protein (PfCSP) plateaued after two immunizations with the same antigen and these Abs masked the epitope, thereby limiting immunodominant B cell responses upon the third immunization with the same antigen. They allowed subdominant responses toward distinct epitopes, thereby contributing to broadening the spectrum of vaccine-induced Abs (**Figure 2**).

Assuming that, to simplify the model, influenza HA has five dominant epitopes in the head, which change in variant viruses, and one conserved subdominant epitope in the stem (73), based upon the epitope masking mechanism, the following scenario can be envisaged (**Figure 3**). If the antigenic distance between the virus (A) that the individual was initially exposed to and the current exposure virus (B) is large, pre-existing anti-head Abs against virus (A) cannot protect from the (B) virus. After infection/vaccination with the virus (A), anti-stem memory B cells are probably also generated but, as seen in the mouse infection case (9), levels of anti-stem Abs are very low. In this case, upon virus (B) infection, because there are no epitope masking Abs for the stem epitope, anti-stem memory B cells are activated. Simultaneously, GC and memory B cells directed towards the unique head region of the new (B) virus are generated from naïve B cells. The anti-stem memory B cells swiftly produce plasmablasts, along with entering GCs and subsequently generating more mature memory B cells. Thus, this individual can be protected from (B) virus due to the *de novo* promptly generated anti-stem Abs and will be prepared for the subsequent variant virus (C) infection due to generating more mature mutated anti-stem memory B cells by acquiring further breadth in GCs. Once the further distant virus (C) infects, even though the anti-stem Abs have declined, high quality anti-stem memory B cells would play a significant role in protection from the (C) virus. Validating this scenario needs further study but, to make high quality anti-stem memory B cells, limiting epitope masking by anti-stem Abs seems to be another option.

## CONCLUDING REMARK

Considerable advances have been made in elucidating the cellular basis and key drivers regulating GC-derived memory B cell differentiation and activation in recent years (74, 75), which can explain the mechanism how the memory B cell pool can deal with the variant viruses. Generation of high quality broadly protective memory B cells against conserved viral epitopes

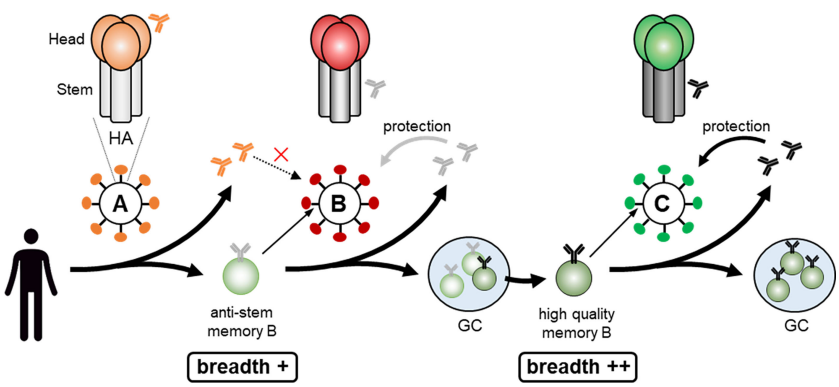


**FIGURE 3** | Making high quality anti-stem memory B cell. Infection with the virus **(A)** results in generation of anti-stem memory B cells and low levels of anti-stem Abs. In this case, as there are no stem epitope masking Abs, anti-stem memory B cells are activated upon virus **(B)** infection, quickly produce anti-stem Abs, along with acquiring further breadth by entering GCs and subsequently generating more mature high quality memory B cells. Once the further distant virus **(C)** infects, high quality anti-stem memory B cells would play a significant role in protection from the virus **(C)**.

remains a continuous challenge to provide long-lasting and cross-protective immunological memory, but the recent progress in this field will facilitate the development of better Ab-based universal vaccine design strategies.

## AUTHOR CONTRIBUTIONS

TI, RS, and TK contributed to conception of the study. TI and TK wrote the manuscript. All authors contributed to the article and approved the submitted version.

## FUNDING

This work was supported by grants from JSPS KAKENHI (JP21H02749), Takeda Science Foundation, the Naito Foundation, and the Sumitomo Foundation to TI, grants from JSPS KAKENHI (JP21H02740) to RS, and grants from JSPS KAKENHI (JP19H01028) to TK.

## ACKNOWLEDGMENTS

We thank P.D. Burrows for critical reading of the manuscript.

## REFERENCES

1. Victora GD, Nussenzweig MC. Germinal Centers. *Annu Rev Immunol* (2012) 30:429–57. doi: 10.1146/annurev-immunol-020711-075032
2. Mesin L, Ersching J, Victora GD. Germinal Center B Cell Dynamics. *Immunity* (2016) 45(3):471–82. doi: 10.1016/j.immuni.2016.09.001
3. Young C, Brink R. The Unique Biology of Germinal Center B Cells. *Immunity* (2021) 54(8):1652–64. doi: 10.1016/j.immuni.2021.07.015
4. Shinnakasu R, Inoue T, Kometani K, Moriyama S, Adachi Y, Nakayama M, et al. Regulated Selection of Germinal-Center Cells Into the Memory B Cell Compartment. *Nat Immunol* (2016) 17(7):861–9. doi: 10.1038/ni.3460
5. Weisel FJ, Zuccarino-Catania GV, Chikina M, Shlomchik MJ. A Temporal Switch in the Germinal Center Determines Differential Output of Memory B and Plasma Cells. *Immunity* (2016) 44(1):116–30. doi: 10.1016/j.immuni.2015.12.004
6. Suan D, Krautler NJ, Maag JLV, Butt D, Bourne K, Hermes JR, et al. CCR6 Defines Memory B Cell Precursors in Mouse and Human Germinal Centers, Revealing Light-Zone Location and Predominant Low Antigen Affinity. *Immunity* (2017) 47(6):1142–53.e1144. doi: 10.1016/j.immuni.2017.11.022
7. Viant C, Weymar GHJ, Escolano A, Chen S, Hartweger H, Cipolla M, et al. Antibody Affinity Shapes the Choice Between Memory and Germinal Center B Cell Fates. *Cell* (2020) 183(5):1298–311.e1211. doi: 10.1016/j.cell.2020.09.063
8. Purtha WE, Tedder TF, Johnson S, Bhattacharya D, Diamond MS. Memory B Cells, But Not Long-Lived Plasma Cells, Possess Antigen Specificities for Viral Escape Mutants. *J Exp Med* (2011) 208(13):2599–606. doi: 10.1084/jem.20110740
9. Leach S, Shinnakasu R, Adachi Y, Momota M, Makino-Okamura C, Yamamoto T, et al. Requirement for Memory B Cell Activation in Protection From Heterologous Influenza Virus Reinfection. *Int Immunol* (2019) 31(12):771–9. doi: 10.1093/intimm/dxz049
10. Andrews SF, Huang Y, Kaur K, Popova LI, Ho IY, Pauli NT, et al. Immune History Profoundly Affects Broadly Protective B Cell Responses to Influenza. *Sci Transl Med* (2015) 7(316):316ra192. doi: 10.1126/scitranslmed.aad0522
11. Kurosaki T, Kometani K, Ise W. Memory B Cells. *Nat Rev Immunol* (2015) 15(3):149–59. doi: 10.1038/nri3802
12. Akkaya M, Kwak K, Pierce SK. B Cell Memory: Building Two Walls of Protection Against Pathogens. *Nat Rev Immunol* (2020) 20(4):229–38. doi: 10.1038/s41577-019-0244-2
13. Ise W, Kurosaki T. Plasma Cell Differentiation During the Germinal Center Reaction. *Immunol Rev* (2019) 288(1):64–74. doi: 10.1111/imr.12751
14. Schwickert TA, Victora GD, Fooksman DR, Kamphorst AO, Mugnier MR, Gitlin AD, et al. A Dynamic T Cell-Limited Checkpoint Regulates Affinity-Dependent B Cell Entry Into the Germinal Center. *J Exp Med* (2011) 208(6):1243–52. doi: 10.1084/jem.20102477
15. Abbott RK, Lee JH, Menis S, Skog P, Rossi M, Ota T, et al. Precursor Frequency and Affinity Determine B Cell Competitive Fitness in Germinal Centers, Tested With Germline-Targeting HIV Vaccine Immunogens. *Immunity* (2018) 48(1):133–46.e136. doi: 10.1016/j.immuni.2017.11.023
16. Yeh CH, Nojima T, Kuraoka M, Kelsoe G. Germinal Center Entry Not Selection of B Cells Is Controlled by Peptide-MHCII Complex Density. *Nat Commun* (2018) 9(1):928. doi: 10.1038/s41467-018-03382-x
17. Glaros V, Rauschmeier R, Artemov AV, Reinhardt A, Ols S, Emmanouilidi A, et al. Limited Access to Antigen Drives Generation of Early B Cell Memory While Restraining the Plasmablast Response. *Immunity* (2021) 54(9):2005–23:e10. doi: 10.1016/j.immuni.2021.08.017
18. Abbott RK, Crotty S. Factors in B Cell Competition and Immunodominance. *Immunol Rev* (2020) 296(1):120–31. doi: 10.1111/imr.12861
19. Victora GD, Schwickert TA, Fooksman DR, Kamphorst AO, Meyer-Hermann M, Dustin ML, et al. Germinal Center Dynamics Revealed by Multiphoton Microscopy With a Photoactivatable Fluorescent Reporter. *Cell* (2010) 143(4):592–605. doi: 10.1016/j.cell.2010.10.032
20. Cyster JG, Allen CDC. B Cell Responses: Cell Interaction Dynamics and Decisions. *Cell* (2019) 177(3):524–40. doi: 10.1016/j.cell.2019.03.016
21. Kennedy DE, Okoreeh MK, Maienschein-Cline M, Ai J, Veselits M, McLean KC, et al. Novel Specialized Cell State and Spatial Compartments Within the Germinal Center. *Nat Immunol* (2020) 21(6):660–70. doi: 10.1038/s41590-020-0660-2
22. Weinstein JS, Herman EI, Lainez B, Licona-Limon P, Esplugues E, Flavell R, et al. TFH Cells Progressively Differentiate to Regulate the Germinal Center Response. *Nat Immunol* (2016) 17(10):1197–205. doi: 10.1038/ni.3554
23. Miyauchi K, Adachi Y, Tonouchi K, Yajima T, Harada Y, Fukuyama H, et al. Influenza Virus Infection Expands the Breadth of Antibody Responses Through IL-4 Signalling in B Cells. *Nat Commun* (2021) 12(1):3789. doi: 10.1038/s41467-021-24090-z
24. Bannard O, McGowan SJ, Ersching J, Ishido S, Victora GD, Shin JS, et al. Ubiquitin-Mediated Fluctuations in MHC Class II Facilitate Efficient Germinal Center B Cell Responses. *J Exp Med* (2016) 213(6):993–1009. doi: 10.1084/jem.20151682
25. Luo W, Weisel F, Shlomchik MJ. B Cell Receptor and CD40 Signaling Are Rewired for Synergistic Induction of the C-Myc Transcription Factor in Germinal Center B Cells. *Immunity* (2018) 48(2):313–26.e315. doi: 10.1016/j.immuni.2018.01.008
26. Ersching J, Efeyan A, Mesin L, Jacobsen JT, Pasqual G, Grabiner BC, et al. Germinal Center Selection and Affinity Maturation Require Dynamic Regulation of Mtorc1 Kinase. *Immunity* (2017) 46(6):1045–58.e1046. doi: 10.1016/j.immuni.2017.06.005
27. Finkin S, Hartweger H, Oliveira TY, Kara EE, Nussenzweig MC. Protein Amounts of the MYC Transcription Factor Determine Germinal Center B Cell Division Capacity. *Immunity* (2019) 51(2):324–36.e5. doi: 10.1016/j.immuni.2019.06.013
28. Pae J, Ersching J, Castro TBR, Schips M, Mesin L, Allon SJ, et al. Cyclin D3 Drives Inertial Cell Cycling in Dark Zone Germinal Center B Cells. *J Exp Med* (2021) 218(4). doi: 10.1084/jem.20201699
29. Jacob J, Przylepa J, Miller C, Kelsoe G. In Situ Studies of the Primary Immune Response to (4-Hydroxy-3-Nitrophenyl)Acetyl. III. The Kinetics of V Region Mutation and Selection in Germinal Center B Cells. *J Exp Med* (1993) 178(4):1293–307. doi: 10.1084/jem.178.4.1293
30. Ziegner M, Steinhauser G, Berek C. Development of Antibody Diversity in Single Germinal Centers: Selective Expansion of High-Affinity Variants. *Eur J Immunol* (1994) 24(10):2393–400. doi: 10.1002/eji.1830241020
31. Kuraoka M, Schmidt AG, Nojima T, Feng F, Watanabe A, Kitamura D, et al. Complex Antigens Drive Permissive Clonal Selection in Germinal Centers. *Immunity* (2016) 44(3):542–52. doi: 10.1016/j.immuni.2016.02.010

32. Tas JM, Mesin L, Pasqual G, Targ S, Jacobsen JT, Mano YM, et al. Visualizing Antibody Affinity Maturation in Germinal Centers. *Science* (2016) 351 (6277):1048–54. doi: 10.1126/science.aad3439
33. Zhang Y, Meyer-Hermann M, George LA, Figge MT, Khan M, Goodall M, et al. Germinal Center B Cells Govern Their Own Fate via Antibody Feedback. *J Exp Med* (2013) 210(3):457–64. doi: 10.1084/jem.20120150
34. Zhang Y, Garcia-Ibanez L, Toellner KM. Regulation of Germinal Center B-Cell Differentiation. *Immunol Rev* (2016) 270(1):8–19. doi: 10.1111/imr.12396
35. Meyer-Hermann M. Injection of Antibodies Against Immunodominant Epitopes Tunes Germinal Centers to Generate Broadly Neutralizing Antibodies. *Cell Rep* (2019) 29(5):1066–73.e1065. doi: 10.1016/j.celrep.2019.09.058
36. Smith KG, Light A, O'Reilly LA, Ang SM, Strasser A, Tarlinton D. Bcl-2 Transgene Expression Inhibits Apoptosis in the Germinal Center and Reveals Differences in the Selection of Memory B Cells and Bone Marrow Antibody-Forming Cells. *J Exp Med* (2000) 191(3):475–84. doi: 10.1084/jem.191.3.475
37. Alameh M-G, Tombácz I, Bettini E, Lederer K, Sittplangkoon C, Wilmore JR, et al. Lipid Nanoparticles Enhance the Efficacy of mRNA and Protein Subunit Vaccines by Inducing Robust T Follicular Helper Cell and Humoral Responses. *Immunity* (2021) 54(12):2877–92.e7. doi: 10.1016/j.immuni.2021.11.001
38. McCarthy KR, Watanabe A, Kuraoka M, Do KT, McGee CE, Sempowski GD, et al. Memory B Cells That Cross-React With Group 1 and Group 2 Influenza A Viruses Are Abundant in Adult Human Repertoires. *Immunity* (2018) 48174-184(1):e179. doi: 10.1016/j.immuni.2017.12.009
39. Wang Y, Shi J, Yan J, Xiao Z, Hou X, Lu P, et al. Germinal-Center Development of Memory B Cells Driven by IL-9 From Follicular Helper T Cells. *Nat Immunol* (2017) 18(8):921–30. doi: 10.1038/ni.3788
40. Inoue T, Shinnakasu R, Kawai C, Ise W, Kawakami E, Sax N, et al. Exit From Germinal Center to Become Quiescent Memory B Cells Depends on Metabolic Reprograming and Provision of a Survival Signal. *J Exp Med* (2021) 218(1). doi: 10.1084/jem.20200866
41. Laidlaw BJ, Schmidt TH, Green JA, Allen CD, Okada T, Cyster JG. The Eph-Related Tyrosine Kinase Ligand Ephrin-B1 Marks Germinal Center and Memory Precursor B Cells. *J Exp Med* (2017) 214(3):639–49. doi: 10.1084/jem.20161461
42. Toboso-Navasa A, Gunawan A, Morlino G, Nakagawa R, Taddei A, Damry D, et al. Restriction of Memory B Cell Differentiation at the Germinal Center B Cell Positive Selection Stage. *J Exp Med* (2020) 217(7). doi: 10.1084/jem.20191933
43. Stewart I, Radtke D, Phillips B, McGowan SJ, Bannard O. Germinal Center B Cells Replace Their Antigen Receptors in Dark Zones and Fail Light Zone Entry When Immunoglobulin Gene Mutations Are Damaging. *Immunity* (2018) 49(3):477–89.e477. doi: 10.1016/j.immuni.2018.08.025
44. Saito M, Novak U, Piovan E, Basso K, Sumazin P, Schneider C, et al. BCL6 Suppression of BCL2 via Miz1 and Its Disruption in Diffuse Large B Cell Lymphoma. *Proc Natl Acad Sci USA* (2009) 106(27):11294–9. doi: 10.1073/pnas.0903854106
45. Huang C, Gonzalez DG, Cote CM, Jiang Y, Hatzi K, Teater M, et al. The BCL6 RD2 Domain Governs Commitment of Activated B Cells to Form Germinal Centers. *Cell Rep* (2014) 8(5):1497–508. doi: 10.1016/j.celrep.2014.07.059
46. Hatzi K, Nance JP, Kroenke MA, Bothwell M, Haddad EK, Melnick A, et al. BCL6 Orchestrates Tfh Cell Differentiation via Multiple Distinct Mechanisms. *J Exp Med* (2015) 212(4):539–53. doi: 10.1084/jem.20141380
47. Linterman MA, Beaton L, Yu D, Ramiscal RR, Srivastava M, Hogan JJ, et al. IL-21 Acts Directly on B Cells to Regulate Bcl-6 Expression and Germinal Center Responses. *J Exp Med* (2010) 207(2):353–63. doi: 10.1084/jem.20091738
48. Laidlaw BJ, Duan L, Xu Y, Vazquez SE, Cyster JG. The Transcription Factor Hhex Cooperates With the Corepressor Tle3 to Promote Memory B Cell Development. *Nat Immunol* (2020) 21(9):1082–93. doi: 10.1038/s41590-020-0713-6
49. Ng S, Nachbagauer R, Balmaseda A, Stadlbauer D, Ojeda S, Patel M, et al. Novel Correlates of Protection Against Pandemic H1N1 Influenza A Virus Infection. *Nat Med* (2019) 25(6):962–7. doi: 10.1038/s41591-019-0463-x
50. Sangesland M, Ronsard L, Kazer SW, Bals J, Boyoglu-Barnum S, Yousif AS, et al. Germline-Encoded Affinity for Cognate Antigen Enables Vaccine Amplification of a Human Broadly Neutralizing Response Against Influenza Virus. *Immunity* (2019) 51(4):735–49.e738. doi: 10.1016/j.immuni.2019.09.001
51. Guthmiller JJ, Lan LY, Fernandez-Quintero ML, Han J, Utset HA, Bitar DJ, et al. Polyreactive Broadly Neutralizing B Cells Are Selected to Provide Defense Against Pandemic Threat Influenza Viruses. *Immunity* (2020) 53 (6):1230–44.e1235. doi: 10.1016/j.immuni.2020.10.005
52. Guthmiller JJ, Utset HA, Wilson PC. B Cell Responses Against Influenza Viruses: Short-Lived Humoral Immunity Against a Life-Long Threat. *Viruses* (2021) 13(6). doi: 10.3390/v13060965
53. Li GM, Chiu C, Wrammert J, McCausland M, Andrews SF, Zheng NY, et al. Pandemic H1N1 Influenza Vaccine Induces a Recall Response in Humans That Favors Broadly Cross-Reactive Memory B Cells. *Proc Natl Acad Sci USA* (2012) 109(23):9047–52. doi: 10.1073/pnas.1118979109
54. Finney J, Watanabe A, Kelsoe G, Kuraoka M. Minding the Gap: The Impact of B-Cell Tolerance on the Microbial Antibody Repertoire. *Immunol Rev* (2019) 292(1):24–36. doi: 10.1111/imr.12805
55. Sabouri Z, Schofield P, Horikawa K, Spierings E, Kipling D, Randall KL, et al. Redemption of Autoantibodies on Anergic B Cells by Variable-Region Glycosylation and Mutation Away From Self-Reactivity. *Proc Natl Acad Sci USA* (2014) 111(25):E2567–2575. doi: 10.1073/pnas.1406974111
56. Burnett DL, Langley DB, Schofield P, Hermes JR, Chan TD, Jackson J, et al. Germinal Center Antibody Mutation Trajectories Are Determined by Rapid Self/Foreign Discrimination. *Science* (2018) 360(6385):223–6. doi: 10.1126/science.aao3859
57. Locci M, Havenar-Daughton C, Landais E, Wu J, Kroenke MA, Arlehamn CL, et al. Human Circulating PD-1+CXCR3-CXCR5+ Memory Tfh Cells Are Highly Functional and Correlate With Broadly Neutralizing HIV Antibody Responses. *Immunity* (2013) 39(4):758–69. doi: 10.1016/j.immuni.2013.08.031
58. Martin-Gayo E, Cronin J, Hickman T, Ouyang Z, Lindqvist M, Kolb KE, et al. Circulating CXCR5(+)CXCR3(+)PD-1(Lo) Tfh-Like Cells in HIV-1 Controllers With Neutralizing Antibody Breadth. *JCI Insight* (2017) 2(2): e89574. doi: 10.1172/jci.insight.89574
59. Lee JH, Hu JK, Georgeson E, Nakao C, Groschel B, Dileepan T, et al. Modulating the Quantity of HIV Env-Specific CD4 T Cell Help Promotes Rare B Cell Responses in Germinal Centers. *J Exp Med* (2021) 218(2). doi: 10.1084/jem.20201254
60. Tan HX, Jegaskanda S, Juno JA, Esterbauer R, Wong J, Kelly HG, et al. Subdominance and Poor Intrinsic Immunogenicity Limit Humoral Immunity Targeting Influenza HA Stem. *J Clin Invest* (2019) 129(2):850–62. doi: 10.1172/JCI123366
61. Gray ES, Madiga MC, Hermanus T, Moore PL, Wibmer CK, Tumba NL, et al. The Neutralization Breadth of HIV-1 Develops Incrementally Over Four Years and Is Associated With CD4+ T Cell Decline and High Viral Load During Acute Infection. *J Virol* (2011) 85(10):4828–40. doi: 10.1128/JVI.00198-11
62. Cirelli KM, Carnathan DG, Nogal B, Martin JT, Rodriguez OL, Upadhyay AA, et al. Slow Delivery Immunization Enhances HIV Neutralizing Antibody and Germinal Center Responses via Modulation of Immunodominance. *Cell* (2019) 177(5):1153–71.e1128. doi: 10.1016/j.cell.2019.04.012
63. Nachbagauer R, Feser J, Naficy A, Bernstein DI, Guptill J, Walter EB, et al. A Chimeric Hemagglutinin-Based Universal Influenza Virus Vaccine Approach Induces Broad and Long-Lasting Immunity in a Randomized, Placebo-Controlled Phase I Trial. *Nat Med* (2021) 27(1):106–14. doi: 10.1038/s41591-020-1118-7
64. Mesin L, Schiepers A, Ersching J, Barbulescu A, Cavazzoni CB, Angelini A, et al. Restricted Clonality and Limited Germinal Center Reentry Characterize Memory B Cell Reactivation by Boosting. *Cell* (2020) 180(1):92–106.e111. doi: 10.1016/j.cell.2019.11.032
65. Turner JS, Zhou JQ, Han J, Schmitz AJ, Rizk AA, Alsoussi WB, et al. Human Germinal Centres Engage Memory and Naive B Cells After Influenza Vaccination. *Nature* (2020) 586(7827):127–32. doi: 10.1038/s41586-020-2711-0
66. Ellebedy AH, Jackson KJ, Kissick HT, Nakaya HI, Davis CW, Roskin KM, et al. Defining Antigen-Specific Plasmablast and Memory B Cell Subsets in Human Blood After Viral Infection or Vaccination. *Nat Immunol* (2016) 17 (10):1226–34. doi: 10.1038/ni.3533
67. Kometani K, Nakagawa R, Shinnakasu R, Kaji T, Rybouchkin A, Moriyama S, et al. Repression of the Transcription Factor Bach2 Contributes to

Predisposition of IgG1 Memory B Cells Toward Plasma Cell Differentiation. *Immunity* (2013) 39(1):136–47. doi: 10.1016/j.immuni.2013.06.011
68. Zuccarino-Catania GV, Sadanand S, Weisel FJ, Tomayko MM, Meng H, Kleinstein SH, et al. CD80 and PD-L2 Define Functionally Distinct Memory B Cell Subsets That Are Independent of Antibody Isotype. *Nat Immunol* (2014) 15(7):631–7. doi: 10.1038/ni.2914
69. Johnson JL, Rosenthal RL, Knox JJ, Myles A, Naradikian MS, Madej J, et al. The Transcription Factor T-Bet Resolves Memory B Cell Subsets With Distinct Tissue Distributions and Antibody Specificities in Mice and Humans. *Immunity* (2020) 52(5):842–55.e846. doi: 10.1016/j.immuni.2020.03.020
70. Wang TT, Maamary J, Tan GS, Bournazos S, Davis CW, Krammer F, et al. Anti-HA Glycoforms Drive B Cell Affinity Selection and Determine Influenza Vaccine Efficacy. *Cell* (2015) 162(1):160–9. doi: 10.1016/j.cell.2015.06.026
71. Bannard O, Cyster JG. Germinal Centers: Programmed for Affinity Maturation and Antibody Diversification. *Curr Opin Immunol* (2017) 45:21–30. doi: 10.1016/j.coi.2016.12.004
72. McNamara HA, Idris AH, Sutton HJ, Vistein R, Flynn BJ, Cai Y, et al. Antibody Feedback Limits the Expansion of B Cell Responses to Malaria Vaccination But Drives Diversification of the Humoral Response. *Cell Host Microbe* (2020) 28572-585(4):e577. doi: 10.1016/j.chom.2020.07.001
73. Angeletti D, Gibbs JS, Angel M, Kosik I, Hickman HD, Frank GM, et al. Defining B Cell Immunodominance to Viruses. *Nat Immunol* (2017) 18 (4):456–63. doi: 10.1038/ni.3680
74. Inoue T, Moran I, Shinnakasu R, Phan TG, Kurosaki T. Generation of Memory B Cells and Their Reactivation. *Immunol Rev* (2018) 283(1):138–49. doi: 10.1111/imr.12640
75. Laidlaw BJ, Cyster JG. Transcriptional Regulation of Memory B Cell Differentiation. *Nat Rev Immunol* (2021) 21(4):209–20. doi: 10.1038/s41577-020-00446-2

**Conflict of Interest:** The authors declare that the research was conducted in the absence of any commercial or financial relationships that could be construed as a potential conflict of interest.

**Publisher's Note:** All claims expressed in this article are solely those of the authors and do not necessarily represent those of their affiliated organizations, or those of the publisher, the editors and the reviewers. Any product that may be evaluated in this article, or claim that may be made by its manufacturer, is not guaranteed or endorsed by the publisher.

frontiers in Immunology

ORIGINAL RESEARCH
published: 03 February 2022
doi: 10.3389/fimmu.2022.817905

# Robust and Functional Immune Memory Up to 9 Months After SARS-CoV-2 Infection: A Southeast Asian Longitudinal Cohort

*Hoa Thi My Vo[1†], Alvino Maestri[1†], Heidi Auerswald[2], Sopheak Sorn[3], Sokchea Lay[1], Heng Seng[4], Sotheary Sann[1], Nisa Ya[1], Polidy Pean[1], Philippe Dussart[2], Olivier Schwartz[5,6], Sovann Ly[4], Timothée Bruel[5,6], Sowath Ly[3], Veasna Duong[2], Erik A. Karlsson[2‡] and Tineke Cantaert[1*‡]*

[1] Immunology Unit, Institut Pasteur du Cambodge, Pasteur Network, Phnom Penh, Cambodia, [2] Virology Unit, Institut Pasteur du Cambodge, Pasteur Network, Phnom Penh, Cambodia, [3] Epidemiology and Public Health Unit, Institut Pasteur du Cambodge, Pasteur Network, Phnom Penh, Cambodia, [4] Department of Communicable Disease Control, Ministry of Health (CDC-MoH), Phnom Penh, Cambodia, [5] Institut Pasteur, Université de Paris, CNRS UMR3569, Virus and Immunity Unit, Paris, France, [6] Vaccine Research Institute, Créteil, France

OPEN ACCESS

**Edited by:**
Kihyuck Kwak,
Yonsei University, South Korea

**Reviewed by:**
Christopher Sundling,
Karolinska Institutet (KI), Sweden
Constantin Joachim Thieme,
Charité Medical University of Berlin, Germany

***Correspondence:**
Tineke Cantaert
tineke.cantaert@pasteur.fr

[†]These authors have contributed equally to this work

[‡]These authors have contributed equally to this work

**Specialty section:**
This article was submitted to Immunological Memory, a section of the journal Frontiers in Immunology

**Received:** 18 November 2021
**Accepted:** 10 January 2022
**Published:** 03 February 2022

**Citation:**
Vo HTM, Maestri A, Auerswald H, Sorn S, Lay S, Seng H, Sann S, Ya N, Pean P, Dussart P, Schwartz O, Ly S, Bruel T, Ly S, Duong V, Karlsson EA and Cantaert T (2022) Robust and Functional Immune Memory Up to 9 Months After SARS-CoV-2 Infection: A Southeast Asian Longitudinal Cohort. Front. Immunol. 13:817905. doi: 10.3389/fimmu.2022.817905

The duration of humoral and cellular immune memory following SARS-CoV-2 infection in populations in least developed countries remains understudied but is key to overcome the current SARS-CoV-2 pandemic. Sixty-four Cambodian individuals with laboratory-confirmed infection with asymptomatic or mild/moderate clinical presentation were evaluated for Spike (S)-binding and neutralizing antibodies and antibody effector functions during acute phase of infection and at 6-9 months follow-up. Antigen-specific B cells, $CD4^+$ and $CD8^+$ T cells were characterized, and T cells were interrogated for functionality at late convalescence. Anti-S antibody titers decreased over time, but effector functions mediated by S-specific antibodies remained stable. S- and nucleocapsid (N)-specific B cells could be detected in late convalescence in the activated memory B cell compartment and are mostly $IgG^+$. $CD4^+$ and $CD8^+$ T cell immune memory was maintained to S and membrane (M) protein. Asymptomatic infection resulted in decreased antibody-dependent cellular cytotoxicity (ADCC) and frequency of SARS-CoV-2-specific $CD4^+$ T cells at late convalescence. Whereas anti-S antibodies correlated with S-specific B cells, there was no correlation between T cell response and humoral immune memory. Hence, all aspects of a protective immune response are maintained up to nine months after SARS-CoV-2 infection and in the absence of re-infection.

**Keywords: SARS-CoV-2, B cell immunity, T cell immunity, antibody effector function, long term immune response**

## INTRODUCTION

In December 2019, a cluster of severe pneumonia of unknown cause was reported to the World Health Organization. Investigation into the etiology revealed a novel betacoronavirus, subsequently named Severe Acute Respiratory Syndrome Coronavirus 2 (SARS-CoV-2), the causative agent of Coronavirus Disease 2019 (COVID-19) (1–3).

Upon infection with SARS-CoV-2, humans generate SARS-CoV-2-specific antibodies, memory B cells, and $CD4^+$ and $CD8^+$ T cells, which all have complementary functions in the clearance of SARS-CoV-2 virions and infected cells (4–6). Mainly structural proteins are targeted by the immune response, such as the membrane (M) and spike (S) protein integrated in the virion envelope, and the nucleoprotein (N), which protects the RNA genome (7–9). The S protein consists of two domains. The S1 region contains the receptor binding domain (RBD) which interacts with the host protein Angiotensin-converting enzyme 2 (ACE2) to mediate cell entry, whereas the S2 domain mediates membrane fusion. The S1 domain with the RBD is a major target of neutralizing antibodies (10, 11). Several studies show correlation between antibodies targeting S and functional neutralization (12–14). In animal models, these neutralizing antibodies are protective against secondary infection (15, 16). In humans, anti-S antibodies and neutralizing antibodies can be detected up to one year post infection (17–19).

Besides neutralization, antibodies activate a variety of effector functions mediated by their Fc domain. These include complement activation, killing of infected cells and phagocytosis of viral particles (20). Indeed, it has been shown that symptomatic and asymptomatic SARS-CoV-2 infection elicit polyfunctional antibodies targeting infected cells (21, 22) and Fc mediated effector activity of antibodies correlates with reduced disease severity and mortality after SARS-CoV-2 infection (23). However, the evolution of this response over time requires further investigation (24, 25).

Persistence of serum antibodies may not be the sole determinant of long-lasting immune memory post infection or vaccination. Anamnestic recall of memory T and B cell populations can also reduce infection or disease at re-exposure (4, 26, 27), with increasing importance as antibody titers wane. Virus-specific memory T and B cells can be detected in at least 50% of the individuals more than eight months post infection (4, 27, 28). Several studies suggest that increased severity of COVID-19 induces a stronger SARS-CoV-2-specific $CD4^+$ T cell response (28–30). However, the magnitude, quality, and protective capacity of cellular responses against SARS-CoV-2 requires further definition (31).

Kinetics and duration of the memory immune responses could depend on a number of factors including disease severity, re-infection, cross-reactivity with human seasonal coronaviruses (hCoVs), ethnic background, age and length of antigenic exposure [reviewed in (31)]. Other human betacoronaviruses, such as hCoV OC43 and HKU1, and zoonotic viruses, such as SARS-CoV−1 and Middle East respiratory syndrome-related coronavirus (MERS-CoV), show waning antibody levels as soon as three months post infection. In contrast, T cell responses are detectable up to 17 years later (32, 33).

Most studies analyzing the evolution of the adaptive immune response to SARS-CoV-2 are conducted in Caucasian populations (31). In South-East Asia, very few studies have been performed, which mainly focused on antibody responses (18, 34–36). Paucity of data from at risk areas and populations can hamper global mitigation and vaccination efforts.

We comprehensively characterized long-lived immune memory in 64 Cambodian individuals with laboratory-confirmed infection experiencing mild/moderate or asymptomatic clinical outcome. Cambodia remained almost completely COVID-19-free in 2020 (37), hence additional exposure to SARS-CoV-2 in this cohort during the follow-up period is highly unlikely.

# RESULTS

## Long-Term Follow-Up of SARS-CoV-2 Imported Cases

Sixty-four individuals with confirmed SARS-CoV-2 were included and re-assessed 6-9 months after infection. SARS-CoV-2 infection was confirmed by positive molecular diagnosis as part of the national surveillance system. Since Cambodia had minimal detection of SARS-CoV-2 during the follow-up period, the probability of re-exposure to SARS-CoV-2 was minimal (37) in 2020. For 33 individuals, we obtained a blood sample 2-9 days after laboratory confirmed infection (**Figure S1A**). For all 64 study participants, between 1 to 15 follow-up nasopharyngeal/oropharyngeal (NP/OP) swab samplings assessed the duration of SARS-CoV-2 RNA shedding during the acute phase of infection *via* RT-PCR (38). Based on the duration of SARS-CoV-2 RNA shedding, 53% of individuals were considered "long shedders" with detection of viral RNA in NP/OP swabs for ≥10 days (**Figure S1B**). Overall, 70% of the patients displayed mild or moderate symptoms, and 30% remained asymptomatic (**Table S1**). For all assays, samples were selected based on availability and quality.

## Asymptomatic and Mild/Moderate Infection Induces a Persisting Anti-Spike Antibody Response

The presence of S-binding antibodies was measured using the S-Flow assay, which sensitively and quantitatively measures anti-S IgG, IgA, and IgM by flow cytometry (21, 39) (**Figure 1A**). The National Institute for Biological Standards and Control (NIBSC) references were utilized to validate the assays and pre-pandemic samples obtained from nineteen individuals were measured to set the cutoff for each assay (**Figure S2**). Anti-S IgM, IgG, and IgA titers decreased significantly between acute phase and late convalescence ($p=0.02$, $p<0.0001$, $p<0.0001$, respectively) (**Figure 1B**). Within the total S-binding antibodies, the percentage of anti-S IgM and IgA decreased whereas anti-S IgG increased over time ($p=0.03$, **Figure 1C**). The detection of neutralizing antibodies was achieved by foci reduction neutralization test using a Cambodian SARS-CoV-2 isolate. There was no difference in the titers of SARS-CoV-2 neutralizing antibodies between the acute and convalescent phase, even though titers tended to decrease over time (**Figure 1D**). Over time, the percentage of individuals positive for anti-S IgM ($p<0.0001$) and anti-S IgA ($p<0.0001$) decreased (**Figure 1E**). In the acute phase, 91% of individuals were positive for anti-S IgG, and only 70% of the individuals were positive for neutralizing antibody titers. Up to nine months post infection, the frequency of individuals positive for anti-S IgG remained stable (88%) whereas the frequency of individuals with neutralizing titers decreased to 56% ($p=0.055$) (**Figure 1E**). Analyzing only individuals with paired

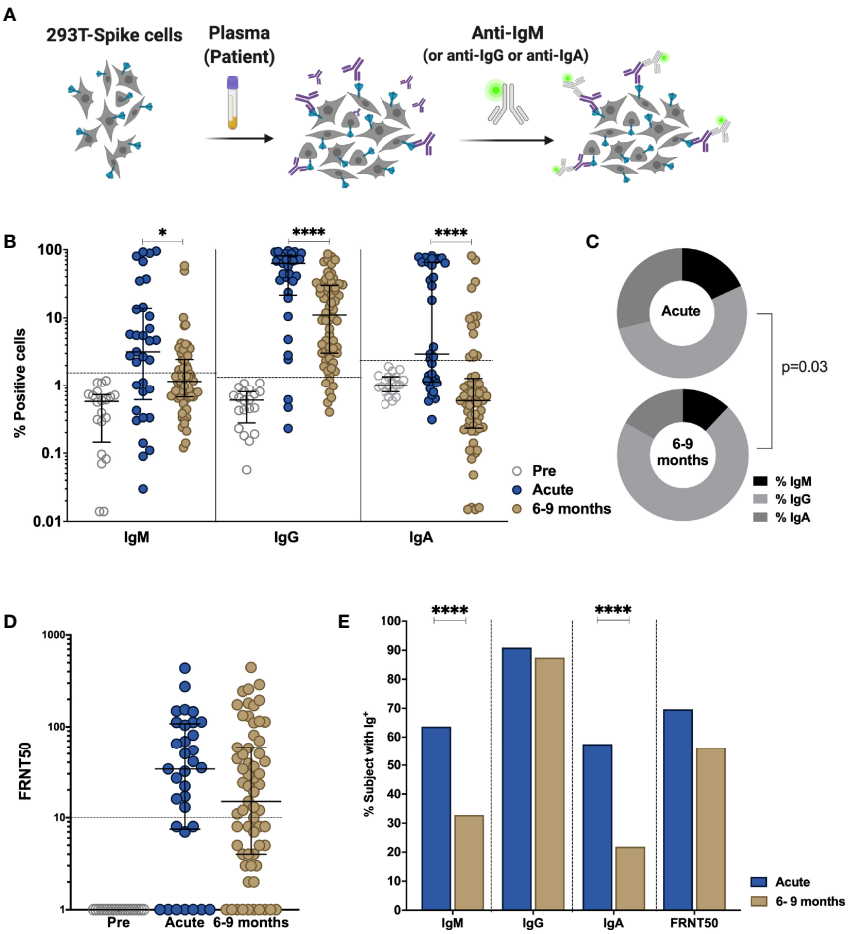


**FIGURE 1** | Comparison of antibody response in SARS-CoV-2-infected individuals during the acute phase and 6-9 months post infection. Non-infected samples obtained before the pandemic (pre), and SARS-Cov-2 infected individuals were sampled 2-9 days post laboratory confirmation and 6-9 months later. **(A)** Schematic model of the S-Flow assay. **(B)** Amount of antibodies against spike protein were reported as percentage of spike-expressing 293T cells bound by IgM, IgG, IgA in the S-Flow assay. **(C)** Pie charts show the proportion of anti-S IgM, IgG and IgA antibodies. **(D)** SARS-CoV-2 neutralizing activity was calculated as FRNT50 titer in foci reduction neutralization test (FRNT). **(E)** Comparison of the percentage of individuals positive for anti-S IgM, IgG, IgA and FRNT50. Statistical comparisons were performed by Mann Whitney test **(B, D)** and Chi-square test **(C, E)**. The dashed line indicates the cutoff for positivity based on values calculated following formula: cut-off = % mean positive cells from 19 pre-pandemic samples + 3x standard deviation. Each dot represents the result from a single individual. Lines represent median and IQR. *p < 0.05 and ****p < 0.0001. Pre-pandemic n=19, acute n=33, 6-9 months n=64.

samples available, revealed similar results as the whole cohort (**Figures S3A, B**). Taken together, these data show that despite decreases in antibody titers over time, the percentage of individuals positive for anti-S IgG remains stable.

## Functional Antibody Response Changes Over Time Post SARS-CoV-2 Infection

Besides neutralization, antibodies can mediate Fc-effector functions, such as complement activation, killing of virus-infected cells and phagocytosis of viral particles (20). To further define the humoral response in these individuals, we assessed antibody effector functions *in vitro*. The NIBSC references were utilized to validate the assays and nineteen pre-pandemic samples were measured to set the cutoff for each assay. Antibody-dependent cellular phagocytosis (ADCP) assay measures the engulfment of neutravidin beads coated with SARS-CoV-2 derived S1 by THP-1 cells (**Figures 2A**, **S4**). A decrease in ADCP can be observed between the acute and late convalescent phase (p=0.005, **Figures 2B, C**). The percentage of subjects with ADCP activity decreased from 73% to 55% over time. However, when calculating the proportion of ADCP within the total anti-S IgG, we observed a significant increase of the proportion of ADCP over time (p=0.003, **Figure 2D**).

Next, to evaluate the contribution of anti-S antibodies to complement dependent cytotoxicity (CDC), we assessed cell death in Raji cells engineered to express S protein in the presence of normal human serum as source of complement (**Figure 2E**, **S5**) (21). No differences in CDC activity was observed between the acute and late convalescent phase, where 60% and 56% of the subjects showed CDC activity, respectively

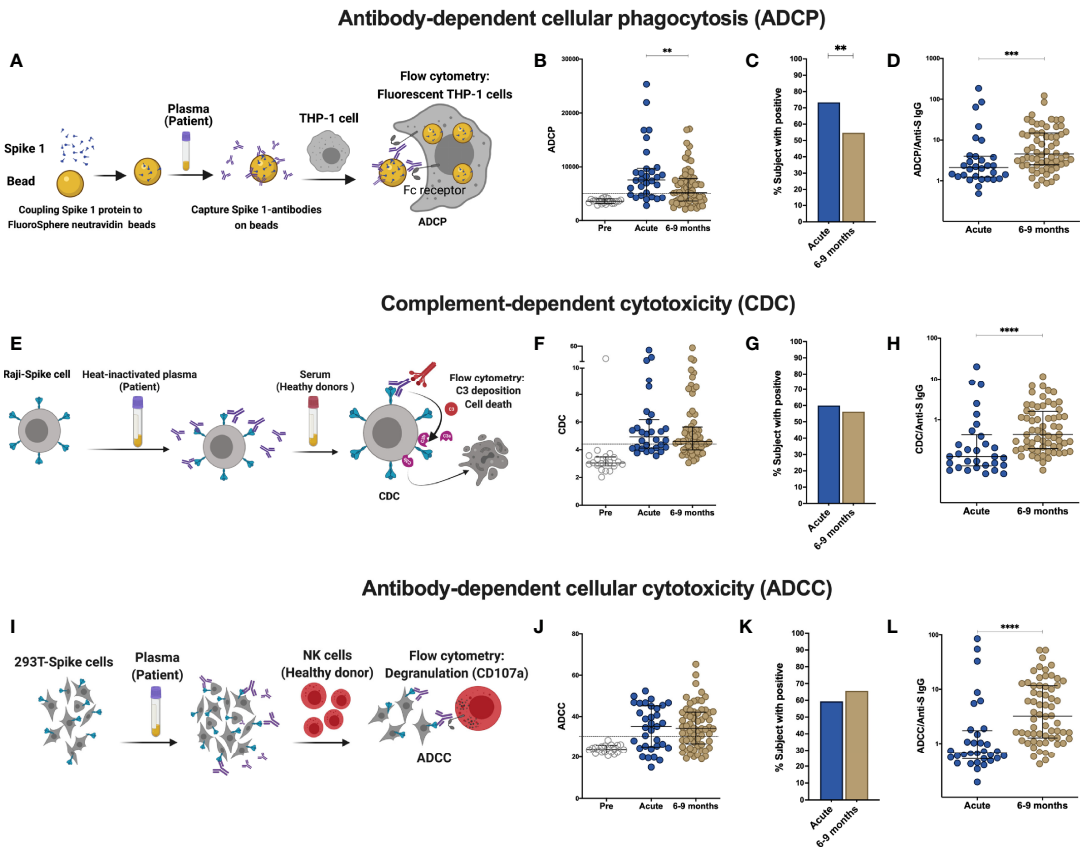


**FIGURE 2** | Comparison of effector function profiles of plasma from SARS-CoV-2-infected individuals during the acute phase and 6-9 months post infection. Non-infected samples obtained before the pandemic (pre), and SARS-Cov-2 infected individuals were sampled 2-9 days post laboratory confirmation and 6-9 months later. **(A)** Schematic representation of the antibody-dependent cellular phagocytosis (ADCP) assay. **(B)** Comparison of ADCP activity in pre-pandemic samples, SARS-CoV-2-infected individuals in the acute phase of infection and 6-9 months later. **(C)** Percentage of individuals with ADCP above the cutoff for positivity. **(D)** Ratio of ADCP to anti-spike IgG measured by S-Flow. **(E)** Schematic representation of complement-dependent cytotoxicity (CDC) assay. **(F)** Comparison of CDC activity in pre-pandemic samples, SARS-CoV-2-infected individuals in the acute phase of infection and 6-9 months later. **(G)** Percentage of individuals with CDC above the cutoff for positivity. **(H)** Ratio of CDC to anti-spike IgG as measured by S-Flow. **(I)** Schematic representation of antibody-dependent cellular cytotoxicity (ADCC). SARS-CoV-2 plasma induced NK degranulation as measured by CD107a staining using spike-expressing 293T cells as target cells. NK cells were isolated from healthy donors. **(J)** Comparison of ADCC activity in pre-pandemic samples, SARS-CoV-2-infected individuals in the acute phase of infection and 6-9 months later. **(K)** Percentage of individuals with ADCC above the cutoff for positivity. **(L)** Ratio of ADCC to anti-spike IgG as measured by S-Flow. Statistical comparisons were performed by Mann Whitney test. The dashed line indicates the cutoff for positivity set based on values calculated following formula: cut-off = % mean positive cells from 19 pre-pandemic samples + 3x standard deviation. Each dot represents result from a single individual. Lines represent median and IQR. **p < 0.01, ***p < 0.001, and ****p < 0.0001. Pre-pandemic: n=19, acute ADCP and CDC: n=30, acute ADCC: n=32, 6-9 months ADCP, CDC and ADCC: n=64.

(**Figures 2F, G**). The proportion of CDC-mediating antibodies within the total anti-S IgG fraction significantly increased between acute and late convalescence (p=0.0002, **Figure 2H**).

Killing of virus-infected cells can also be mediated by activated NK cells, after binding of immunocomplexes to CD16 (20). Therefore, antibody-dependent cellular cytotoxicity (ADCC) activity was measured using S-expressing 293T cells as target cells with degranulation measured by CD107a staining in primary NK cells as a readout for ADCC (**Figures 2I**, **S6**). ADCC activity did not change between the acute and late convalescent phase (**Figures 2J, K**). At both time points, 59% - 66% of individuals showed anti-S mediated ADCC activity. However, similar to ADCP and CDC, the proportion of ADCC-mediating antibodies within the fraction of anti-S IgG increased significantly over time (p<0.0001, **Figure 2L**).

Analyzing only individuals with paired samples available, revealed similar results as the cohort as a whole (**Figures S3C–H**). Overall, these data show that antibody effector functions mediated by S-specific antibodies remain stable over time and that the proportion of the functional antibody response within the total anti-S antibodies increases over time.

## SARS-CoV-2 Infection Induces a Sustained Memory B Cell Compartment Reacting Against Spike and Nucleocapsid Protein 6–9 Months After Infection

Upon re-infection, memory B cells are rapidly activated to differentiate into antibody-producing plasmablasts and/or re-

initiate germinal centers in the case of secondary heterologous infection with antigenically similar pathogens (40). Therefore, they may play an important role in long-term immune memory to SARS-CoV-2 and their evolving variants. We assessed the phenotype and frequency of antigen-specific memory B cells from 40 SARS-CoV-2 infected individuals in the cohort by staining with site-specific biotinylated recombinant S1 and N protein (**Figures 3A**, **S7A, B**). At late convalescence, 0.10% of median of the total $CD27^+$ B cells are S1-specific, whereas 0.66% of median are N-specific ($p<0.0001$, **Figure 3B**). We observed the highest frequencies of S1-specific and N-specific B cells in the activated memory B cell compartment ($CD27^+CD38^+$) compared to plasma blast ($CD27^+CD38^{hi}$) and resting memory compartments ($CD27^+CD38^-$) (**Figures 3C, D**) (41, 42). The proportion of $CD27^+CD38^+$ S1-specific B cells (median=75%, IQR=30%) is significantly increased compared to the proportion of $CD27^+CD38^+$ N-specific B cells (median=39%, IQR=26%, Mann-Whitney Test, $p<0.0001$) (**Figure 3E**). Moreover, the

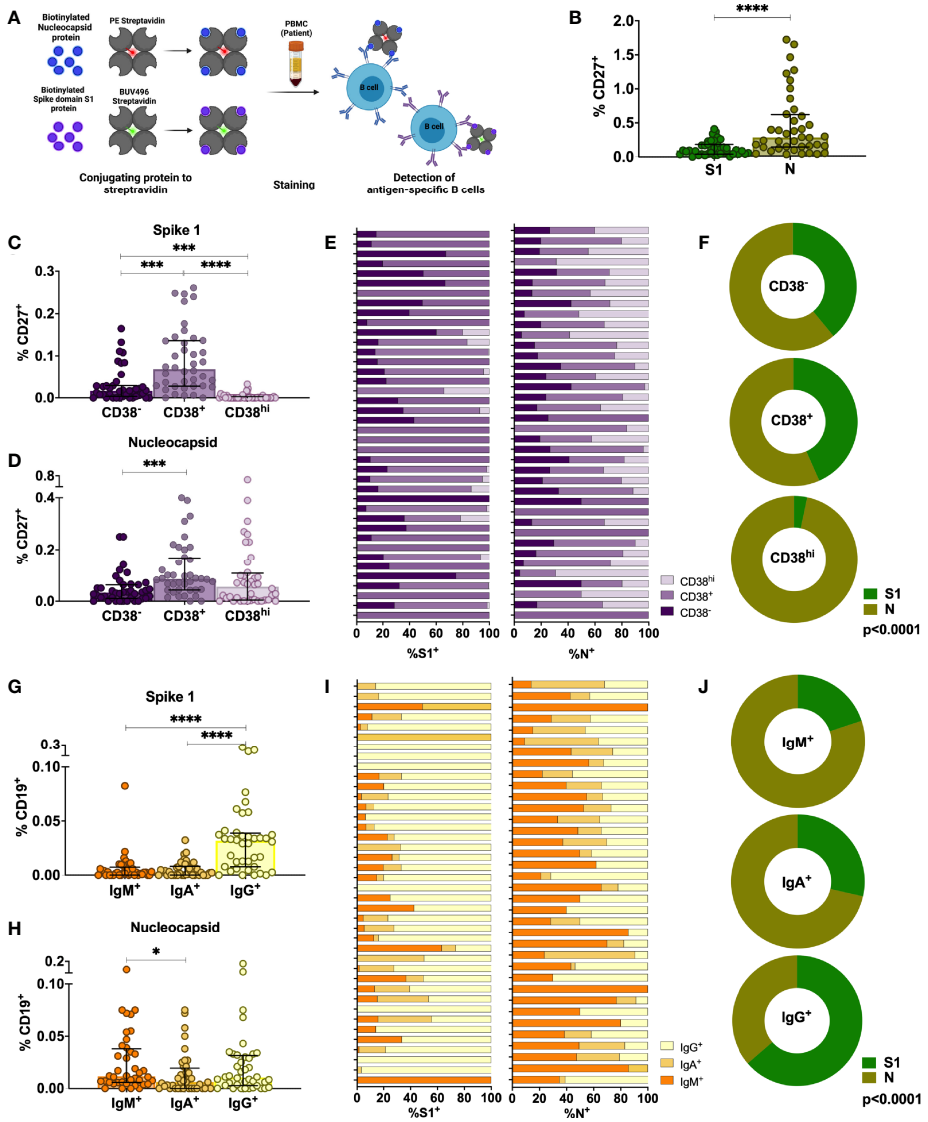


**FIGURE 3** | Characterization of antigen-specific memory B cells in the peripheral blood of individuals infected with SARS-CoV-2 6-9 months after infection. **(A)** Schematic representation of the memory B cell assay. **(B)** Comparison of percentages of S1-specific or N-specific memory B cells ($CD19^+CD27^+$). **(C, D)** Percentages of S1- and N-specific B cells among resting memory B cells ($CD38^-$), activated memory B cells ($CD38^+$) or plasmablasts within the $CD27^+$ memory B cell population. **(E, F)** Proportion of S1-specific and N-specific $CD27^+CD19^+$ B cell subsets for each individual and the whole cohort **(G, H)** Percentages of S1- and N-specific cells in non-class-switched B cells ($IgD^-IgM^+$) or class-switched B cells ($IgD^-IgA^+$ or $IgD^-IgG^+$). **(I, J)** Proportion of S1-specific and N-specific switched and unswitched $CD19^+$ B cells for each individual and for the whole cohort. Statistical comparisons were performed by Mann-Whitney test **(B)**, Wilcoxon Rank Sum test **(C, D, G, H)** or Chi-square test **(F, J)**. Each dot represents result from a single individual. Lines represent median and IQR (n=40). *$p < 0.05$, ***$p < 0.001$, and ****$p < 0.0001$. n = 40. S1, subunit 1 of spike protein; N, Nucleocapsid protein.

proportion of S1- versus N-specific B cells varies within each CD27$^+$ B cell subset (p<0.0001, **Figure 3F**). We next analyzed S1- and N-specific B cells within the unswitched (IgD$^-$IgM$^+$) and switched (IgD$^-$IgG$^+$ and IgD$^-$IgA$^+$) B cell compartments (**Figure S7A**). S1-specific B cells were mainly IgD$^-$IgG$^+$, whereas N-specific B cells were either IgD$^-$IgM$^+$ or IgD$^-$IgG$^+$ (**Figures 3G, H**). The proportion of IgD$^-$IgG$^+$ S1-specific B cells (median=75%, IQR=24%) was significantly increased compared to the proportion of IgD$^-$IgG$^+$ N-specific B cells (median=37%, IQR=17%) (p<0.0001) (**Figure 3I**). Therefore, within each switched B cell subset, the proportion of S1- versus N-specific B cells was different (p<0.0001) (**Figure 3J**). Taken together, SARS-CoV-2 infection induces a robust memory B cell response targeting both S and N.

## SARS-CoV-2 Infection Induces Mainly Spike and Membrane Protein-Specific Memory CD4$^+$ and CD8$^+$ T Cells That Are Maintained Up to 6–9 Months After Infection

In addition to humoral immune memory, the generation and maintenance of virus-specific cellular immune responses is critical to help prevent reinfection. Long-term maintenance and phenotypes of SARS-CoV-2-specific memory T cell responses are still under investigation (4, 43, 44). SARS-CoV-2-specific CD4$^+$ and CD8$^+$ T cells were assessed in 33 individuals at late convalescence by incubating PBMCs with peptide pools covering immunodominant sequences of the viral S1, M and N protein (**Figure 4A**). Post incubation, activation induced marker (AIM) assays identified CD4$^+$ antigen-specific cells using OX40$^+$CD137$^+$ combined with phenotypic markers to measure different memory and T helper (Th) subsets (**Figures S8A–D**). Percentages of both S1- and M-specific CD4$^+$ T cells were significantly increased compared to the percentage of N-specific cells (p<0.0001, p=0.0002), **Figure 4B**). Phenotypically, 42% of virus-specific T cells displayed an effector memory phenotype (CD45RA$^-$CCR7$^+$) and 87% of the cells showed a Th1-skewed phenotype (CXCR3$^+$CCR6$^-$) (**Figures 4C, D**). Comparing the memory phenotype of S1-, M- and N-specific cells, we observed that a lower proportion of S1-specific cells displayed an effector memory phenotype (23%) compared to M-specific cells (41%, p=0.0457) and N-specific cells (58%, p<0.0001) (**Figure S9A**). Moreover, 97% of M-specific cells showed a Th1-skewed phenotype compared to only 65% (p<0.0001) of the S1-specific cells and 71% (p=0.0130) of the N-specific cells (**Figure S9B**). In eight individuals, sufficient cell numbers were available to assess functionality by cytokine production after peptide stimulation using a multi-parameter *ex vivo* intracellular cytokine staining (ICS) assay (**Figure S8E**). SARS-CoV-2-specific CD4$^+$ T cells produced Interleukin (IL)-2 (36%) or IL-6 (28%) after peptide stimulation, and were polyfunctional (**Figures 4E, F**). Percentages of IL-2$^+$ and IL-17$^+$ cells were significantly higher after S1 stimulation compared to M stimulation (p=0.046, p=0.017) (**Figure S9C**).

Next, we assessed the frequency and phenotype of cytotoxic CD8$^+$ T cells by AIM assay using CD69$^+$CD137$^+$ to identify antigen-specific CD8$^+$ T cells. Frequency of total SARS-CoV-2-specific CD8$^+$ cells is 0.44% (median) (**Figure 5A**) with 61% of

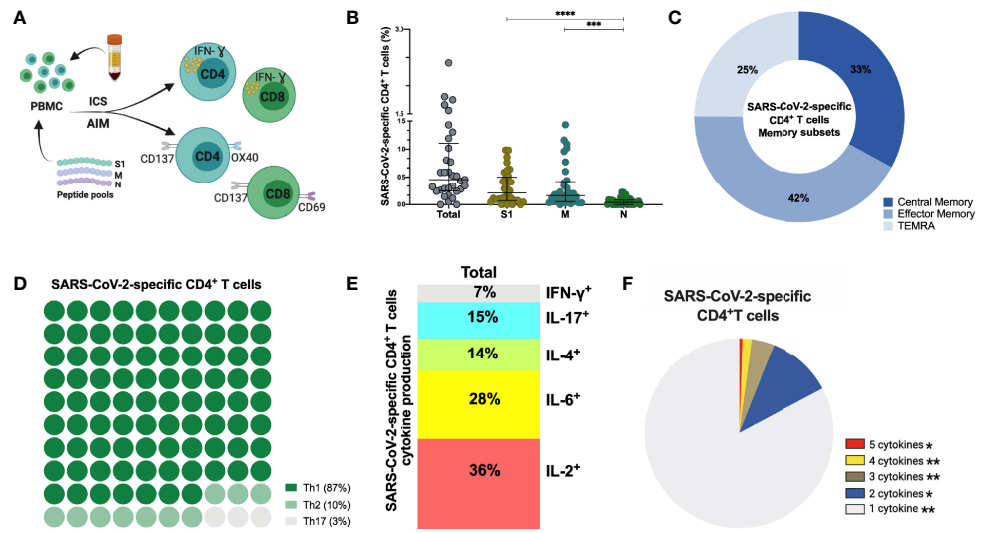


**FIGURE 4** | SARS-CoV-2-specific CD4$^+$ T cells 6-9 months post-infection. **(A)** Schematic representation of the CD4$^+$ T cell assay **(B)** Frequency (percentage of CD4$^+$ T cells) of total SARS-CoV-2-specific CD4$^+$ T cells after overnight stimulation with S, M and N peptide pools as assessed by induced expression of OX40 and CD137. Each dot represents result from a single individual (n=33). Lines represent median and IQR. **(B)** Distribution of SARS-CoV-2–specific CD4$^+$ T cells among central memory, effector memory, and terminally differentiated effector memory cells (TEMRA). **(C)** Frequencies of SARS-CoV-2-specific CD4$^+$ T helper (Th) subset. **(D)** Cytokine production and **(E)** pie chart representing the multifunctional SARS-CoV-2-specific CD4$^+$ T cell response assessed by intracellular cytokine staining after incubation with SARS-CoV-2 peptides compared to unstimulated control, n=8. SARS-CoV-2 specific activation and cytokine production were calculated by subtracted the unstimulated control from the SARS-CoV-2 peptide stimulated condition. Statistical comparisons were performed by Kruskal-Wallis test **(B)** and Wilcoxon Rank Sum test **(F)**. *p < 0.05, **p < 0.01, ***p < 0.001, ****p < 0.0001. S1, subunit 1 of spike protein; M, membrane protein; N, nucleocapsid protein.

these SARS-CoV-2-specific CD8$^+$ T cells being terminally differentiated effector memory cells (TEMRA, CD45RA$^+$CCR7$^-$) (**Figures 5B**, **S9D**). No differences were observed between S1-, M- and N-specific CD8$^+$ T cells. Similar to antigen-specific CD4$^+$ T cells, SARS-CoV-2-specific CD8$^+$ T cells produced either IL-2 (56%) or IL-6 (16%) after peptide stimulation, and were polyfunctional (**Figures 5C, D**), (**Figure S9E**). Interestingly, 2/33 (6%) individuals displayed no CD4$^+$ T cell reactivity, and 6/33 (19%) individuals lacked a CD8$^+$ T cell response after stimulation. In summary, sustained and functional CD4$^+$ and CD8$^+$ T cell responses are detected in the study participants, even after experiencing only mild or asymptomatic SARS-CoV-2 infection. These data suggest that SARS-CoV-2 can induce a long-lived cellular immune response, which could confer protection after reinfection or could be reactivated with vaccination.

## Symptomatic Infection Is Associated With Increased ADCC Activity and Increased Frequency of SARS-CoV-2-Specific CD4$^+$ T Cells Observed 6–9 Months After Infection

In order to assess if symptomatic disease is associated to altered immune memory formation, we compared the functional immune response between asymptomatic and symptomatic patients with mild/moderate clinical presentation. Overall, no differences occurred in the titers of anti-S IgM, IgA, IgG, neutralization or antibody-effector functions assessed in the acute phase of infection (**Figures 6A**, **S10**). At late convalescence, symptomatic disease resulted in increased ADCC activity compared to asymptomatic individuals (p=0.0034) (**Figure 6A**). Other Fc-mediated effector functions, such as ADCP and CDC and neutralizing titers were not different between the patients (**Figure S10**). Percentages of N-specific CD27$^+$ B cells, but not S1-specific, were increased in asymptomatic individuals versus patients who were symptomatic (p=0.051) (**Figure 6B**). Symptomatic disease resulted in increased percentage of SARS-CoV-2-specific CD4$^+$ T cells (p=0.0018) with a central memory phenotype (p=0.0498) (**Figures 6C, D**), but no differences were observed in the CD8$^+$ T cell compartment (**Figure S10**).

These data suggest that the outcome of acute infection has an imprint on the memory immune response with implications for response to subsequent infection or vaccination.

## Correlations Between Various Aspects of the Functional Anti-Viral Memory Response

In order to assess the relation between antibody titers, functional humoral immune memory, and the cellular T and B cell

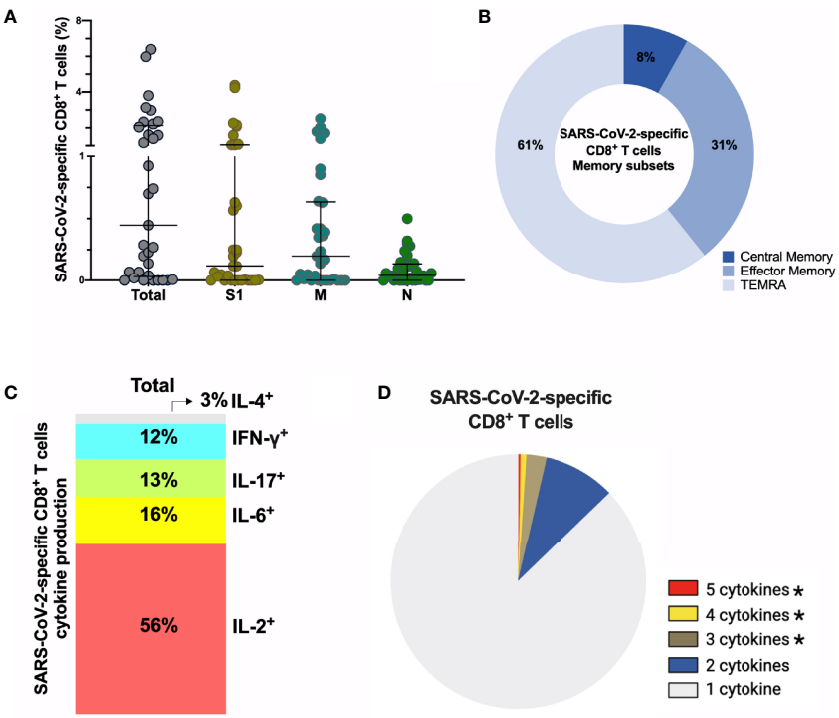


**FIGURE 5** | SARS-CoV-2-specific CD8$^+$ T cells 6-9 months post-infection. **(A)** Frequency (percentage of CD8$^+$ T cells) of total SARS-CoV-2-specific CD8$^+$ T cells after overnight stimulation with S, M and N peptide pools as assessed by induced expression of CD69 and CD137. Each dot represents result of a single individual (n=33). Lines represent median and IQR. **(B)** Distribution of SARS-CoV-2-specific CD8$^+$ T cells among central memory, effector memory, and terminally differentiated effector memory cells (TEMRA). **(C)** Cytokine production and **(D)** pie chart representing the multifunctional CD8$^+$ T of SARS-Cov-2-specific T cells assessed by intracellular cytokine staining after incubation with SARS-CoV-2 peptides compared to unstimulated control, n=8. SARS-CoV-2 specific activation and cytokine production were calculated by subtracted the unstimulated control from the SARS-CoV-2 peptide stimulated condition. **(A)** Kruskal-Wallis test and **(D)** Wilcoxon Rank Sum test. *p < 0.05. S1, subunit 1 of spike protein; M, membrane protein; N, nucleocapsid protein.

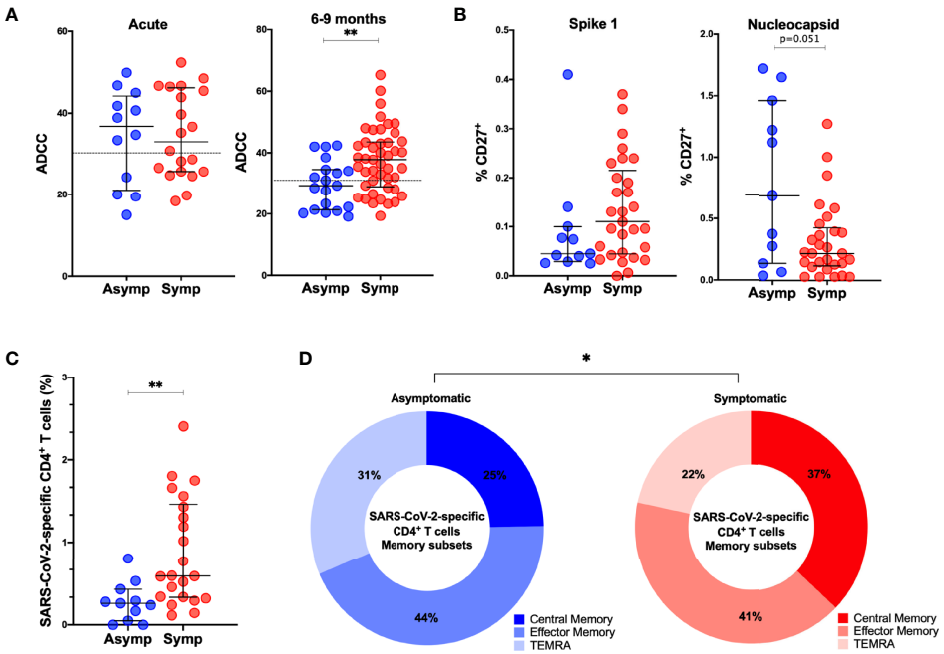


**FIGURE 6** | Comparison of adaptive immune memory in asymptomatic and symptomatic individuals. **(A)**. Comparisons of ADCC activity in asymptomatic (asymp; n=12) versus symptomatic (symp; n=20) individuals in the acute phase and 6-9 months after confirmed infection using 293T-spike cells as target cell. Percentage of CD107a positive cells is measured as readout for ADCC. **(B)** Comparison of percentages of S1-specific or N-specific memory B cells ($CD19^+CD27^+$) between 11 asymptomatic individuals and 29 symptomatic individuals. **(C)** Frequency (percentage of $CD4^+$ T cells) of total SARS-CoV-2-specific $CD4^+$ T cells after overnight stimulation with peptide pools comparing asymptomatic individuals (asymp; n=11) with symptomatic patients (symp; n=22). **(D)** Comparison of $CD4^+$ T cell memory phenotype between asymptomatic individuals (asymp; n=11) and symptomatic patients (symp; n=22). Statistical comparisons were performed by **(A–C)** Mann Whitney tests and **(D)** Chi-square test for trend *p < 0.05, **p < 0.01.

compartment we performed extensive correlation analysis (**Figure 7A**). Age correlated to anti-S antibody titers and S1-specific $CD19^+IgD^-IgG^+$ and $CD19^+CD27^+$B cells. In the acute phase of infection, anti-S IgG, IgM and IgA titers, functionality, measured by seroneutralization, and effector functions correlated. Seroneutralization, anti-S IgA, and ADCC correlated over time, albeit not very strong. Of note, viral shedding did not correlate with anti-SARS-CoV-2 immunity (**Figure 7A**), and subdividing individuals into short or long viral RNA shedding using an arbitrary cut-off of 10 days did not yield any differences in SARS-CoV-2 specific immune responses (**Figure S11**).

At late convalescence, anti-S IgG correlated with all three effector functions, but not with neutralizing capacity. Within the B cell compartment, N-specific $IgD^-IgG^+$, $IgD^-IgA^+$ and $CD27^+$ B cells correlated to one another, as did S1-specific $IgD^-IgG^+$, $IgD^-IgA^+$ and $CD27^+$ B cells. No correlation was identified between S1- and N-specific B cells. Anti-S IgG titers, ADCP, and CDC correlated with S1-specific $IgD^-IgG^+$ and $CD27^+$ B cells. The S-specific $CD4^+$ T cell responses correlated with S-specific $CD8^+$ T cell responses, but did not correlate to antibody titers nor to effector functions or to S1-specific B cells.

Next, we assessed in more detail the relationship between the different effector functions at late convalescence. We included 56 individuals with measurable anti-S IgG above the cutoff based on the pre-pandemic samples (**Figures 1**, **7B**). We found that plasma from each individual could induce neutralization or at least one antibody-effector function (ADCP, CDC and ADCC). In 11 out of the 56 individuals (19.6%), both neutralization titers and all antibody-effector functions could be measured. Eighteen out of the 56 individuals (32,1%) had measurable antibody-effector functions, but no neutralizing titers, while in 4 out of the 56 (7.1%) individuals only neutralizing titers were detected (**Figure 7B**).

We further detailed if individuals showed measurable immune responses in one or multiple immune compartments at 6-9 months post infection. In twenty individuals we assessed in parallell anti-S IgG, S1-specific B cells and S-specific T cells. We set an arbitrary cutoff for positive B and T cell responses at 0.1% of S-specific $CD27^+$ B, $CD4^+$ T and $CD8^+$ T cells. Four out of the 20 individuals (20.0%) had responses in all compartments. Three individuals (15.0%) showed only measurable anti-S IgG titers. Moreover, 7 individuals (35.0%) had anti-S IgG titers and detectable S1-specific $CD27^+$ B cells but no S-specific T cell responses. In contrast, 9 (45.0%) individuals had measurable S-specific T cell responses, but no S1-specific B cell responses or anti-S antibody titers (**Figure 7C**).

Overall, different aspects of a functional immune memory response do not fully correlate with one another and require separate evaluation when considering long-term immune memory to SARS-CoV-2.

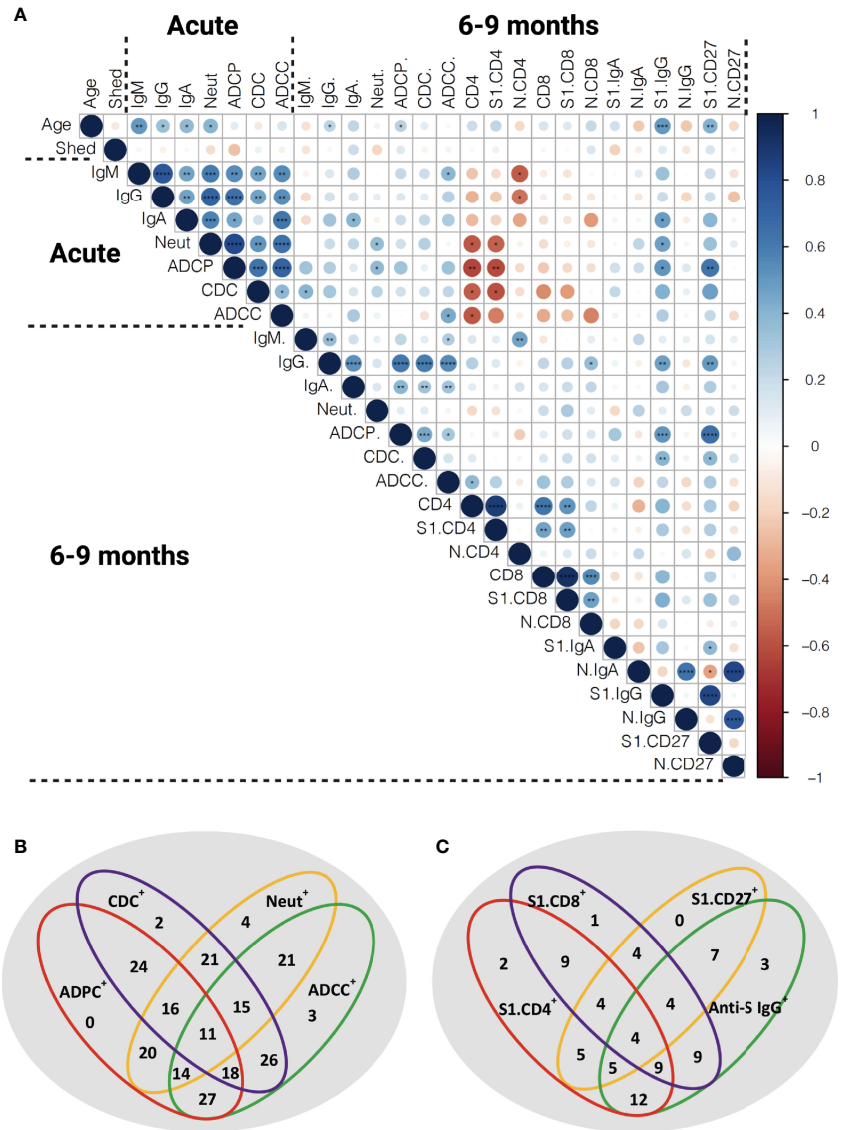


**FIGURE 7** | Correlation of the functional anti-SARS-CoV-2 immune responses. **(A)** Spearman correlation matrix showing humoral immune memory and effector functions measured in the acute phase and 6-9 months post infection were correlated to each other and to frequencies of antigen-specific B and T cells measured 6-9 months after infection. Red represents a negative correlation between two variables and blue indicates a positive correlation. The size of the dot represents the magnitude of the correlation coefficient. Statistical analysis was performed with spearman correlation test. *p <0.05, **p < 0.01, ***p < 0.001, ****p < 0.001. IgM: anti-S IgM titers, IgG: anti-S IgG titers, IgA: anti-S IgA titers, Neut: FRNT50 titers, CD4: total SARS-CoV-2 specific $CD4^+$ T cells, S1.CD4: S-specific $CD4^+$ T cells, N.CD4: N-specific $CD4^+$ T cells, CD8: total SARS-CoV-2 specific $CD8^+$ T cells, S1.CD8: S-specific $CD8^+$ T cells, N.CD8: N-specific $CD8^+$ T cells, S1.IgA: S1-specific $IgD^-IgA^+$ B cells, N.IgA: N-specific $IgD^-IgA^+$ B cells, S1. IgG: S1-specific $IgD^-IgG^+$ B cells, N.IgG: N-specific $IgD^-IgG^+$ B cells, S1.CD27: S1-specific $CD27^+$ B cells, N.CD27: N-specific $CD27^+$ B cells. **(B)** Venn diagram showing the relation of anti-S humoral immune responses at late convalescence. All individuals with detectable anti-S IgG titers are included (n=56). **(C)** Venn diagram showing the relation of anti-S IgG, S1-specific $CD27^+$ B cells and S1-specific T cells at late convalescence. The cutoffs for S1-specific CD27+ B cell response and S-specific $CD4^+$ and $CD8^+$ T cell responses were arbitrarily set above 0.1% (n =20).

## DISCUSSION

In this study, we investigated a partially asymptomatic cohort of Cambodian individuals in the acute and late convalescent phase for anti-S antibody titers, neutralization and effector functions, as well as SARS-CoV-2-specific B and T cell responses. As Cambodia was relatively COVID-19-free throughout 2020 (45), it is highly unlikely this cohort had additional exposure events after inclusion in this study, that could have boosted their immune memory to SARS-CoV-2. One limitation is the uncertainty of the exact timing of exposure/infection, as infections were identified by screening at entry into Cambodia rather than in a direct surveillance or community cohort.

Studies assessing long-term immune memory to SARS-CoV-2 in Asian populations are scarce (18, 34–36, 46). Historically,

the population in East Asia seems to be more exposed to coronavirus-like viruses as only East Asian population show genetic adaptation to coronaviruses (47). The main natural reservoir of SARS-related coronaviruses is believed to be Horseshoe bats (genus *Rhinolophus*), which are endemic to Southeast Asia and China (48–51). Whether possible cross-reactivity to other coronavirus-like viruses or hCoVs may have influenced the adaptive immune response to SARS-CoV-2 in Southeast Asian populations remained to be investigated.

As shown in previous studies anti-S IgM, IgG and IgA titers declined over time and anti-S IgG becomes the major isotype at late convalescence (4, 52, 53). In this study, IgA titers were the most affected over time. The formation of anti-S IgA is shown to be dependent on local lung inflammation (6, 54, 55) hence titers decline the strongest in asymptomatic/mild patients. Titers of neutralizing antibodies are reported to reach their maximum within the first month after infection and then decay, but mostly remain detectable six months and even up to one year after infection (4, 12). A relatively low rate of individuals retained neutralizing antibodies at late convalescence in this cohort (56%) as most longitudinal studies found 76-98% of individuals remaining positive (4, 21). This might be attributed to the absence of possible re-exposure and/or the consequence of asymptomatic/mild infection (12, 27, 43, 53). One caveat is that it is possible that the humoral responses for some donors were still on the rise and had not peaked by the detection at the acute timepoint.

In contrast with other papers, neutralizing titers did not correlate to anti-S IgG antibodies at late convalescence. This might be due to the genetic background or previous immunity to other hCoVs of the participants inducing antibodies binding to different viral epitopes, or could be due to the different technique to measure anti-S binding and neutralizing antibodies (56, 57).

Fc-mediated effector functions contribute to clearance of virus-infected cells but are often critically overlooked. SARS-CoV-2 infection induces Fc-mediated effector functions irrespective of disease outcome (21–23). Antibody effector functions develop rapidly after infection and correlate with anti-S IgG and neutralizing titers in the acute phase and at late convalescence (21, 22). In this current study, we assessed three antibody effector functions using cell-based assays. Between 55-66% of individuals showed antibody effector function activity up to nine months after infection. Also, ADCC persisted in a higher percentage of individuals compared to neutralization or other effector functions (24, 25). We report here the maintenance of CDC over time suggesting that both ADCC and CDC can contribute to protection from re-infection. ADCP levels decreased over time which could have consequences for antigen presentation and macrophage activation upon re-infection (58). Interestingly, the ratio of S-mediated effector functions over total anti-S IgG increases over time. Together with reports showing the evolution of the BCR repertoire over time (27, 59, 60), these data indicate ongoing affinity maturation and evolution of the antibody response to a more functional response. Therefore, measurement of only S-binding antibodies at late convalescence does not reflect their function.

S-, RBD- and N-specific memory B cells are maintained more than six months post symptom onset and their frequency increased over time (4, 61, 62). In this cohort, S1-and N-specific memory B cells persisted up to 6-9 months post infection with some variability between individuals. One of the caveats of this study is that the cut-off for positive staining in antigen-specific B/T cells is arbitrary, which may lead to over-estimate the true number. The percentage of S1-specific IgG B cells correlated with S-specific IgG antibodies, and S1-specific B cells displayed an activated phenotype. This suggests that these B cells could be recruited after secondary exposure with SARS-CoV-2 and might confer some level of protection against infection with new variants or could be re-activated after vaccination *via* additional diversification trough germinal center responses (40, 63).

Anti-SARS-CoV-2 T cell immune memory was assessed by AIM, which is a sensitive assay that provides a broader picture of the overall antigen-specific T cell response, compared to cytokine-detection based assays (8, 64). Persistence of functional memory T cells after SARS-CoV-2 infection has been reported, also after asymptomatic infection (4, 65). Similar to other reports, virus-specific memory $CD4^+$ T cells were skewed to a Th1 or Th1/Th17 profile and displayed mainly an effector memory ($CD45RA^-CCR7^-$) phenotype (28, 65, 66). Virus-specific $CD8^+$ T cells consisted mostly of cells with a TEMRA phenotype, a compartment of cytotoxic $CD8^+$ T with limited proliferative potential (66). Polyfunctional virus-specific $CD4^+$ and $CD8^+$ T cells could be detected, mainly secreting IL-2 (18, 43), albeit we could only include few individuals in this analysis. Similar to other long-term cohorts, virus-specific $CD4^+$ and $CD8^+$ cells can be detected in up to 90% - 70% of the individuals, respectively (31). Hence, cellular immune responses might confer protection after reinfection with variants of concern (67).

Differences in frequency and phenotype of N- and S-specific B and T cells has been reported before (4, 5, 28, 43). This might be due to the difference in antigen availability, persistence, and immunological context. Together with other envelope proteins, S proteins cover the surface of the virus and bind to the host cell, while the N protein underlies viral packaging and hence is less accessible (68). The N protein is more conserved among coronaviruses (68), whereas S protein and especially the RBD-bearing S1 subunit are more prone for acquiring mutations (69, 70). Consequently, anti-N IgG rather than anti-S1 IgG can be found in individuals not exposed to SARS-CoV-2 (68, 71, 72). This might explain the observed higher frequency of N-specific B cells in our study.

Correlations between $CD4^+$ T cells and humoral responses can be observed in some long-term cohorts (28, 30, 73, 74) but not all (4). In this study, there was no correlation between the S-specific cellular and humoral immune compartment at late convalescence. Importantly, in 45% of the individuals anti-S $CD4^+$ and $CD8^+$ T cell responses could be detected but their anti-S antibody titers were below the pre-pandemic detection threshold. Therefore, neither anti-S IgG nor neutralizing antibodies are a good proxy to determine the cellular response to SARS-CoV-2. Interestingly, we showed that 32% of the

individuals had measurable antibody-effector functions, but no neutralizing titers, while in 7% of the individuals only neutralizing titers were detected. Hence, subtle differences in anti-S antibody titers, neutralization and Fc-related functions might lead to a different disease outcome upon re-exposure. Therefore, serological testing alone might not be sufficient to understand the full spectrum of long-term immune memory generated after SARS-CoV-2 infection.

In this cohort, the duration of SARS-CoV-2 RNA shedding did not correlate with the magnitude of anti-SARS-CoV-2 immunity, either measured in the acute phase or at late convalescence, which is in contrast to previous studies (12, 34, 75) and could be explained by the inclusion of mainly asymptomatic and mild cases.

The development, characteristics and functionality of the totality of long-term immune memory in asymptomatic infected individuals remains to be further characterized. We observed an increase of ADCC at late convalescence in patients who had mild/moderate disease compared to asymptomatic individuals. This observation is in line with studies showing increased anti-S IgG afucosylation in severe patients compared to mild and asymptomatic cases (76, 77). Indeed, afucosylated monoclonal antibodies can cause elevated ADCC though increased IgG-FcγRIIIa affinity (78, 79). More severe COVID-19 induced a stronger SARS-CoV-2-specific $CD4^+$ T cell response (28, 29). We confirm and extend these data as we observed lower levels of virus-specific $CD4^+$ T cells in asymptomatic individuals compared to mild/moderate cases. These data suggest that different disease outcome after infection results in altered long-term immune memory, which could shape the response to subsequent infection or vaccination.

Taken together, our work shows additional evidence of long-term and persistent immune memory after asymptomatic and mild SARS-CoV-2 infection. Furthermore, this cohort describes the immune response in individuals of Asian origin and in the absence of re-exposure to SARS-CoV-2. We show the persistence of humoral immune memory, antibody effector functions, and virus-specific memory T and B cells 6-9 months after infection, which do not correlate to each other. These data enhance our understanding of long-term functional immune memory.

# MATERIALS AND METHODS

## Human Subjects

Ethical approval for the study was obtained from the National Ethics Committee of Health Research of Cambodia. Written informed consent was obtained from all participants prior to inclusion in the study. Pre-pandemic blood samples were obtained from clinically healthy individuals included in the dengue vaccine initiative study in 2015-2016. Clinically healthy adult volunteers who presented at the International Vaccination Centre, Institut Pasteur du Cambodge before the onset of the pandemic were included to validate the antigen-specific B and T cell staining. Acute SARS-CoV-2 infected patients were identified *via* screening of imported cases in Cambodia between 6$^{th}$ March to 12$^{th}$ August 2020. All laboratory confirmed cases are quarantined and monitored for symptoms. Moreover, 1-15 follow-up nasopharyngeal/oropharyngeal swab samplings for SARS-CoV-2 detection were conducted to assess SARS-CoV-2 RNA shedding. Patients were only discharged after two consecutive negative RT-PCR tests within 48h. Symptomatic patients displayed mild/moderate symptoms such as running nose, cough, fever and difficult to breath. In total, we included 64 individuals for follow up. In 33 individuals, 2-9 days after laboratory confirmation, a blood sample was obtained. A second blood sample was obtained 6-9 months later from all 64 study participants. Participant characteristics and clinical signs are summarized in **Table S1**. Plasma was collected and stored at -80°C, The PBMCs were isolated *via* Ficoll-Paque separation, cryopreserved in 10% DMSO/FBS and stored in liquid nitrogen until analysis. The National Institute for Biological Standards and Control (NIBSC) 20/130 (research reagent) and 20/118 (reference panel) have been obtained from WHO Solidarity II, the global serologic study for COVID-19.

## SARS-CoV-2 Detection

Molecular detection of SARS-CoV-2 in combined nasopharyngeal/oropharyngeal swabs was performed as previously described (38). Briefly, RNA was extracted with the QIAamp Viral RNA Mini Kit (Qiagen) and real-time RT-PCR assays for SARS-CoV-2 RNA detection were performed in using primers/probes from Charité Virologie [Berlin, Germany (80)] to detect both E and RdRp genes.

## Virus Neutralization Assay

The detection of neutralizing antibodies was achieved by foci reduction neutralization test (FRNT) similar as described before (81) and adapted to SARS-CoV-2. Briefly, serial diluted, heat-treated plasma samples were incubated with a Cambodian SARS-CoV-2 isolate (ancestral strain; GISAID: EPI_ISL_956384 (38);) for 30min at 37°C and 5% $CO_2$. The mixtures were distributed on African green monkey kidney cells (VeroE6; ATCC CRL-1586) and incubated again for 30min 37°C and 5% $CO_2$. Afterwards, the mixtures were replaced by an overlay medium containing 2% carboxymethyl cellulose (Sigma-Aldrich) in Dulbecco's modified Eagle medium (DMEM; Sigma-Aldrich) supplemented with 3% FBS (Gibco) and 100 U/mL penicillin-streptomycin (Gibco). Infection was visualized 16-18h after inoculation by staining of infected cells with a SARS-CoV-2-specific antibody (rabbit, antibodies-online GmbH), targeting the S2 subunit of the viral spike protein, and afterwards with antibody anti-rabbit IgG HRP conjugate (goat; antibodies-online GmbH). Finally, cells were incubated with TrueBlue TMB substrate (KPL), and infection events appear as stained foci and were counted with an ELISPOT reader (AID Autoimmune Diagnostika GmbH, Strassberg, Germany). The amount of neutralizing antibodies is expressed as the reciprocal serum dilution that induces 50% reduction of infection (FRNT50) compared to the positive control (virus only) and is calculated by log probit regression analysis (SPSS for Windows, Version 16.0, SPSS Inc., Chicago, IL, USA). FRNT50 titers below 10 are considered negative.

## S-Expressing Cell Lines

Transfected cell lines, Raji (ATCC® CCL-86™) and 293T (ATCC® CRL-3216™), with SARS-Cov-2 spike plasmid or a control plasmid using Lipofectamine 2000 (Life technologies) are kind gifts from Olivier Schwartz, Institut Pasteur, Paris, France (21). Spike-expressing Raji cells and Raji control cells were cultured at 37°C, 5% CO2 in RPMI medium while 293T-spike cells and 293T control cells were cultured in DMEM medium. All media were completed with 10% FBS (Gibco, MT, USA), 1% L glutamine (Gibco), 1% penicillin/streptomycin and puromycin (1 µg/mL, Gibo™) for cell selection during the culture.

## S-Flow Assay

The S-Flow assay was performed as previously described (39). Briefly, plasma samples were diluted (1:200) in 1xPBS with 2mM EDTA and 0.5% BSA (PBS/BSA/EDTA) and incubated with 293T-spike cells (80000 cells/100µl) for 30 minutes on ice. The cells were washed with PBS/BSA/EDTA and stained either with anti-IgM PE (dilution 1:100, Biolegend) and anti-IgG Alexa Fluor™ 647 (dilution 1:600, Thermo Fisher) or anti-IgA Alexa Fluor 647 (dilution 1:800, Jakson ImmunoResearch) for 30 minutes on ice. The cells were washed with 1xPBS and fixed using buffer of the True-Nuclear Transcription Factor Staining kit (Biolegend). After fixing, the cells were washed and resuspended in 1xPBS. The results were acquired using FACS Canto II, BD Biosciences. The gating strategy for anti-IgM, anti-IgG or anti-IgA positive cells was based on the 293T control cells incubated with negative SARS-CoV-2 reference plasma. The data were reported as percentage of positive cells for anti-IgM, anti-IgG or anti-IgA. The NIBSC Research Reagent (20/130) and panel (20/118) (WHO Solidarity II) was utilized to set the cutoff for positivity based on the background staining of the negative SARS-CoV-2 plasma and calculated following formula: cut-off= % positive cells + 2x standard deviation.

## Antibody Dependent Cellular Phagocytosis (ADCP) Assay

THP-1 cells (ATCC® TIB-202™) were used as phagocytic cells. For this, 1 µg of biotinylated S1 protein (Genscripts) was used to saturate the binding sites on 1 µl of FluoroSphere neutravidin beads (Thermo Fisher) overnight at 4°C. Excess protein was removed by washing the pelleted beads. The protein-coated beads were incubated with 40 µl heated-inactivated plasma diluted in complete RPMI (1:40) for 15 minutes at room temperature. Then, $5x10^4$ THP-1 cells suspended in 50 µl complete RPMI were added to the complex and incubated for 16 hours at 37°C, 5% $CO_2$. After incubation, the cells were washed with 1xPBS and fixed using buffer in True-Nuclear Transcription Factor Staining kit (Biolegend). After fixing, the cells were washed and resuspended in 1xPBS. The samples were analyzed using FACS Canto II, BD Biosciences. Phagocytosis activity was scored by the integrate mean fluorescence intensity (iMFI) value (% positive fluorescence THP-1 cells x MFI of the positive fluorescence THP-1 cells).

## Complement Dependent Cytotoxicity (CDC) Assay

The assay used spike-expressing Raji cells as target cells, pooled serum (4 healthy donors) as complement source and heated-inactivated patient plasma as antibody source. In short, 50 µl of heated-inactivated plasma (1:50) were incubated with Raji-spike cells for 30 minutes at 37°C, 5% $CO_2$. Afterward, 50 µl of complete RPMI containing 15% of pooled serum was added into the cells and incubated at 37°C, 5% $CO_2$ for 14 hours. The cells were washed with PBS and stained with Zombie Aqua viability dye (BioLegend) for 20 minutes on ice and then stained anti-APC C3/C3b/iC3b antibody (Cedarlane) for 30 minutes on ice. The cells were fixed with fixation buffer in True-Nuclear Transcription Factor Staining kit (Biolegend) for 20 minutes on ice. After fixing, the cells were washed and resuspended in 1xPBS. The samples were acquired using FACS Canto II, BD Biosciences. The results were reported as percentage of cell death and MFI of C3 deposition on the cells.

## Antibody-Dependent Cellular Cytotoxicity (ADCC) Assay

The assay used 293T-spike cells as a target cell and purified NK cells from healthy donor PMBCs as effector cells. First, 293T-spike cells were incubated with heated-inactivated patient plasma diluted in complete DMEM medium (1:50) at 37°C, 5% $CO_2$ for 30 minutes. The NK cells were enriched by magnetic negative selection (Miltenyi) according to manufactor's instruction. The 293T-spike cells were washed five times with complete RPMI medium. The NK cells were mixed with 293T-spike cells at a ratio 1:1 at final volume of 100 µl complete RPMI. Anti-CD107a and Monensin (Biolegend) 1:1000 dilution were added to the suspension and incubated at 37°C, 5% $CO_2$ for 6 hours. The cells were washed with 1xPBS and stained with Zombie Aqua viability dye (BioLegend) for 20 minutes on ice. Then the cells were stained with anti-CD3 and anti-CD56 for 30 minutes on ice. The cells were washed and fixed/permeabilized using True-Nuclear Transcription Factor Staining kit (Biolegend) for 20 minutes on ice. After staining, the cells were washed and resuspended in 1xPBS. The samples were acquired using FACS Canto II, BD Biosciences.

## Detection of Antigen-Specific Memory B Cells

Biotinylated SARS-CoV-2 S1 protein and biotinylated SARS-CoV-2 N protein were purchased from GenScript. The biotinylated proteins were combined with different streptavidin (SA) fluorophore conjugates, BUV496 (BD Biosciences) and PE (Biolegend), respectively, at 1:1 molar ratio. Briefly, each SA was added gradually (3 times, every 20 minutes) to 20 µl of each biotinylated protein (1 µM) on ice. The reaction was quenched with D-biotin (GeneCopeia) at 50:1 molar ratio to SA for a total

probe volume of 30 µl for 30 minutes on ice. Probes were then used immediately for staining. Each staining used 5 µl of probe. Shortly, patient PBMCs was washed with 1xPBS and stained with Zombie Aqua viability dye (BioLegend) for 10 minutes on ice. The cells were stained with the probes. Then the cells were washed and stained with anti-IgG antibody, for 30 minutes on ice. After that, the cells were washed and stained with master mix containing of anti-CD3, anti-CD19, anti-CD27, anti-CD38, anti-IgD, anti-IgM and anti-IgA antibodies for 30 minutes on ice Antibodies are listed in **Table S2**. After staining, the cells were washed and resuspended in 1xPBS with 2% FBS. The samples were analyzed using FACS Aria, BD Biosciences. The flow cytometry gating strategy to classify memory B cell subsets and switched B cells is shown in **Figure S7**. Overall, 40 samples were of sufficient quality and were included in the analysis.

## Activation-Induced Markers (AIM) T Cell Assay

Antigen-specific $CD4^+$ and $CD8^+$ T cells, as well as memory T cells and T helper subsets were assessed by Activation-Induced Marker (AIM) assay (4, 8). Cells were cultured at 37°C, 5% $CO_2$, in the presence of SARS-CoV-2-specific S1, M and N protein pools [1 µg/mL] (PepTivator® SARS-CoV-2 regents; Miltenyi Biotec) in 96-well U-bottom plates at 0,5-1x$10^6$ PBMCs per well. After 24 hours, cells were washed in 1xPBS supplemented with 0.5% bovine serum albumin (BSA) and 2 mM EDTA (FACS buffer) and stained with Zombie Aqua Fixable Viability kit (Biolegend) and incubated for 20 min at 4°C followed by surface staining for 30 min at 4°C. Stained cells were washed and resuspended in FACS buffer and analyzed using a FACSAria Fusion (BD Biosciences). Antibodies are listed in **Table S2**. Negative controls without peptide stimulation were included for each donor. Antigen-specific $CD4^+$ and $CD8^+$ T cells were measured subtracting the background (unstimulated control) from the peptide-stimulated sample. Negative results were set to zero. Data were analyzed with FlowJo software version 10.7.1 (FlowJo LLC). Overall, 33 samples were of sufficient quality and were included in the analysis.

## Intracellular Staining (ICS) Assay

Functional SARS-CoV-2-specific $CD4^+$ and $CD8^+$ T cells were assessed by surface and intracellular staining in a subset of individuals if sufficient amount of PBMCs were obtained (n=8). Cells were cultured at 37°C, 5% CO2, in the presence of SARS-CoV-2-specific S1, M and N protein pools separately [1 µg/mL each] (PepTivator® SARS-CoV-2 reagents; Miltenyi Biotec), Monensin (Biolegend) 1:1000 dilution and anti-Human CD28/CD49d purified [100 µg/mL] (BD Bioscience) in 96-well U-bottom plates at 0,5-1x$10^6$ PBMCs per well. After 6 hours, cells were washed in FACS buffer and stained using a Zombie Aqua Fixable Viability kit (Biolegend) and incubated for 20 minutes at 4°C. Cells were then washed in PBS and fixed/permeabilized with True-Nuclear™ Transcription Factor Buffer Set (Biolegend). Surface (CD3, CD4 and CD8) and intracellular markers (IFN-γ, IL-2, IL-4, IL-6 and IL-17) were detected *via* the subsequent addition of directly conjugated antibodies incubating for 30 minutes at 4°C. Antibodies are listed in **Table S2**. Stained cells were finally washed and resuspended in FACS buffer and analyzed using a FACSAria Fusion (BD Biosciences). Antigen-specific $CD4^+$ and $CD8^+$ T cells were measured subtracting the background (unstimulated control) from the peptide-stimulated sample. Negative results were set to zero. Data were analyzed with FlowJo software version 10.7.1 (FlowJo LLC).

## Statistical Analysis

Calculations, figures and statistics were made using Prism 9 (GraphPad Software) or RStudio (Version 1.2.1335). The data were tested for statistical normality before applying the appropriate statistical tests. All information about sample sizes and statistical tests performed were shown in the figure legends. Spearman correlation plot was calculated and visualized with the following packages: FactoMineR, factoextra (https://cran.r-project.org/web/packages/factoextra/index.html) and corrplot (https://github.com/taiyun/corrplot) in R (Version 3.6.1) and RStudio (Version 1.2.1335).

# DATA AVAILABILITY STATEMENT

The original contributions presented in the study are included in the article/**Supplementary Material**. Further inquiries can be directed to the corresponding author.

# ETHICS STATEMENT

The studies involving human participants were reviewed and approved by National Ethics Committee of Health Research Cambodia (approval number 020-316). The patients/participants provided their written informed consent to participate in this study.

# AUTHOR CONTRIBUTIONS

Conceptualization: TC, PD, and EK. Methodology: HV, AM, HA, SovL, SSa, NY, and PP. Investigation: HV, AM, HA, TB, VD, TC, and EK. Visualization: HV, AM, HA, and SokL. Funding acquisition: TC, HA, and PD. Patient inclusion: HS and SSo. Cohort management and patient selection: SovL and SowL. Project administration: TC, EK, PP, and PD. Supervision: HV, AM, BT, OS, VD, EK, and TC. Writing: original draft: HV, AM, HA, TB, EK, and TC. Writing: review and editing: HV, AM, HA, TB, VD, OS, EK, and TC. All authors contributed to the article and approved the submitted version.

# FUNDING

The Howard Hughes Medical Institute (HHMI)–Wellcome Trust (208710/Z/17/Z to TC), « URGENCE COVID-19 » fundraising campaign of Institut Pasteur (TC, HA, and PD).

HA is supported by the German Centre for International Migration and Development (CIM).

## ACKNOWLEDGMENTS

This publication has been supported by WHO Solidarity II, global serologic study for COVID-19, with funding from the German Federal Ministry of Health (BMG) COVID-19 Research and development to WHO. We would like to acknowledge all patients that participated to the study. We would like to thank Borita Heng for her technical assistance.

## SUPPLEMENTARY MATERIAL

The Supplementary Material for this article can be found online at: https://www.frontiersin.org/articles/10.3389/fimmu.2022.817905/full#supplementary-material

## REFERENCES

1. Chen N, Zhou M, Dong X, Qu J, Gong F, Han Y, et al. Epidemiological and Clinical Characteristics of 99 Cases of 2019 Novel Coronavirus Pneumonia in Wuhan, China: A Descriptive Study. *Lancet* (2020) 395:507–13. doi: 10.1016/S0140-6736(20)30211-7
2. Guan WJ, Ni ZY, Hu Y, Liang WH, Ou CQ, He JX, et al. Clinical Characteristics of Coronavirus Disease 2019 in China. *N Engl J Med* (2020) 382:1708–20. doi: 10.1056/NEJMoa2002032
3. Zhu N, Zhang D, Wang W, Li X, Yang B, Song J, et al. A Novel Coronavirus From Patients With Pneumonia in China, 2019. *N Engl J Med* (2020) 382:727–33. doi: 10.1056/NEJMoa2001017
4. Dan JM, Mateus J, Kato Y, Hastie KM, Yu ED, Faliti CE, et al. Immunological Memory to SARS-CoV-2 Assessed for Up to 8 Months After Infection. *Science* (2021) 371:eabf4063. doi: 10.1126/science.abf4063
5. Hartley GE, Edwards ESJ, Aui PM, Varese N, Stojanovic S, McMahon J, et al. Rapid Generation of Durable B Cell Memory to SARS-CoV-2 Spike and Nucleocapsid Proteins in COVID-19 and Convalescence. *Sci Immunol* (2020) 5:e01991-20. doi: 10.1126/sciimmunol.abf8891
6. Sherina N, Piralla A, Du L, Wan H, Kumagai-Braesch M, Andréll J, et al. Persistence of SARS-CoV-2-Specific B and T Cell Responses in Convalescent COVID-19 Patients 6-8 Months After the Infection. *Med (N Y)* (2021) 2:281–95.e284. doi: 10.1016/j.medj.2021.02.001
7. Wang M-Y, Zhao R, Gao LJ, Gao XF, Wang DP, Cao JM. SARS-CoV-2: Structure, Biology, and Structure-Based Therapeutics Development. *Front Cell Infect Microbiol* (2020) 10:724. doi: 10.3389/fcimb.2020.587269
8. Grifoni A, Weiskopf D, Ramirez SI, Mateus J, Dan JM, Moderbacher CR, et al. Targets of T Cell Responses to SARS-CoV-2 Coronavirus in Humans With COVID-19 Disease and Unexposed Individuals. *Cell* (2020) 181:1489–501.e1415. doi: 10.1016/j.cell.2020.05.015
9. Yoshida S, Ono C, Hayashi H, Fukumoto S, Shiraishi S, Tomono K, et al. SARS-CoV-2-Induced Humoral Immunity Through B Cell Epitope Analysis in COVID-19 Infected Individuals. *Sci Rep* (2021) 11:5934. doi: 10.1038/s41598-021-85202-9
10. Wang Q, Zhang Y, Wu L, Niu S, Song C, Zhang Z, et al. Structural and Functional Basis of SARS-CoV-2 Entry by Using Human Ace2. *Cell* (2020) 181:894–904.e899. doi: 10.1016/j.cell.2020.03.045
11. Yan R, Zhang Y, Li Y, Xia L, Guo Y, Zhou Q. Structural Basis for the Recognition of SARS-CoV-2 by Full-Length Human ACE2. *Science* (2020) 367:1444–8. doi: 10.1126/science.abb2762
12. Dispinseri S, Secchi M, Pirillo MF, Tolazzi M, Borghi M, Brigatti C, et al. Neutralizing Antibody Responses to SARS-CoV-2 in Symptomatic COVID-19 is Persistent and Critical for Survival. *Nat Commun* (2021) 12:2670. doi: 10.1038/s41467-021-22958-8
13. Wajnberg A, Amanat F, Firpo A, Altman DR, Bailey MJ, Mansour M, et al. Robust Neutralizing Antibodies to SARS-CoV-2 Infection Persist for Months. *Science* (2020) 370:1227. doi: 10.1126/science.abd7728
14. Legros V, Denolly S, Vogrig M, Boson B, Siret E, Rigaill J, et al. A Longitudinal Study of SARS-CoV-2-Infected Patients Reveals a High Correlation Between Neutralizing Antibodies and COVID-19 Severity. *Cell Mol Immunol* (2021) 18:318–27. doi: 10.1038/s41423-020-00588-2
15. Yu J, Tostanoski LH, Peter L, Mercado NB, McMahan K, Mahrokhian SH, et al. DNA Vaccine Protection Against SARS-CoV-2 in Rhesus Macaques. *Science* (2020) 369:806–11. doi: 10.1126/science.abc6284
16. Schäfer A, Muecksch F, Lorenzi JCC, Leist SR, Cipolla M, Bournazos S, et al. Antibody Potency, Effector Function, and Combinations in Protection and Therapy for SARS-CoV-2 Infection *In Vivo*. *J Exp Med* (2021) 218:e20201993. doi: 10.1084/jem.20201993
17. Capetti AF, Borgonovo F, Mileto D, Gagliardi G, Mariani C, Lupo A, et al. One-Year Durability of Anti-Spike IgG to SARS-CoV-2: Preliminary Data From the AntiCROWN Prospective Observational Study One Year Durability of COVID-19 Anti-Spike IgG. *J Infect* (2021) 83:237–79. doi: 10.1016/j.jinf.2021.05.023
18. Kang CK, Kim M, Lee S, Kim G, Choe PG, Park WB, et al. Longitudinal Analysis of Human Memory T-Cell Response According to the Severity of Illness Up to 8 Months After SARS-CoV-2 Infection. *J Infect Dis* (2021) 224:39–48. doi: 10.1093/infdis/jiab159
19. Wang Z, Muecksch F, Schaefer-Babajew D, Finkin S, Viant C, Gaebler C, et al. Naturally Enhanced Neutralizing Breadth Against SARS-CoV-2 One Year After Infection. *Nature* (2021) 595:426–31. doi: 10.1038/s41586-021-03696-9
20. Bournazos S, Ravetch JV. Fcγ Receptor Function and the Design of Vaccination Strategies. *Immunity* (2017) 47:224–33. doi: 10.1016/j.immuni.2017.07.009
21. Dufloo J, Grzelak L, Staropoli I, Madec Y, Tondeur L, Anna F, et al. Asymptomatic and Symptomatic SARS-CoV-2 Infections Elicit Polyfunctional Antibodies. *Cell Rep Med* (2021) 2:100275. doi: 10.1016/j.xcrm.2021.100275
22. Natarajan H, Crowley AR, Butler SE, Xu S, Weiner JA, Bloch EM, et al. Markers of Polyfunctional SARS-CoV-2 Antibodies in Convalescent Plasma. *mBio* (2021) 12:e00765-00721. doi: 10.1128/mBio.00765-21
23. Zohar T, Loos C, Fischinger S, Atyeo C, Wang C, Slein MD, et al. Compromised Humoral Functional Evolution Tracks With SARS-CoV-2 Mortality. *Cell* (2020) 183:1508–19.e1512. doi: 10.1016/j.cell.2020.10.052
24. Anand SP, Prévost J, Nayrac M, Beaudoin-Bussières G, Benlarbi M, Gasser R, et al. Longitudinal Analysis of Humoral Immunity Against SARS-CoV-2 Spike in Convalescent Individuals Up to Eight Months Post-Symptom Onset. *Cell Rep Med* (2021) 2:100290. doi: 10.1016/j.xcrm.2021.100290
25. Lee WS, Selva KJ, Davis SK, Wines BD, Reynaldi A, Esterbauer R, et al. Decay of Fc-Dependent Antibody Functions After Mild to Moderate COVID-19. *Cell Rep Med* (2021) 2(6):100296. doi: 10.1016/j.xcrm.2021.100296
26. Bonifacius A, Tischer-Zimmermann S, Dragon AC, Gussarow D, Vogel A, Krettek U, et al. COVID-19 Immune Signatures Reveal Stable Antiviral T Cell Function Despite Declining Humoral Responses. *Immunity* (2021) 54:340–54.e346. doi: 10.1016/j.immuni.2021.01.008
27. Gaebler C, Wang Z, Lorenzi JCC, Muecksch F, Finkin S, Tokuyama M, et al. Evolution of Antibody Immunity to SARS-CoV-2. *Nature* (2021) 591:639–44. doi: 10.1038/s41586-021-03207-w
28. Zuo J, Dowell AC, Pearce H, Verma K, Long HM, Begum J, et al. Robust SARS-CoV-2-Specific T Cell Immunity is Maintained at 6 Months Following Primary Infection. *Nat Immunol* (2021) 22:620–6. doi: 10.1038/s41590-021-00902-8
29. Wheatley AK, Juno JA, Wang JJ, Selva KJ, Reynaldi A, Tan HX, et al. Evolution of Immune Responses to SARS-CoV-2 in Mild-Moderate COVID-19. *Nat Commun* (2021) 12:1162. doi: 10.1038/s41467-021-21444-5
30. Peluso MJ, Deitchman AN, Torres L, Iyer NS, Munter SE, Nixon CC, et al. Long-Term SARS-CoV-2-Specific Immune and Inflammatory Responses in Individuals Recovering From COVID-19 With and Without Post-Acute Symptoms. *Cell Rep* (2021) 36:109518. doi: 10.1016/j.celrep.2021.109518

31. Sette A, Crotty S. Adaptive Immunity to SARS-CoV-2 and COVID-19. *Cell* (2021) 184:861–80. doi: 10.1016/j.cell.2021.01.007
32. Le Bert N, Tan AT, Kunasegaran K, Tham CYL, Hafezi M, Chia A, et al. SARS-CoV-2-Specific T Cell Immunity in Cases of COVID-19 and SARS, and Uninfected Controls. *Nature* (2020) 584:457–62. doi: 10.1038/s41586-020-2550-z
33. Sariol A, Perlman S. Lessons for COVID-19 Immunity From Other Coronavirus Infections. *Immunity* (2020) 53:248–63. doi: 10.1016/j.immuni.2020.07.005
34. Noh JY, Kwak JE, Yang JS, Hwang SY, Yoon JG, Seong H, et al. Longitudinal Assessment of Anti-SARS-CoV-2 Immune Responses for Six Months Based on the Clinical Severity of COVID-19. *J Infect Dis* (2021) 224:754–63. doi: 10.2139/ssrn.3719075
35. Ravichandran S, Lee Y, Grubbs G, Coyle EM, Klenow L, Akasaka O, et al. Longitudinal Antibody Repertoire in "Mild" Versus "Severe" COVID-19 Patients Reveals Immune Markers Associated With Disease Severity and Resolution. *Sci Adv* (2021) 7:eabf2467. doi: 10.1126/sciadv.abf2467
36. Long Q-X, Jia YJ, Wang X, Deng HJ, Cao XX, Yuan J, et al. Immune Memory in Convalescent Patients With Asymptomatic or Mild COVID-19. *Cell Discov* (2021) 7:18. doi: 10.1038/s41421-021-00250-9
37. WHO. *In COVID-19: Situation Reports*. Geneva: WHO Coronavirus (Covid-19) (2021). p. 21.
38. Auerswald H, Yann S, Dul S, In S, Dussart P, Martin NJ, et al. Assessment of Inactivation Procedures for SARS-CoV-2. *J Gen Virol* (2021) 102:001539. doi: 10.1099/jgv.0.001539
39. Grzelak L, Temmam S, Planchais C, Demeret C, Tondeur L, Huon C, et al. A Comparison of Four Serological Assays for Detecting Anti-SARS-CoV-2 Antibodies in Human Serum Samples From Different Populations. *Sci Transl Med* (2020) 12:eabc3103. doi: 10.1126/scitranslmed.abc3103
40. Mesin L, Schiepers A, Ersching J, Barbulescu A, Cavazzoni CB, Angelini A, et al. Restricted Clonality and Limited Germinal Center Reentry Characterize Memory B Cell Reactivation by Boosting. *Cell* (2020) 180:92–106.e111. doi: 10.1016/j.cell.2019.11.032
41. Bohnhorst J, Bjørgan MB, Thoen JE, Natvig JB, Thompson KM. Bm1-Bm5 Classification of Peripheral Blood B Cells Reveals Circulating Germinal Center Founder Cells in Healthy Individuals and Disturbance in the B Cell Subpopulations in Patients With Primary Sjögren's Syndrome. *J Immunol* (2001) 167:3610–8. doi: 10.4049/jimmunol.167.7.3610
42. Wei C, Anolik J, Cappione A, Zheng B, Pugh-Bernard A, Brooks J, et al. A New Population of Cells Lacking Expression of CD27 Represents a Notable Component of the B Cell Memory Compartment in Systemic Lupus Erythematosus. *J Immunol* (2007) 178:6624–33. doi: 10.4049/jimmunol.178.10.6624
43. Rodda LB, Netland J, Shehata L, Pruner KB, Morawski PA, Thouvenel CD, et al. Functional SARS-CoV-2-Specific Immune Memory Persists After Mild COVID-19. *Cell* (2021) 184:169–83.e117. doi: 10.1016/j.cell.2020.11.029
44. Peng Y, Mentzer AJ, Liu G, Yao X, Yin Z, Dong D, et al. Broad and Strong Memory CD4+ and CD8+ T Cells Induced by SARS-CoV-2 in UK Convalescent Individuals Following COVID-19. *Nat Immunol* (2020) 21:1336–45. doi: 10.1038/s41590-020-0782-6
45. WHO. COVID-19 Situation Report. Geneva: WHO Coronavirus (COVID-19). (2021). Available at: https://www.who.int/emergencies/diseases/novel-coronavirus-2019/situation-reports/ Assessed in 21st.June.2021.
46. Chia WN, Zhu F, Ong SWX, Young BE, Fong SW, Le Bert N, et al. Dynamics of SARS-CoV-2 Neutralising Antibody Responses and Duration of Immunity: A Longitudinal Study. *Lancet Microbe* (2021) 2:e240–9. doi: 10.1016/S2666-5247(21)00025-2
47. Zeberg H, Pääbo S. The Major Genetic Risk Factor for Severe COVID-19 is Inherited From Neanderthals. *Nature* (2020) 587:610–2. doi: 10.1038/s41586-020-2818-3
48. Zhou P, Yang XL, Wang XG, Hu B, Zhang L, Zhang W, et al. A Pneumonia Outbreak Associated With a New Coronavirus of Probable Bat Origin. *Nature* (2020) 579:270–3. doi: 10.1038/s41586-020-2012-7
49. Wacharapluesadee S, Tan CW, Maneeorn P, Duengkae P, Zhu F, Joyjinda Y, et al. Evidence for SARS-CoV-2 Related Coronaviruses Circulating in Bats and Pangolins in Southeast Asia. *Nat Commun* (2021) 12:972. doi: 10.1038/s41467-021-21240-1
50. Delaune D, Hul V, Karlsson EA, Hassanin A, Ou TP, Baidaliuk A, et al. A Novel SARS-CoV-2 Related Coronavirus in Bats From Cambodia. *Nat Commun* (2021) 12:6563. doi: 10.1038/s41467-021-26809-4
51. Souilmi Y, Lauterbur ME, Tobler R, Huber CD, Johar AS, Moradi SV, et al. An Ancient Viral Epidemic Involving Host Coronavirus Interacting Genes More Than 20,000 Years Ago in East Asia. *Curr Biol* (2021) 31:3504–14.e3509. doi: 10.1016/j.cub.2021.05.067
52. Van Elslande J, Gruwier L, Godderis L, Vermeersch P. Estimated Half-Life of SARS-CoV-2 Anti-Spike Antibodies More Than Double the Half-Life of Anti-Nucleocapsid Antibodies in Healthcare Workers. *Clin Infect Dis* (2021) 73:2366–8. doi: 10.1093/cid/ciab219
53. Harrington WE, Trakhimets O, Andrade DV, Dambrauskas N, Raappana A, Jiang Y, et al. Rapid Decline of Neutralizing Antibodies is Associated With Decay of IgM in Adults Recovered From Mild COVID-19. *Cell Rep Med* (2021) 2:100253. doi: 10.1016/j.xcrm.2021.100253
54. Guo L, Ren L, Yang S, Xiao M, Chang D, Yang F, et al. Profiling Early Humoral Response to Diagnose Novel Coronavirus Disease (COVID-19). *Clin Infect Dis* (2020) 71:778–85. doi: 10.1093/cid/ciaa310
55. Cervia C, Nilsson J, Zurbuchen Y, Valaperti A, Schreiner J, Wolfensberger A, et al. Systemic and Mucosal Antibody Responses Specific to SARS-CoV-2 During Mild Versus Severe COVID-19. *J Allergy Clin Immunol* (2021) 147:545–57.e549. doi: 10.1016/j.jaci.2020.10.040
56. Sterlin D, Mathian A, Miyara M, Mohr A, Anna F, Claër L, et al. IgA Dominates the Early Neutralizing Antibody Response to SARS-CoV-2. *Sci Transl Med* (2021) 13:eabd2223. doi: 10.1126/scitranslmed.abd2223
57. Gasser R, Cloutier M, Prévost J, Fink C, Ducas É, Ding S, et al. Major Role of IgM in the Neutralizing Activity of Convalescent Plasma Against SARS-CoV-2. *Cell Rep* (2021) 34:108790. doi: 10.1016/j.celrep.2021.108790
58. Tay MZ, Wiehe K, Pollara J. Antibody-Dependent Cellular Phagocytosis in Antiviral Immune Responses. *Front Immunol* (2019) 10:332. doi: 10.3389/fimmu.2019.00332
59. Sakharkar M, Rappazzo CG, Wieland-Alter WF, Hsieh CL, Wrapp D, Esterman ES, et al. Prolonged Evolution of the Human B Cell Response to SARS-CoV-2 Infection. *Sci Immunol* (2021) 6:eabg6916. doi: 10.1126/sciimmunol.abg6916
60. Dugan HL, Stamper CT, Li L, Changrob S, Asby NW, Halfmann PJ, et al. Profiling B Cell Immunodominance After SARS-CoV-2 Infection Reveals Antibody Evolution to Non-Neutralizing Viral Targets. *Immunity* (2021) 54:1290–303.e1297. doi: 10.1016/j.immuni.2021.05.001
61. Robbiani DF, Gaebler C, Muecksch F, Lorenzi JCC, Wang Z, Cho A, et al. Convergent Antibody Responses to SARS-CoV-2 in Convalescent Individuals. *Nature* (2020) 584:437–42. doi: 10.1038/s41586-020-2456-9
62. Kreer C, Zehner M, Weber T, Ercanoglu MS, Gieselmann L, Rohde C, et al. Longitudinal Isolation of Potent Near-Germline SARS-CoV-2-Neutralizing Antibodies From COVID-19 Patients. *Cell* (2020) 182:843–54.e812. doi: 10.1016/j.cell.2020.06.044
63. Perugino CA, Liu H, Feldman J, Hauser BM, Jacob-Dolan C, Nathan A, et al. Preferential Expansion of Cross-Reactive Pre-Existing Switched Memory B Cells That Recognize the SARS-CoV-2 Omicron Variant Spike Protein. *medRxiv* (2022) 2021:2012.2030.21268554. doi: 10.1101/2021.12.30.21268554
64. Reiss S, Baxter AE, Cirelli KM, Dan JM, Morou A, Daigneault A, et al. Comparative Analysis of Activation Induced Marker (AIM) Assays for Sensitive Identification of Antigen-Specific CD4 T Cells. *PloS One* (2017) 12:e0186998. doi: 10.1371/journal.pone.0186998
65. Sekine T, Perez-Potti A, Rivera-Ballesteros O, Strålin K, Gorin JB, Olsson A, et al. Robust T Cell Immunity in Convalescent Individuals With Asymptomatic or Mild COVID-19. *Cell* (2020) 183:158–68.e114. doi: 10.1016/j.cell.2020.08.017
66. Cohen KW, Linderman SL, Moodie Z, Czartoski J, Lai L, Mantus G, et al. Longitudinal Analysis Shows Durable and Broad Immune Memory After SARS-CoV-2 Infection With Persisting Antibody Responses and Memory B and T Cells. *Cell Rep Med* (2021) 2:100354. doi: 10.1016/j.xcrm.2021.100354
67. Keeton R, Tincho MB, Ngomti A, Baguma R, Benede N, Suzuki A, et al. SARS-CoV-2 Spike T Cell Responses Induced Upon Vaccination or Infection Remain Robust Against Omicron. *medRxiv* (2021) 2021:2012.2026.21268380. doi: 10.1101/2021.12.26.21268380
68. Cubuk J, Alston JJ, Incicco JJ, Singh S, Stuchell-Brereton MD, Ward MD, et al. The SARS-CoV-2 Nucleocapsid Protein is Dynamic, Disordered, and Phase

Separates With RNA. *Nat Commun* (2021) 12:1936. doi: 10.1038/s41467-021-21953-3
69. Laha S, Chakraborty J, Das S, Manna SK, Biswas S, Chatterjee R. Characterizations of SARS-CoV-2 Mutational Profile, Spike Protein Stability and Viral Transmission. *Infect Genet Evol* (2020) 85:104445. doi: 10.1016/j.meegid.2020.104445
70. Korber B, Fischer WM, Gnanakaran S, Yoon H, Theiler J, Abfalterer W, et al. Tracking Changes in SARS-CoV-2 Spike: Evidence That D614G Increases Infectivity of the COVID-19 Virus. *Cell* (2020) 182:812–27.e819. doi: 10.1016/j.cell.2020.06.043
71. Ng KW, Faulkner N, Cornish GH, Rosa A, Harvey R, Hussain S, et al. Preexisting and *De Novo* Humoral Immunity to SARS-CoV-2 in Humans. *Science* (2020) 370:1339. doi: 10.1126/science.abe1107
72. Song G, He WT, Callaghan S, Anzanello F, Huang D, Ricketts J, et al. Cross-Reactive Serum and Memory B-Cell Responses to Spike Protein in SARS-CoV-2 and Endemic Coronavirus Infection. *Nat Commun* (2021) 12:2938. doi: 10.1038/s41467-021-23074-3
73. Bartsch YC, Fischinger S, Siddiqui SM, Chen Z, Yu J, Gebre M, et al. Discrete SARS-CoV-2 Antibody Titers Track With Functional Humoral Stability. *Nat Commun* (2021) 12:1018. doi: 10.1038/s41467-021-21336-8
74. Pušnik J, Richter E, Schulte B, Dolscheid-Pommerich R, Bode C, Putensen C, et al. Memory B Cells Targeting SARS-CoV-2 Spike Protein and Their Dependence on CD4(+) T Cell Help. *Cell Rep* (2021) 34(13):109320. doi: 10.1016/j.celrep.2021.109320
75. Vibholm LK, Nielsen SSF, Pahus MH, Frattari GS, Olesen R, Andersen R, et al. SARS-CoV-2 Persistence is Associated With Antigen-Specific CD8 T-Cell Responses. *EBioMedicine* (2021) 64:103230. doi: 10.1016/j.ebiom.2021.103230
76. Chakraborty S, Gonzalez J, Edwards K, Mallajosyula V, Buzzanco AS, Sherwood R, et al. Proinflammatory IgG Fc Structures in Patients With Severe COVID-19. *Nat Immunol* (2021) 22:67–73. doi: 10.1038/s41590-020-00828-7
77. Larsen MD, de Graaf EL, Sonneveld ME, Plomp HR, Nouta J, Hoepel W, et al. Afucosylated IgG Characterizes Enveloped Viral Responses and Correlates With COVID-19 Severity. *Science* (2021) 371:eabc8378. doi: 10.1126/science.abc8378
78. Shields RL, Lai J, Keck R, O'Connell LY, Hong K, Meng YG, et al. Lack of Fucose on Human IgG1 N-Linked Oligosaccharide Improves Binding to Human Fcgamma RIII and Antibody-Dependent Cellular Toxicity. *J Biol Chem* (2002) 277:26733–40. doi: 10.1074/jbc.M202069200
79. Pereira NA, Chan KF, Lin PC, Song Z. The "Less-is-More" in Therapeutic Antibodies: Afucosylated Anti-Cancer Antibodies With Enhanced Antibody-Dependent Cellular Cytotoxicity. *MAbs* (2018) 10:693–711. doi: 10.1080/19420862.2018.1466767
80. Corman VM, Landt O, Kaiser M, Molenkamp R, Meijer A, Chu DK, et al. Detection of 2019 Novel Coronavirus (2019-Ncov) by Real-Time RT-PCR. *Euro Surveill* (2020) 25:2000045. doi: 10.2807/1560-7917.ES.2020.25.3.2000045
81. Auerswald H, Boussioux C, In S, Mao S, Ong S, Huy R, et al. Broad and Long-Lasting Immune Protection Against Various Chikungunya Genotypes Demonstrated by Participants in a Cross-Sectional Study in a Cambodian Rural Community. *Emerg Microbes Infect* (2018) 7:13. doi: 10.1038/s41426-017-0010-0

**Conflict of Interest:** The authors declare that the research was conducted in the absence of any commercial or financial relationships that could be construed as a potential conflict of interest.

**Publisher's Note:** All claims expressed in this article are solely those of the authors and do not necessarily represent those of their affiliated organizations, or those of the publisher, the editors and the reviewers. Any product that may be evaluated in this article, or claim that may be made by its manufacturer, is not guaranteed or endorsed by the publisher.

frontiers in Immunology

MINI REVIEW
published: 17 February 2022
doi: 10.3389/fimmu.2021.804808

# Progress and Challenges Toward Generation and Maintenance of Long-Lived Memory T Lymphocyte Responses During COVID-19

*Swatantra Kumar*[†], *Shailendra K. Saxena*[*†], *Vimal K. Maurya and Anil K. Tripathi*

*Centre for Advanced Research (CFAR), Faculty of Medicine, King George's Medical University (KGMU), Lucknow, India*

OPEN ACCESS

**Edited by:**
*Jin-Hwan Han, Merck, United States*

**Reviewed by:**
*Russell Kabir, Anglia Ruskin University, United Kingdom*

***Correspondence:**
*Shailendra K. Saxena*
*shailen@kgmcindia.edu*

[†]*These authors have contributed equally to this work and share first authorship*

**Specialty section:**
*This article was submitted to T Cell Biology, a section of the journal Frontiers in Immunology*

**Received:** *29 October 2021*
**Accepted:** *13 December 2021*
**Published:** *17 February 2022*

**Citation:**
*Kumar S, Saxena SK, Maurya VK and Tripathi AK (2022) Progress and Challenges Toward Generation and Maintenance of Long-Lived Memory T Lymphocyte Responses During COVID-19. Front. Immunol. 12:804808. doi: 10.3389/fimmu.2021.804808*

Severe acute respiratory syndrome coronavirus 2 (SARS-CoV-2) causing the coronavirus disease 2019 (COVID-19) pandemic is a serious global threat until we identify the effective preventive and therapeutic strategies. SARS-CoV-2 infection is characterized by various immunopathological consequences including lymphocyte activation and dysfunction, lymphopenia, cytokine storm, increased level of neutrophils, and depletion and exhaustion of lymphocytes. Considering the low level of antibody-mediated protection during coronavirus infection, understanding the role of T cell for long-term protection is decisive. Both $CD4^+$ and $CD8^+$ T cell response is imperative for cell-mediated immune response during COVID-19. However, the level of $CD8^+$ T cell response reduced to almost half as compared to $CD4^+$ after 6 months of infection. The long-term protection is mediated *via* generation of immunological memory response during COVID-19. The presence of memory $CD4^+$ T cells in all the severely infected and recovered individuals shows that the memory response is predominated by $CD4^+$ T cells. Prominently, the antigen-specific $CD4^+$ and $CD8^+$ T cells are specifically observed during day 0 to day 28 in COVID-19-vaccinated individuals. However, level of antigen-specific T memory cells in COVID-19-vaccinated individuals defines the long-term protection against forthcoming outbreaks of SARS-CoV-2.

**Keywords: SARS-CoV-2, COVID-19, T cell response, B cell response, immunopathogenesis, cytokine storm, memory T cell response**

## INTRODUCTION

The global emergence of Severe acute respiratory syndrome coronavirus 2 (SARS-CoV-2) caused the pandemic coronavirus disease (COVID-19), affecting at least 243 million cases with 4.9 million deaths (1). SARS-CoV-2 belongs to *Coronaviridae* which is a family of diverse enveloped RNA viruses of positive sense (2). SARS-CoV-2 is primarily transmitted *via* direct, indirect, or close contact with respiratory droplets generated by infected individuals through sneezing, coughing, talking, or singing. However, other possible routes of transmission occur *via* fomite, blood-borne,

fecal–oral, mother-to-child, and animal-to-human transmission (3). Among the coronaviruses (CoVs), SARS-CoV-2 is the seventh coronavirus that infected humans. The size of the SARS-CoV-2 genome ranges from 27 to 32 kb which comprises of 6–11 open reading frames (ORFs). Among all the ORFs, the replicase (ORF1a/ORF1b), spike (S), membrane (M), envelope (E), and nucleocapsid (N) are the six functional ORFs, whereas seven putative ORFs encode for accessory proteins, which are interspersed in between the structural genes. The replicase gene encompasses 67% of the genome that encodes for a large polyprotein (pp1ab) that gets processed into 16 non-structural proteins (nsps) (4, 5). SARS-CoV-2 infection initiates upon attachment of spike glycoprotein with the ACE2 receptor and consequent priming of spike protein through host cell serine protease TMPRSS2 (6). Following entry, viral RNA is released into the cytoplasm which instantly undergoes translation to generate ORF1a and ORF1b (7). Crystal structures of crucial SARS-CoV-2 proteins have been resolved which are crucial for the designing of effective therapeutic strategies (8–11). However, understanding of SARS-CoV-2 immunopathology and immune response is crucial for designing effective vaccines and immunotherapeutics (12). Importantly, understating of effector T and B cell response is vital for controlling SARS-CoV-2 infection and crucial to providing long-lasting protection *via* generation of antigen-specific immunological memory response (13, 14). This strategy may help us to implement more effective vaccines in the mass population for reducing the burden of COVID-19 (15, 16).

## IMMUNOPATHOLOGY OF SARS-CoV-2 INFECTION

COVID-19 represents a complex profile with heterogeneous clinical manifestations (17). Most of the SARS-CoV-2 infections are asymptomatic and may present mild to moderate clinical symptoms of upper respiratory tract whereas around 15% of the cases result in severe pneumonia and approximately 5% of the cases result in acute respiratory distress syndrome (ARDS) or multiple-organ dysfunction due to septic shock (18). Severe patients are identified with bilateral lung involvement where 80% of the severe cases necessitate oxygenation, of which 30%–40% need mechanical ventilation. Importantly, 80%–90% of the severe cases of mechanical ventilation is the prime cause of COVID-19-associated mortality (19). Critically ill or severe COVID-19 patients are characterized as lymphocyte activation identified as increased levels of CD38, CD69, and CD44 T cell activation markers and exhaustion of T cells identified as the increased expression of T cell immunoglobulin domain and mucin domain-3 (TIM3), programmed cell death protein-1 (PD1), and killer cell lectin-like receptor subfamily C member 1 (NKG2A) (20). Therefore, lymphopenia or lymphocytopenia has been found as a decisive feature of severe cases of COVID-19 (21). In addition, the level of neutrophils is strikingly higher whereas the levels of monocytes, eosinophils, and basophiles have been found to be reduced (22). Importantly, severe cases of COVID-19 are identified as uncontrolled inflammatory response known as cytokine storm where IL-6, IL-1β, IL-10, and IFN-γ have been found to be significantly higher (23). Moreover, patients are identified with the higher level of immunoglobulin G (IgG) and total antibodies (24). Non-survivors are identified as elevated levels of C-reactive proteins, serum ferritin, lactate dehydrogenase, and serum IL-6 as compared with survivors (25). Analysis of the postmortem samples showed the infiltration of lymphocytes and macrophages in the lungs as well as hemophagocytosis in reticuloendothelial organs and bone marrow (26). The SARS-CoV-2-induced lung injury is characterized by diffuse alveolar damages in the pulmonary vessels identified as platelet fibrin microthrombi (27, 28). Altogether, this hyperinflammatory response during COVID-19 suggests the involvement of diverse COVID-19 immunopathologies and host immune responses. Classification of the severity of the disease is crucial for the gradient-based treatment of COVID-19. So far, the radiological imaging of pulmonary systems and other auxiliary examinations are exhibited for the classification of the disease severity (29). However, the blood profiling of the patients is a cost-effective examination of the severe cases.

## CYTOKINE STORM DURING COVID-19

In addition to T and B cell response, elevated levels of cytokines are associated with the disease severity and mortality during SARS-CoV-2 infection (30). Activation of coagulation pathways as an immune response mechanism against SARS-CoV-2 infection is associated with the hyperactivation of proinflammatory cytokine production and multi organ failures (31). Importantly, some of the crucial cytokines such as CCL7, CXCL10, and IL-1 receptor antagonist are associated with the increased viral load, pulmonary dysfunction and damage, and mortality (32, 33). Severe COVID-19 patients have been shown to exhibit higher levels of IL-2, IL-6, IL-10, IL-1, GSCF, MCP-1, TNF-α, and MIP1A (34, 35). Interestingly, the peak plasma levels of IL-6 have been shown to be less as compared with the patients with hyperinflammatory ARDS, cytokine release syndrome, and sepsis (**Figure 1**) (36).

## T CELL RESPONSE DURING COVID-19

Similar to other respiratory viral infections, lymphocyte response is crucial during SARS-CoV-2 infection. Response of lymphocytes specifically T cells is vital since the cellular immune response is exhibited *via* T cells which are involved in the direct killing of the virus-infected cells *via* cytotoxic T lymphocyte $CD8^+$ T cells and $CD4^+$ T cell-mediated $CD8^+$ T cell priming and induction of B cell differentiation into plasma cells to produce virus-specific antibodies (37). Response of both T and B cells during SARS-CoV-2 infection has been detected in the blood approximately 1 week after the onset of

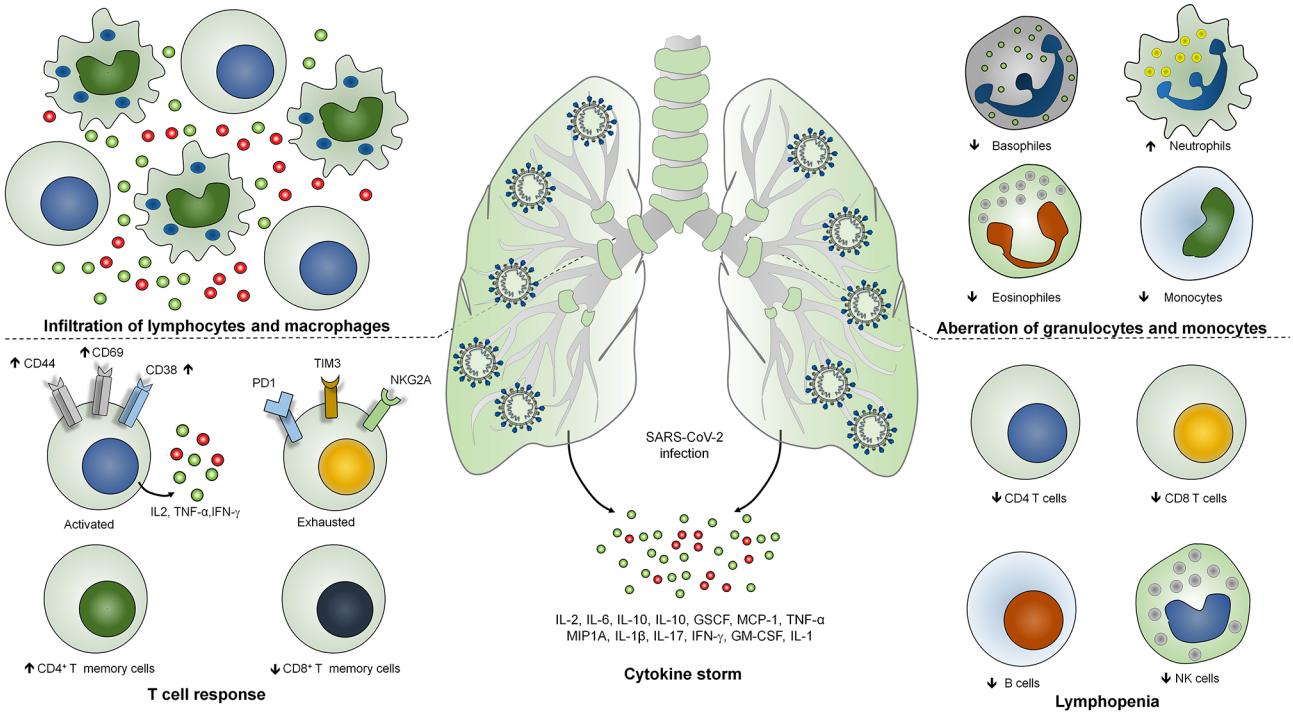


**FIGURE 1** | Immunopathogenesis of SARS-COV-2 infection. Severe COVID-19 is identified with infiltration of lymphocytes and macrophages in the lungs, lymphopenia or lymphocytopenia where reduction in the number of $CD4^+$, $CD8^+$ T cells, B cells and NK cells occurs. SARS-CoV-2 infection is identified with the lymphocyte activation with increased expression of CD38, CD69 and CD44 activation markers and T cell exhaustion identified as T cell immunoglobulin domain and mucin domain-3 (TIM3), programmed cell death protein-1 (PD1), and killer cell lectin-like receptor subfamily C member 1 (NKG2A) markers. Level of neutrophils is strikingly higher whereas the level of monocytes, eosinophils and basophiles has been found to be reduced. Severe COVID-19 patients have been shown to exhibits higher levels of IL-2, IL-6, IL-10, IL-1, GSCF, MCP-1, TNF-α, MIP1A, IFN-γ, IL-1 and GM-CSF.

symptoms (38). Studies are suggesting that the activation of $CD8^+$ T cells is greater than the $CD4^+$ T cell response which was observed by the higher expression of activation markers HLA-DR and CD38 (39). Response of a high magnitude of $CD8^+$ T cells was observed in the mild cases of COVID-19 which may define the protective role of these cells (40). However, severe cases of COVID-19 have been shown to exhibit the terminally differentiated or exhausted $CD8^+$ T cells with an increased expression of inhibitory receptors including TIM3, PD1, CTLA4, LAG3, CD39, and NKG2A showing the characteristic of T cell dysfunction. However, some reports are suggesting that SARS-CoV-2-infected individuals exhibit functional $CD8^+$ T cells identified by PD-1 (41). These data also suggest the hyperactivation of antigen-specific $CD8^+$ T cells might be the cause of disease severity (42). Interestingly, $CD4^+$ T cell response has been observed against spike glycoprotein in the recovered patients (43) whereas $CD8^+$ T cell response was specifically attributed toward the internal proteins of SARS-CoV-2 (44). The six predominant epitopes have been identified to be involved in the T cell response where three epitopes are from spike and two from membrane proteins and one is from nucleocapsid (45). In addition, a significant $CD4^+$ T cell response was found to be specific against spike, nsp3, nsp4, ORF3s, ORF7a, nsp12, and ORF8 (46).

## B CELL RESPONSE DURING COVID-19

In patients of COVID-19, B cell response has been found to be elicited against nucleocapsid protein which concomitantly exhibited with T follicular helper cell response after 1 week of onset of symptoms (47). Strikingly, antibody response against spike glycoprotein was observed 4–8 days after the onset of symptoms (38, 48). Neutralizing antibody response against spike glycoprotein was found to be generated after 2 to 3 weeks (49). A subset of individuals has been found to be incapable of developing long-lasting antibody response and therefore might be prone to the reinfections (50, 51). Importantly, SARS-CoV-2 infection has been shown to be involved in antibody-dependent enhancement of infection mediated by IgG receptors FcγRIIA and FcγRIIIA (52). Strikingly, despite of the presence of the anti-SARS-CoV-2 RBD antibody of serum neutralization activity, effector B cell response is linked with poor clinical outcome and disease severity of the COVID-19 patients (53). The B cell response during SARS-CoV-2 infection mimic the patients reported with active autoimmune processes and human systemic lupus erythematosus (54). In spite of productive humoral response marked by higher antibody-secreting cells (ASCs), expansion was associated with the more severe infections in a subset of COVID-19 patients; neutralizing

antibodies were found to provide ineffective protection against SARS-CoV-2 infection (55).

## LYMPHOPENIA IN SEVERE COVID-19

Lymphopenia or lymphocytopenia has been found as the key immunopathological characteristic of severe COVID-19 cases where 20% of the severe cases showed a low T cell count (56). More specifically, $CD8^+$ T cells remains low as a result of COVID-19-associated lymphopenia (57). In addition, the level of memory $T_H$ cells identified as triple-positive cells ($CD3^+CD4^+$ and $CD45RO^+$) has been found to be reduced (58). The probable reason for the lymphopenia has been suggested *via* four ways, namely, SARS-CoV-2 directly infecting the lymphocytes causing lymphocyte programmed cell death, damage to the lymphoid organs, hyperinflammation-mediated lymphocyte dysfunction probably *via* TNF-α and IL-6, and metabolic molecule-mediated lymphocyte dysfunction (59). All of the probable mechanisms result in lymphopenia, and therefore, admitted patients may be immediately subjected to T cell count which suggests the severity of the case (60).

## MEMORY T CELL RESPONSE DURING SARS-COV-2 INFECTION

Although neutralizing antibody response is important for protection against SARS-CoV-2 infection, long-term protection is required from the onset of infection during reexposure of infection and therefore is crucial for designing effective vaccine candidates for COVID-19 which aims to generate robust memory response upon reexposure. Memory T and B cell responses are the most vital immunological responses, which provide long-term protection against any infections. Recovered COVID-19 patients have been shown to exhibit robust and broad memory $CD4^+$ and $CD8^+$ T cell responses (45, 61). Human peripheral $CD4^+$ T cells can be classified based on their activity during antigen reexposure where naïve cells can be characterized as $CCR7^+$ and $CD45RA^+$ cells, and central and effector memory cells are characterized as $CCR7^+$ $CD45RA^-$ and $CCR7^-$ $CD45RA^-$, respectively. Recovered convalescent patients who were recently discharged from the hospital and 2 to 4 weeks after being declared virus-free have been shown to exhibit persistent memory $CD4^+$ T cell response as well as effector memory-circulating T follicular helper (cTfh) cells (47, 62). Unlike SARS-CoV infection, where memory $CD8^+$ T cell response was found to be higher as compared with the memory $CD4^+$ T cell response which persists for more than 6 years (63, 64), SARS-CoV-2-infected recovered patients showed memory $CD4^+$ T cells in all patients where memory $CD8^+$ T cells are present in 70% individuals, suggesting that memory response in severe cases is predominated by $CD4^+$ Tm cells (45). In addition, all memory T cell responses have been observed against structural proteins of SARS-CoV after 9 and 11 years of recovery (65).

## GENERATION OF ANTIGEN-PRIMED T CELLS DURING NATURAL COVID-19 INFECTION

Antigen-primed T cells are crucial to effectively countering the SARS-CoV-2 infection mediated by both $CD4^+$ and $CD8^+$ Teff cells (66). T cell response investigated against nucleocapsid (N) protein has been shown to exhibit robust IFN-γ response after 17 years of SARS-CoV infection against N peptides. Interestingly, PBMCs collected from these individuals elicited a similar response against N peptides from SARS-CoV-2. SARS-CoV-2-infected individuals exhibit N protein-specific T cell repertoires which are the part of individuals with a history of SARS-CoV infection (67). Prominently, T cell response has been investigated in COVID-19 patients 6 months after the infection. IFN-γ ELISPOT analysis revealed the presence of predominant antigen-specific $CD4^+$ T cells with robust IL-2 expression (68). However, $CD8^+$ response was found to be half as compared to the $CD4^+$ T cell response which is mostly seen against non-spike proteins (68, 69). The level of T cell response can be strongly correlated with the magnitude of peak antibody level specific against spike and RBD (68). These data suggest that infection with betacoronaviruses induces long-lasting T cell-mediated immunity that will prevent COVID-19 survivors to be infected from forthcoming severe infections.

## LYMPHOCYTE RESPONSE AGAINST COVID-19-VACCINATED INDIVIDUALS

Considering the crucial role of T cell-mediated immunity during SARS-CoV-2 infection, it is imperative to understand the T cell response during COVID-19 vaccination. A replication-deficient simian adenoviral vector-based vaccine, ChAdOx1 nCoV-19 (AZD1222), has been shown to induce discrete clusters of populations of lymphocyte (70). These clusters were identified as $Ki\text{-}67^+$ as proliferating population and $CD69^+$ as activated population for both $CD4^+$ and $CD8^+$ T cells. Interestingly, terminally differentiating T cells identified as $CD57^+$ and $KLRG1^+$ were not detected showing a reduced low cytotoxicity response upon AZD1222 vaccination. Upon vaccination, anti-SARS-CoV-2 spike IgG1 and IgG3 responses have been detected at day 14 that further increased by day 28. However, by day 56, these responses were found to be similar to those by day 14. Importantly, IgG1 responses were detected in half, whereas IgG3 was detected in almost all the recruited vaccinated individuals (71). Similar to the COVID-19 patients, T cell responses were measured in AZD1222-vaccinated individuals using IFN-γ ELISpot assay which was peaked at day 14. Spike-specific cytokine response measured by intracellular cytokine staining

(ICS) showed that $CD4^+$ T cell response is heavily responsive toward secretion of Th1 cytokines specifically IL-2 and IFN-γ (**Figure 2**). Assessment of combination of cytokines shows that these responses are primarily dominated by monofunctional IFN-γ $CD8^+$ T cells (71).

Considering the emergence of newer SARS-CoV-2 variants including Omicron, the efficacy of COVID-19 vaccines is crucial to be explored (72). Prominently, sera collected from the second dose of BNT162b2-vaccinated individuals show neutralizing Abs response against several of the emerging SARS-CoV-2 variants (73). Importantly, detection of IFN-γ, IL-12p70, and IL-2 but not IL-4 or IL-5 showed the promising $T_H1$ response along with the absence of deleterious $T_H2$ immune response (74). Likewise, the mRNA-1273 vaccine has been shown to elicit strong CD4 cytokine response specifically type 1 helper T cells (75). Importantly, no correlation of T cell response has been found in these vaccinated individuals toward common cold coronaviruses (CCCs). These vaccines show enhanced T cell response toward peptides derived from SARS-CoV-2 spike as well as toward HCoV-NL63 spike peptides (76).

## CONCLUSIONS

Severe COVID-19 cases are associated with the macrophage and lymphocyte infiltration to the lungs, which results in lung injury *via* activation of lymphocytes and hyperinflammatory responses. The T cell response is crucial as compared with the B cell response due to inability of antibody-mediated neutralization of SARS-CoV-2 and its level of reduction in long-term protection. Memory $CD4^+$ T cell response is higher as compared with the memory $CD8^+$ T cell response which might be linked with the compromised long-lasting protection. Considering the presence of memory T cell responses against structural proteins of SARS-CoV after 9 and 11 years of recovery, long-term protection against COVID-19 depends upon the presence of antigen-specific memory T cell response against SARS-CoV-2 which is predominated by $CD4^+$ T cells. However, lymphopenia has been also reported in various severe infections, which results in compromised immune response and death. COVID-19-vaccinated individuals show presence of antigen-specific $CD4^+$ and $CD8^+$ T cells observed

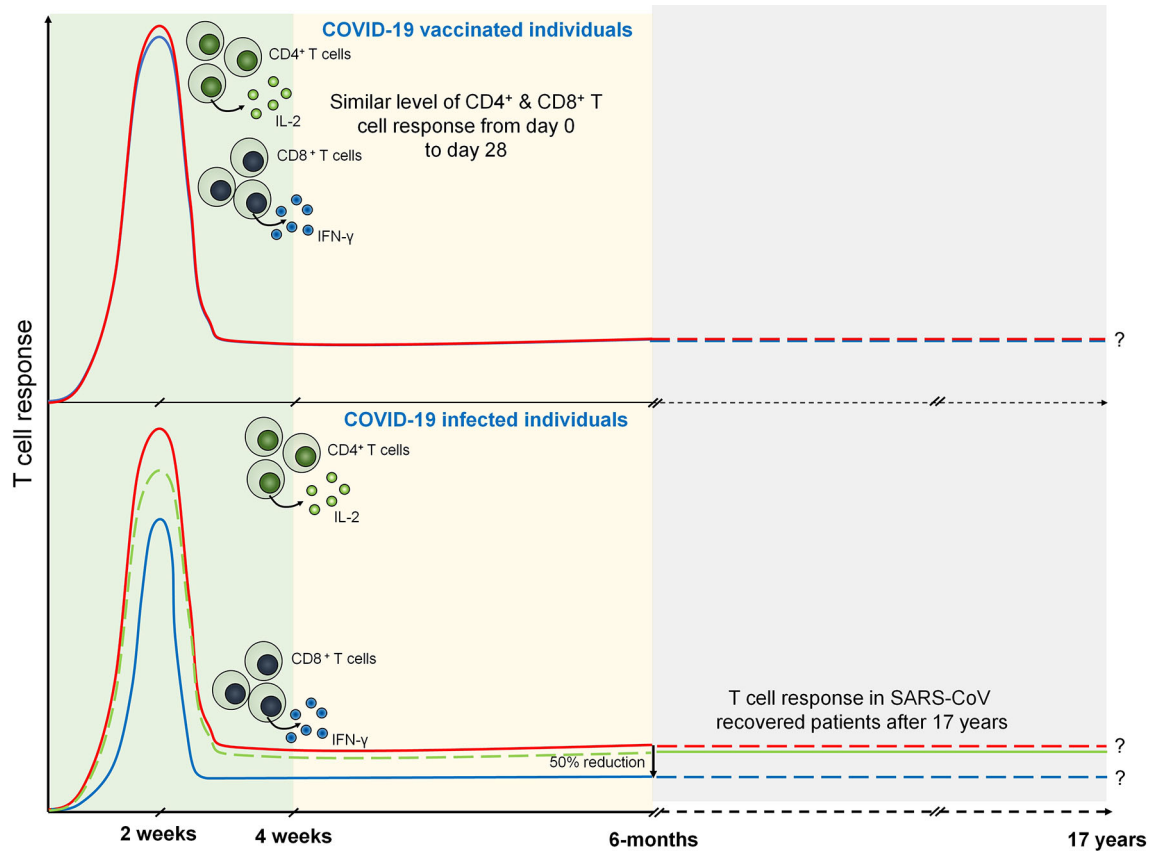


**FIGURE 2** | T cell response during COVID-19 and vaccinated individuals. Both $CD4^+$ (marked by IL-2 expression) and $CD8^+$ T (marked by IFN-γ expression) cell response are peaked at 14 days from the onset of infection. However, after 6 months of COVID-19 infection $CD8^+$ T cell response becomes half of the $CD4^+$ T cell response. SARS-CoV specific T cell response is seen after 17 years that may suggests the persistence of antigen specific memory T cells. Similarly, T cell response are seen in COVID-19 vaccinated individuals which are prominently observed in day 0 to day 28.

on day 0 to day 28. However, the level of these cells in COVID-19-vaccinated individuals defines the long-term protection against forthcoming outbreaks of SARS-CoV-2.

## FUTURE PERSPECTIVES

The number of SARS-CoV-2 infection is continuously rising with the emergence of more mutant strains. A comprehensive understanding of immunological response is crucial for the development of effective immunotherapy and vaccines. Considering the inability of complete protection mediated by antibody response, understanding of memory cell response during SARS-CoV-2 infection is crucial for developing the effective vaccine for long-term protection. Therefore, more clinical studies are required that focus on the memory T cell response during COVID-19 and its associated pathophysiology in natural infection and vaccinated individuals. Therefore, it is really important to look at the specificity of the currently developed vaccine candidates for its effectiveness and protection. Majority of the currently developed vaccines are based on the spike glycoprotein; however, we should also focus on the importance of other structural and non-structural proteins for the development of effective COVID-19 vaccine. Emergence of SARS-CoV-2 variants imposes imperative concerns for COVID-19 vaccination due to their vaccine breakthrough cases. Therefore, the ideal vaccine may focus on the protection against various predominant SARS-CoV-2 variants and be able to induce effective memory T cell generation for long-term protection.

## AUTHOR CONTRIBUTIONS

SS and SK conceived the idea. SK, VM, and SS collected the data, devised the initial draft, and reviewed the final draft. SS, SK, VM, and AT finalized the draft for submission. All authors contributed to the article and approved the submitted version.

## ACKNOWLEDGMENTS

The authors are grateful to the Vice Chancellor, King George's Medical University (KGMU) Lucknow, for the encouragement for this work. The authors have no other relevant affiliations or financial involvement with any organization or entity with a financial interest in or financial conflict with the subject matter or materials discussed in the manuscript apart from those disclosed.

## REFERENCES

1. *Coronavirus Disease (COVID-19) Pandemic*. World Health Organization (WHO). Available at: https://www.who.int/emergencies/diseases/novel-coronavirus-2019 (Accessed on 27 Oct 2021).
2. Gorbalenya AE, Baker SC, Baric RS, de Groot RJ, Drosten C, Gulyaeva AA, et al. (Coronaviridae Study Group of the International Committee on Taxonomy of Viruses). The Species Severe Acute Respiratory Syndrome-Related Coronavirus: Classifying 2019-Ncov and Naming it SARS-CoV-2. *Nat Microbiol* (2020) 5(4):536–44. doi: 10.1038/s41564-020-0695-z
3. *Transmission of SARS-CoV-2: Implications for Infection Prevention Precautions*. World Health Organization (WHO). Available at: https://www.who.int/news-room/commentaries/detail/transmission-of-sars-cov-2-implications-for-infection-prevention-precautions (Accessed on 27 Oct 2021).
4. Kumar S, Saxena SK. Structural and Molecular Perspectives of SARS-CoV-2. *Methods* (2021) 195:23–8. doi: 10.1016/j.ymeth.2021.03.007
5. Kumar S, Nyodu R, Maurya VK, Saxena SK. Morphology, Genome Organization, Replication, and Pathogenesis of Severe Acute Respiratory Syndrome Coronavirus 2 (SARS-CoV-2). *Coronavirus Dis 2019 (COVID-19)* (2020) 30:23–31. doi: 10.1007/978-981-15-4814-7_3
6. Hoffmann M, Kleine-Weber H, Schroeder S, Krüger N, Herrler T, Erichsen S, et al. SARS-CoV-2 Cell Entry Depends on ACE2 and TMPRSS2 and Is Blocked by a Clinically Proven Protease Inhibitor. *Cell* (2020) 181(2):271–80.e8. doi: 10.1016/j.cell.2020.02.052
7. V'kovski P, Kratzel A, Steiner S, Stalder H, Thiel V. Coronavirus Biology and Replication: Implications for SARS-CoV-2. *Nat Rev Microbiol* (2021) 19 (3):155–70. doi: 10.1038/s41579-020-00468-6
8. Yan R, Zhang Y, Li Y, Xia L, Guo Y, Zhou Q. Structural Basis for the Recognition of SARS-CoV-2 by Full-Length Human ACE2. *Science* (2020) 367(6485):1444–8. doi: 10.1126/science.abb2762
9. Zhang L, Lin D, Sun X, Curth U, Drosten C, Sauerhering L, et al. Crystal Structure of SARS-CoV-2 Main Protease Provides a Basis for Design of Improved α-Ketoamide Inhibitors. *Science* (2020) 368(6489):409–12. doi: 10.1126/science.abb3405
10. Kang S, Yang M, Hong Z, Zhang L, Huang Z, Chen X, et al. Crystal Structure of SARS-CoV-2 Nucleocapsid Protein RNA Binding Domain Reveals Potential Unique Drug Targeting Sites. *Acta Pharm Sin B* (2020) 10 (7):1228–38. doi: 10.1016/j.apsb.2020.04.009
11. Krafcikova P, Silhan J, Nencka R, Boura E. Structural Analysis of the SARS-CoV-2 Methyltransferase Complex Involved in RNA Cap Creation Bound to Sinefungin. *Nat Commun* (2020) 11(1):3717. doi: 10.1038/s41467-020-17495-9
12. Wheatley AK, Juno JA, Wang JJ, Selva KJ, Reynaldi A, Tan HX, et al. Evolution of Immune Responses to SARS-CoV-2 in Mild-Moderate COVID-19. *Nat Commun* (2021) 12(1):1162. doi: 10.1038/s41467-021-21444-5
13. Cox RJ, Brokstad KA. Not Just Antibodies: B Cells and T Cells Mediate Immunity to COVID-19. *Nat Rev Immunol* (2020) 20(10):581–2. doi: 10.1038/s41577-020-00436-4
14. Sherina N, Piralla A, Du L, Wan H, Kumagai-Braesch M, Andréll J, et al. Persistence of SARS-CoV-2-Specific B and T Cell Responses in Convalescent COVID-19 Patients 6-8 Months After the Infection. *Med (N Y)* (2021) 2 (3):281–95.e4. doi: 10.1016/j.medj.2021.02.001
15. Kabir R, Mahmud I, Chowdhury MTH, Vinnakota D, Jahan SS, Siddika N, et al. COVID-19 Vaccination Intent and Willingness to Pay in Bangladesh: A Cross-Sectional Study. *Vaccines (Basel)* (2021) 9(5):416. doi: 10.3390/vaccines9050416
16. Chowdhury MTH, Hoque Apu E, Nath SK, Noor AE, Podder CP, Mahmud I, et al. Exploring the Knowledge, Awareness and Practices of COVID-19 Among Dentists in Bangladesh: A Cross-Sectional Investigation. *J Oral Res* (2021) 10(3):1–12. doi: 10.21203/rs.3.rs-56753/v1
17. Yuki K, Fujiogi M, Koutsogiannaki S. COVID-19 Pathophysiology: A Review. *Clin Immunol* (2020) 215:108427. doi: 10.1016/j.clim.2020.108427
18. Cao X. COVID-19: Immunopathology and Its Implications for Therapy. Nature Reviews. *Immunology* (2020) 20(5):269–70. doi: 10.1038/s41577-020-0308-3
19. Yang X, Yu Y, Xu J, Shu H, Xia J, Liu H, et al. Clinical Course and Outcomes of Critically Ill Patients With SARS-CoV-2 Pneumonia in Wuhan, China: A Single-Centered, Retrospective, Observational Study. *Lancet Respir Med* (2020) 8(5):475–81. doi: 10.1016/S2213-2600(20)30079-5

20. Yang L, Liu S, Liu J, Zhang Z, Wan X, Huang B, et al. COVID-19: Immunopathogenesis and Immunotherapeutics. *Signal Transduct Target Ther* (2020) 5(1):128. doi: 10.1038/s41392-020-00243-2
21. Zhao Q, Meng M, Kumar R, Wu Y, Huang J, Deng Y, et al. Lymphopenia Is Associated With Severe Coronavirus Disease 2019 (COVID-19) Infections: A Systemic Review and Meta-Analysis. *Int J Infect Dis* (2020) 96:131–5. doi: 10.1016/j.ijid.2020.04.086
22. Sun DW, Zhang D, Tian RH, Li Y, Wang YS, Cao J, et al. The Underlying Changes and Predicting Role of Peripheral Blood Inflammatory Cells in Severe COVID-19 Patients: A Sentinel? *Clin Chim Acta* (2020) 508:122–9. doi: 10.1016/j.cca.2020.05.027
23. Costela-Ruiz VJ, Illescas-Montes R, Puerta-Puerta JM, Ruiz C, Melguizo-Rodríguez L. SARS-CoV-2 Infection: The Role of Cytokines in COVID-19 Disease. *Cytokine Growth Factor Rev* (2020) 54:62–75. doi: 10.1016/j.cytogfr.2020.06.001
24. Hou H, Wang T, Zhang B, Luo Y, Mao L, Wang F, et al. Detection of IgM and IgG Antibodies in Patients With Coronavirus Disease 2019. *Clin Transl Immunol* (2020) 9(5):e01136. doi: 10.1002/cti2.1136
25. Poggiali E, Zaino D, Immovilli P, Rovero L, Losi G, Dacrema A, et al. Lactate Dehydrogenase and C-Reactive Protein as Predictors of Respiratory Failure in CoVID-19 Patients. *Clin Chim Acta* (2020) 509:135–8. doi: 10.1016/j.cca.2020.06.012
26. Gustine JN, Jones D. Immunopathology of Hyperinflammation in COVID-19. *Am J Pathol* (2021) 191(1):4–17. doi: 10.1016/j.ajpath.2020.08.009
27. Rapkiewicz AV, Mai X, Carsons SE, Pittaluga S, Kleiner DE, Berger JS, et al. Megakaryocytes and Platelet-Fibrin Thrombi Characterize Multi-Organ Thrombosis at Autopsy in COVID-19: A Case Series. *EClinicalMedicine* (2020) 24:100434. doi: 10.1016/j.eclinm.2020.100434
28. Borczuk AC, Salvatore SP, Seshan SV, Patel SS, Bussel JB, Mostyka M, et al. COVID-19 Pulmonary Pathology: A Multi-Institutional Autopsy Cohort From Italy and New York City. *Mod Pathol* (2020) 33(11):2156–68. doi: 10.1038/s41379-020-00661-1
29. Verity R, Okell LC, Dorigatti I, Winskill P, Whittaker C, Imai N, et al. Estimates of the Severity of Coronavirus Disease 2019: A Model-Based Analysis. *Lancet Infect Dis* (2020) 20(6):669–77. doi: 10.1016/S1473-3099(20)30243-7
30. Del Valle DM, Kim-Schulze S, Huang HH, Beckmann ND, Nirenberg S, Wang B, et al. An Inflammatory Cytokine Signature Predicts COVID-19 Severity and Survival. *Nat Med* (2020) 26(10):1636–43. doi: 10.1038/s41591-020-1051-9
31. Jose RJ, Manuel A. COVID-19 Cytokine Storm: The Interplay Between Inflammation and Coagulation. *Lancet Respir Med* (2020) 8(6):e46–7. doi: 10.1016/S2213-2600(20)30216-2
32. Vaninov N. In the Eye of the COVID-19 Cytokine Storm. *Nat Rev Immunol* (2020) 20(5):277. doi: 10.1038/s41577-020-0305-6
33. Elrobaa IH, New KJ. COVID-19: Pulmonary and Extra Pulmonary Manifestations. *Front Public Health* (2021) 9:711616. doi: 10.3389/fpubh.2021.711616
34. Noroozi R, Branicki W, Pyrc K, Łabaj PP, Pospiech E, Taheri M, et al. Altered Cytokine Levels and Immune Responses in Patients With SARS-CoV-2 Infection and Related Conditions. *Cytokine* (2020) 133:155143. doi: 10.1016/j.cyto.2020.155143
35. Costela-Ruiz VJ, Illescas-Montes R, Puerta-Puerta JM, Ruiz C, Melguizo-Rodríguez L. SARS-CoV-2 Infection: The Role of Cytokines in COVID-19 Disease. *Cytokine Growth Factor Rev* (2020) 54:62–75. doi: 10.1016/j.cytogfr.2020.06.001
36. Leisman DE, Ronner L, Pinotti R, Taylor MD, Sinha P, Calfee CS, et al. Cytokine Elevation in Severe and Critical COVID-19: A Rapid Systematic Review, Meta-Analysis, and Comparison With Other Inflammatory Syndromes. *Lancet Respir Med* (2020) 8(12):1233–44. doi: 10.1016/S2213-2600(20)30404-5
37. Swadling L. Maini MK. T Cells in COVID-19 - United in Diversity. *Nat Immunol* (2020) 21(11):1307–8. doi: 10.1038/s41590-020-0798-y
38. Tay MZ, Poh CM, Rénia L, MacAry PA, Ng LFP. The Trinity of COVID-19: Immunity, Inflammation and Intervention. *Nat Rev Immunol* (2020) 20(6):363–74. doi: 10.1038/s41577-020-0311-8
39. Chen Z, John Wherry E. T Cell Responses in Patients With COVID-19. *Nat Rev Immunol* (2020) 20(9):529–36. doi: 10.1038/s41577-020-0402-6
40. De Biasi S, Meschiari M, Gibellini L, Bellinazzi C, Borella R, Fidanza L, et al. Marked T Cell Activation, Senescence, Exhaustion and Skewing Towards TH17 in Patients With COVID-19 Pneumonia. *Nat Commun* (2020) 11(1):3434. doi: 10.21203/rs.3.rs-23957/v1
41. Rha MS, Jeong HW, Ko JH, Choi SJ, Seo IH, Lee JS, et al. PD-1-Expressing SARS-CoV-2-Specific CD8+ T Cells Are Not Exhausted, But Functional in Patients With COVID-19. *Immunity* (2021) 54(1):44–52.e3. doi: 10.1016/j.immuni.2020.12.002
42. Kang CK, Han GC, Kim M, Kim G, Shin HM, Song KH, et al. Aberrant Hyperactivation of Cytotoxic T-Cell as a Potential Determinant of COVID-19 Severity. *Int J Infect Dis* (2020) 97:313–21. doi: 10.1016/j.ijid.2020.05.106
43. Braun J, Loyal L, Frentsch M, Wendisch D, Georg P, Kurth F, et al. SARS-CoV-2-Reactive T Cells in Healthy Donors and Patients With COVID-19. *Nature* (2020) 587(7833):270–4. doi: 10.1038/s41586-020-2598-9
44. Mathew D, Giles JR, Baxter AE, Oldridge DA, Greenplate AR, Wu JE, et al. Deep Immune Profiling of COVID-19 Patients Reveals Distinct Immunotypes With Therapeutic Implications. *Science* (2020) 369(6508):eabc8511. doi: 10.1126/science.abc8511
45. Peng Y, Mentzer AJ, Liu G, Yao X, Yin Z, Dong D, et al. Broad and Strong Memory CD4+ and CD8+ T Cells Induced by SARS-CoV-2 in UK Convalescent Individuals Following COVID-19. *Nat Immunol* (2020) 21(11):1336–45. doi: 10.1038/s41590-020-0782-6
46. Grifoni A, Weiskopf D, Ramirez SI, Mateus J, Dan JM, Moderbacher CR, et al. Targets of T Cell Responses to SARS-CoV-2 Coronavirus in Humans With COVID-19 Disease and Unexposed Individuals. *Cell* (2020) 181(7):1489–501.e15. doi: 10.1016/j.cell.2020.05.015
47. Gong F, Dai Y, Zheng T, Cheng L, Zhao D, Wang H, et al. Peripheral CD4+ T Cell Subsets and Antibody Response in COVID-19 Convalescent Individuals. *J Clin Invest* (2020) 130(12):6588–99. doi: 10.1172/JCI141054
48. Tan YJ, Goh PY, Fielding BC, Shen S, Chou CF, Fu JL, et al. Profiles of Antibody Responses Against Severe Acute Respiratory Syndrome Coronavirus Recombinant Proteins and Their Potential Use as Diagnostic Markers. *Clin Diagn Lab Immunol* (2004) 11(2):362–71. doi: 10.1128/cdli.11.2.362-371.2004
49. Wajnberg A, Amanat F, Firpo A, Altman DR, Bailey MJ, Mansour M, et al. Robust Neutralizing Antibodies to SARS-CoV-2 Infection Persist for Months. *Science* (2020) 370(6521):1227–30. doi: 10.1126/science.abd7728
50. Goldman JD, Wang K, Roltgen K, Nielsen SCA, Roach JC, Naccache SN, et al. Reinfection With SARS-CoV-2 and Failure of Humoral Immunity: A Case Report. *medRxiv* (2020) 2020.09.22.20192443. doi: 10.1101/2020.09.22.20192443
51. Townsend JP, Hassler HB, Wang Z, Miura S, Singh J, Kumar S, et al. The Durability of Immunity Against Reinfection by SARS-CoV-2: A Comparative Evolutionary Study. *Lancet Microbe* (2021) 2(12):e666–75. doi: 10.1016/S2666-5247(21)00219-6
52. Maemura T, Kuroda M, Armbrust T, Yamayoshi S, Halfmann PJ, Kawaoka Y. Antibody-Dependent Enhancement of SARS-CoV-2 Infection Is Mediated by the IgG Receptors Fcγriia and Fcγriiia But Does Not Contribute to Aberrant Cytokine Production by Macrophages. *mBio* (2021) 12(5):e0198721. doi: 10.1128/mBio.01987-21
53. Zohar T, Loos C, Fischinger S, Atyeo C, Wang C, Slein MD, et al. Compromised Humoral Functional Evolution Tracks With SARS-CoV-2 Mortality. *Cell* (2020) 183(6):1508–19.e12. doi: 10.1016/j.cell.2020.10.052
54. Woodruff MC, Ramonell RP, Nguyen DC, Cashman KS, Saini AS, Haddad NS, et al. Extrafollicular B Cell Responses Correlate With Neutralizing Antibodies and Morbidity in COVID-19. *Nat Immunol* (2020) 21(12):1506–16. doi: 10.1038/s41590-020-00814-z
55. Varnaitė R, García M, Glans H, Maleki KT, Sandberg JT, Tynell J, et al. Expansion of SARS-CoV-2-Specific Antibody-Secreting Cells and Generation of Neutralizing Antibodies in Hospitalized COVID-19 Patients. *J Immunol* (2020) 205(9):2437–46. doi: 10.4049/jimmunol.2000717
56. Zhao Q, Meng M, Kumar R, Wu Y, Huang J, Deng Y, et al. Lymphopenia Is Associated With Severe Coronavirus Disease 2019 (COVID-19) Infections: A Systemic Review and Meta-Analysis. *Int J Infect Dis* (2020) 96:131–5. doi: 10.1016/j.ijid.2020.04.086
57. Westmeier J, Paniskaki K, Karaköse Z, Werner T, Sutter K, Dolff S, et al. Impaired Cytotoxic $CD8^+$ T Cell Response in Elderly COVID-19 Patients. *mBio* (2020) 11(5):e02243–20. doi: 10.1128/mBio.02243-20

58. Mahmoudi S, Rezaei M, Mansouri N, Marjani M, Mansouri D. Immunologic Features in Coronavirus Disease 2019: Functional Exhaustion of T Cells and Cytokine Storm. *J Clin Immunol* (2020) 40(7):974–6. doi: 10.1007/s10875-020-00824-4
59. Vabret N, Britton GJ, Gruber C, Hegde S, Kim J, Kuksin M, et al. Immunology of COVID-19: Current State of the Science. *Immunity* (2020) 52(6):910–41. doi: 10.1016/j.immuni.2020.05.002
60. Tan L, Wang Q, Zhang D, Ding J, Huang Q, Tang YQ, et al. Lymphopenia Predicts Disease Severity of COVID-19: A Descriptive and Predictive Study. *Signal Transduct Target Ther* (2020) 5(1):33. doi: 10.1038/s41392-020-0148-4
61. Cañete PF, Vinuesa CG. COVID-19 Makes B Cells Forget, But T Cells Remember. *Cell* (2020) 183(1):13–5. doi: 10.1016/j.cell.2020.09.013
62. Sekine T, Perez-Potti A, Rivera-Ballesteros O, Strålin K, Gorin JB, Olsson A, et al. Robust T Cell Immunity in Convalescent Individuals With Asymptomatic or Mild COVID-19. *Cell* (2020) 183(1):158–68.e14. doi: 10.1016/j.cell.2020.08.017
63. Oh HL, Chia A, Chang CX, Leong HN, Ling KL, Grotenbreg GM, et al. Engineering T Cells Specific for a Dominant Severe Acute Respiratory Syndrome Coronavirus CD8 T Cell Epitope. *J Virol* (2011) 85(20):10464–71. doi: 10.1128/JVI.05039-11
64. Janice Oh HL, Ken-En Gan S, Bertoletti A, Tan YJ. Understanding the T Cell Immune Response in SARS Coronavirus Infection. *Emerg Microbes Infect* (2012) 1(9):e23. doi: 10.1038/emi.2012.26
65. Ng OW, Chia A, Tan AT, Jadi RS, Leong HN, Bertoletti A, et al. Memory T Cell Responses Targeting the SARS Coronavirus Persist Up to 11 Years Post-Infection. *Vaccine* (2016) 34(17):2008–14. doi: 10.1016/j.vaccine.2016.02.063
66. Brunk F, Moritz A, Nelde A, Bilich T, Casadei N, Fraschka SAK, et al. SARS-CoV-2-Reactive T-Cell Receptors Isolated From Convalescent COVID-19 Patients Confer Potent T-Cell Effector Function. *Eur J Immunol* (2021) 51 (11):2651–64. doi: 10.1002/eji.202149290
67. Le Bert N, Tan AT, Kunasegaran K, Tham CYL, Hafezi M, Chia A, et al. SARS-CoV-2-Specific T Cell Immunity in Cases of COVID-19 and SARS, and Uninfected Controls. *Nature* (2020) 584(7821):457–62. doi: 10.1038/s41586-020-2550-z
68. Zuo J, Dowell AC, Pearce H, Verma K, Long HM, Begum J, et al. Robust SARS-CoV-2-Specific T Cell Immunity is Maintained at 6 Months Following Primary Infection. *Nat Immunol* (2021) 22(5):620–6. doi: 10.1038/s41590-021-00902-8
69. Matyushenko V, Isakova-Sivak I, Kudryavtsev I, Goshina A, Chistyakova A, Stepanova E, et al. Detection of Ifnγ-Secreting $CD4^+$ and $CD8^+$ Memory T Cells in COVID-19 Convalescents After Stimulation of Peripheral Blood Mononuclear Cells With Live SARS-CoV-2. *Viruses* (2021) 13(8):1490. doi: 10.3390/v13081490
70. Lineburg KE, Neller MA, Ambalathingal GR, Le Texier L, Raju J, Swaminathan S, et al. Rapid Whole-Blood Assay to Detect SARS-CoV-2-Specific Memory T-Cell Immunity Following a Single Dose of AstraZeneca ChAdOx1-S COVID-19 Vaccine. *Clin Transl Immunol* (2021) 10(8):e1326. doi: 10.1002/cti2.1326
71. Ewer KJ, Barrett JR, Belij-Rammerstorfer S, Sharpe H, Makinson R, Morter R, et al. T Cell and Antibody Responses Induced by a Single Dose of ChAdOx1 Ncov-19 (AZD1222) Vaccine in a Phase 1/2 Clinical Trial. *Nat Med* (2021) 27 (2):270–8. doi: 10.1038/s41591-020-01194-5
72. Saxena SK, Kumar S, Ansari S, Paweska JT, Maurya VK, Tripathi AK, et al. Characterization of the Novel SARS-CoV-2 Omicron (B.1.1.529) Variant of Concern and Its Global Perspective. *J Med Virol* (2022) 1–7. doi: 10.1002/jmv.27524
73. Liu J, Liu Y, Xia H, Zou J, Weaver SC, Swanson KA, et al. BNT162b2-Elicited Neutralization of B.1.617 and Other SARS-CoV-2 Variants. *Nature* (2021) 596(7871):273–5. doi: 10.1038/s41586-021-03693-y
74. Sahin U, Muik A, Derhovanessian E, Vogler I, Kranz LM, Vormehr M, et al. COVID-19 Vaccine BNT162b1 Elicits Human Antibody and TH1 T Cell Responses. *Nature* (2020) 586(7830):594–9. doi: 10.1038/s41586-020-2814-7
75. Anderson EJ, Rouphael NG, Widge AT, Jackson LA, Roberts PC, Makhene M, et al. Safety and Immunogenicity of SARS-CoV-2 mRNA-1273 Vaccine in Older Adults. *N Engl J Med* (2020) 383(25):2427–38. doi: 10.1056/NEJMoa2028436
76. Woldemeskel BA, Garliss CC, Blankson JN. SARS-CoV-2 mRNA Vaccines Induce Broad CD4+ T Cell Responses That Recognize SARS-CoV-2 Variants and HCoV-Nl63. *J Clin Invest* (2021) 131(10):e149335. doi: 10.1172/JCI149335


**Conflict of Interest:** The authors declare that the research was conducted in the absence of any commercial or financial relationships that could be construed as a potential conflict of interest.

frontiers in Immunology

ORIGINAL RESEARCH
published: 04 March 2022
doi: 10.3389/fimmu.2022.839922

# Persistence of Immune Response in Health Care Workers After Two Doses BNT162b2 in a Longitudinal Observational Study

*Jonas Herzberg[1*†], Bastian Fischer[2†], Christopher Lindenkamp[2], Heiko Becher[3], Ann-Kristin Becker[4], Human Honarpisheh[1], Salman Yousuf Guraya[5], Tim Strate[1] and Cornelius Knabbe[2]*

[1] Department of Surgery, Krankenhaus Reinbek St. Adolf-Stift, Reinbek, Germany, [2] Institut für Laboratoriums- und Transfusionsmedizin, Herz- und Diabeteszentrum Nordrhein-Westfalen, Universitätsklinik der Ruhr-Universität Bochum, Bad Oeynhausen, Germany, [3] Institute of Medical Biometry and Epidemiology, University Medical Center Hamburg-Eppendorf, Hamburg, Germany, [4] Asklepios Klinik Harburg, Abteilung für Psychiatrie und Psychotherapie, Hamburg, Germany, [5] Clinical Sciences Department, College of Medicine, University of Sharjah, Sharjah, United Arab Emirates

OPEN ACCESS

**Edited by:**
Sejin Im,
Sungkyunkwan University,
South Korea

**Reviewed by:**
Xionglin Fan,
Huazhong University of Science and Technology, China
Thorsten Demberg,
Baylor College of Medicine,
United States

***Correspondence:**
Jonas Herzberg
jonas.herzberg@krankenhaus-reinbek.de

[†]These authors share first authorship

**Specialty section:**
This article was submitted to Immunological Memory, a section of the journal Frontiers in Immunology

**Received:** 20 December 2021
**Accepted:** 07 February 2022
**Published:** 04 March 2022

**Citation:**
Herzberg J, Fischer B, Lindenkamp C, Becher H, Becker AK, Honarpisheh H, Guraya SY, Strate T and Knabbe C (2022) Persistence of Immune Response in Health Care Workers After Two Doses BNT162b2 in a Longitudinal Observational Study. Front. Immunol. 13:839922. doi: 10.3389/fimmu.2022.839922

**Background:** The mRNA-based vaccine BNT162b2 of BioNTech/Pfizer has shown high efficacy against SARS-CoV-2 infection and a severe course of the COVID-19 disease. However, little is known about the long-term durability of the induced immune response resulting from the vaccination.

**Methods:** In a longitudinal observational study in employees at a German hospital we compared the humoral and cellular immune response in 184 participants after two doses of the BioNTech/Pfizer vaccine (BNT162b2) with a mid-term follow-up after 9 months. Anti-SARS-CoV-2 binding antibodies were determined using both a quantitative and a semi-quantitative assay. For a qualitative assessment of the humoral immune response, we additionally measured neutralizing antibodies. Cellular immune response was evaluated by measuring Interferon-gamma release after stimulating blood-cells with SARS-CoV-2 specific peptides using a commercial assay.

**Results:** In the first analysis, a 100% humoral response rate was described after two doses of BNT162b2 vaccine with a mean antibody ratio of 8.01 ± 1.00. 9 months after the second dose of BNT162b2, serological testing showed a significant decreased mean antibody ratio of 3.84 ± 1.69 ($p < 0.001$). Neutralizing antibodies were still detectable in 96% of all participants, showing an average binding inhibition value of 68.20% ± 18.87%. Older age ($p < 0.001$) and obesity ($p = 0.01$) had a negative effect on the antibody persistence. SARS-CoV-2 specific cellular immune response was proven in 75% of individuals (mean Interferon-gamma release: 579.68 mIU/ml ± 705.56 mIU/ml).

**Conclusion:** Our data shows a declining immune response 9 months after the second dose of BNT162b2, supporting the potentially beneficial effect of booster vaccinations, the negative effect of obesity and age stresses the need of booster doses especially in these groups.

**Keywords: SARS-CoV-2, humoral and cellular immunity, health care worker, immunological memory, vaccination, BNT162b2**

## INTRODUCTION

In order to fight the global coronavirus disease 2019 (COVID-19) pandemic, a variety of vaccines were applied worldwide, beginning in December 2020, and were felt to be the pivoting point in this pandemic situation. The mRNA vaccines, provided by BioNTech/Pfizer (BNT162b2) and Moderna (Spikevax) have shown high efficacy in clinical trials and real-world-data (1, 2). Until now, real-world-data regarding the persistence of the induced humoral and especially cellular immune response post-vaccination are rare.

Even in short-term studies, elderly people were reported to have a less intense immune response after two doses of the BioNTech/Pfizer vaccine BNT162b2 (3, 4). This was also seen in patients under immunosuppression, such as after organ transplantation (5).

Initial studies reported a decrease in antibodies after 6 months (4, 6) or a correlating increased number of infections after complete vaccination (7); but data regarding the longitudinal serological dynamics of immunization after BNT162b2 vaccine is limited.

In this trial we report the mid-term dynamics of immune response, 9 months after second dose of BNT162b2, by determining anti-SARS-CoV-2-immunglobulin G (IgG) antibodies, T-cell-response and neutralizing antibodies. The study cohort consisted of a well-defined group of health care employees, known to be under a higher risk for COVID-19.

## METHODS

### Study Design

In April 2020 we initiated a longitudinal study in health care workers measuring sero-epidemiological data during the COVID-19 pandemic (8). All employees of the secondary care hospital located in the province of Schleswig-Holstein near the border of the city of Hamburg in Northern Germany were invited to participate. All employees were offered vaccination against SARS-CoV-2 starting in December 2020. In April 2021, all participants were invited to provide a blood specimen to evaluate the antibody prevalence after vaccination or infection (9).

For this study, an additional analysis of all participants around 9 months after second dose of BioNTech/Pfizer vaccine was made to evaluate the longitudinal persistence of the vaccine-induced immune response.

All blood samples were collected on November $13^{th}$ – $14^{th}$ 2021 and all participants were asked to complete an additional questionnaire, regarding post-vaccination reactions and previous SARS-CoV-2 infections.

All participants provided written and informed consent prior to enrolment. This study was prospectively registered at the German Clinical Trial Register (DRKS00021270) after approval by the Ethics Committee of the Medical Association Schleswig-Holstein. All study activities were conducted in accordance with the Declaration of Helsinki.

### Anti-SARS-CoV-2-IgG Antibodies

The fully automated semiquantitative anti-SARS-CoV-2-ELISA (IgG) from Euroimmun (Lübeck, Germany) was used to detect the S1 domain of the SARS-CoV-2 spike-protein. In accordance to the manufacturer this test shows a specificity of 99.0% and sensitivity of 93.8% (10). As this was the same test used within the previous analyses, a longitudinal comparability was ensured. This ELISA calculates a ratio of the extinction of patient sample over the extinction of the calibrator and therefor no unit is used. A ratio below 0.8 was considered negative, a ratio ≥ 0.8 to < 1.1 was considered equivocal, and a ratio ≥ 1.1 was considered positive as defined by the manufacturer.

In addition, a fully automated quantitative anti-SARS-CoV-2-assay (IgG) from Abbott (Chicago, USA) was performed. In keeping with the WHO-standard, data were expressed in Binding Antibody Units per ml (BAU/ml). Samples were marked seronegative below 7.1 BAU/ml whereas values above 7.1 BAU/ml were determined to be positive, as mentioned by the manufacturer.

### Neutralizing Antibodies Against SARS-CoV-2

All samples were analyzed for neutralizing anti-SARS-CoV-2 antibodies using the NeutraLISA™ SARS-CoV-2 Neutralization Antibody Detection KIT (Euroimmun, Lübeck, Germany) in accordance to the manufacturer's instructions. Binding inhibition values above 35% were considered positive, whereas values between 20% and 35% were considered equivocal.

### T-Cell-Response

Cellular immunity to SARS-CoV-2 was assessed by using an Interferon (IFN)-gamma release assay (IGRA) from Euroimmun (Quan-T-cell SARS-CoV-2 kit). The assay was performed according to manufacturer´s instructions. In brief, 500 µl of heparinized blood was stimulated with SARS-CoV-2 specific peptides covering regions of the viral S1-domain. After incubating the tubes (37°C, 22 h), plasma was collected and tested for Interferon-gamma release using an ELISA-assay (Quan T-cell ELISA, Euroimmun). Background IFN-gamma values were assessed by incubating blood without prior peptide-stimulation. As a positive control, blood cells were stimulated with mitogen, resulting in a broad and unspecific IFN-gamma secretion. IFN-gamma concentration was expressed as mIU/ml. Values >200 mIU/ml were considered positive, whereas values between 100-200 mIU/ml were considered equivocal.

### Statistical Analysis

IBM SPSS Statistics Version 25 (IBM Co., Armonk, NY, USA) was used for statistical analysis. Graphics were elaborated using IBM SPSS Statistics Version 25 (IBM Co., Armonk, NY, USA) and GraphPad Prism 9.

All variables are presented as means with standard deviation. Categorical variables are shown as numbers with percentages. Fisher's exact test or chi-square test was used to determine relationships between categorical variables depending on size of groups. Exact 95% confidence intervals were provided where

appropriate. Differences between groups were analyzed using Wilcoxon test. Inter-group differences were analyzed using Mann-Whitney-U test or Kruskal-Wallis-test. A linear regression analysis was done to investigate the joint effect of age, sex, body mass index and current smoking on antibody and t-cell response using the backward selection method. The t-cell response had a skewed distribution and was logarithmized for the regression analysis. A p-value < 0.05 was considered statistically significant.

# RESULTS

A total of 184 participants provided a blood sample 9 months (range 7-9 months) after receiving their second dose of BioNTech/Pfizer. This meant a follow-up rate of 58.41% compared to the analysis after the second dose of vaccine (315 participants in April 2021) (9).

In this follow-up, the study characteristics did not differ significant to the previous follow-ups with 73.4% female and 26.6% male and a mean age of 46.32 ± 10.91 years. 3 participants reported a previous SARS-CoV-2 infection. Of these, 1 was reported prior to vaccination, and 2 cases occurred between the second dose of vaccine and this follow-up (**Table 1**). These participants are included in the following analysis.

## Anti-SARS-CoV-2-IgG

In the previous analysis, all participants showed a positive antibody-ratio after two doses of BioNTech/Pfizer, whereas two participants seroconverted to an equivocal result in this follow-up after 9 months. The antibody-ratio was significantly lower in the follow-up analysis after 9 months (8.01 ± 1.00. vs. 3.84 ± 1.69; p < 0.001) (**Figure 1**).

The mean reduction of the IgG antibody-ratio was 53.11% ± 17.95%.

In order to further improve the assessment of the humoral immune response, quantification of anti-SARS-CoV-2 antibodies was performed according to WHO standards (BAU/ml). All participants showed antibody levels above the manufacturer's cutoff (mean: 124.67 ± 104.41 BAU/ml) (**Figure 2**).

## Neutralizing Antibodies

Overall, 96% of study-participants showed neutralizing antibodies against SARS-CoV-2. Our data show a mean binding inhibition capability of 68.20% ± 18.87% 9 months after the second vaccination using BioNTech/Pfizer vaccine (**Figure 3**).

## T-Cell Response

9 months after the second dose of the BioNTech/Pfizer vaccine, 73.4% of participants had a detectable T-cell-immune response. There was no significant correlation of the positivity in relation to the sex, obesity or smoking behavior. The mean IFN-gamma concentration was 579.68 mlU/ml ± 705.56 mlU/ml within this study cohort (**Figure 4**).

We identified several factors associated with a lower T-cell response and a lower level of neutralizing antibodies (**Table 2**). A BMI above 30 (p = 0.004) and smoking (p = 0.034) was associated with a reduced level of neutralizing antibodies. The distribution of sex (p = 0.656) and age (p = 0.135) did not differ significantly in the group of obese participants. This was also seen for the group of smoking participants with a mean age of 46.36 ± 10.80 years (sex: p = 0.854; age: p = 0.739). Male participants showed a lower T-cell response at this timepoint, whereas this difference remained insignificant following the Mann-Whitney-U-test.

During the 9 months follow-up period, the antibody-ratio showed a significant decrease in older participants (p = 0.003 following the Kruskal-Wallis-test) (**Figure 5A**).

There was also a statistically significant decrease in neutralizing antibodies (p = 0.001) (**Figure 5B**), but the reduction in INF-gamma-level remained statistically insignificant (p = 0.218).

Comparing the cellular and humoral immune response, we could not find a significant correlation between these two (**Figure 6**).

The additionally performed linear regression analysis confirmed the univariate analyses regarding the differences in persisting immune response after 9 months. A significant negative effect on antibody persistence was observed for older (p < 0.001) and obese (p = 0.01) participants. Smoking had also a negative effect, with p-value slightly above the limit (p = 0.08) **Table 3** gives the regression estimates and the corresponding p-values and 95% confidence intervals. Sex had no effect. The same result was also found for neutralizing antibodies as dependent variable. **Table 4** gives the corresponding results. Thus, the estimated neutralizing antibodies value for a nonsmoker, age 50 and BMI 25 is 68.705%.

# DISCUSSION

This study analyzes the persistence of the humoral and cellular response, including neutralizing antibodies, to BioNTech/Pfizer

**TABLE 1** | Immune status of previously infected and vaccinated participants in comparison to the mean values of the study cohort.

| Participant | Time since infection [months] | Anti-SARS-CoV-2-IgG [BAU/ml] | Neutralizing antibodies [%] | Interferon-gamma [mIU/ml] |
|---|---|---|---|---|
| A | 17.5 | 314.40 | 97.26 | 645.60 |
| B | 8.5 | 304.30 | 96.87 | 170.00 |
| C | 6.5 | 26.90 | 39.12 | 1216.20 |
| **Study cohort** | | **Anti-SARS-CoV-2-IgG [BAU/ml] (mean ± SD)** | **Neutralizing antibodies [%] (mean ± SD)** | **Interferon-gamma [mIU/ml] (mean ± SD)** |
| n = 184 | — — | 124.67 ± 104.41 | 68.20 ± 18.87 | 579.68 ± 705.56 |

*SD, standard deviation.*

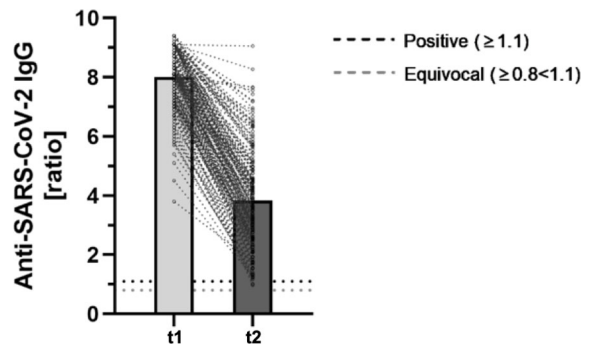


**FIGURE 1** | Comparing anti-SARS-CoV-2-IgG ratios 2 months after second BNT162b2-dose (t1) and a mid-term follow-up 9 months after second dose (t2) (n = 184). The fully automated anti-SARS-CoV-2-ELISA from Euroimmun was used to determine semiquantitative IgG-antibody ratios. As defined by the manufacturer, ratios ≥ 1.1 were considered positive (horizontal black dotted line). Ratios ≥ 0.8 < 1.1 were considered equivocal (horizontal gray dotted line).

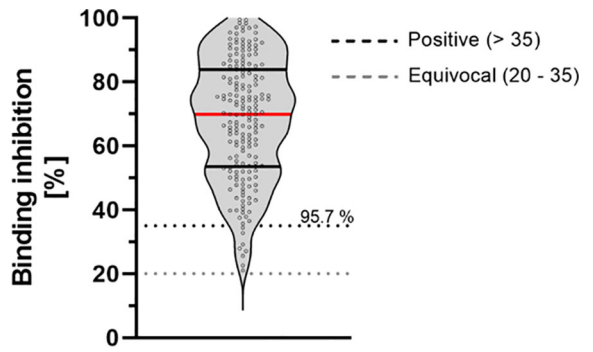


**FIGURE 3** | Binding inhibition capability of neutralizing antibodies 9 months after vaccination with BioNTech/Pfizer vaccine BNT162b2. Neutralizing anti-SARS-CoV-2 antibodies were determined using the NeutraLISA™ SARS-CoV-2 Neutralization Antibody Detection KIT from Euroimmun. According to the manufacturer, binding inhibition values above 35% were considered positive (horizontal black dotted line), whereas values between 20% and 35% were considered equivocal (horizontal gray dotted line). Red line marks the mean. The dashed lines show the positive (light gray)- and equivocal (dark gray) cutoffs specified by the manufacturer.

vaccine in a well-defined group of hospital employees as part of a longitudinal evaluation.

Up until now, little is known about the persistence of the immune response after vaccination with BioNTech/Pfizer. This study reveals a significant antibody decrease in a mid-term-follow-up in all subgroups, affecting especially older people and people with a high BMI.

## Immune Response After 9 Months

Currently there is minimal data about the long-lasting effect following active immunization with mRNA vaccines.

In our cohort, the antibody ratio decreased in the 9-month follow-up to about the half of the initial value. This was not surprising, as first half-year follow-ups showed a decrease during that timeframe (4), and it is well known, that not all plasmablasts commit as memory plasma cells (11, 12).

The decreased antibody ratio is also detected in the decreased neutralization capacity. Several studies found this decrease to begin as early as 3 months after vaccination (4, 13).

Discussing the long-lasting effect of mRNA vaccines (such as the one from BioNTech/Pfizer) in protecting against COVID-19 disease, the role of cellular immunity in addition to humoral response might be important but is often disregarded due to elaborate assays, which are not feasible in standard-laboratories. We determined cellular immunity in a simplified approach by

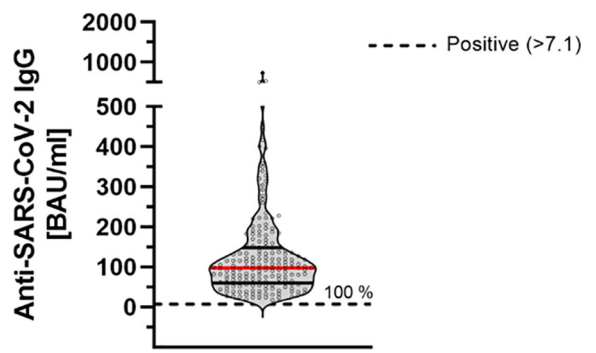


**FIGURE 2** | Quantitative determination of anti-SARS-CoV-2-IgG antibodies 9 months after second dose of BNT162b2 (n = 184). Anti-SARS-CoV-2-IgG antibodies were determined using a quantitative assay from Abbott. In keeping with the WHO-standard, data were expressed in Binding Antibody Units per ml (BAU/ml). Samples were marked seronegative below 7.1 BAU/ml whereas values above 7.1 BAU/ml were determined to be positive (horizontal black dotted line), as mentioned by the manufacturer. Red line marks the mean. The dashed gray line marks the positive cutoff specified by the manufacturer.

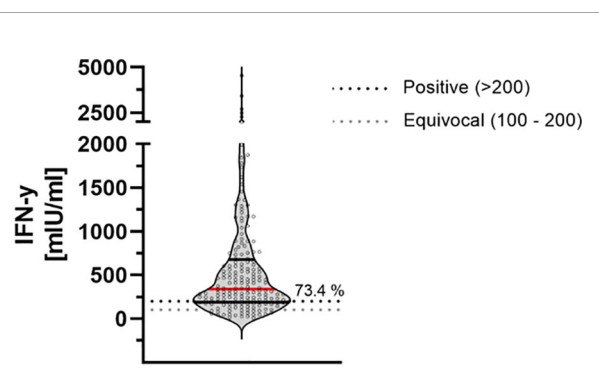


**FIGURE 4** | T-cell-response assessed by measuring IFN-gamma release 9 months after second dose of BNT162b2. Cellular immunity to SARS-CoV-2 was assessed by using an Interferon (IFN)-gamma release assay (IGRA) from Euroimmun (Quan-T-cell SARS-CoV-2 kit). Values > 200 mIU/ml were considered positive (horizontal black dotted line), whereas values between 100-200 mIU/ml were considered equivocal (horizontal gray dotted line). Red line marks the mean. The dashed lines show the positive (light gray)- and equivocal (dark gray) cutoffs specified by the manufacturer.

**TABLE 2 |** Participants 9 months after second dose of BioNTech/Pfizer vaccine (n = 184).

| | Antibody ratio after 9 months, M ± SD | p-value | Reduction of initial antibody response (%), M ± SD | p-value | T-cell response, M ± SD | p-value | Neutralizing antibodies (%), M ± SD | p-value |
|---|---|---|---|---|---|---|---|---|
| **All (n = 184)** | 3.84 ±1.69 | | 53.11 ± 17.95 | | 579.68 ± 705.56 | | 68.20 ± 18.87 | |
| **Sex** | | | | | | | | |
| Male (n = 49) | 3.84 ± 1.71 | 0.938[a] | 52.32 ± 17.98 | 0.712[a] | 492.17 ± 528.48 | 0.146[a] | 66.98 ± 20.93 | 0.805[a] |
| Female (n = 135) | 3.84 ± 1.68 | | 53.39 ± 18.00 | | 611.44 ± 758.94 | | 68.65 ± 18.12 | |
| **Smoking** | | | | | | | | |
| Yes (n = 52)[+] | 3.45 ± 1.56 | 0.062[a] | 56.80 ± 16.25 | 0.120[a] | 512.60 ± 726.06 | 0.162[a] | 63.59 ± 18.84 | 0.034[a] |
| No (n = 132) | 3.99 ± 1.72 | | 51.65 ± 18.43 | | 606.10 ± 698.35 | | 70.03 ± 18.64 | |
| **Obesity** | | | | | | | | |
| Yes (n = 30)[#] | 3.19 ± 1.70 | 0.012[a] | 59.16 ± 18.82 | 0.020[a] | 451.80 ± 475.61 | 0.306[a] | 58.68 ± 20.20 | 0.004[a] |
| No (n = 154) | 3.96 ± 1.66 | | 51.92 ± 17.60 | | 604.58 ± 740.75 | | 70.07 ± 18.09 | |
| **Age groups** | | | | | | | | |
| <30 (n = 13) | 4.92 ± 1.95 | 0.003[b] | 42.86 ± 21.82 | 0.008[b] | 465.95 ± 523.68 | 0.216[b] | 78.60 ± 19.89 | 0.001[b] |
| 31-39 (n = 40) | 4.45 ± 1.66 | | 46.99 ± 18.08 | | 753.12 ± 980.72 | | 74.37 ± 18.62 | |
| 40-49 (n = 57) | 3.77 ± 1.47 | | 53.58 ± 16.17 | | 568.40 ± 678.75 | | 69.32 ± 15.95 | |
| 50-59 (n = 47) | 3.36 ± 1.61 | | 57.65 ± 16.80 | | 468.27 ± 565.18 | | 62.07 ± 20.29 | |
| >60 (n = 27) | 3.36 ± 1.75 | | 58.19 ± 17.89 | | 595.19 ± 549.00 | | 62.13 ± 17.48 | |

*M, mean.*
*SD, standard deviation.*
[a]*Mann-Whitney-U-test.*
[b]*Kruskal-Wallis-Test.*
[+]*Including 9 male and 21 female participants.*
[#]*Including 13 male and 39 female participants.*
*Obesity is defined as a Body mass index above 30.*

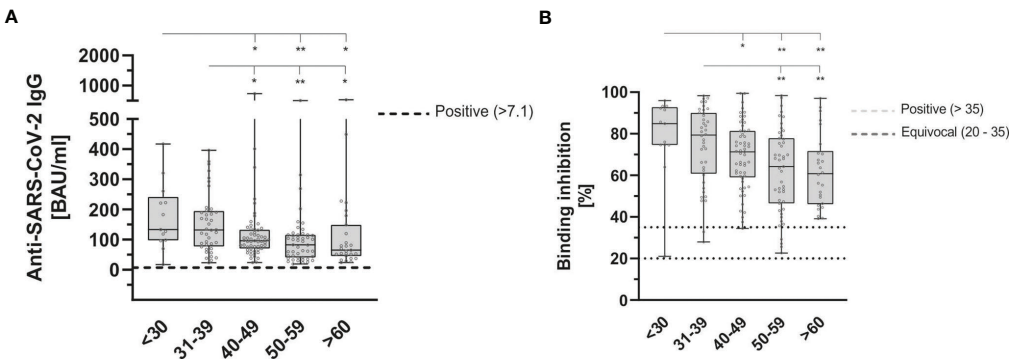


**FIGURE 5** | Age dependent anti-SARS-CoV-2-IgG binding antibodies **(A)** and neutralizing antibodies **(B)** 9 months after second dose of BioNTech/Pfizer vaccine with both, significantly reduced in older participants (p = 0.003 and p = 0.001, respectively). Anti-SARS-CoV-2-IgG antibodies were determined using a quantitative assay from Abbott. In keeping with the WHO-standard, data were expressed in Binding Antibody Units per ml (BAU/ml). Samples were marked seronegative below 7.1 BAU/ml whereas values above 7.1 BAU/ml were determined to be positive (horizontal black dotted line), as mentioned by the manufacturer. Neutralizing anti-SARS-CoV-2 antibodies were determined using the NeutraLISA™ SARS-CoV-2 Neutralization Antibody Detection KIT from Euroimmun. According to the manufacturer, binding inhibition values above 35% were considered positive (horizontal black dotted line), whereas values between 20% and 35% were considered equivocal (horizontal gray dotted line). Cohorts were grouped as follows (in years): <30 (n = 13), 31-39 (n = 40), 40-49 (n = 57), 50-59 (n = 47), >60 (n = 27). *p < 0.05; **p < 0.01 (Mann-Whitney U-test).

IFN-gamma release after stimulation of blood-cells with specific SARS-CoV-2 peptides.

In our cohort, 73.40% showed a detectable T-cell response even 9 months after vaccination. This is in line with data presented by Naaber et al. for their 6-months follow-up (4), and in keeping with the initial phase I/II trial showing an activation of T-cells after using mRNA vaccines (14).

Compared to our data, Tober-Lau et al. determined a higher median IFN-gamma release six months after BNT162b2-vaccination within their HCW-cohort using the same IGRA-assay (1198.0 mIU/ml vs. 412.0 mIU/ml) (15). In addition, binding inhibition capability of neutralizing antibodies was considerably lower within our cohort (88.1% vs. 68.2%). Reasons for this may be the different time points of examination after second vaccination (9 vs. 6 months) and the higher average age of our cohort (46 vs 35 years). Referring to the same kits used the decreasing immune response was also seen in reconvalescent patients, whereas the authors only have reported the positivity rate instead of the values measured (16).

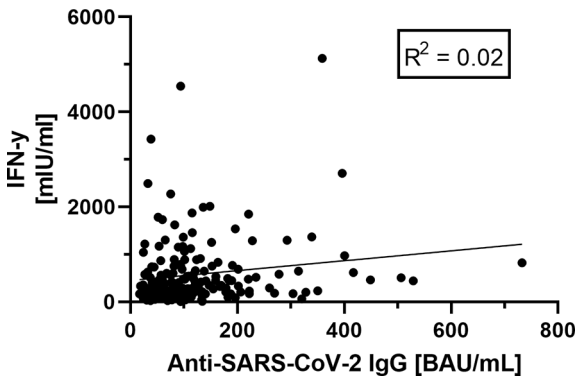


**FIGURE 6** | Correlation between humoral (anti-SARS-CoV-2-IgG antibodies)- and cellular (Interferon-gamma release) immunity. No correlation between humoral and cellular immunity values could be shown ($R^2$ = 0.02), based on the data shown before.

## Factors Associated With a Reduced Immune Response to SARS-CoV-2

In our follow-up study, we found a correlation between age, obesity and smoking with respect to almost all considered immune responses.

As shown in previous studies, we confirmed the negative correlation between antibody responses and the age of vaccinated individuals (3, 4). In addition to the reduced antibody response after vaccination older people are known to have a faster decrease after vaccination (4). Interestingly, obese participants with a BMI higher than 30 showed a significantly higher decrease in the antibody ratio and also significantly lower neutralizing antibodies not only in the univariate analysis but also following the regression analysis. This effect was first described by Watanabe et al. (17) and seen by Malavazos et al. (18) in the first months after vaccination.

The effect of smoking immediately after vaccination was already discussed (9, 17) and is reported to influence the effectiveness of other vaccines due to a general immunosuppression caused by smoking (17, 19). In this 9-month evaluation, for the only significant difference was with respect to neutralizing antibodies.

These findings are important as obese people and elderly are known to have a higher risk not only for SARS-CoV-2 infection, but especially for a severe course of COVID-19 (20, 21). Further studies are needed to evaluate the longitudinal course of cellular and humoral immune response not only after two doses of BioNTech/Pfizer but also after a third dose.

## Limitation

The major limitation of this trial is its single-center design. Due to the inclusion of hospital employees, women are relatively overrepresented and other groups with a higher risk are underrepresented. Especially elderly participants, with an age over 70 years, are not included in this study.

It cannot be excluded that there were asymptomatic, undetected SARS-CoV-2 infections among the participants during the 9 months after second vaccination, which may lead to a slight bias in the results.

Further differentiations concerning the humoral immune response (such as IgG subclasses or antibody glycosylation patterns) or the cellular immune response (*e.g.* distinguishing between CD4 and CD8 T-cells) could provide further important aspects. However, these analyses should be carried out by specialized working groups.

Due to the use of different methods, it was not possible to compare the absolute values of antibody concentrations, T-cell responses or neutralizing antibodies over the follow-up-period. Therefore, a convincing calculation of the half-life of the immune response is not possible.

Further evaluations of antibody response after vaccination are needed, to investigate the longitudinal persistence of antibodies and the possible need for further booster vaccinations.

**TABLE 3** | Linear regression for Anti-SARS-CoV-2 antibody ratio as dependent variable and smoking, age and BMI as covariable.

| Variable | | Parameter Estimate | p-value | 95% CI |
|---|---|---|---|---|
| (Intercept) | $\alpha$ | 1.249 | <0.001 | (1.168, 1.329) |
| BMI -25* | $\beta_1$ | -0.0182 | 0.01 | (-0.032, -0.0043) |
| Current smoking (yes) | $\beta_2$ | -0.128 | 0.08 | (-0.273, 0.017) |
| Age -50* | $\beta_3$ | -0.0115 | <0.001 | (-0.0175, -0.00544) |

*CI, confidence interval; BMI, body mass index.*
*$R^2$ = 0.13*
**linear transformation of BMI (minus 25) and Age (minus 50).*

**TABLE 4** | Linear regression for neutralizing antibodies as dependent variable and smoking, age and BMI as covariable.

| Variable | | Parameter Estimate | p-value | 95% CI |
|---|---|---|---|---|
| (Intercept) | $\alpha$ | 68.705 | <0.001 | (65.47, 71.94) |
| BMI -25* | $\beta_1$ | -0.687 | 0.02 | (-1.24, -0.13) |
| Current smoking (yes) | $\beta_2$ | -5.51 | 0.06 | (-11.32, 0.303) |
| Age -50* | $\beta_3$ | -0.423 | <0.001 | (-0.665, -0.180) |

*CI, confidence interval; BMI, body mass index.*
*$R^2$ = 0.13.*
**linear transformation of BMI (minus 25) and Age (minus 50).*

## CONCLUSION

This study showed an age-dependent decrease of vaccine-induced anti-SARS-CoV-2-IgG antibodies in a midterm-follow-up after 9 months. People with a higher risk for a severe COVID-19-disease course, such as elderly or obese people, showed a reduced immune response at this timepoint after vaccination. These results encourage the use, and need, of so-called booster doses 6 months after the second dose of the BioNTech/Pfizer vaccine BNT162b2, especially in vulnerable individuals such as elderly or obese people.

## DATA AVAILABILITY STATEMENT

The raw data supporting the conclusions of this article will be made available by the authors on reasonable request, without undue reservation.

## ETHICS STATEMENT

The studies involving human participants were reviewed and approved by Ethics Committee of the Medical Association Schleswig-Holstein. The participants provided their written informed consent to participate in this study.

## AUTHOR CONTRIBUTIONS

JH and BF conducted the research and wrote the manuscript. These authors contributed equally to this research. CL and BF performed the assays. HB supervised the statistical analysis. A-KB, HH, and SG reviewed the manuscript. TS initiated the research and supervised the study. TS and CK reviewed the final draft of this article and provided logistic support. All authors have critically reviewed and approved the final draft and are responsible for the content of the manuscript.

## ACKNOWLEDGMENTS

We would like to thank all team members at the Krankenhaus Reinbek St. Adolf-Stift, and all participating laboratories that analyzed these additional samples in a phase of high workload. Thanks also to Rebecca Zimmer (linguistic enrichment) for her intense and rapid help.

## REFERENCES

1. Pawlowski C, Lenehan P, Puranik A, Agarwal V, Venkatakrishnan AJ, Niesen MJM, et al. FDA-Authorized mRNA COVID-19 Vaccines are Effective Per Real-World Evidence Synthesized Across a Multi-State Health System. *Med* (2021) 2:979–992.e8. doi: 10.1016/j.medj.2021.06.007
2. Thompson MG, Burgess JL, Naleway AL, Tyner HL, Yoon SK, Meece J, et al. Interim Estimates of Vaccine Effectiveness of BNT162b2 and mRNA-1273 COVID-19 Vaccines in Preventing SARS-CoV-2 Infection Among Health Care Personnel, First Responders, and Other Essential and Frontline Workers - Eight U.S. Locations, December 2020-March 2021. *MMWR Morb Mortal Wkly Rep* (2021) 70:495–500. doi: 10.15585/mmwr.mm7013e3
3. Müller L, Andrée M, Moskorz W, Drexler I, Walotka L, Grothmann R, et al. Age-Dependent Immune Response to the Biontech/Pfizer BNT162b2 COVID-19 Vaccination. *Clin Infect Dis* (2021) 73:2065–72. doi: 10.1093/cid/ciab381
4. Naaber P, Tserel L, Kangro K, Sepp E, Jürjenson V, Adamson A, et al. Dynamics of Antibody Response to BNT162b2 Vaccine After Six Months: A Longitudinal Prospective Study. *Lancet Reg Heal Eur* (2021) 10:100208. doi: 10.1016/j.lanepe.2021.100208
5. Schramm R, Costard-Jäckle A, Rivinius R, Fischer B, Müller B, Boeken U, et al. Poor Humoral and T-Cell Response to Two-Dose SARS-CoV-2 Messenger RNA Vaccine BNT162b2 in Cardiothoracic Transplant Recipients. *Clin Res Cardiol* (2021) 110:1142–9. doi: 10.1007/s00392-021-01880-5
6. Tartof SY, Slezak JM, Fischer H, Hong V, Ackerson BK, Ranasinghe ON, et al. Effectiveness of mRNA BNT162b2 COVID-19 Vaccine Up to 6 Months in a Large Integrated Health System in the USA: A Retrospective Cohort Study. *Lancet (London England)* (2021) 398:1407–16. doi: 10.1016/S0140-6736(21)02183-8
7. Keehner J, Horton LE, Binkin NJ, Laurent LC, Pride D, Longhurst CA, et al. Resurgence of SARS-CoV-2 Infection in a Highly Vaccinated Health System Workforce. *N Engl J Med* (2021) 385:1330–2. doi: 10.1056/NEJMc2112981
8. Herzberg J, Vollmer T, Fischer B, Becher H, Becker A-K, Sahly H, et al. A Prospective Sero-Epidemiological Evaluation of SARS-CoV-2 Among Health Care Workers in a German Secondary Care Hospital. *Int J Infect Dis* (2021) 102:136–43. doi: 10.1016/j.ijid.2020.10.026
9. Herzberg J, Vollmer T, Fischer B, Becher H, Becker A-K, Honarpisheh H, et al. SARS-CoV-2-Antibody Response in Health Care Workers After Vaccination or Natural Infection in a Longitudinal Observational Study. *Vaccine* (2022) 40:206–12. doi: 10.1016/J.VACCINE.2021.11.081
10. Okba NMA, Müller MA, Li W, Wang C, GeurtsvanKessel CH, Corman VM, et al. Severe Acute Respiratory Syndrome Coronavirus 2-Specific Antibody Responses in Coronavirus Disease Patients. *Emerg Infect Dis* (2020) 26:1478–88. doi: 10.3201/eid2607.200841
11. Khodadadi L, Cheng Q, Radbruch A, Hiepe F. The Maintenance of Memory Plasma Cells. *Front Immunol* (2019) 10:721. doi: 10.3389/fimmu.2019.00721
12. Quast I, Tarlinton D. B Cell Memory: Understanding COVID-19. *Immunity* (2021) 54:205–10. doi: 10.1016/j.immuni.2021.01.014
13. Souza WM, Amorim MR, Sesti-Costa R, Coimbra LD, Brunetti NS, Toledo-Teixeira DA, et al. Neutralisation of SARS-CoV-2 Lineage P.1 by Antibodies Elicited Through Natural SARS-CoV-2 Infection or Vaccination With an Inactivated SARS-CoV-2 Vaccine: An Immunological Study. *Lancet Microbe* (2021) 2:e527–35. doi: 10.1016/S2666-5247(21)00129-4
14. Sahin U, Muik A, Derhovanessian E, Vogler I, Kranz LM, Vormehr M, et al. COVID-19 Vaccine BNT162b1 Elicits Human Antibody and TH1 T Cell Responses. *Nature* (2020) 586:594–9. doi: 10.1038/s41586-020-2814-7
15. Tober-Lau P, Schwarz T, Vanshylla K, Hillus D, Gruell H, Group ES, et al. Long-Term Immunogenicity of BNT162b2 Vaccination in the Elderly and in Younger Health Care Workers. *medRxiv* (2021) 2021.08.26.21262468. doi: 10.1101/2021.08.26.21262468
16. Schiffner J, Backhaus I, Rimmele J, Schulz S, Möhlenkamp T, Klemens JM, et al. Long-Term Course of Humoral and Cellular Immune Responses in Outpatients After SARS-CoV-2 Infection. *Front Public Heal* (2021) 9:732787. doi: 10.3389/fpubh.2021.732787
17. Watanabe M, Balena A, Tuccinardi D, Tozzi R, Risi R, Masi D, et al. Central Obesity, Smoking Habit, and Hypertension are Associated With Lower Antibody Titres in Response to COVID-19 mRNA Vaccine. *Diabetes Metab Res Rev* (2022) 38:e3465. doi: 10.1002/dmrr.3465
18. Malavazos AE, Basilico S, Iacobellis G, Milani V, Cardani R, Boniardi F, et al. Antibody Responses to BNT162b2 mRNA Vaccine: Infection-Naïve Individuals With Abdominal Obesity Warrant Attention. *Obes (Silver Spring)* (2021). doi: 10.1002/oby.23353
19. Winter AP, Follett EAC, McIntyre J, Stewart J, Symington IS. Influence of Smoking on Immunological Responses to Hepatitis B Vaccine. *Vaccine* (1994) 12:771–2. doi: 10.1016/0264-410X(94)90283-6

20. Nakeshbandi M, Maini R, Daniel P, Rosengarten S, Parmar P, Wilson C, et al. The Impact of Obesity on COVID-19 Complications: A Retrospective Cohort Study. *Int J Obes (Lond)* (2020) 44:1832–7. doi: 10.1038/s41366-020-0648-x
21. Stanetić K, Stanetić B, Petrović V, Marković B, Kević V, Todorović N, et al. The Influence of Different Risk Factors on COVID-19 Outcomes in Adult Patients - An Observational-Descriptive Study. *Acta Med Acad* (2021) 50:308–16. doi: 10.5644/ama2006-124.348

**Conflict of Interest:** The authors declare that the research was conducted in the absence of any commercial or financial relationships that could be construed as a potential conflict of interest.

**Publisher's Note:** All claims expressed in this article are solely those of the authors and do not necessarily represent those of their affiliated organizations, or those of the publisher, the editors and the reviewers. Any product that may be evaluated in this article, or claim that may be made by its manufacturer, is not guaranteed or endorsed by the publisher.

frontiers in Immunology

ORIGINAL RESEARCH
published: 29 March 2022
doi: 10.3389/fimmu.2022.823652

# Adult Memory T Cell Responses to the Respiratory Syncytial Virus Fusion Protein During a Single RSV Season (2018–2019)

*Brittani N. Blunck[1], Laura S. Angelo[1], David Henke[1], Vasanthi Avadhanula[1], Matthew Cusick[2], Laura Ferlic-Stark[1], Lynn Zechiedrich[1,3,4], Brian E. Gilbert[1] and Pedro A. Piedra[1,5]**

[1] Department of Molecular Virology and Microbiology, Baylor College of Medicine, Houston, TX, United States, [2] Department of Pathology, University of Michigan, Ann Arbor, MI, United States, [3] Verna and Marrs McLean Department of Biochemistry and Molecular Biology, Baylor College of Medicine, Houston, TX, United States, [4] Department of Pharmacology and Chemical Biology, Baylor College of Medicine, Houston, TX, United States, [5] Department of Pediatrics, Baylor College of Medicine, Houston, TX, United States

OPEN ACCESS

**Edited by:**
*Eui Ho Kim,*
*Institut Pasteur Korea, South Korea*

**Reviewed by:**
*Efrain Guzman,*
*Oxford BioMedica, United Kingdom*
*Karen Bohmwald,*
*Pontificia Universidad Católica de Chile, Chile*

***Correspondence:**
*Pedro A. Piedra*
*ppiedra@bcm.edu*

**Specialty section:**
*This article was submitted to Immunological Memory, a section of the journal Frontiers in Immunology*

**Received:** *27 November 2021*
**Accepted:** *02 March 2022*
**Published:** *29 March 2022*

**Citation:**
*Blunck BN, Angelo LS, Henke D, Avadhanula V, Cusick M, Ferlic-Stark L, Zechiedrich L, Gilbert BE and Piedra PA (2022) Adult Memory T Cell Responses to the Respiratory Syncytial Virus Fusion Protein During a Single RSV Season (2018–2019). Front. Immunol. 13:823652. doi: 10.3389/fimmu.2022.823652*

Respiratory Syncytial Virus (RSV) is ubiquitous and re-infection with both subtypes (RSV/A and RSV/B) is common. The fusion (F) protein of RSV is antigenically conserved, induces neutralizing antibodies, and is a primary target of vaccine development. Insight into the breadth and durability of RSV-specific adaptive immune response, particularly to the F protein, may shed light on susceptibility to re-infection. We prospectively enrolled healthy adult subjects ($n$ = 19) and collected serum and peripheral blood mononuclear cells (PBMCs) during the 2018–2019 RSV season. Previously, we described their RSV-specific antibody responses and identified three distinct antibody kinetic profiles associated with infection status: uninfected ($n$ = 12), acutely infected ($n$ = 4), and recently infected ($n$ = 3). In this study, we measured the longevity of RSV-specific memory T cell responses to the F protein following natural RSV infection. We stimulated PBMCs with overlapping 15-mer peptide libraries spanning the F protein derived from either RSV/A or RSV/B and found that memory T cell responses mimic the antibody responses for all three groups. The uninfected group had stable, robust memory T cell responses and polyfunctionality. The acutely infected group had reduced polyfunctionality of memory T cell response at enrollment compared to the uninfected group, but these returned to comparable levels by end-of-season. The recently infected group, who were unable to maintain high levels of RSV-specific antibody following infection, similarly had decreased memory T cell responses and polyfunctionality during the RSV season. We observed subtype-specific differences in memory T cell responses and polyfunctionality, with RSV/A stimulating stronger memory T cell responses with higher polyfunctionality even though RSV/B was the dominant subtype in circulation. A subset of individuals demonstrated an overall deficiency in the generation of a durable RSV-specific adaptive immune response.

Because memory T cell polyfunctionality may be associated with protection against re-infection, this latter group would likely be at greater risk of re-infection. Overall, these results expand our understanding of the longevity of the adaptive immune response to the RSV fusion protein and should be considered in future vaccine development efforts.

**Keywords: respiratory syncytial virus (RSV), infection, fusion protein, peptide library, memory T cell, polyfunctionality, viral immunity**

## INTRODUCTION

RSV is a major global health burden as it is a leading cause of acute lower respiratory infection (ALRI) in young children and the elderly (1). RSV causes approximately 22% of all severe ALRI worldwide resulting in over 30 million annual cases and 3 million hospitalizations. These hospitalizations result in 55,000–199,000 deaths, 50,000–75,000 of which are in-hospital deaths in children under the age of 5 years (1, 2). In addition to infants and young children, RSV causes significant morbidity and mortality in older adults and immunocompromised individuals, with a similar disease burden to influenza (3–6).

Immune responses to the initial and subsequent RSV exposures are non-sterilizing, as evidenced by re-infection throughout life (6, 7). This inadequate immune response is not caused by the viral evasion of the immune system seen with other respiratory viruses, including influenza, and is most notable in human challenge studies showing that individuals can be re-infected within two months with identical viral inoculum (7). Why or how the primary immune response fails to protect from subsequent RSV exposure remains unclear. RSV-specific serum antibody, particularly neutralizing antibody, increases protection against re-infection and reduces severe disease in young children, young adults, and the elderly (8–13). Maternal-infant cord blood demonstrates that neutralizing activity correlates with protection of infants from severe disease (14). However, older adults hospitalized with RSV have levels of neutralizing antibody that are considered protective in young children (15), implying that either their repertoire of neutralizing antibodies are less effective or there are other more critical mediators of protection in this population. Therefore, the pathogenesis of disease in re-infection in older adults is likely to require immune mechanisms of protection that are different from that required for the initial infection in infants and young children. Fatal infant cases of RSV demonstrate an almost complete absence of T cells and NK cells in the lungs, illustrating a critical role for these immune cells in controlling viral replication and clearance (16). Conversely, T cells have been implicated in the disease pathogenesis of RSV by causing rampant inflammation (17–19). The longevity and durability of the T cell response following natural RSV-infection in RSV-primed individuals and its role in providing protection from re-infection or severe disease remains unclear.

The F protein, which mediates fusion between the viral and host cell membranes, is the primary focus of the neutralizing antibody response (20). It is also largely conserved between the two subtypes, RSV/A and RSV/B (21), making it a primary target of vaccination efforts (22). An enhanced understanding of the range and longevity of the RSV-specific adaptive immune response, particularly to the F protein, may shed light on the susceptibility to re-infection throughout life. In this study, we evaluated the RSV-specific memory T cell responses to the F protein in healthy adult subjects over the course of a single RSV season and found that memory T cell responses followed the three distinct antibody kinetic profiles that are associated with their RSV infection status: uninfected, acutely infected, and recently infected (23).

## MATERIALS AND METHODS

### Study Design

Healthy adults were eligible for enrollment into a longitudinal prospective study during the 2018–2019 RSV season in Houston, Texas, United States, as described previously (23). The Institutional Review Board at Baylor College of Medicine approved the study protocol prior to initiation of the study. Written informed consent was obtained from all enrolled participants prior to any study related procedures. Briefly, nineteen healthy adults were enrolled and completed the study. Blood samples were collected at three time points (Visits 1, 2, and 3), which occurred in November 2018, January 2019, and May 2019, respectively. RSV infection status was determined by changes in RSV neutralizing antibody titers using four qualified microneutralization assays (24) utilizing prototypic (RSV/A/Tracy and RSV/B/18537) and contemporaneous (RSV/A/Ontario and RSV/B/Buenos Aires) isolates. Volunteers with less than a four-fold change in RSV neutralizing antibody activity over the course of the season by all four assays were defined as uninfected; those with four-fold or greater increases between two consecutive study visits by one or more assay were defined as having an acute RSV infection; and those with a four-fold or greater decrease in neutralizing antibody titer at their second visit by one or more assay were defined as having a recent infection prior to enrollment, indicating we missed the baseline titer prior to RSV infection (23).

### Peripheral Blood Mononuclear Cell Isolation

Blood was collected in sodium citrate CPT tubes (BD Vacutainer, Cat. #62761) and processed within four hours of collection. PBMCs were isolated by centrifugation for 30 minutes at 1800 x g (RCF) at room temperature (21°C). Cells were washed 3 times in phosphate buffered saline (PBS) with centrifugation at 300 x g (RCF) for 10 minutes at room temperature (21°C). Cells were

frozen in 10% dimethyl sulfoxide (DMSO) in fetal bovine serum (FBS) and stored in liquid nitrogen.

## Fusion Protein Peptide Library Generation

Overlapping peptide libraries of the full-length RSV F0 protein derived from RSV/A/Ontario (GenBank ID: AZQ19478.1) was custom ordered (Genentech, San Francisco, CA) and RSV/B/B1 (Swiss-Prot ID: O36634) was obtained from JPT (Berlin, Cat. #PM-HRSVB-FGF0). Each library contained 141 15-mer peptides with an 11 amino acid overlap (25, 26). Each peptide library was reconstituted in DMSO and stored at -80°C in single use aliquots.

## *In Vitro* Stimulation and Multiparametric Flow Cytometry

PBMCs were rapidly thawed in a 37°C water bath and added dropwise into pre-warmed R10 medium (RPMI 1640 + 10% FBS). Cells were washed in R10 medium to remove excess DMSO, and viable cells were counted using trypan blue exclusion. Cells were resuspended at 1.5 x $10^6$ cells/mL in 5 mL of R10 medium in 50 mL conical tubes and rested overnight at 37°C in 5% $CO_2$. Tubes were placed at a 5° angle, and the cap loosened to allow for maximum oxygenation (27). After resting overnight, samples were plated into 96-well round bottom plates. Cells were stimulated with either R10 medium alone (negative unstimulated control), PMA/ionomycin (positive control), the RSV/A/Ontario F (RSV $F_A$) protein peptide library, or the RSV/B/B1 F (RSV $F_B$) protein peptide library. Both RSV $F_A$ and RSV $F_B$ protein peptide library contained anti-CD28 and anti-CD49d co-stimulatory agents (Becton-Dickinson Biosciences, Franklin Lakes, NJ Cat. #347690) with brefeldin A, monensin, and anti-CD107a antibody. Stimulation was for 6 hours at 37°C in 5% $CO_2$ (28, 29). Following stimulation, cells were washed in PBS (without $Ca^{++}$ or $Mg^{++}$), and viability dye (ThermoFisher Scientific, Waltham, NJ) was added to enable gating out any non-viable cells. Fc-blocking was performed to reduce non-specific binding of antibodies using 5% FBS in PBS. Extracellular antibodies were then added and incubated for 20 minutes in the dark at room temperature. Following washing, cells were fixed and permeabilized (BD Cyto Fixation/Permeabilization kit, Cat #554714) for 20 minutes in the dark at 4°C. Cells were washed twice with BD CytoWash solution (BD Cyto Fixation/Permeabilization kit, Cat #554714). Antibodies for intracellular markers were then added for intracellular staining and incubated for 30 minutes in the dark at 4°C. Cells were washed twice in BD CytoWash solution and then cells were resuspended in 1% paraformaldehyde prior to acquisition. In total, samples were stained with a pool of fluorescence-conjugated antibodies for CD45, CD56, CD16, CD3, CD4, CD8, CD45RO, CD107a, TNFα, IFNγ, and PD-1. Cells were analyzed on an LSRII-Fortessa flow cytometer running DiVa software (Becton-Dickinson Biosciences, Franklin Lakes, NJ), and data were analyzed using FlowJo (version 10.7.1; TreeStar, OR) and Simplified Presentation of Incredibly Complex Evaluations (SPICE; National Institute of Health, Bethesda, MD) software. Viable lymphocytes were identified by forward- and side-scatter, single-cell discrimination, live/dead measurements using viability dye exclusion, and expression of the pan-lymphocyte marker CD45.

## Uniform Manifold Approximation and Projection Visualization of Flow Cytometric Data

Contour plots were generated using 'contour' visualization in FlowJo (using equal probability contouring). For uniform manifold approximation and projection (UMAP) analysis, all samples were down-sampled to 5,000 cells using the DownSample plugin (v3.3) available on FlowJo Exchange. All samples were concatenated to create a single, 1,140,000 cell composite, and a UMAP algorithm for dimensionality reduction was applied using the UMAP plugin (v3.1) available on FlowJo Exchange (30, 31). The composite sample was then re-gated as indicated for all primary and secondary populations to aid in visual overlays in exploration of the UMAP projections. Density plots representing 90% of the total gated cells by RSV infection status or stimulation were superimposed upon UMAP projections to visualize differences by study visit.

## Simplified Presentation of Incredibly Complex Evaluation Analysis

Simplified Presentation of Incredibly Complex Evaluation (SPICE) is a software that can be used to analyze multivariate data sets for which a series of nominal measurements and a single continuous measurement is available. We employed SPICE software in our study as a means to visually inspect and represent the polyfunctionality of T cell subsets in response to stimulation with either RSV $F_A$ or RSV $F_B$ protein peptide libraries (32). SPICE analysis is largely qualitative rather than quantitative and is used to provide an overall commentary of the trends in the data. No statistical conclusions were drawn from the SPICE data and we do not refer to any differences in polyfunctional responses as "significant" since other methods were used to determine statistical significance throughout the manuscript.

## High Resolution Human Leukocyte Antigen-Typing

Blood was collected in Acid Citrate Dextrose tubes (Becton-Dickinson Biosciences, Franklin Lakes, NJ) and DNA was extracted from whole blood using the Qiagen EZ1® DNA Blood 350 µl Kit (Qiagen, Hilden, Germany) with the EZ1 Advanced system. After extraction, DNA concentration and quality were measured with the Qiagen Qiexpert spectrophotometer. Next generation sequencing (NGS) human leukocyte antigen (HLA)-typing for HLA-A, -B, -C, -DRB1, -DRB3/4/5, -DQB1, -DQA1, -DPB1, and -DPA1 was done using MIA FORA kit (Immucor, Norcross, GA), according to the manufacturer's instructions. Briefly, after long-range PCR amplification of each HLA gene, DNA fragments (500–900 bp) were selected, amplified, cleaned, and sequenced on a MiSeq using MiSeq Reagent Kits v2 (300 cycles) (Illumina, San Diego, CA). Samples were analyzed using MIA FORA NGS software.

## Prediction of RSV/A and RSV/B F Protein T Cell Epitopes

T cell epitopes within the RSV $F_A$ and RSV $F_B$ protein peptide libraries were predicted using the Immune Epitope Database and Analysis Resource (IEDB, National Institute of Allergy and Infectious Disease, Bethesda, MD) major histocompatibility complex (MHC)-I and MHC-II binding algorithms (33, 34). Only HLA alleles from our cohort were included in the predictions and allele-specific percentile ranks of all algorithms queried by the IEDB tool were utilized (35). A percentile rank is generated by comparing the predicted binding affinity of a selected peptide against that of a large set of similarly sized peptides randomly selected from the SWISS-PROT database (36). Percentile rank provides a uniform scale allowing comparisons across different predictors. A lower percentile rank indicates higher affinity. Predicted hits were further refined to those specifically within our peptide libraries utilizing a threshold of <5% for both MHC-I and MHC-II.

## Statistical Analysis

A repeated measures mixed model analysis was performed to assess differences in expression of each functional marker among the three RSV infection status groups and three study visits. The covariance structure and diagnostic plots of the residuals were examined to assess the validity of the model assumptions for a repeated measures analysis of variance approach. The analysis first determined whether the visit by infection status interaction term in the model was significant by the omnibus F-test. Pairwise comparisons were conducted only of the mean percentage difference between the visits within each infection status group for a total of nine *a priori* comparisons per functional marker. Statistical significance was indicated for $P$ values $\leq 0.05$. No correction was made for multiple comparisons. T cell and neutralizing antibody scores were calculated by quartile ranking responses, where the top quartile received a score of 4 and the lowest quartile received a score of 1. Populations of T cells that received scores included: total T cells, $CD4^+$ memory T cells, $CD8^+$ memory T cells and $CD4^+/CD8^+$ memory T cells which were summed for each individual to create a composite score with a range of 4–16. Separate T cell composite scores were calculated for responses to the RSV $F_A$ and RSV $F_B$ protein peptide libraries. Neutralizing antibody score was calculated by quartile ranking neutralizing antibody titers to RSV/A/Tracy, RSV/B/18537, RSV/A/Ontario, and RSV/B/Buenos Aires which were summed for each individual to create a composite score with a range of 4–16. Pearson's correlation coefficients were calculated between T cell scores to each peptide library and corresponding neutralizing antibody scores. Statistical analyses were performed using Stata 14 (Stata Corp, College Station, Texas).

# RESULTS

## Demographics

Healthy adults under the age of 65 with no underlying conditions were enrolled during the 2018–2019 RSV season, where RSV/B was the dominant circulating subtype, as described previously (23). There were three RSV infection status groups, which were defined by changes in neutralizing antibody titer: uninfected (n=12), acutely infected (n=4), and recently infected (n=3). Volunteers with less than a four-fold change in RSV neutralizing antibody activity over the course of the season by all four assays were defined as uninfected; those with four-fold or greater increases between two consecutive study visits by one or more assay were defined as having an acute RSV infection; and those with a four-fold or greater decrease in neutralizing antibody titer at their second visit by one or more assay were defined as having a recent infection prior to enrollment, indicating we missed the baseline titer prior to RSV infection. Ages ranged from 23–59, with no discernable difference detected among age, gender, or ethnicity across infection status (23).

## Total T Cell Responses to RSV F Protein Peptide Libraries

To compare functional responses of T cells among the three infection status groups, we first analyzed the total T cell response ($CD3^+$,$CD56^-$; **Figure 1**) by measuring the expression of four functional markers: CD107a, IFNγ, TNFα, and PD-1 using the antibody panel shown in **Supplementary Table 1**. A representative gating strategy is shown in **Supplementary Figure 1A**. All gates were set from fluorescence minus one (FMO) controls (**Supplementary Figure 1B**). CD107a (also known as LAMP-1) is a marker of degranulation of cytolytic T cells, whereas IFNγ and TNFα are pro-inflammatory cytokines, and PD-1 is a surface protein that negatively regulates immune responses, which serves as a marker of T cell exhaustion (37–39). In addition to analyzing single expression of these four markers, we also analyzed the polyfunctionality of the T cell response since the magnitude of a T-cell response as measured by a single parameter does not fully reflect its functional potential (40). Higher polyfunctionality can indicate a higher quality anti-viral immune response and is often used to evaluate the quality of vaccine-induced immune responses. Several studies have provided compelling evidence that the quality of the T cell response is a crucial factor in defining a protective T cell response (40–48). Consistent with the stability of their neutralizing antibody response (23), the uninfected group had a stable total T cell response over the course of the RSV season as measured by either single functional marker expression (**Figures 1A–D**) or polyfunctionality (as defined by dark blue and yellow pie slices) of activation markers CD107a, IFNγ, and TNFα (**Figure 1E**). The acutely infected group had minimal changes in single activation marker expression throughout the season but had significantly higher PD-1 expression at enrollment (Visit 1; **Figures 1A–E**). The T cells from the acutely infected group also displayed less polyfunctionality at enrollment compared to the uninfected group but regained polyfunctionality, comparable to the levels in the uninfected group by Visit 3. This pattern is similar to that observed with the neutralizing antibody responses for the acutely infected and uninfected groups (**Figure 1E**) (23). The total T cell response of the recently infected group followed a pattern similar to their neutralizing antibody response. There was

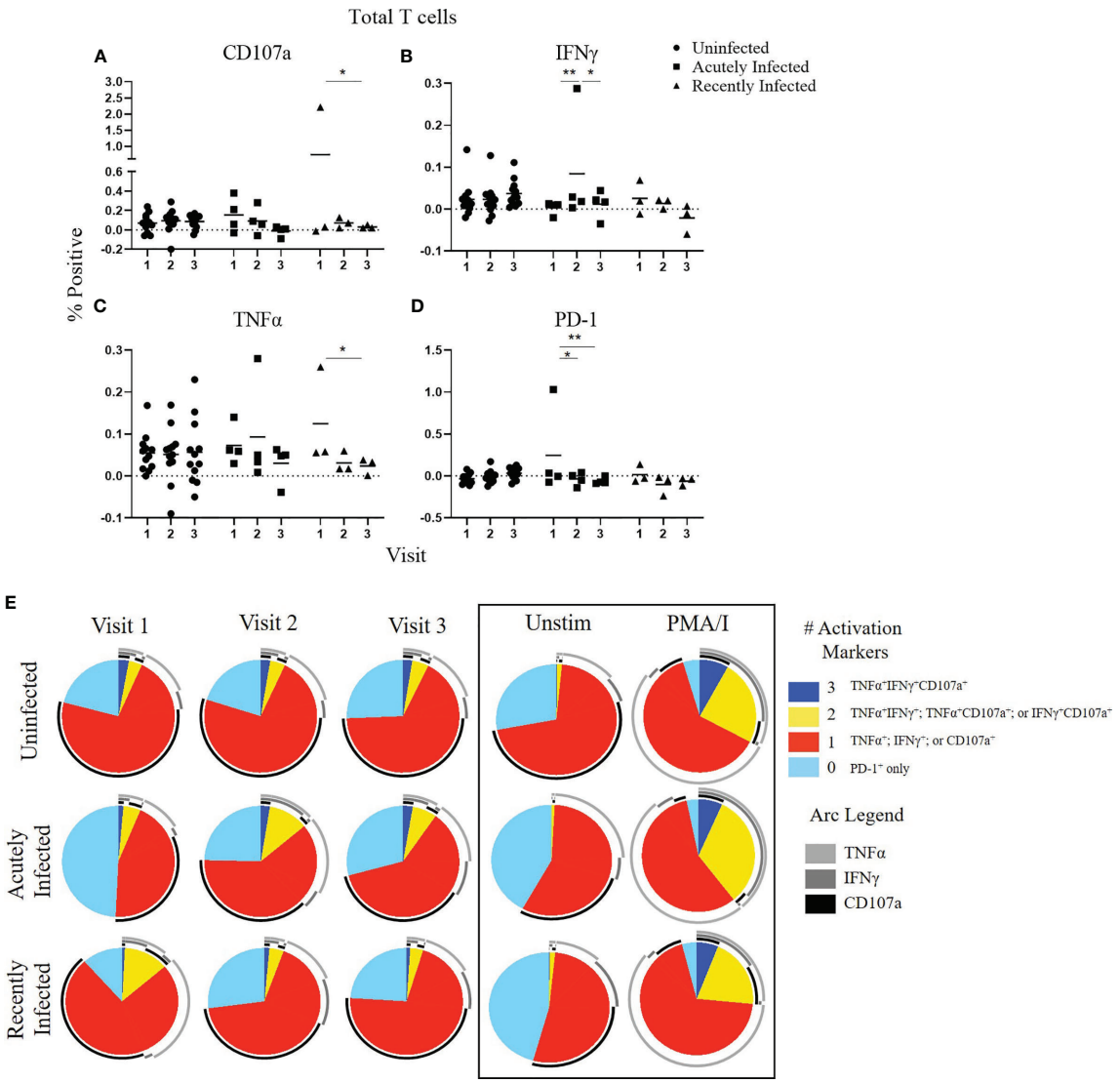


**FIGURE 1** | Total T cell responses to the RSV F protein peptide libraries as a function of RSV infection status and study visit. **(A–D)** Individual functional marker expression following stimulation with the RSV/A F (RSV $F_A$) protein peptide library by RSV infection status: uninfected ($n$ = 12), acutely infected ($n$ = 4), and recently infected ($n$ = 3). PBMCs from adult volunteers were stimulated with the RSV $F_A$ protein peptide library and the expression of CD107a, IFNγ, TNFα, and PD-1 were measured relative to the unstimulated controls by flow cytometry. These values are reported as percent positive of total $CD3^+$ T cells. Each symbol represents the response from a single individual. The thick horizontal bar indicates the mean of all responses within each group at that visit. A significant pairwise comparison of mean percentage difference between visits within a group is denoted by a thin horizontal bar with $^*P \leq 0.05$, $^{**}P \leq 0.01$. **(E)** Polyfunctional T cell responses to RSV $F_A$ protein peptide library by RSV infection status. Simplified Presentation of Incredibly Complex Evaluations (SPICE) software was used for the identification of total T cells expressing the various activation markers. Pie charts show the frequency in which PBMCs produced the various combinations of the activation markers CD107a, IFNγ, and TNFα; or expressed PD-1 alone. Background (determined from the media-stimulated negative controls) was subtracted from all samples and negative values were set to zero. Surrounding arcs denote the specific markers produced by the cells in each pie segment. Representative negative and positive controls across all study visits are boxed.

a significant decline in CD107a and TNFα expression over the course of the season (**Figures 2A, C**), as well as a reduction of polyfunctionality, although polyfunctionality remained low in comparison to the uninfected group at Visit 3 (**Figure 2E**). Total polyfunctional profiles with combinations of all four functional markers (CD107a, IFNγ, TNFα, and PD-1) followed similar patterns as described for the polyfunctional profiles of the three activation markers (**Supplementary Figure 2**). Additionally, all trends observed with the RSV $F_A$ protein peptide library were also observed following stimulation with the RSV $F_B$ F protein peptide library (data not shown).

## Uniform Manifold Approximation and Projection Analysis

We next wanted to consider whether there were global differences in T cells by RSV infection status or by RSV

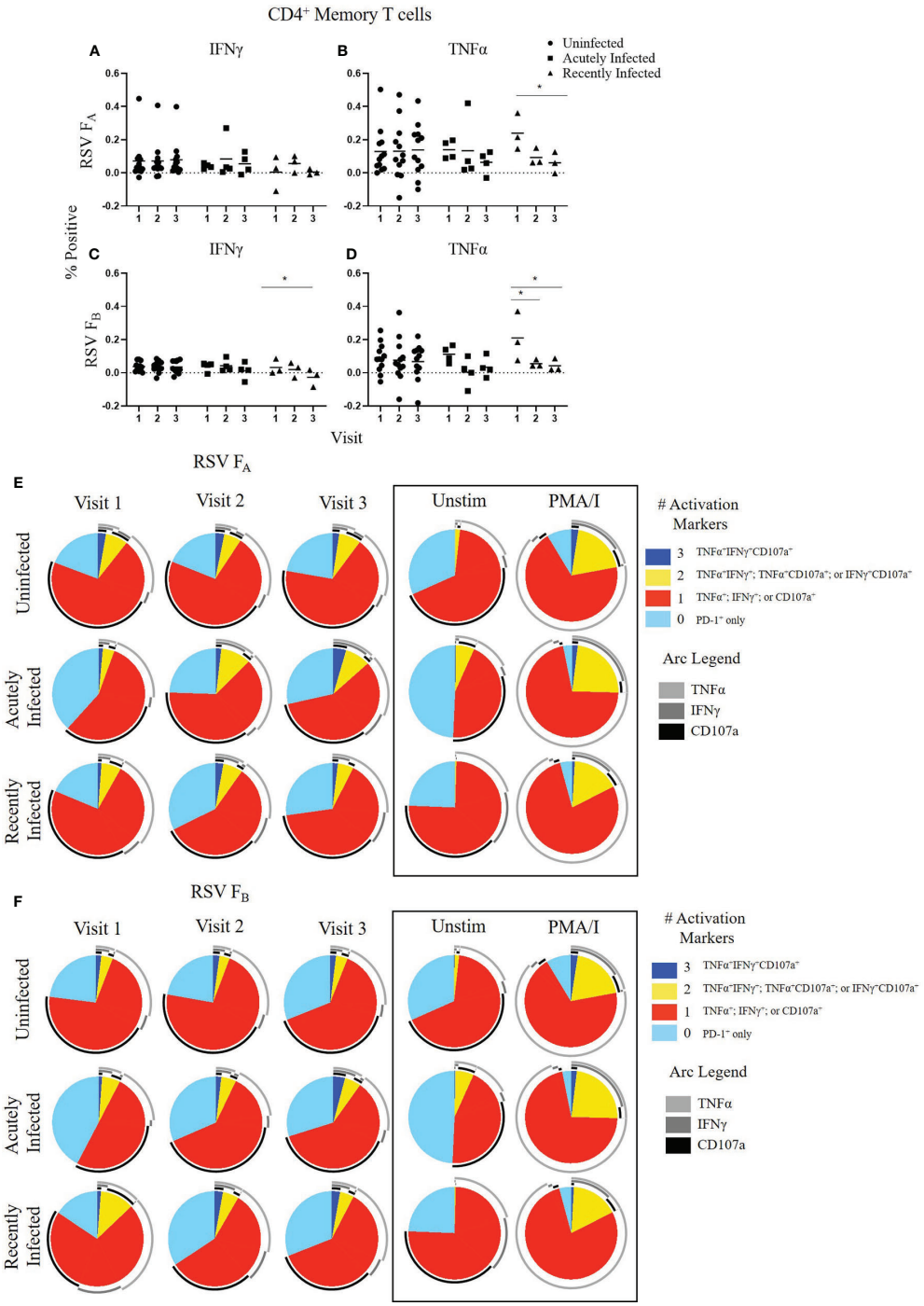


**FIGURE 2** | CD4+ Memory T cell responses to the RSV F protein peptide libraries by RSV infection status and study visit. **(A–D)** Individual functional marker expression by RSV infection status: uninfected ($n$ = 12), acutely infected ($n$ = 4), and recently infected ($n$ = 3). PBMCs were stimulated *in vitro* with RSV $F_A$ **(A, B)** or RSV $F_B$ **(C, D)** F protein peptide libraries. Marker expression is shown as percentage of total CD4+ memory T cells. symbol represents the response from a single individual. The thick horizontal bar indicates the mean of all responses within each group at that visit. A significant pairwise comparison of mean percentage difference between visits within a group is denoted by a thin horizontal bar with $^*P \leq 0.05$. **(E, F)** Polyfunctional CD4+ memory T cell responses to RSV $F_A$ or RSV $F_B$ protein peptide libraries as a function of RSV infection status and study visit. Simplified Presentation of Incredibly Complex Evaluations (SPICE) analysis was performed for the identification of CD4+ memory T cells expressing multiple activation markers. Pie charts show the frequency in which PBMCs produced the various combinations of the activation markers CD107a, IFNγ, and TNFα; or expressed PD-1 alone. Background (determined from the media-stimulated negative controls) was subtracted from all samples and negative values were set to zero. Surrounding arcs denote the specific markers produced by the cells in each pie segment. Representative negative and positive controls across all study visits are boxed.

subtype. To aid in exploration of the dataset, we created a composite sample by representative down-sampling (5,000 cells per sample) flow cytometry results obtained from each study subject at each study visit using the DownSample plugin (v3.3) available on FlowJo Exchange. A sample UMAP algorithm for dimensionality reduction was applied to gated live T lymphocytes ($CD45^+CD3^+CD56^-$) composite sample and assessed all additional fluorescence markers (**Supplementary Figure 3**). Cells from the composite sample were mapped in Cartesian space (**Supplementary Figure 3A**). Gating on T cell subsets following the strategy outlined in **Supplementary Figure 1**, confirmed that UMAP analysis clustered distinct cell phenotypes (**Supplementary Figure 3B**). We compared UMAP clustering among infection status groups to understand whether there are global differences in T cell populations in response to stimulation with the RSV F protein peptide libraries that could explain, at least in part, the different antibody kinetic profiles of our cohort (**Supplementary Figure 3C**).

We found that whereas there were variations within each infection status group at the various study visits, there were no variations associated with infection status (**Supplementary Figure 3C**). To assess whether there were RSV subtype-specific differences, we compared T cell responses following stimulation with the two different RSV F protein peptide libraries (**Supplementary Figure 3D**) and found that there was no difference. Virus-specific T cell responses are rare events. Therefore, these results were not surprising and indicate that any differences in responses among the subject groups or RSV virus-subtypes were based upon functionality rather than broad T cell phenotype.

## $CD4^+$ Memory T Cell Responses to RSV F Protein Peptide Libraries

We evaluated $CD4^+$ memory T cell ($CD45RO^+CD4^+$ T cells) responses (**Figure 2** and **Supplementary Figure 4**). CD107a and PD-1 expression did not change significantly within any of the groups following stimulation with either the RSV $F_A$ or RSV $F_B$ protein peptide library and are therefore not shown. As observed with the total T cell response, the uninfected group had a very stable $CD4^+$ memory T cell response to both F protein peptide libraries over the course of the RSV season as measured by single functional marker expression (**Figures 2A–D**) or by polyfunctionality of the activation markers (**Figures 2E, F**). The acutely infected group also had a very stable $CD4^+$ memory T cell response by single functional marker analysis (**Figures 2A–D**), but polyfunctional analyses revealed a distinct profile to that of the uninfected group with changes in polyfunctionality over the study duration when stimulated with either RSV $F_A$ or RSV $F_B$ protein peptide libraries (**Figures 2E, F**). The acutely infected group had a polyfunctional profile driven by increased PD-1 expression and reduced polyfunctionality compared to the uninfected group at enrollment (Visit 1). Polyfunctionality increased over the RSV season in the acutely infected group and more closely resembles that of the uninfected group by Visit 3. The recently infected group had significant decreases in $CD4^+$ memory T cell single marker expression of IFNγ, and TNFα over the course of the season but had only subtle changes in polyfunctionality over the RSV season (**Figures 2B, C**). The recently infected group had an increased double functionality (co-expression of two activation markers, indicated by yellow pie slice) and reduced triple functionality (co-expression of all 3 activation markers, indicated by dark blue) compared to the uninfected group at Visit 1. By Visit 3, however, the polyfunctional profile of $CD4^+$ memory T cells was comparable to that of the uninfected group.

## $CD8^+$ Memory T Cell Responses to RSV F Protein Peptide Libraries

We then evaluated $CD8^+$ memory T cell ($CD45RO^+CD8^+$ T cells) responses (**Figure 3**, and **Supplementary Figures 5**, **6**). The expression of single functional markers by $CD8^+$ memory T cells remained the same for each infection status for the duration of the study (**Supplementary Figure 5**). Although the expression of single functional markers was both low and stable, the polyfunctional profiles were distinct among the three groups (**Figure 3** and **Supplementary Figure 6**). Like the other subsets, the polyfunctionality of the $CD8^+$ memory T cell response in the uninfected group was consistent across the three study visits to both RSV F protein peptide libraries (**Figures 3A, B**). In the acutely infected group, there was a lack of triple functionality toward the RSV $F_A$ protein peptide library at enrollment (Visit 1; **Figure 3A**). Polyfunctionality in the acutely infected group expanded following infection at Visit 2 but retracted by Visit 3 to levels slightly lower than the uninfected group. Polyfunctionality of $CD8^+$ memory T cells toward the RSV $F_B$ protein peptide library in the acutely infected group was nearly absent over the study period (**Figure 3B**). The $CD8^+$ memory T cell response of the recently infected group was distinct from that of the uninfected or acutely infected group and displayed very little polyfunctionality toward either peptide library. This distinct profile is quite notable, particularly at Visit 1, when combinations of all four functional markers were analyzed (**Supplementary Figure 6**).

## $CD4^+/CD8^+$ Memory T Cell Responses to RSV F Protein Peptide Libraries

$CD4^+/CD8^+$ double positive T cells make up a low frequency of total T cells and can express memory markers such as CD45RO. Their role in viral immunity and cancer is hotly debated, though there is evidence they may have enhanced anti-viral capabilities (49–52). We therefore analyzed the $CD4^+/CD8^+$ memory T cell response among the infection status groups and found that the trends mimic those of the canonical $CD4^+$ or $CD8^+$ memory T cell response (**Supplementary Figure 7**). Similar to the other subsets of T cells, the uninfected group had very consistent levels of $CD4^+/CD8^+$ memory T cell response over the RSV season to both RSV F protein peptide libraries. The acutely infected group had a significant decrease in TNFα expression following infection, but by Visit 3 TNFα expression had returned to levels observed at enrollment. The recently infected group had

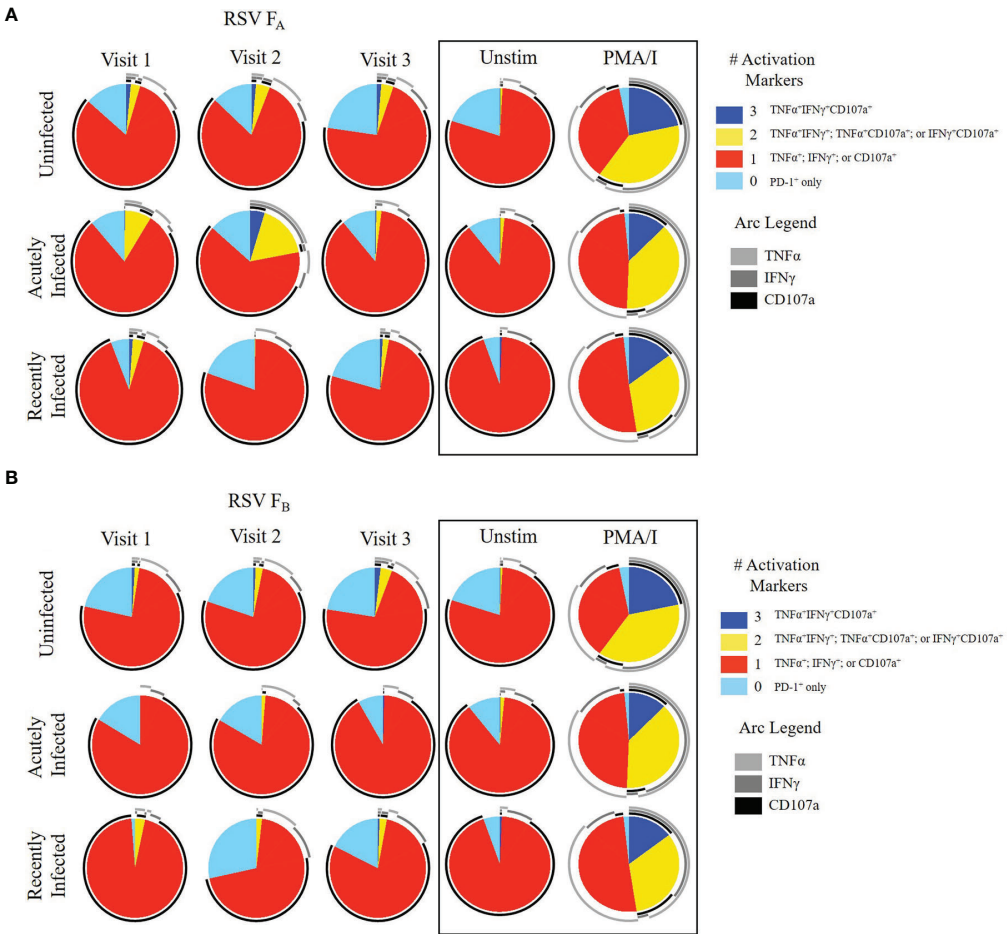


**FIGURE 3** | $CD8^+$ Memory T cell responses to RSV F protein peptide libraries as a function of RSV infection status and study visit. Polyfunctional $CD8^+$ Memory T cell responses to **(A)** RSV $F_A$ or **(B)** RSV $F_B$ protein peptide libraries by RSV infection status: uninfected ($n$ = 12), acutely infected ($n$ = 4), and recently infected ($n$ = 3). Simplified Presentation of Incredibly Complex Evaluations (SPICE) analysis was performed for the identification of $CD8^+$ memory T cells expressing multiple cytokines. Pie charts show the frequency in which PBMCs produced the various combinations of the activation markers CD107a, IFNγ, and TNFα; or expressed PD-1 alone. Background (determined from the media-stimulated negative controls) was subtracted from all samples and negative values were set to zero. Surrounding arcs denote the specific markers produced by the cells in each pie segment. Representative negative and positive controls across all study visits are boxed.

a significant decrease in CD107a expression over the RSV season. Taken altogether, responses of all T cell subsets, as measured by both the magnitude of single parameters and polyfunctionality, closely mimics that observed in the antibody kinetic profiles by RSV infection status (23).

## Subtype-Specific Differences in T Cell Responses to RSV F Protein Peptide Libraries

Because we observed differences between the responses to the RSV $F_A$ and RSV $F_B$ protein peptide libraries across all infection groups and T cell subsets, we combined these data for all 19 adults at each timepoint to assess viral subtype-specific differences in T cell responses. In total T cells, the RSV $F_A$ protein peptide library induced higher expression of each individual activation marker (CD107a, IFNγ, and TNFα) than the RSV $F_B$ protein peptide library (**Figures 4A–D**). Whereas this trend is only significant at Visit 3 for IFNγ and TNFα expression, the trend was consistent at every timepoint for these three activation markers. PD-1 expression, however, was similar between the two peptide libraries, indicating that stimulation with the RSV $F_B$ peptide library is not simply exhausting the T cells. There was also decreased polyfunctionality of the total T cell response when stimulated with the RSV $F_B$ protein peptide library compared to the RSV $F_A$ library at all three timepoints (**Figures 4E, F**).

We tested whether a specific compartment of the T cell response is driving these RSV subtype-specific differences. $CD4^+$ memory T cells demonstrated significantly higher CD107a, IFNγ, and TNFα expression at most time points when stimulated with RSV $F_A$ versus RSV $F_B$ protein peptide library (**Figures 5A–D**). There was also a subtle increased

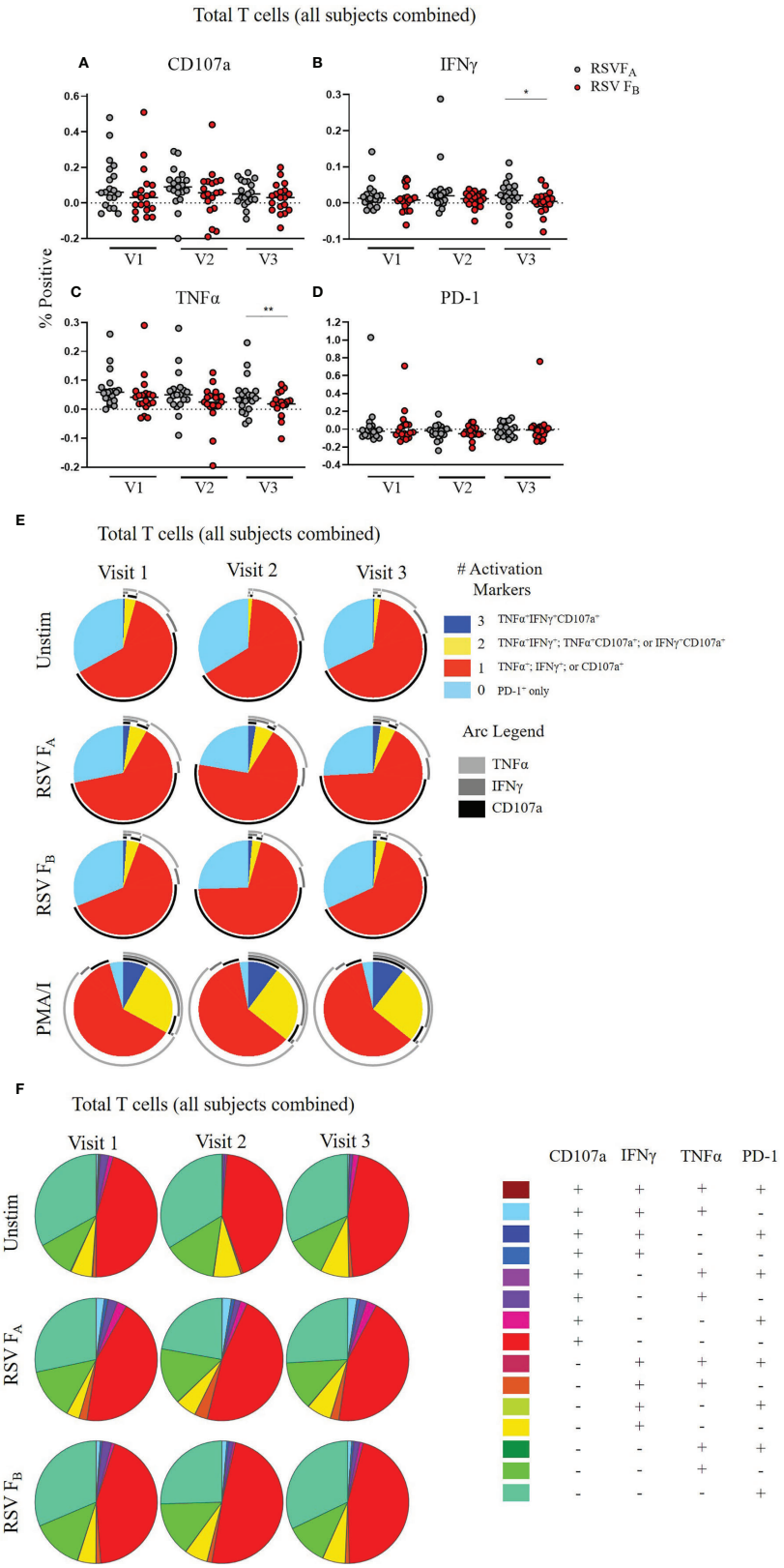


**FIGURE 4** | Continued

**FIGURE 4 |** RSV subtype-specific differences in total T cell responses to RSV F protein peptide libraries for all study subjects. **(A–D)** Individual functional marker expression following stimulation with either peptide library ($n$ = 19). PBMCs were stimulated with either RSV $F_A$ or RSV $F_B$ peptide library and expression of CD107a, IFNγ, TNFα, and PD-1 were measured by flow cytometry and reported as a percentage of total T cells. Each symbol represents the response from a single individual. The thick horizontal bar indicates the mean of all responses within each group at that visit. A significant pairwise comparison of mean percentage difference between visits within a group is denoted by a thin horizontal bar with $^*P \leq 0.05$, $^{**}P \leq 0.01$. V1, Visit 1; V2, Visit 2; V3, Visit 3. **(E)** Polyfunctionality of activation markers in total T cell responses as a function of stimulation type and study visit. Pie charts show the frequency in which PBMCs produced the various combinations of the activation markers CD107a, IFNγ, and TNFα; or expressed PD-1 alone. Background (determined from the media-stimulated negative controls) was subtracted from all samples and negative values were set to zero. Surrounding arcs denote the specific markers produced by the cells in each pie segment. Representative negative and positive controls across all study visits are boxed. **(F)** Total polyfunctionality of total T cells by stimulation and study visit. Pie segments indicate frequency of cells producing combinations of all four functional markers CD107a, IFNγ, and TNFα and PD-1. Background (determined from the media-only negative controls) was subtracted from all samples and negative values were set to zero.

polyfunctionality of $CD4^+$ memory T cells stimulated with the RSV $F_A$ library (**Figures 5E, F**). $CD8^+$ memory T cells displayed subtle differences in single marker expression between the two F protein peptide libraries, with significantly higher expression of CD107a at Visit 1 and IFNγ at Visit 2 (**Figures 6A–D**). There was a marked reduction in polyfunctionality of $CD8^+$ memory T cells when stimulated with RSV $F_B$ protein peptide library compared with the RSV $F_A$ protein peptide library (**Figures 6E, F**). Therefore, memory T cells from both major subsets ($CD4^+$ and $CD8^+$), drive these RSV subtype-specific differences in responses.

## RSV-Subtype Specific Differences in T Cell Responses Are Not Due to HLA-Haplotypes

Although the RSV/A/Ontario and RSV/B/B1 F protein sequences utilized to construct the F protein peptide libraries are very highly conserved (91% sequence homology), even small amino acid changes can lead to alternative T cell epitope recognition by individuals with specific HLA genotypes, which could potentially explain the RSV subtype-related differences in the T cell responses we observed. To test whether these subtype-specific differences are due to alternate epitope recognition originating from the HLA-restriction of the subjects in our cohort, we performed high resolution HLA-typing on all subjects in the study. We then predicted HLA-restricted epitopes within the RSV F protein (RSV/A/Ontario and RSV/B/B1) utilizing MHC class I and class II predictive algorithms (data not shown). We mapped these potential epitopes along the RSV F protein sequences to identify potential epitope 'hotspots' within each peptide library (data not shown). We found similar hotspots by subtype where the highest T cell epitope predictions (lowest rank scores) for MHC class II are consistently near the N terminus and between aa 150–250. The list of potential epitopes was refined by utilizing only those contained within both peptide libraries. Both subtypes had similar predicted epitopes within the 15mer peptide libraries (data not shown), indicating the RSV subtype-specific differences in T cell response do not stem from an inability of the adults in our cohort to respond to the peptide libraries because of antigen presentation.

## RSV-Specific T Cell and Neutralizing Antibody Responses Are Correlated

Finally, we tested the relationship between T cell and neutralizing antibody responses among RSV infection status or RSV subtype (**Figure 7** and **Supplementary Figure 8**). We were interested in determining if individuals with higher RSV-specific T cell activity also had higher RSV-specific neutralizing antibody levels. We used quartile-ranking of T cell and neutralizing antibody responses to test this hypothesis. We found that T cell and antibody scores were not correlated at Visit 1 or 2 but were highly correlated at Visit 3 for both RSV subtypes (**Figure 7A** and **Supplementary Figure 8A**). We found that the uninfected group was distributed evenly among the quartiles at Visits 1 and 2 (**Figure 7B** and **Supplementary Figure 8B**). At Visit 3 there was a significant correlation of the RSV $F_A$ T cell score and neutralizing antibody score in the uninfected group. There are, however, individuals with low quartile scores in the uninfected group, suggesting a small subset of this group may now be susceptible to re-infection. The acutely infected group had scores in the low quartile ranges for both antibody and T cell scores at Visit 1 but, following re-infection, these individuals ended in the high quartiles for both responses, suggesting protection from re-infection. Although not statistically significant, both RSV $F_A$ and RSV $F_B$ T cell scores nonetheless were highly correlated at Visit 3 (RSV $F_A$: $r = 0.730$; RSV $F_B$: $r = 0.880$). At enrollment, the recently infected group was in the high quartiles, but dropped to the low quartiles by Visit 2. The correlation coefficient for the recently infected group is undefined at Visit 3, suggesting no relationship between T cell and antibody responses. Therefore, by Visit 3, individuals who were high T cell responders were also high neutralizing antibody responders and those with low T cell responses had low neutralizing antibody responses.

# DISCUSSION

In this study we analyzed the memory T cell response to RSV F protein peptide libraries in a cohort of healthy adults with three distinct antibody kinetic profiles corresponding to their RSV infection status. We found that memory T cell responses mimic previously published antibody responses observed for the three distinct RSV infection status groups (23). Both the acutely and recently infected groups had reduced T cell polyfunctionality compared to the uninfected group at enrollment (Visit 1: early in the RSV season), indicating that higher RSV-specific memory T cell polyfunctionality may protect against re-infection. T cells from the acutely infected group displayed higher PD-1 expression, particularly at enrollment and even without stimulation, suggesting that these individuals' T cells may have

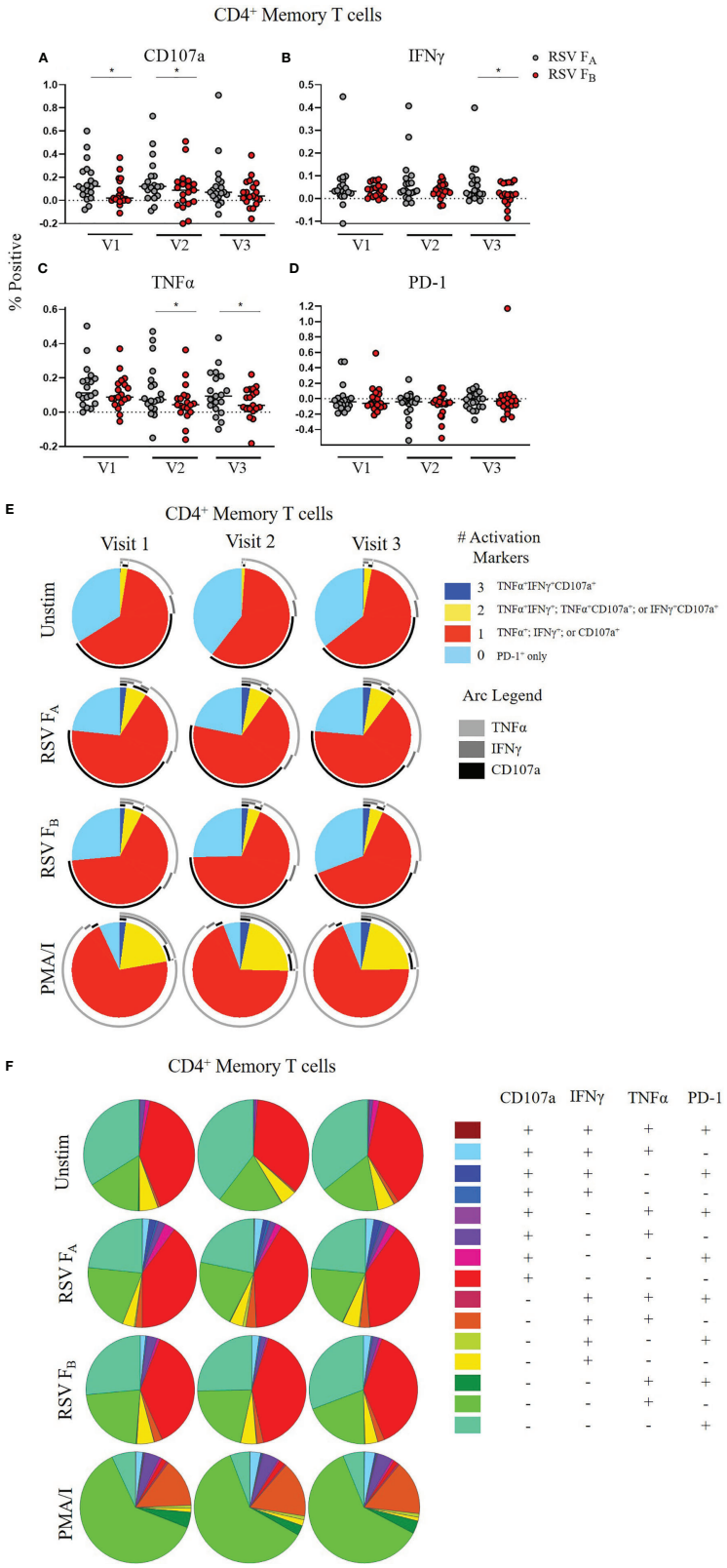


**FIGURE 5** | Continued

**FIGURE 5 |** RSV subtype-specific differences in $CD4^+$ Memory T cell responses to RSV F protein peptide libraries for all study participants. **(A–D)** Individual functional marker expression. PBMCs were stimulated *in vitro* with RSV $F_A$ **(A, B)** or RSV $F_B$ **(C, D)** peptide libraries ($n$ = 19). Expression of CD107a, IFNγ, TNFα, and PD-1 was measured by flow cytometry and reported as a percentage of $CD4^+$ memory T cells. Each symbol represents the response from a single individual. The thick horizontal bar indicates the mean of all responses within each group at that visit. A significant pairwise comparison of mean percentage difference between visits within a group is denoted by a thin horizontal bar with $^*P \leq 0.05$. V1, Visit 1; V2, Visit 2; V3, Visit 3. **(E)** Polyfunctionality of activation markers in $CD4^+$ memory T cell responses by stimulation and study visit. Pie charts represent the mean frequencies of responding $CD4^+CD45RO^+$ T cells following stimulation with RSV $F_A$ or RSV $F_B$ protein peptide library. Pie charts indicate frequency of cells producing combinations of the activation markers CD107a, IFNγ, and TNFα or expressing PD-1 alone. Background (determined from the media-only negative controls) was subtracted from all samples and negative values were set to zero. **(F)** Total polyfunctionality of $CD4^+$ memory T cells by stimulation and study visit. Pie segments indicate frequency of cells producing combinations of all four functional markers CD107a, IFNγ, and TNFα and PD-1. Background (determined from the media-only negative controls) was subtracted from all samples and negative values were set to zero.

been exhausted prior to infection, which may predispose them to RSV re-infection. Higher expression of PD-1 may also play an inhibitory role during the $CD8^+$ T effector cell transition to impair T cell differentiation and subsequent viral clearance during acute infection (38, 39). Additional studies with a larger cohort are warranted to test whether polyfunctionality of memory T cells can be used as a correlate of infection in the adult population.

Increased individual functional marker expression and increased polyfunctionality across all T cell subsets to the RSV $F_A$ F protein peptide library rather than the RSV $F_B$ protein peptide library was unexpected, as RSV/B was the dominant circulating subtype during the study period (23). Additionally, the highest fold changes in neutralizing antibody were detected to a prototypic B strain (RSV/B/18537), which is analogous to the RSV/B/B1 strain used for generating the F protein peptide library used in this study, and the lowest fold changes were detected to a contemporaneous RSV/A strain (RSV/A/ON) (23). Although the reason for this is unknown, the difference in subtype-specific T cell responses raises several interesting questions. Is this higher T cell response to the RSV $F_A$ protein peptide library characteristic of adults in general? If so, do the elderly consistently have a stronger T cell response to RSV/A F protein? Do these lower T cell responses to the RSV $F_B$ protein peptide library make adults more susceptible to RSV/B than RSV/A infections? Or is this difference in response reflective of what these particular adults were primed with in prior respiratory seasons? Additional studies testing the T cell responses of older adults, particularly with emphasis on polyfunctionality, as well as the frequency and severity of re-infection by subtype in this population, are warranted. These subtype-related differences have implications for vaccine development, as most vaccine candidates are derived from a single RSV/A strain (prototypic GA1). Our data indicate that adults may need additional protection from RSV/B, so bivalent vaccines containing both RSV subtypes may be warranted, at least for the older adult population.

The recently infected group had a significant decrease in memory T cell single marker expression over the RSV season and marked reduction of polyfunctionality of memory T cells in comparison with the uninfected group at Visit 3, implying these individuals have a lower overall quality of RSV-specific T cell response. Taken together with the antibody response profiles of these individuals (23), these results suggest an overall inability to sustain long-lived memory from both B and T cell responses. The rapid decay of antibody observed in the recently infected group closely resembles the natural decay of immunoglobulin in the absence of newly generated antibody (53, 54). This decay indicates that the antibody response in these individuals could be driven primarily by short-lived circulating plasma blasts that can secrete large amounts of antibody rapidly following infection rather than long-lived plasma cells that typically reside in bone marrow and maintain high levels of antibody long-term (55). Short-lived circulating plasma blasts are typically derived from an extrafollicular response unlike long-lived plasma cells, which are thought to be generated primarily through germinal center responses (55). We hypothesize that individuals in the recently infected group are predisposed to elicit primarily an extrafollicular rather than germinal center response to RSV infection. Predisposition toward an extrafollicular-dominant T cell response may have arisen during the primary exposure in infancy or, more likely, during multiple re-infection events throughout life.

The short-lived antibody response may not be limited to RSV but may hold true for other seasonal respiratory viruses. Indeed, we observed a rapid loss of hMPV-specific antibody responses within this cohort (23). Mechanistic studies aimed at elucidating the underlying cause of these various infection kinetic profiles of long-term memory will have significant impact on vaccine development for respiratory pathogens at large.

Whether or not there is a relationship between the T cell response and a known correlate of protection, neutralizing antibody, is unclear. By the end of our study period, we saw a significant correlation between T cell response scores (to both RSV subtypes) and neutralizing antibody scores. This correlation indicates that individuals with high neutralizing antibody responses are likely to have strong T cell responses (and *vice versa*). It is not surprising that the highest correlation is at Visit 3 compared to earlier study visits, as a limitation of the study is the timing of sample collections to capture the kinetics of T cell responses immediately following infection. As infections were defined using fold-changes in neutralizing antibody rather than PCR, the exact timing of RSV infection in the infected groups is unknown. Therefore, we are best able to detect a relationship at Visit 3, when all subjects have reached a steady-state in their RSV-specific immune response. A relationship between neutralizing antibody and T cell responses suggests that including T cell scores and using them in conjunction with neutralizing antibody responses may strengthen the ability to use them as a correlate of infection and help to identify individuals at higher risk for re-infection. Furthermore, there are differences in

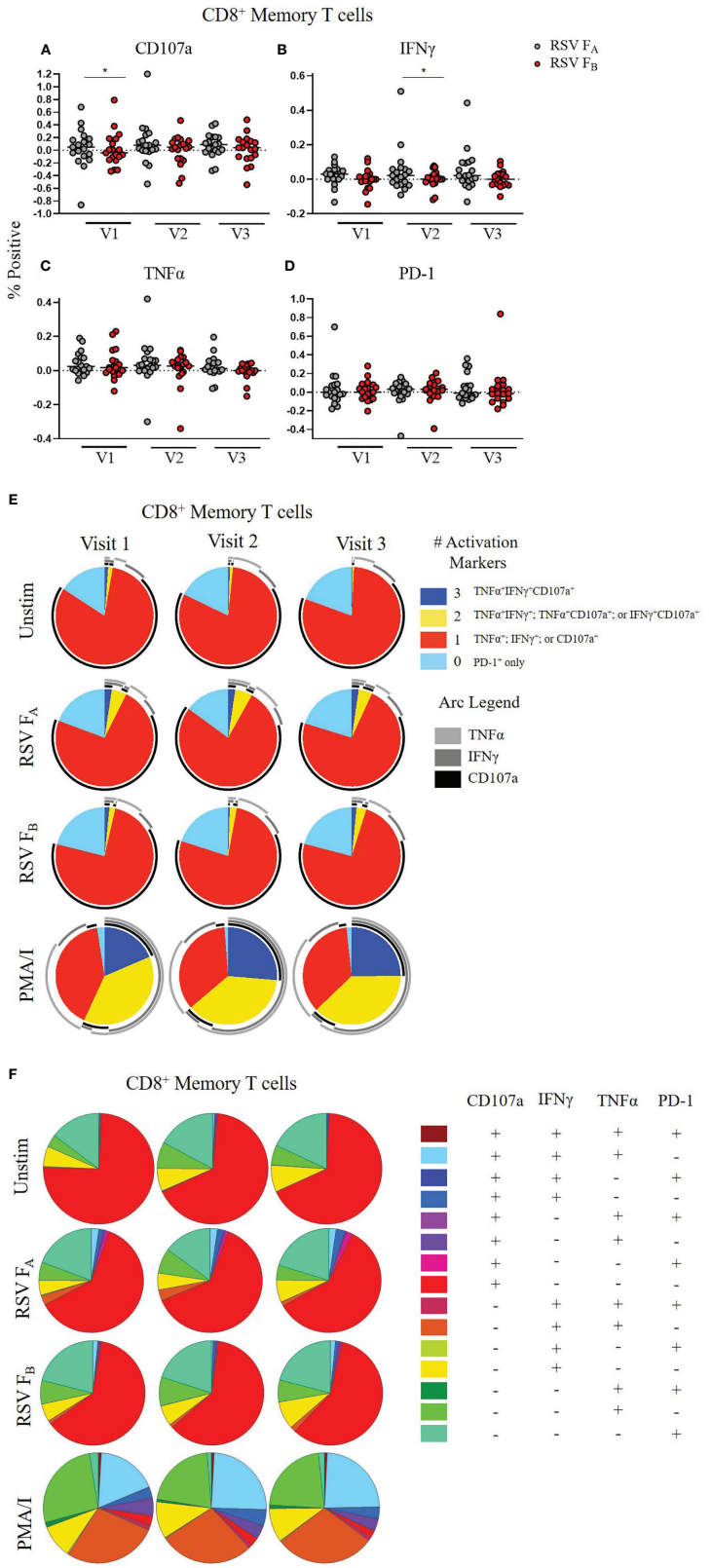


**FIGURE 6 |** Continued

**FIGURE 6 |** RSV subtype-specific differences in $CD8^+$ Memory T cell responses to RSV F protein peptide libraries for all study participants. **(A–D)** Individual functional marker expression. PBMCs were stimulated *in vitro* with RSV $F_A$ **(A, B)** or RSV $F_B$ **(C, D)** peptide libraries ($n$ = 19). Expression of CD107a, IFNγ, TNFα, and PD-1 was measured by ICS and reported as a percentage of $CD8^+$ memory T cells. Each symbol represents the response from a single individual. The thick horizontal bar indicates the mean of all responses within each group at that visit. A significant pairwise comparison of mean percentage difference between visits within a group is denoted by a thin horizontal bar with $^*P \leq 0.05$. V1, Visit 1; V2, Visit 2; V3, Visit 3. **(E)** Polyfunctionality of activation markers in $CD8^+$ memory T cell responses by stimulation and study visit. Pie charts represent the mean frequencies of responding $CD8^+CD45RO^+$ T cells following stimulation with RSV $F_A$ or RSV $F_B$ peptide library. Pie charts indicate frequency of cells producing combinations of the activation markers CD107a, IFNγ, and TNFα or expressing PD-1 alone. Background (determined from the media-only negative controls) was subtracted from all samples and negative values were set to zero. **(F)** Total polyfunctionality of $CD8^+$ memory T cells by stimulation and study visit. Pie segments indicate frequency of cells producing combinations of all four functional markers CD107a, IFNγ, and TNFα and PD-1. Background (determined from the media-only negative controls) was subtracted from all samples and negative values were set to zero.

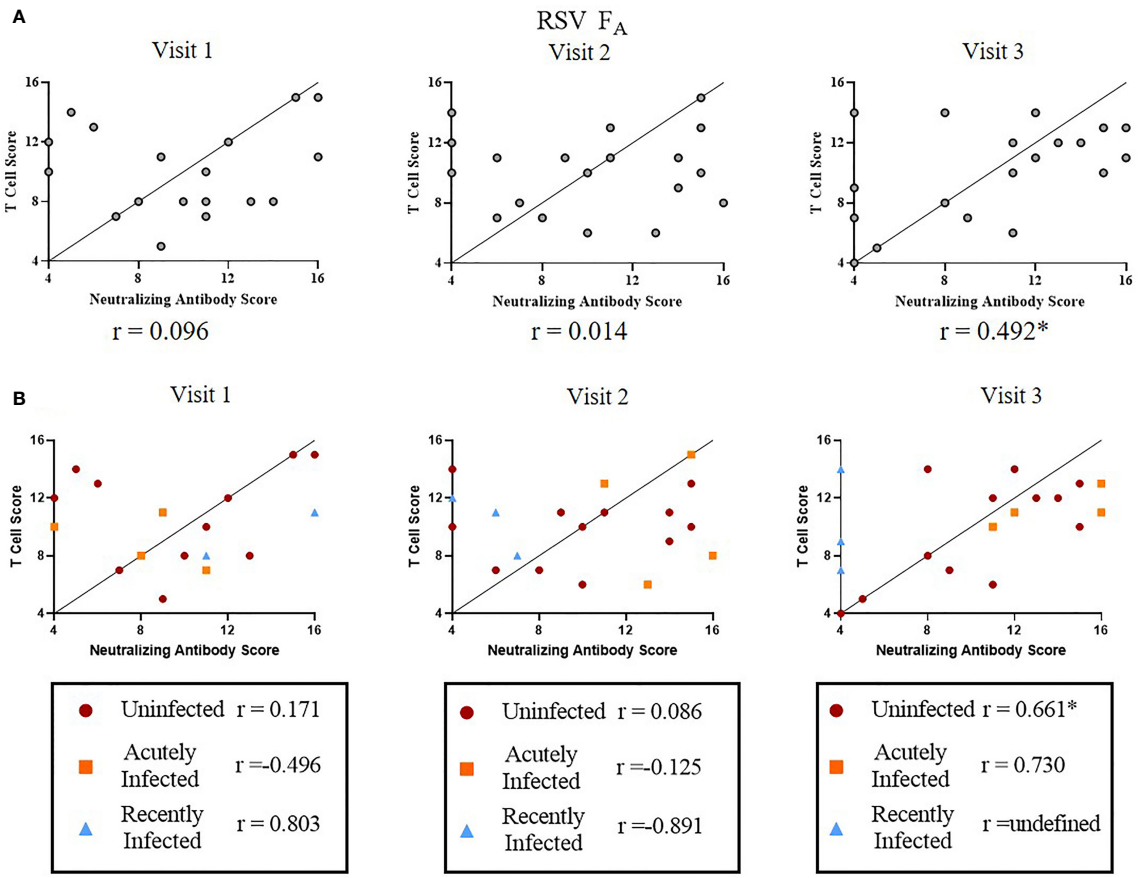


**FIGURE 7** | Correlation between RSV $F_A$ T cell and neutralizing antibody responses. A significant linear relationship between T cell score and neutralizing antibody score is denoted by a correlation coefficient (r) with $^*P \leq 0.05$. **(A)** Correlation between RSV $F_A$ T cell score with neutralizing antibody score by study visit ($n$ = 19). **(B)** Correlation between RSV $F_A$ T cell scores with neutralizing antibody score by RSV infection status and study visit. Uninfected ($n$ = 12), acutely infected ($n$ = 4), or recently infected ($n$ = 3) individuals are shown.

the scores by RSV infection status. The two infection groups have opposite patterns in that, the acutely infected group starts within the lowest quartile scores for both T cell and antibody responses, but by the end of the season have the highest for both. The recently infected group starts with high scores for both responses, but by the end of the season there is no relationship between scores. Together, these results strengthen the hypothesis that combined use of T cell scores and neutralizing antibody scores can be used as a correlate of infection.

In summary, we identified three distinct T cell immune responses to the RSV F protein peptide libraries that reflect three distinct antibody kinetic profiles. This increased understanding of how long RSV-subtype specific memory T cell responses persist and how this longevity relates to antibody responses increases our knowledge of how some adults become susceptible to re-infection. This knowledge is vital for developing an efficacious RSV vaccine, particularly in older adult populations where pre-existing immunity may need to be 're-

trained' for establishing an optimal and durable immune response upon vaccination.

## DATA AVAILABILITY STATEMENT

The original contributions presented in the study are included in the article/**Supplementary Materials**. Further inquiries can be directed to the corresponding author.

## ETHICS STATEMENT

The studies involving human participants were reviewed and approved by Institutional Review Board at Baylor College of Medicine. The patients/participants provided their written informed consent to participate in this study.

## AUTHOR CONTRIBUTIONS

BNB, PAP, BEG, and LZ designed the study, BNB performed data collection, BNB, LSA, LFS, DH, and PAP planned and conducted data analysis, LSA, VA, LFS, and MC helped with acquisition of data, all authors contributed to interpretation of data and to the decision to publish. BNB completed first and subsequent drafts of the manuscript, and all authors provided feedback and approved the final manuscript.

## FUNDING

Funding was from discretionary funds from PAP and BEG, and NIH grant R01GM115501 to LZ. This project was further supported by the Cytometry and Cell Sorting Core at Baylor College of Medicine with funding from the CPRIT Core Facility Support Award (CPRIT-RP180672), the NIH (CA125123 and RR024574) and the assistance of Joel M. Sederstrom.

## SUPPLEMENTARY MATERIAL

The Supplementary Material for this article can be found online at: https://www.frontiersin.org/articles/10.3389/fimmu.2022.823652/full#supplementary-material

## REFERENCES

1. Shi T, McAllister DA, O'Brien KL, Simoes EAF, Madhi SA, Gessner BD, et al. Global, Regional, and National Disease Burden Estimates of Acute Lower Respiratory Infections Due to Respiratory Syncytial Virus in Young Children in 2015: A Systematic Review and Modelling Study. *Lancet* (2017) 390:946–58. doi: 10.1016/S0140-6736(17)30938-8
2. Nair H, Nokes DJ, Gessner BD, Dherani M, Madhi SA, Singleton RJ, et al. Global Burden of Acute Lower Respiratory Infections Due to Respiratory Syncytial Virus in Young Children: A Systematic Review and Meta-Analysis. *Lancet* (2010) 375(9725):1545–55. doi: 10.1016/S0140-6736(10)60206-1
3. Shi T, Arnott A, Semogas I, Falsey AR, Openshaw P, Wedzicha JA, et al. The Etiological Role of Common Respiratory Viruses in Acute Respiratory Infections in Older Adults: A Systematic Review and Meta-Analysis. *J Infect Dis* (2020) 222(Supplement_7):S563–9. doi: 10.1093/infdis/jiy662
4. Shi T, Denouel A, Tietjen AK, Campbell I, Moran E, Li X, et al. Global Disease Burden Estimates of Respiratory Syncytial Virus-Associated Acute Respiratory Infection in Older Adults in 2015: A Systematic Review and Meta-Analysis. *J Infect Dis* (2020) 222(Supplement_ 7):S577–83. doi: 10.1093/infdis/jiz059
5. Branche AR, Falsey AR. Respiratory Syncytial Virus Infection in Older Adults: An Under-Recognized Problem. *Drugs Aging* (2015) 32(4):261–9. doi: 10.1007/s40266-015-0258-9
6. Walsh EE, Falsey AR. Respiratory Syncytial Virus Infection in Adult Populations. *Infect Disord Drug Targets* (2012) 12(2):98–102. doi: 10.2174/187152612800100116
7. Hall CB, Walsh EE, Long CE, Schnabel KC. Immunity to and Frequency of Re-Infection With Respiratory Syncytial Virus. *J Infect Dis* (1991) 163(4):693–8. doi: 10.1093/infdis/163.4.693
8. Piedra PA, Jewell AM, Cron SG, Atmar RL, Glezen PW. Correlates of Immunity to Respiratory Syncytial Virus (RSV)-Associated Hospitalization: Establishment of Minimum Protective Threshold Levels of Serum Neutralizing Antibodies. *Vaccine* (2003) 21(24):3479–82. doi: 10.1016/S0264-410X(03)00355-4
9. Stensballe LG, Ravn H, Kristensen K, Agerskov K, Meakins T, Aaby P, et al. Respiratory Syncytial Virus Neutralizing Antibodies in Cord Blood, Respiratory Syncytial Virus Hospitalization, and Recurrent Wheeze. *J Allergy Clin Immunol* (2009) 123(2):398–403. doi: 10.1016/j.jaci.2008.10.043
10. Piedra PA, Hause AM, Aideyan L. Respiratory Syncytial Virus (RSV): Neutralizing Antibody, a Correlate of Immune Protection. In: RA Tripp, PA Jorquera, editors. *Human Respiratory Syncytial Virus*, vol. 1442. New York, NY:Humana Press (2016). p. 77–91. doi: 10.1007/978-1-4939-3687-8_7
11. Luchsinger V, Piedra PA, Ruiz M, Zunino E, Martínez MA, Machado C, et al. Role of Neutralizing Antibodies in Adults With Community-Acquired Pneumonia by Respiratory Syncytial Virus. *Clin Infect Dis Off Publ Infect Dis Soc Am* (2012) 54(7):905–12. doi: 10.1093/cid/cir955
12. Terrosi C, Di Genova G, Martorelli B, Valentini M, Cusi MG. Humoral Immunity to Respiratory Syncytial Virus in Young and Elderly Adults. *Epidemiol Infect* (2009) 137(12):1684–6. doi: 10.1017/S0950268809002593
13. Lee FE-H, Walsh EE, Falsey AR, Betts RF, Treanor JJ. Experimental Infection of Humans With A2 Respiratory Syncytial Virus. *Antiviral Res* (2004) 63 (3):191–6. doi: 10.1016/j.antiviral.2004.04.005
14. Glezen WP, Paredes A, Allison JE, Taber LH, Frank AL. Risk of Respiratory Syncytial Virus Infection for Infants From Low-Income Families in Relationship to Age, Sex, Ethnic Group, and Maternal Antibody Level. *J Pediatr* (1981) 98(5):708–15. doi: 10.1016/s0022-3476(81)80829-3
15. Falsey AR, Walsh EE. Relationship of Serum Antibody to Risk of Respiratory Syncytial Virus Infection in Elderly Adults. *J Infect Dis* (1998) 177(2):463–6. doi: 10.1086/517376
16. Welliver TP, Reed JL, Welliver RCSr. Respiratory Syncytial Virus and Influenza Virus Infections: Observations From Tissues of Fatal Infant Cases. *Pediatr Infect Dis J* (2008) 27(10 Suppl):S92–6. doi: 10.1097/INF.0b013e318168b706
17. Graham BS, Bunton LA, Wright PF, Karzon DT. Role of T Lymphocyte Subsets in the Pathogenesis of Primary Infection and Rechallenge With Respiratory Syncytial Virus in Mice. *J Clin Invest* (1991) 88(3):1026–33. doi: 10.1172/JCI115362
18. Cannon MJ, Openshaw PJ, Askonas BA. Cytotoxic T Cells Clear Virus But Augment Lung Pathology in Mice Infected With Respiratory Syncytial Virus. *J Exp Med* (1988) 168(3):1163–8. doi: 10.1084/jem.168.3.1163
19. Schmidt ME, Knudson CJ, Hartwig SM, Pewe LL, Meyerholz DK, Langlois RA, et al. Memory CD8 T Cells Mediate Severe Immunopathology Following

Respiratory Syncytial Virus Infection. *PloS Pathog* (2018) 14(1):e1006810. doi: 10.1371/journal.ppat.1006810
20. Melero JA, Mas V, McLellan JS. Structural, Antigenic, and Immunogenic Features of Respiratory Syncytial Virus Glycoproteins Relevant for Vaccine Development. *Vaccine* (2017) 35(3):461–8. doi: 10.1016/j.vaccine.2016.09.045
21. Hause AM, Henke DM, Avadhanula V, Shaw CA, Tapia LI, Piedra PA. Sequence Variability of the Respiratory Syncytial Virus (RSV) Fusion Gene Among Contemporary and Historical Genotypes of RSV/A and RSV/B. *PloS One* (2017) 12(4):e0175792. doi: 10.1371/journal.pone.0175792
22. WHO Vaccine Pipeline Tracker. Available at: https://docs.google.com/spreadsheets/d/19otvINcayJURCMg76xWO4KvuyedYbMZDcXqbyJGdcZM/pubhtml (Accessed on 15 July 2021).
23. Blunck BN, Aideyan L, Ye X, Avadhanula V, Ferlic-Stark L, Zechiedrich L, et al. A Prospective Surveillance Study on the Kinetics of the Humoral Immune Response to the Respiratory Syncytial Virus Fusion Protein in Adults in Houston, Texas. *Vaccine* (2021) 39(8):1248–56. doi: 10.1016/j.vaccine.2021.01.045
24. Piedra PA, Grace S, Jewell A, Spinelli S, Bunting D, Hogerman DA, et al. Purified Fusion Protein Vaccine Protects Against Lower Respiratory Tract Illness During Respiratory Syncytial Virus Season in Children With Cystic Fibrosis. *Pediatr Infect Dis J* (1996) 15(1):23–31. doi: 10.1097/00006454-199601000-00006
25. Bell MJ, Burrows JM, Brennan R, Miles JJ, Tellam J, McCluskey J, et al. The Peptide Length Specificity of Some HLA Class I Alleles Is Very Broad and Includes Peptides of Up to 25 Amino Acids in Length. *Mol Immunol* (2009) 46 (8-9):1911–7. doi: 10.1016/j.molimm.2008.12.003
26. Chicz RM, Urban RG, Lane WS, Gorga JC, Stern LJ, Vignali DA, et al. Predominant Naturally Processed Peptides Bound to HLA-DR1 Are Derived From MHC-Related Molecules and Are Heterogeneous in Size. *Nature* (1992) 358(6389):764–8. doi: 10.1038/358764a0
27. Wang L, Hückelhoven A, Hong J, Jin N, Mani J, Chen BA, et al. Standardization of Cryopreserved Peripheral Blood Mononuclear Cells Through a Resting Process for Clinical Immunomonitoring–Development of an Algorithm. *Cytomet A* (2016) 89(3):246–58. doi: 10.1002/cyto.a.22813
28. Savic M, Dembinski JL, Kim Y, Tunheim G, Cox RJ, Oftung F, et al. Epitope Specific T-Cell Responses Against Influenza A in a Healthy Population. *Immunology* (2016) 147(2):165–77. doi: 10.1111/imm.12548
29. Peng Y, Mentzer AJ, Liu G, Yao X, Yin Z, Dong D, et al. Broad and Strong Memory $CD4^+$ and $CD8^+$ T Cells Induced by SARS-CoV-2 in UK Convalescent Individuals Following COVID-19. *Nat Immunol* (2020) 21 (11):1336–45. doi: 10.1038/s41590-020-0782-6
30. McInnes L, Healy J. *UMAP: Uniform Manifold Approximation and Projection for Dimension Reduction*. Preprint (2018) 3 (29):861. doi: 10.21105/joss.00861.
31. McInnes L, Healy J, Saul N, Großberger L. UMAP: Uniform Manifold Approximation and Projection. *J Open Source Software* (2018) 3:861. doi: 10.21105/joss.00861
32. Roederer M, Nozzi JL, Nason MC. SPICE: Exploration and Analysis of Post-Cytometric Complex Multivariate Datasets. *Cytomet A* (2011) 79(2):167–74. doi: 10.1002/cyto.a.21015
33. Zhang Q, Wang P, Kim Y, Haste-Andersen P, Beaver J, Bourne PE, et al. Immune Epitope Database Analysis Resource (IEDB-Ar). *Nucleic Acids Res* (2008) 36(Web Server issue):W513–8. doi: 10.1093/nar/gkn254
34. Vita R, Overton JA, Greenbaum JA, Ponomarenko J, Clark JD, Cantrell JR, et al. The Immune Epitope Database (IEDB) 3.0. *Nucleic Acids Res* (2015) 43 (Database issue):D405–12. doi: 10.1093/nar/gku938
35. Kim Y, Ponomarenko J, Zhu Z, Tamang D, Wang P, Greenbaum J, et al. Immune Epitope Database Analysis Resource. *Nucleic Acids Res* (2012) 40 (Web Server issue):W525–30. doi: 10.1093/nar/gks438
36. Wang P, Sidney J, Kim Y, Sette A, Lund O, Nielsen M, et al. Peptide Binding Predictions for HLA DR, DP and DQ Molecules. *BMC Bioinf* (2010) 11:568. doi: 10.1186/1471-2105-11-568
37. Terahara K, Ishii H, Nomura T, Takahashi N, Takeda A, Shiino T, et al. Vaccine-Induced CD107a+ CD4+ T Cells Are Resistant to Depletion Following AIDS Virus Infection. *J Virol* (2014) 88(24):14232–40. doi: 10.1128/JVI.02032-14
38. Jubel JM, Barbati ZR, Burger C, Wirtz DC, Schildberg FA. The Role of PD-1 in Acute and Chronic Infection. *Front Immunol* (2020) 11:487. doi: 10.3389/fimmu.2020.00487
39. Ahn E, Araki K, Hashimoto M, Li W, Riley JL, Cheung J, et al. Role of PD-1 During Effector CD8 T Cell Differentiation. *Proc Natl Acad Sci USA* (2018) 115(18):4749–54. doi: 10.1073/pnas.1718217115
40. Seder R, Darrah P, Roederer M. T-Cell Quality in Memory and Protection: Implications for Vaccine Design. *Nat Rev Immunol* (2008) 8:247–58. doi: 10.1038/nri2274
41. Makedonas G, Betts MR. Polyfunctional Analysis of Human T Cell Responses: Importance in Vaccine Immunogenicity and Natural Infection. *Springer Semin Immunopathol* (2006) 28(3):209–19. doi: 10.1007/s00281-006-0025-4
42. Betts MR, Nason MC, West SM, De Rosa SC, Migueles SA, Abraham J, et al. HIV Nonprogressors Preferentially Maintain Highly Functional HIV-Specific CD8+ T Cells. *Blood* (2006) 107(12):4781–9. doi: 10.1182/blood-2005-12-4818
43. Casazza JP, Betts MR, Price DA, Precopio ML, Ruff LE, Brenchley JM, et al. Acquisition of Direct Antiviral Effector Functions by CMV-Specific CD4+ T Lymphocytes With Cellular Maturation. *J Exp Med* (2006) 203(13):2865–77. doi: 10.1084/jem.20052246
44. Darrah PA, Patel DT, De Luca PM, Lindsay RW, Davey DF, Flynn BJ, et al. Multifunctional TH1 Cells Define a Correlate of Vaccine-Mediated Protection Against Leishmania Major. *Nat Med* (2007) 13(7):843–50. doi: 10.1038/nm1592
45. Precopio ML, Betts MR, Parrino J, Price DA, Gostick E, Ambrozak DR, et al. Immunization With Vaccinia Virus Induces Polyfunctional and Phenotypically Distinctive CD8+ T Cell Responses. *J Exp Med* (2007) 204 (6):1405–16. doi: 10.1084/jem.20062363
46. Wille-Reece U, Flynn BJ, Loré K, Koup RA, Kedl RM, Mattapallil JJ, et al. HIV Gag Protein Conjugated to a Toll-Like Receptor 7/8 Agonist Improves the Magnitude and Quality of Th1 and CD8+ T Cell Responses in Nonhuman Primates. *Proc Natl Acad Sci USA* (2005) 102(42):15190–4. doi: 10.1073/pnas.0507484102
47. Kannanganat S, Ibegbu C, Chennareddi L, Robinson HL, Amara RR. Multiple-Cytokine-Producing Antiviral CD4 T Cells Are Functionally Superior to Single-Cytokine-Producing Cells. *J Virol* (2007) 81:8468–76. doi: 10.1128/JVI.00228-07
48. Tilton JC, Luskin MR, Johnson AJ, Manion JM, Hallahan CW, Metcalf JA, et al. Changes in Paracrine Interleukin-2 Requirement, CCR7 Expression, Frequency, and Cytokine Secretion of Human Immunodeficiency Virus-Specific CD4+ T Cells Are a Consequence of Antigen Load. *J Virol* (2007) 81(6):2713–25. doi: 10.1128/JVI.01830-06
49. Frahm MA, Picking RA, Kuruc JD, McGee KS, Gay CL, Eron JJ, et al. CD4 +CD8+ T Cells Represent a Significant Portion of the Anti-HIV T Cell Response to Acute HIV Infection. *J Immunol* (2012) 188(9):4289–96. doi: 10.4049/jimmunol.1103701
50. Suni MA, Ghanekar SA, Houck DW, Maecker HT, Wormsley SB, Picker LJ, et al. CD4(+)CD8(dim) T Lymphocytes Exhibit Enhanced Cytokine Expression, Proliferation and Cytotoxic Activity in Response to HCMV and HIV-1 Antigens. *Eur J Immunol* (2001) 31(8):2512–20. doi: 10.1002/1521-4141(200108)31:8<2512::aid-immu2512>3.0.co;2-m
51. Nguyen P, Melzer M, Beck F, Krasselt M, Seifert O, Pierer M, et al. Expansion of CD4+CD8+ Double-Positive T Cells in Rheumatoid Arthritis Patients Is Associated With Erosive Disease. *Rheumatology* (2022) 61(3):1282–7. doi: 10.1093/rheumatology/keab551
52. Nascimbeni M, Shin EC, Chiriboga L, Kleiner DE, Rehermann B. Peripheral CD4 (+)CD8(+) T Cells Are Differentiated Effector Memory Cells With Antiviral Functions. *Blood* (2004) 104(2):478–86. doi: 10.1182/blood-2003-12-4395
53. Vieira P, Rajewsky K. The Half-Lives of Serum Immunoglobulins in Adult Mice. *Eur J Immunol* (1988) 18(2):313–6. doi: 10.1002/eji.1830180221
54. Mankarious S, Lee M, Fischer S, Pyun KH, Ochs HD, Oxelius VA, et al. The Half-Lives of IgG Subclasses and Specific Antibodies in Patients With Primary Immunodeficiency Who Are Receiving Intravenously Administered Immunoglobulin. *J Lab Clin Med* (1988) 112(5):634–40.
55. Weisel FJ, Zuccarino-Catania GV, Chikina M, Shlomchik MJ. A Temporal Switch in the Germinal Center Determines Differential Output of Memory B and Plasma Cells. *Immunity* (2016) 44(1):116–30. doi: 10.1016/j.immuni.2015.12.004

**Conflict of Interest:** The authors declare that the research was conducted in the absence of any commercial or financial relationships that could be construed as a potential conflict of interest.

this article, or claim that may be made by its manufacturer, is not guaranteed or endorsed by the publisher.

frontiers | Frontiers in Immunology

ORIGINAL RESEARCH
published: 21 June 2022
doi: 10.3389/fimmu.2022.917905

# Comparison of IgA, IgG, and Neutralizing Antibody Responses Following Immunization With Moderna, BioNTech, AstraZeneca, Sputnik-V, Johnson and Johnson, and Sinopharm's COVID-19 Vaccines

*Tomabu Adjobimey[1,2*], Julia Meyer[1], Leander Sollberg[1], Michael Bawolt[1], Christina Berens[1], Peđa Kovačević[3], Anika Trudić[4,5], Marijo Parcina[1†] and Achim Hoerauf[1,6†]*

[1] Institute of Medical Microbiology, Immunology and Parasitology (IMMIP), University Hospital Bonn, Bonn, Germany, [2] Faculté des Sciences et Techniques (FAST), Université d'Abomey Calavi, Abomey-Calavi, Bénin, [3] Medical Intensive Care Unit, University Clinical Center of Republic of Srpska, Banja Luka, Bosnia and Herzegovina, [4] Faculty of Medicine, University of Novi Sad, Novi Sad, Serbia, [5] Institute for Pulmonary Diseases of Vojvodina, Sremska Kamenica, Serbia, [6] Bonn-Cologne Site, German Center for Infectious Disease Research (DZIF), Bonn, Germany

OPEN ACCESS

**Edited by:**
Kihyuck Kwak,
Yonsei University, South Korea

**Reviewed by:**
Thorsten Demberg,
Baylor College of Medicine,
United States
Pean Polidy,
Institut Pasteur du Cambodge,
Cambodia

***Correspondence:**
Tomabu Adjobimey
Tomabu.Adjobimey@ukb.uni-bonn.de

†These authors have contributed equally to this work

**Specialty section:**
This article was submitted to B Cell Biology, a section of the journal Frontiers in Immunology

**Received:** 11 April 2022
**Accepted:** 25 May 2022
**Published:** 21 June 2022

**Citation:**
Adjobimey T, Meyer J, Sollberg L, Bawolt M, Berens C, Kovačević P, Trudić A, Parcina M and Hoerauf A (2022) Comparison of IgA, IgG, and Neutralizing Antibody Responses Following Immunization With Moderna, BioNTech, AstraZeneca, Sputnik-V, Johnson and Johnson, and Sinopharm's COVID-19 Vaccines. Front. Immunol. 13:917905. doi: 10.3389/fimmu.2022.917905

In an ongoing multinational trial, we obtained blood samples from 365 volunteers vaccinated with mRNA vaccines (Moderna, BioNTech), viral DNA-vectored vaccines (AstraZeneca, Sputnik-V, and Johnson and Johnson), or the attenuated virus vaccine from Sinopharm. After collecting reactogenicity data, the expression of S-Protein binding IgG and IgA was analyzed using an automated sandwich ELISA system. Serum neutralizing potentials were then investigated using an ACE-2-RBD neutralizing assay. Moderna's vaccine induced the highest amounts of SARS-CoV-2 specific neutralizing antibodies compared to the other groups. In contrast, Sinopharm and Johnson and Johnson's vaccinees presented the lowest SARS-CoV-2-specific antibody titers. Interestingly, moderate to high negative correlations between age and virus-specific IgG expression were observed in the Johnson and Johnson ($\rho$ =-0.3936) and Sinopharm ($\rho$ =-0.6977) groups according to Spearman's rank correlation analysis. A negative correlation was seen between age and IgA expression in the Sputnik-V group ($\rho$ =-0.3917). The analysis of virus neutralization potentials in age categories demonstrated that no significant neutralization potential was observed in older vaccinees (61and 80 years old) in the Sputnik-V Johnson and Johnson and Sinopharm vaccinees' groups. In contrast, neutralization potentials in sera of Moderna, BioNTech, and AstraZeneca vaccinees were statistically comparable in all age categories. Furthermore, while the AstraZeneca vaccine alone induced moderate IgG and IgA expression, the combination with Moderna or BioNTech mRNA vaccines induced significantly higher antibody levels than a double dose of AstraZeneca and similar IgG expression and neutralization potential compared to Moderna or BioNTech vaccines used alone. These results suggest that mRNA vaccines are the most immunogenic after two doses. DNA vectored vaccines from AstraZeneca and Sputnik-V presented lower but significant antibody expression and virus neutralizing properties after two doses. The lowest

antibody and neutralization potential were observed in the Sinopharm or Johnson and Johnson vaccinees. Especially elderly over 60 presented no significant increase in neutralizing antibodies after vaccination. The data also indicate that heterologous vaccination strategies combining the AstraZeneca DNA vectored vaccines and mRNA vaccines are more effective in the induction of neutralizing antibodies compared to their homologous counterparts.

**Keywords: SARS-CoV-2, COVID-19 vaccines, neutralizing antibodies, ELISA, IgA, IgG**

## INTRODUCTION

Since it began in November 2019, the COVID-19 pandemic has caused significant morbidity and mortality worldwide and major social, educational, and economic disruptions. It is the most serious global health crisis ever experienced in modern history (1). Seniors and persons with comorbidities are at the highest risk for COVID-19 complications (2). Globally, as of April 8$^{th,}$ 2022, there have been 494 587 638 confirmed cases of COVID-19, including 6 170 283 deaths, reported to the WHO (3). Recent data indicate increasing SARS-CoV-2 infection rates and COVID-19 in younger adults due to the occurrence of new virus variants (4, 5). In this context, vaccine rollout represents a tool of choice to fight the pandemic. Several groups developed vaccines to prevent the infection and control the pandemic. The amount of resources and the extraordinary speed of vaccine development against COVID-19 are unique in human history (6). While the WHO declared COVID-19 a pandemic in March 2020, less than nine months later, more than 60 vaccines entered clinical trials, with 13 in Phase III clinical trials at the end of 2020 (7). New technologies, accumulated expertise during the development of vaccines against related viruses like MERS-CoV or SARS-CoV-1, as well as existing production platforms have made this fulminant acceleration possible (8). As of April 5$^{th,}$ 2022, a total of 11 250 782 214 vaccine doses have been administered worldwide (3). Currently available vaccines against COVID-19 include Messenger ribonucleic acid (mRNA) vaccines like Moderna's Spikevax and Pfizer-BioNTech's Comirnaty, recombinant adenovirus vectored vaccines such as Vaxzevria from Oxford-AstraZeneca, Janssen from Johnson & Johnson Pharm, and Sputnik-V from the Gamaleya Research Center in Russia. The Chinese pharmaceutical firm Sinopharm opted for a more classical approach using inactivated viruses and proposed the BIBP COVID-19-vaccine, also known as BBIBP-CorV. All these vaccine candidates have been authorized for human use in many countries (9). The approval of these vaccines offers a highly effective tool for the global control of the COVID-19 pandemic. While the high-speed vaccine development is undoubtedly a scientific and technological success, it has also raised concerns about safety and efficacy in the global population (10). In this context, independent evaluations of the safety and effectiveness of these vaccines are highly needed.

Humoral immune responses and particularly neutralizing antibodies are key elements of the adaptive immunity against acutely cytopathic viruses such as the SARS-CoV-2 (11–13). Gamma (IgG) and alpha (IgA) immunoglobulins are the first and second most abundant immunoglobins in human serum, respectively (14). There is increasing evidence that neutralizing responses correlate with protection against COVID-19 (15). Both IgG and IgA were reported to mediate viral neutralization in COVID-19 patients, and their neutralization potential is the key mechanism supporting the efficacy of convalescent plasma in the treatment of severe COVID-19 patients (16–19). While IgG is the main antibody in the blood and most tissues, IgA is the most abundant antibody on mucosal surfaces (14, 20), including the respiratory mucosa, main entry, and replication site of SARS-CoV-2 in the human body (20–23). Investigations in influenza and SARS-CoV-2 infections suggested higher antiviral properties for IgA in comparison to IgG (24, 25), suggesting a key role for IgA in protective immunity against SARS-CoV-2. However, limited data exist on IgG and IgA responses after COVID-19 vaccinations. In the present study, we compared SARS-CoV-2 spike antigen-specific serum IgA and IgG expression as well as virus neutralization potential in individuals vaccinated with five different COVID-19 vaccines, including mRNA vaccines from Pfizer-BioNTech and Moderna, viral DNA vectored vaccines from Johnson & Johnson, Oxford-AstraZeneca, and Sputnik-V, as well as the inactivated virus vaccine from Sinopharm (BIBP COVID-19-vaccine). In the present study, we investigated the humoral immune response in blood samples from volunteers vaccinated with mRNA vaccines (Moderna, BioNTech), viral DNA-vectored vaccines (AstraZeneca, Sputnik-V, and Johnson and Johnson), or the inactivated virus vaccine from Sinopharm.

## MATERIAL AND METHODS

### Participants, Sample Collection, and Ethics

The study was conducted between January 2021 and October 2021 at the Institute of Medical Microbiology, Immunology and Parasitology (IMMIP) of the University Hospital of Bonn and is part of an ongoing survey. Volunteers were recruited in Bonn (Germany), in Sremska Kamenica (Serbia), and in Banja Luka (Bosnia and Herzegovina). A total of 365 (122 men and 243 women) were included in the study. Each volunteer recruited for the study gave informed consent to participate. Ethics approval for the study was obtained from the ethical boards of the University Hospital Bonn (Lfd.Nr.439/20) and the Faculty of Medicine of the University of Novi Sad (FN.198/02).

Epidemiological and clinical characteristics of study participants are summarized in **Table 1**. Venous blood was collected 14-30 days after the last vaccination dose using the S-Monovette SERUM GEL blood collection system (Sarstedt AG, Nümbrecht, Germany). Characteristics of all vaccines investigated during the study are listed in **Table 2**. Donors with immune deficiency or using immunosuppressive treatment were excluded from the analyses.

## Reactogenicity Analysis

Reactogenicity investigations were done using questionnaires designed by the investigators and delivered to the participants. The survey was done 2 to 3 weeks after each vaccine shot. Participants who agreed to participate gave written consent and filled a form with their demographics, including sex, age, earlier infection with SARS-CoV-2, and the observed side effects. All responses were included anonymously.

## Enzyme-Linked Immunosorbent Assay (ELISA) for the Detection of SARS-COV-2 Specific IgG and IgA

To detect the levels of SARS-CoV-2 specific antibodies, the Euroimmun SARS-CoV-2 IgG/IgA ELISA kit (Euroimmun, Lübeck, Germany) was used, according to the manufacturer's instructions. Serum samples were diluted 1:101 in the provided sample buffer and incubated at 37° C for 60 min in a 96-well microtiter plate. Washings and incubation cycles were performed automatically using the predesigned program of Euroimmun's Analyzer I automate. Optical densities (OD) were measured at 450 nm. SARS-CoV-2 specific immunoglobulin G and A expressions were calculated, and results were interpreted as per the manufacturer's protocol.

## Neutralizing Antibody Level

To test the neutralizing potential of SARS-CoV-2 specific antibodies in the sera of vaccinated individuals, SARS-CoV-2 antibody neutralizing immunoassay kits (ThermoFisher Scientific) were used according to the manufacturer's instructions. Briefly, 100 µL of controls and 1:5 diluted sera from fully vaccinated or unvaccinated individuals were added to the wells of microplates pre-coated with SARS-CoV-2 receptor-binding domain (RBD) protein. The plates were then incubated for 1 hour to allow neutralizing antibodies present in the samples to bind to RBD specifically. After 3 washes with the provided wash solution, 100 µL of biotinylated 1x ACE2 and samples were incubated for an additional 1h. After incubation, samples were washed 3 times, and 100 µL of 1x Streptavidin-HRP was added to each well. Plates were then incubated for an additional 30 min, and 50µL of stop solution containing 2N $H_2SO_4$ was added to stop the reaction. Signal development is indirectly proportional to the amount of specific neutralizing antibodies present. Plates were measured at 450 nm with the SpectraMax Pro plate reader (Molecular Devices), and neutralization potential was calculated according to the provided controls.

## Statistics

Descriptive demographic and clinical data analyses are presented as mean ± SD when continuous and as proportions (%) when categorical. All graphs were generated using GraphPad Prism 8 (La Jolla, CA, USA). p values were calculated using the Kruskal Wallis test. Dunnett's multiple comparison test was used to compare all settings to the control (Unvaccinated), and Dunn's *post hoc* test was used to compare all groups. Significance is accepted if $p < 0.05$.

# RESULTS

## Lowest Systemic Reactogenicity After Vaccination With Sinopharm's BIBP COVID-19 Vaccine

We first analyzed the reactogenicity of the different vaccines using an appropriate questionnaire. The most common local symptoms were pain at the site of injection and skin rash. Minor systemic side effects were seen in all groups. More severe systemic effects, including musculoskeletal symptoms, fever, and headache for more than 3 days, were observed in the Moderna (10%), AstraZeneca (11%), Johnson and Johnson (5.9%), and Sputnik-V (7.2%) groups. No severe systemic effect was reported in the BioNTech group. Sinopharm's BIBP COVID-19 vaccinees presented the lowest percentage of adverse reactions. Indeed, 93.2% % of the participants who received this vaccine declared having experienced no systemic side effects (**Figure 1**).

**TABLE 1** | Epidemiological and clinical characteristics of study participants.

| | Moderna | BioNTech/ Pfizer | AstraZeneca | Johnson and Johnson | Sputnik-V | Sinopharm | AstraZeneca+ Moderna | AstraZeneca+ BioNtech | Total vaccinated | Controls |
|---|---|---|---|---|---|---|---|---|---|---|
| **Sample size (N=)** | 41 | 92 | 52 | 34 | 35 | 28 | 43 | 40 | 365 | 30 |
| **Mean age** | 18-85 | 20-88 | 20-82 | 20-71 | 18-78 | 26-74 | 20-6 | 20-98 | 18-98 | 18-78 |
| **(Min-Max, Mean** | (42.1 ± | (44.3 ± | (42.9. ± 16.9) | (35.5 ± 15.6) | (36.0 ± | (33.6 ± | (42.1. ± 20.2) | (45.9. ± 25.2) | (45.7. ± | (33.9 ± |
| **±SD) in years** | 15.8) | 18.5) | | | 10.7) | 15.0) | | | 17.7) | 25.3) |
| **Sex (M/F)** | 13/28 | 37/55 | 14/38 | 23/11 | 11/24 | 11/17 | 6/37 | 7/33 | | 12/18 |
| **Hypertension (N=)** | 5 | 25 | 8 | 5 | 3 | 4 | 2 | 6 | 58 | 3 |
| **BMI (Mean±SD)** | 24.4±4.6 | 26.7±7.5 | 26.4±5.0 | 25.2 ±6.2 | 25.6±4.5 | 26.5±4.5 | 22.7±6.2 | 25.6±5.7 | 25.3±5.9 | 25.4± 3.5 |

**TABLE 2** | Characteristics of investigated vaccines.

| Vaccine Name | Manufacturers | Active component First dose | Active component Second dose | Type | References |
|---|---|---|---|---|---|
| **mRNA-1273** | Moderna, Massachusetts, USA | 100 µg mRNA | 100 µg mRNA | mRNA-based | Baden LR, El Sahly HM, Essink B, Kotloff K, Frey S, Novak R, et al. Efficacy and Safety of the Mrna-1273 Sars-Cov-2 Vaccine. *N Engl J Med* (2021) 384(5):403-16. Epub 20201230. doi: 10.1056/NEJMoa2035389. |
| **Comirnaty** | BioNTech SE, Mainz Germany Pfizer Inc, New York, USA | 30 µg mRNA | 30 µg mRNA | mRNA-based | Polack FP, Thomas SJ, Kitchin N, Absalon J, Gurtman A, Lockhart S, et al. Safety and Efficacy of the Bnt162b2 Mrna Covid-19 Vaccine. *N Engl J Med* (2020) 383 (27):2603-15. Epub 20201210. doi: 10.1056/NEJMoa2034577. |
| **Vaxzevria** | AstraZeneca Corporation, Cambridge, UK | $5\times10^{10}$ viral particles | $5\times10^{10}$ viral particles | Adenovirus-vectored | Falsey AR, Sobieszczyk ME, Hirsch I, Sproule S, Robb ML, Corey L, et al. Phase 3 Safety and Efficacy of Azd1222 (Chadox1 Ncov-19) Covid-19 Vaccine. *N Engl J Med* (2021) 385(25):2348-60. Epub 20210929. doi: 10.1056/NEJMoa2105290. |
| **Ad26.COV2.S** | Johnson & Johnson, New Jersey, USA | $5\times10^{10}$ viral particles | – | Adenovirus-vectored | Sadoff J, Gray G, Vandebosch A, Cardenas V, Shukarev G, Grinsztejn B, et al. Safety and Efficacy of Single-Dose Ad26.Cov2.S Vaccine against Covid-19. *N Engl J Med* (2021) 384(23):2187-201. Epub 20210421. doi: 10.1056/NEJMoa2101544. |
| **Gam-COVID-Vac** | Gamaleya National Research Centre for Epidemiology and Microbiology, Moscow, Russia | (1.0±0.5) x $10^{11}$ viral particles | (1.0±0.5) x $10^{11}$ viral particles | Adenovirus-vectored | Logunov DY, Dolzhikova IV, Shcheblyakov DV, Tukhvatulin AI, Zubkova OV, Dzharullaeva AS, et al. Safety and Efficacy of an Rad26 and Rad5 Vector-Based Heterologous Prime-Boost Covid-19 Vaccine: An Interim Analysis of a Randomised Controlled Phase 3 Trial in Russia. *Lancet* (2021) 397(10275):671-81. Epub 20210202. doi: 10.1016/S0140-6736(21)00234-8. |
| **BBIBP-CorV** | Sinopharm, Beijing, China | 6.5 U (4 µg) of inactivated SARS-CoV-2 antigens | 6.5 U (4 µg) of inactivated SARS-CoV-2 antigens | Inactivated virus | WHO. Background Document on the Inactivated Covid-19 Vaccine Bibp Developed by China National Biotec Group (Cnbg), Sinopharm, 7 May 2021. (2021). |

## Higher Expression of SARS-CoV-2-Specific IgG and IgA in mRNA Vaccinated Individuals

To investigate the levels of SARS-CoV-2 specific antibody expression in the different groups of vaccinees, we analyzed S-protein specific IgG and IgA in the sera of vaccinated individuals 3-6 weeks after full vaccination. The results indicate that mRNA vaccines generally induced the highest amounts of SARS-CoV-2-reactive IgG and IgA. The Moderna vaccine induced slightly more IgG and IgA compared to the BioNTech vaccine. AstraZeneca and Sputnik-V induced comparable amounts of SARS-CoV-2 specific IgG. However, IgA expression was higher

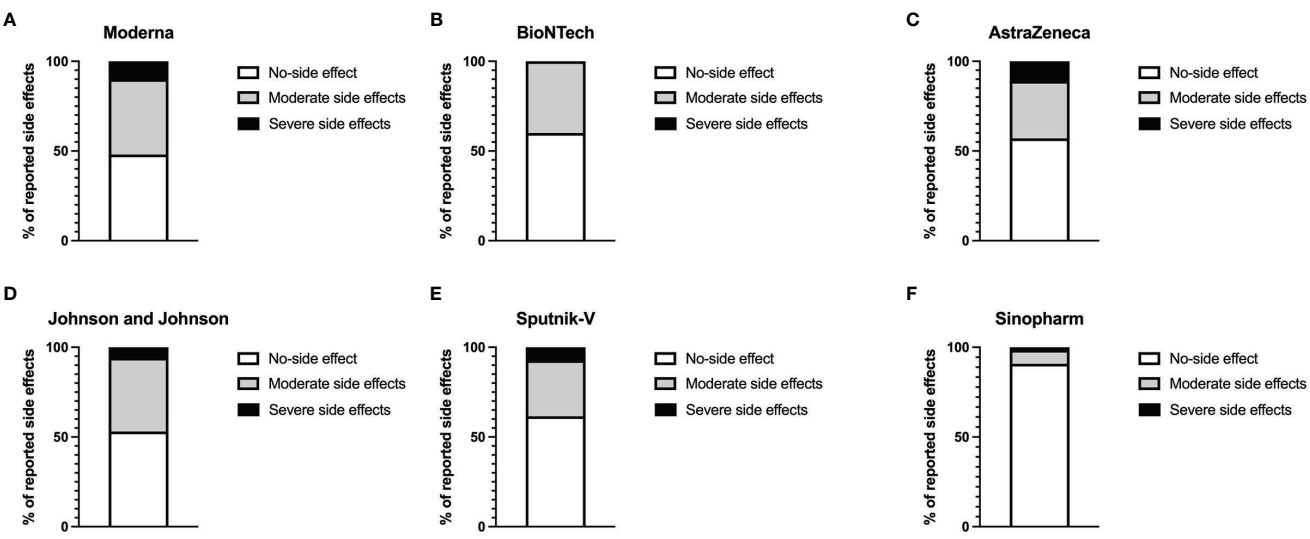


**FIGURE 1** | Level of reported systemic adverse reactions. Graphs represent the proportion of individuals presenting side effects in Moderna **(A)**, BioNTech **(B)**, AstraZeneca **(C)**, Johnson and Johnson **(D)**, Sputnik-V **(E)**, and Sinopharm **(F)** vaccinees. The white parts of the histograms indicate the percentage of persons with no systemic side effects. The grey portions represent the percentage of people with mild side effects, while the dark parts indicate the percentages of individuals with severe side effects.

in the Sputnik-V group compared to the AstraZeneca group. The IgG expression in these two groups was significantly higher compared to the unvaccinated controls but lower compared to both mRNA vaccines. In contrast, the amount of SARS-CoV-2-specific IgG in the Johnson and Johnson and Sinopharm groups was moderately increased compared to the unvaccinated control group. However, differences to the control group were statistically not significant ($p > 0.999$ and $p=0.860$, respectively). However, while SARS-CoV-2 specific IgA was significant in the Johnson & Johnson group ($p=0.004$), no statistical difference was seen between Sinopharm and the control groups ($p= 0.2287$) in regard to SARS-CoV-2-specific IgA expression (**Figure 2**).

## Low Level of SARS-CoV-2-Specific Neutralizing Antibodies in Sera of Sinopharm and Johnson and Johnson Vaccinated Individuals

Next, we determined the level of SARS-CoV-2-specific neutralizing antibodies in sera of vaccinated individuals. The data suggest Moderna and BioNTech groups exhibited the highest neutralization potential compared to the unvaccinated controls and all other groups. These data confirmed that mRNA COVID-19 vaccines induce antibodies with the highest neutralizing potential. In line with their antibody levels, AstraZeneca and Sputnik-V groups exhibited similar and significant neutralization potential compared to the unvaccinated controls. In contrast, no significant difference was seen between the Johnson and Johnson and Sinopharm groups and the control group in terms of SARS-CoV-2 neutralization potential (**Figure 3**).

## Negative Correlation Between Age and IgG Production in Johnson and Johnson and Sinopharm Vaccinees

To determine the impact of age on vaccine induced antibody production, Spearman's correlation test was used to investigate the relationship between the age of the vaccinees and the amplitude of SARS-CoV-2 specific IgA and IgG expression after vaccination with Moderna, BioNTech, AstraZeneca, Johnson, and Johnson, Sputnik-V and Sinopharm vaccines. No correlation was seen between age and SARS-CoV-2 specific

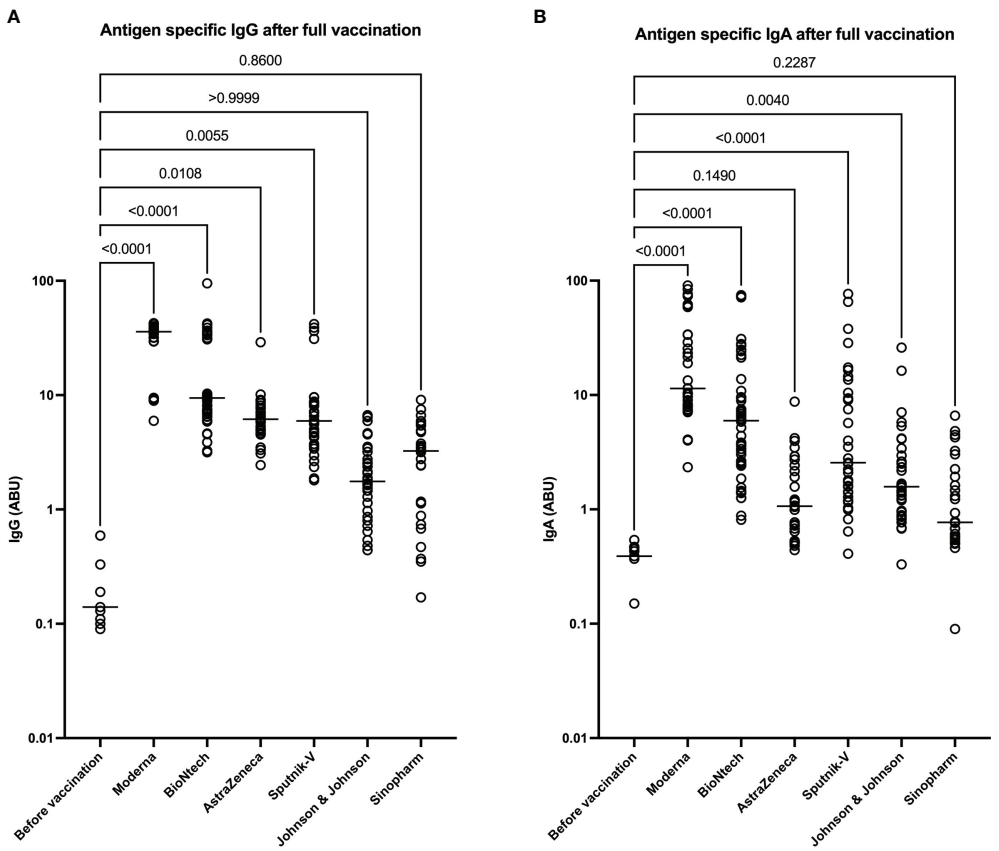


**FIGURE 2** | Higher expression of SARS-CoV-2 reactive IgG and IgA after immunization mRNA vaccines. Graphs represent the expression SARS-CoV-2 spike-protein binding IgG **(A)** and IgA **(B)** in arbitrary binding units (ABU). Each symbol represents individual donors. Indicated p values were calculated using the Kruskal-Wallis test followed by Dunnett's *post hoc* to compare each group to the controls before vaccination. Bars represent the median antibody expression in each group. Significance is accepted if $p < 0.05$.

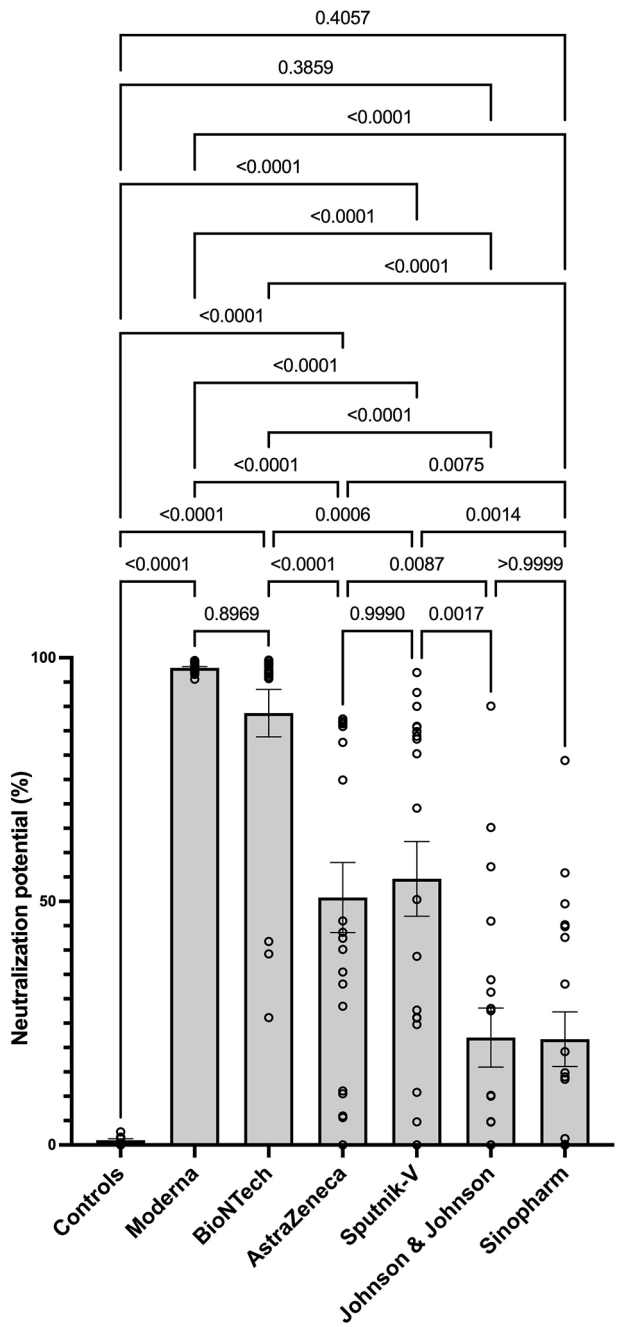


**FIGURE 3** | Higher neutralizing potential of mRNA vaccines in mRNA-vaccinated individuals. The graph represents the relative neutralizing antibody expression observed using sera from each vaccination group. Each symbol represents individual donors. Indicated p values were calculated using Kruskal-Wallis 'test followed by Dunn's comparison *post hoc* to compare all groups. Bars represent the mean ± SEM percentage of relative neutralizing antibody expression in each group. Significance is accepted if $p < 0.05$.

antibody expression in the Moderna, BioNTech, and AstraZeneca groups (**Figures 4A–F**). In sera of Sputnik-V vaccinees, a moderate negative antibody-age correlation was observed for IgA ($\rho$ = -0.3917), whereas a trend was visible for IgG ($\rho$ = -0.2540) (**Figures 4G, H**). In the Johnson and Johnson group, a moderate negative correlation was seen for IgG ($\rho$ = -g0.3936) was seen between age and SARS-CoV-2-specific IgG expression (**Figures 4I, J**). A stronger negative correlation was seen between the expression SARS-CoV-2-specific IgG and age in the Sinopharm group ($\rho$ = -0.6977) (**Figures 4K, L**).

## Low SARS-CoV-2 Specific Antibody Expression and Neutralizing Potential in Older Johnson and Johnson and Sinopharm Vaccinees

The strongest negative correlations between age and antibody expression were observed in the Sputnik-V, Johnson and Johnson, and Sinopharm groups. To further investigate the impact of age on the humoral immune response in these groups, the relative expression of neutralizing antibodies was analyzed in 3 different age categories: 18-40, 41-60, and 61-80+. For Sputnik-V, Johnson and Johnson, and Sinopharm groups, no significant neutralization potential was observed in the elderly between 61and 80 years old. Low to moderate neutralization potentials were measured in the age categories of 41 to 60 years old. Differences to the control group were significant in the age category of 18-40 years old in all groups of vaccinees and in the category of 41-60 years old for Johnson and Johnson and Sinopharm vaccinees. In contrast, a trend was seen for Sputnik-V in this age category (**Figures 5A–C**). In contrast, neutralization potentials were statistically comparable in the different age categories in sera of Moderna, BioNTech, and AstraZeneca vaccinees (**Figures 5D–F**).

## Robust Antibody Production and Neutralization Potential After AstraZeneca-mRNA Vaccine Combinations

We next compared the antibody responses with a double shot of AstraZeneca, Moderna, and BioNTech with the combinations AstraZeneca/Moderna or AstraZeneca/BioNTech. Our data showed that the combinations of AstraZeneca with a second dose of Moderna or BioNTech are significantly more effective at inducing SARS-CoV-2 specific IgG and IgA compared to 2 doses of AstraZeneca. In addition, IgA levels were higher in the homologous Moderna group compared to the AstraZeneca-Moderna group. No significant difference was seen between the AstraZeneca-BioNTech group and the homologous BioNTech group (**Figures 6A, B**). These results were also reflected by the neutralization data. Indeed, neutralization potentials in sera of AstraZeneca/Modern and AstraZeneca/BioNTech groups were significantly higher compared to the groups who received 2 doses of AstraZeneca. In addition, while few individuals of the BioNTech group presented neutralization potentials lower than 70% in the AstraZeneca and BioNTech groups, all tested volunteers exhibited in the AstraZeneca/BioNTech group neutralizing potentials above 95% (**Figure 6C**).

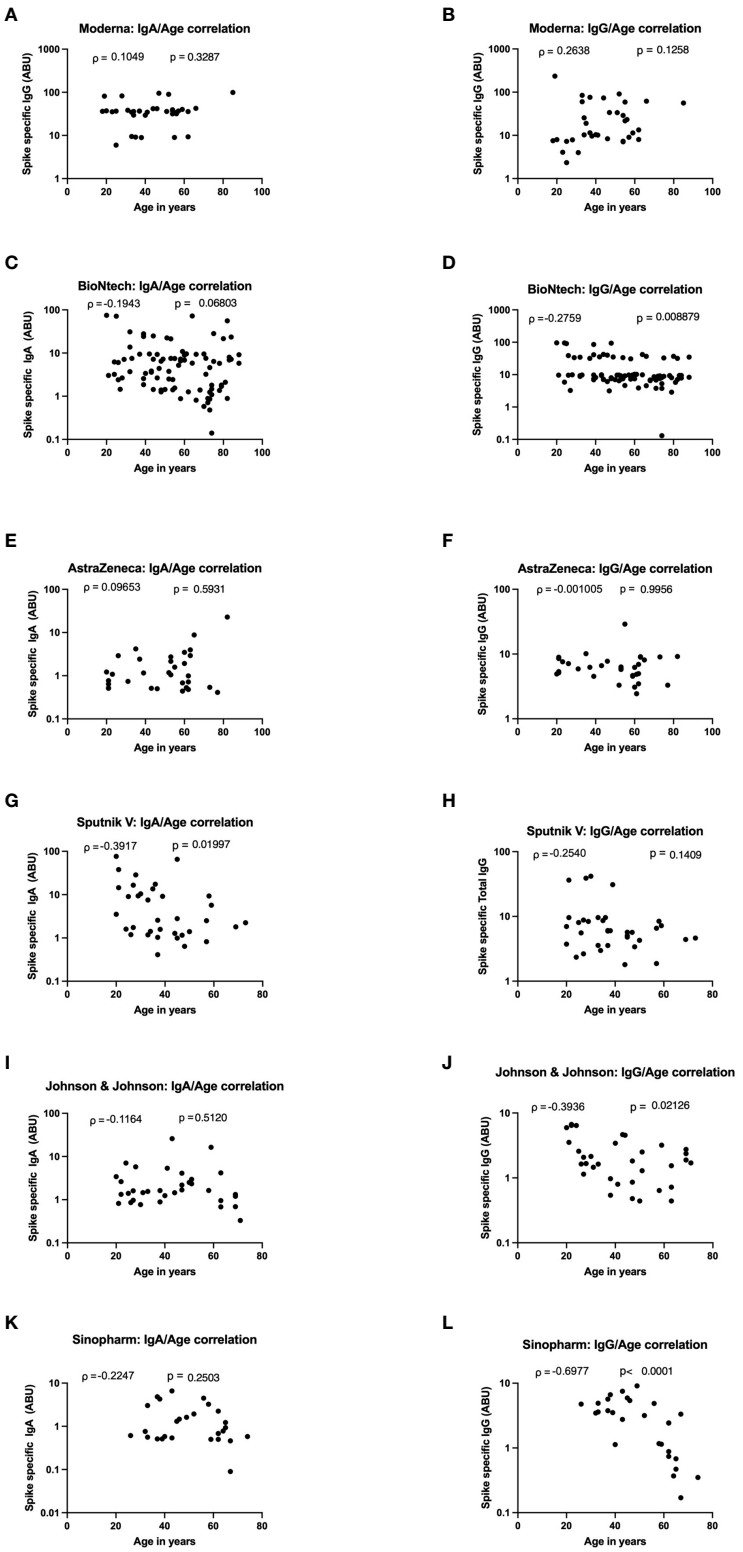


**FIGURE 4** | Strong age-dependent decrease of vaccine-induced antibody decrease in Sputnik-V, Johnson and Johnson, and Sinopharm vaccinees. Graphs represent the correlation of SARS-CoV-2 specific spike-protein binding IgG and IgA with age in Moderna (**A**, **B**), BioNTech (**C**, **D**), AstraZeneca (**E**, **F**), Sputnik-V (**G**, **H**), Johnson and Johnson (**I**, **J**), and Sinopharm (**K**, **L**) vaccinees. Dots represent individual donors. Indicated r values were calculated using Spearman's rank-order analysis.

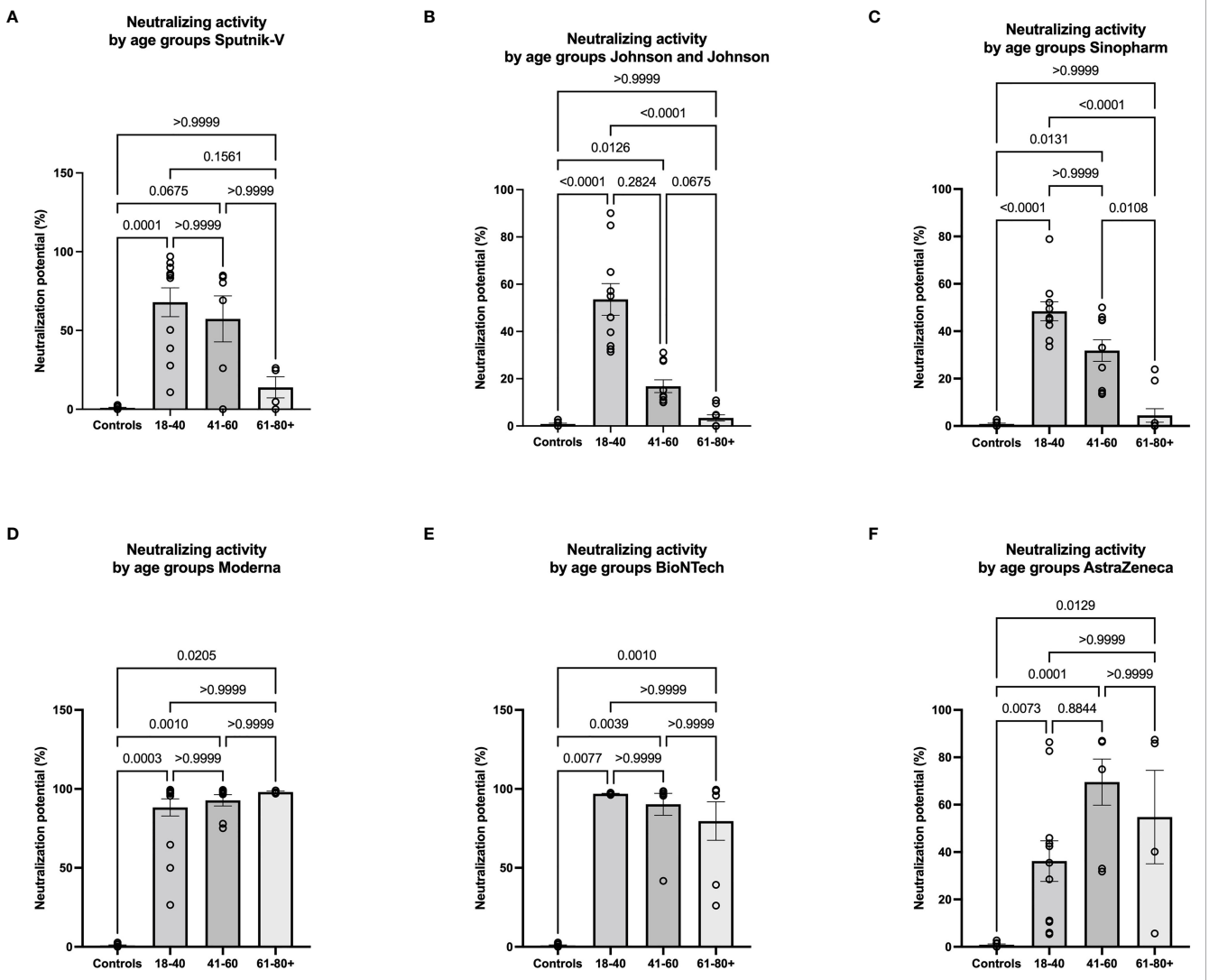


**FIGURE 5** | Low neutralizing antibody response in older vaccinees of Sputnik-V, Johnson and Johnson, and Sinopharm groups. Graphs represent the relative expression of neutralizing antibodies observed using sera from Sputnik-V **(A)**, Johnson and Johnson **(B)**, Sinopharm **(C)**, Moderna **(D)**, BioNTech **(E)**, and AstraZeneca **(F)** vaccinees in 3 different age categories: 18-40, 41-60, and 61-80+ years old. Each symbol represents individual donors. Indicated p values were calculated using Kruskal-Wallis 'test followed by Dunn's comparison *post hoc* to compare all groups. Bars represent the mean percentages of relative neutralizing antibody expression ± SEM. Significance is accepted if $p < 0.05$.

## DISCUSSION

In this study based on 365 vaccinated participants, we showed that post-vaccine anti-spike IgG responses significantly vary according to the vaccine type. mRNA vaccines from Moderna and BioNTech induced the highest amount of spike-specific IgG and IgA antibodies and a high serum neutralization potential. High antibody levels in mRNA vaccinees were also observed in other studies (26). The data suggest a high seroconversion and antibody-mediated virus neutralization potential in mRNA-vaccinated individuals.

Comparatively, DNA vectored vaccines Sputnik-V and AstraZeneca induced similar amounts of SARS-CoV-2 specific IgG. Interestingly, higher IgA expression was seen in the Sputnik-V group compared to the AstraZeneca group. Both groups, however, presented similar levels of neutralizing antibodies. These data can be explained by the fact that Sputnik-V and the AstraZeneca vaccine are very similar in their conception and principle of action. For both vaccines, the gene coding for the SARS-CoV-2 spike protein is introduced into an adenovirus vector. The main difference between these two vector vaccines is that Sputnik-V uses two different vectors, the rAd26 for priming and Ad5 in the booster dose (27), while AstraZeneca includes the spike protein gene in the ChAdOx1 viral vector (28, 29).

Our results clearly showed a weaker performance for the Johnson and Johnson vaccine compared to mRNA and the other

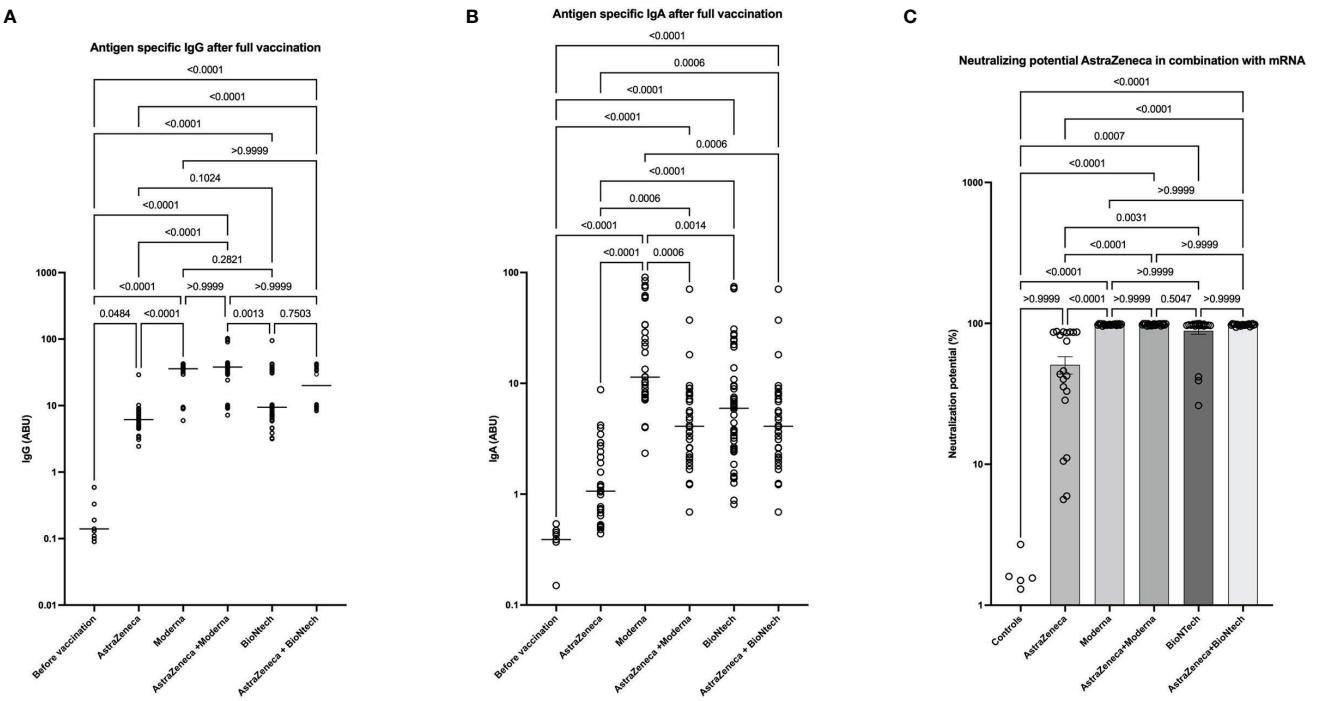


**FIGURE 6** | High neutralizing antibody expression in AstraZeneca- mRNA vaccine combinations. Graphs represent the expression of SARS-CoV-2 specific spike-protein binding IgG **(A)**, IgA **(B)**, and neutralizing antibody expression **(C)** observed in the sera of people that received homologous (AstraZeneca, Moderna, or BioNTech) 's COVID-19 vaccines or heterologous vaccine doses (AstraZeneca-Moderna or AstraZeneca-BioNTech). Each symbol represents individual donors. Indicated p values were calculated using Kruskal-Wallis 'test followed by Dunn's comparison *post hoc* to compare all groups. Bars represent the median **(A, B)** of SARS-CoV-2 spike protein-specific antibody expression in each group in arbitrary binding units (ABU) or the means ± SEM percentages of relative neutralizing antibody expression **(C)**. Significance is accepted if $p < 0.05$.

DNA vectored vaccines. Indeed, the Johnson and Johnson vaccine induced relatively low spike-specific IgG, and the sera of vaccinees from this group exhibit no significant neutralizing potential compared to the unvaccinated controls. Similar findings were obtained in a larger survey by Self et al., where postvaccination anti-spike and anti-RBD IgG levels were seen to be significantly lower in persons vaccinated with Johnson and Johnson than Moderna or Pfizer-BioNTech vaccines (26). This weak performance can be explained by the fact that the Johnson and Johnson vaccine required only one dose. In line with our data, the American Food and Drug Administration (FDA) has recently amended the Emergency Use Authorizations (EUA) for the Janssen COVID-19 vaccine to include the use of a booster dose to be administrated to all recipients of the Johnson and Johnson vaccine. They may choose to receive either an additional full dose of Janssen's vaccine or a full dose of an mRNA vaccine (30).

An even weaker performance was observed for the Sinopharm vaccine. In line with our data, a recent study in Bahrain showed that in a group of 22 persons vaccinated with a double dose of the Sinopharm vaccine, 20 were infected with SARS-CoV-2 (31). Saeed et al., after analyzing the expression of spike-specific antibody levels in 2868 COVID-19 vaccinated individuals with the Sinopharm vaccine in Iran, came to the conclusion that two doses of Sinopharm may not be adequate to provide long-lasting immunity against SARS-CoV-2 (32).

It is, however, noticeable that the Sinopharm vaccine used whole inactivated SARS-CoV-2 viral particles (33) so that our analyses of spike protein reactivity may miss the full extent of immune reactions to this vaccine. Further investigations are required to explore the responses to other viral proteins. Interestingly, despite its weak performance in terms of neutralizing antibody induction, our data indicate that the Sinopharm vaccine has the mildest side effects compared to the other vaccines. These data align with recent findings suggesting that both doses of the Sinopharm COVID-19 vaccine induce mild and common side effects (34, 35).

Nonetheless, correlation analyses of antigen-specific antibody expression with the age of the vaccinees revealed negative correlations between age and antibody expression, especially in Sputnik-V, Johnson and Johnson, and Sinopharm groups. Further analyses revealed that younger vaccinees with 18-40 years in these groups exhibit significant antibody and neutralizing potential compared to older vaccinees. In the age group of 41–60-year-olds, the antibody expression and neutralizing activity were lower but still significant compared to the unvaccinated controls. Thus, while neutralization potential in 18-60 years old Johnson and Johnson and Sinopharm vaccinees was significant, no significance was seen when considering older adults (60-80+ years). Our results on the Sinopharm vaccine are in line with recent data by Ferenci

et al., indicating that antibody production after BBIBP-CorV vaccination was strongly reduced with increasing age (35).

Our data also suggest a higher risk of post-vaccination COVID-19 infection in this age category after Sputnik-V, Johnson and Johnson, and Sinopharm vaccines. This finding, together with the emergence of new virus variants, is very worrying since this very same population of the elderly is considered at high risk of developing severe forms of COVID-19. The negative impact of immune senescence on vaccine efficacy is well known in both human and animal models (36, 37). In Influenza vaccination, for example, it was shown that age-dependent reduction of the expression of critical regulators of B cell maturation and class switch recombination such as Blimp-1, E47, and AID, leads to the production of fewer functional antibodies in the elderly (38). However, such an age-dependent reduction of B cell functions alone is insufficient to explain the weaker SARS-CoV-2 specific antibody induction in older DNA-vectored vaccinees. Indeed, in our investigation, mRNA vaccinees seem to be unaffected. Additional mechanisms inherent to the dose and type of vaccines may contribute to this weak performance in older DNA vectored vaccinees. One factor could be the adenovirus vectors themselves. Indeed, emerging data suggest that immune responses to proteins encoded by the adenovirus vectors reduce antibody responses to the spike protein (39). It may be assumed that older vaccinees who have probably experienced several adenovirus infections might be more likely to exhibit cross-reactive immune responses against adenovirus vectors. To minimize this risk, manufacturers have used different strategies. Johnson & Johnson and AstraZeneca vaccines employed adenoviral strains (ChAd26 and ChAdY25, respectively) exclusively found in chimpanzees (40, 41). In contrast, the Sputnik V vaccine was developed using two different human adenoviral vectors for the first (rAd26) and the second (rAd5) vaccine dose (42). Despite these preventive measures, anti-vector immunity may at least partially contribute to the weaker performance of adenovirus-vectored vaccines, particularly observed in older vaccinees. Further investigations are required to fully elucidate the underlying mechanisms of the observed lower antibody response in this group of vaccinees. Implications for the millions of people who received these vaccines worldwide also need to be addressed. Booster doses with the more effective mRNA vaccines should be considered.

During our survey, the German Standing Vaccination Committee (STIKO), taking into account concerns after several reports of rare but serious blood clots in young adults (43, 44), recommended after AstraZeneca a second dose of one of the 2 available mRNA vaccines to individuals that received the first dose of AstraZeneca. We therefore also analyzed the antibody responses after this mixed vaccination strategy. The data clearly suggest a more robust SARS-CoV-2 specific IgG and IgA expression after this vaccination schedule. Similar data were found in Spain, where preliminary data on 600 AstraZeneca primed vaccinees demonstrated that a BioNTech second dose remarkably boosted antibody responses (45). Our data further confirmed that the mix-and-match COVID-19 vaccination strategy triggered a stronger antibody production than two doses of a single vaccine. Noticeable was, however, that Moderna vaccinees conserved the highest SARS-CoV-2 specific IgA expression compared to all other groups.

The findings in this report are subject to three major limitations. First, antibody specificity and neutralization potential were not tested against emerging variants of concern. Indeed, an increasing concern is whether the vaccines currently available can protect against emerging SARS-CoV-2 variants (46–48). The study was largely performed before the predominance of the Delta (B.1.617.2) and the emergence of the Omicron variants in Europe (5). Further investigations are required to analyze in-depth the antibody responses to different SARS-CoV-2 variants. Second, the present study did not investigate the durability of neutralizing antibody expression after full vaccination with the different vaccines and vaccine combinations. Emerging lines of evidence suggest that antibody levels after COVID-19 vaccination may drop at different rates depending on various factors, including the type of vaccine, infection before or after vaccination, age, sex, T-cell response, and the interval between vaccine injections (49, 50). Therefore, additional investigations are required to better define the stability of immune effectors after COVID-19 vaccination. Third, while our data focus on antibody responses, T cell reactivity and T cell memory might represent another important mechanism for long-lasting vaccine-induced protection.

The present study compared the efficacy of the 6 major COVID-19 vaccines currently available (Moderna, BioNTech, AstraZeneca, Johnson and Johnson, Sputnik-V, and Sinopharm's COVID-19 vaccines). Our findings suggest that mRNA vaccines induced the highest titers of SARS-CoV-2 specific neutralizing antibodies. While all 6 vaccines have moderate reactogenicity and induce functional neutralizing antibodies in vaccinees, low antibody-mediated protection is seen in the elderly vaccinated with DNA-vectored vaccines. Our data also demonstrated that heterologous vaccination strategies using priming with the AstraZeneca followed by a boost with an mRNA vaccine induced more robust antibody expression and virus neutralization potential compared to their homologous counterparts.

## DATA AVAILABILITY STATEMENT

The original contributions presented in the study are included in the article/supplementary material. Further inquiries can be directed to the corresponding author.

## ETHICS STATEMENT

The studies involving human participants were reviewed and approved by Ethical board of the University Hospital Bonn. Ethical board of the Faculty of Medicine of the University of Novi Sad. The patients/participants provided their written informed consent to participate in this study.

## AUTHOR CONTRIBUTIONS

TA and AH conceived the study and were in charge of overall coordination. TA, JM, LS, and MB carried out the experiments. JM, MP, CB, PK, and AT contributed to sample collection. TA, AH, JM

and MP analyzed the data and contributed to the interpretation of the results. TA wrote the manuscript. All authors provided critical feedback and helped shape the research, analysis, and manuscript.

## FUNDING

AH is funded by the Deutsche Forschungsgemeinschaft (DFG, German Research Foundation) under Germany's Excellence Strategy – EXC2151 – 390873048". The funders had no role in study design, data collection, analysis, decision to publish, or manuscript preparation.

## ACKNOWLEDGMENTS

The authors thank the diagnostic team at IMMIP for their technical support.

## REFERENCES

1. Arabi YM, Murthy S, Webb S. Covid-19: A Novel Coronavirus and a Novel Challenge for Critical Care. *Intensive Care Med* (2020) 46(5):833–6. doi: 10.1007/s00134-020-05955-1
2. Ramasamy MN, Minassian AM, Ewer KJ, Flaxman AL, Folegatti PM, Owens DR, et al. Safety and Immunogenicity of Chadox1 Ncov-19 Vaccine Administered in a Prime-Boost Regimen in Young and Old Adults (Cov002): A Single-Blind, Randomised, Controlled, Phase 2/3 Trial. *Lancet* (2021) 396(10267):1979–93. doi: 10.1016/S0140-6736(20)32466-1
3. WHO. *Coronavirus Disease (Covid-19) Dashboard (2021)* (2021). Available at: https://covid19.who.int/.
4. Polack FP, Thomas SJ, Kitchin N, Absalon J, Gurtman A, Lockhart S, et al. Safety and Efficacy of the Bnt162b2 Mrna Covid-19 Vaccine. *N Engl J Med* (2020) 383(27):2603–15. doi: 10.1056/NEJMoa2034577
5. Kandeel M, Mohamed MEM, Abd El-Lateef HM, Venugopala KN, El-Beltagi HS. Omicron Variant Genome Evolution and Phylogenetics. *J Med Virol* (2021) 94. doi: 10.1002/jmv.27515
6. Ball P. The Lightning-Fast Quest for Covid Vaccines - and What It Means for Other Diseases. *Nature* (2021) 589(7840):16–8. doi: 10.1038/d41586-020-03626-1
7. WHO. *The Covid-19 Vaccine Tracker and Landscape Compiles Detailed Information of Each Covid-19 Vaccine Candidate in Development by Closely Monitoring Their Progress Through the Pipeline* (2021). Available at: https://www.who.int/publications/m/item/draft-landscape-of-covid-19-candidate-vaccines.
8. Bok K, Sitar S, Graham BS, Mascola JR. Accelerated Covid-19 Vaccine Development: Milestones, Lessons, and Prospects. *Immunity* (2021) 54 (8):1636–51. doi: 10.1016/j.immuni.2021.07.017
9. He Q, Mao Q, Zhang J, Bian L, Gao F, Wang J, et al. Covid-19 Vaccines: Current Understanding on Immunogenicity, Safety, and Further Considerations. *Front Immunol* (2021) 12:669339. doi: 10.3389/fimmu.2021.669339
10. Wong LP, Alias H, Danaee M, Ahmed J, Lachyan A, Cai CZ, et al. Covid-19 Vaccination Intention and Vaccine Characteristics Influencing Vaccination Acceptance: A Global Survey of 17 Countries. *Infect Dis Poverty* (2021) 10 (1):122. doi: 10.1186/s40249-021-00900-w
11. Dorner T, Radbruch A. Antibodies and B Cell Memory in Viral Immunity. *Immunity* (2007) 27(3):384–92. doi: 10.1016/j.immuni.2007.09.002
12. Ellinger B, Bojkova D, Zaliani A, Cinatl J, Claussen C, Westhaus S, et al. A Sars-Cov-2 Cytopathicity Dataset Generated by High-Content Screening of a Large Drug Repurposing Collection. *Sci Data* (2021) 8(1):70. doi: 10.1038/s41597-021-00848-4
13. Zhu N, Wang W, Liu Z, Liang C, Wang W, Ye F, et al. Morphogenesis and Cytopathic Effect of Sars-Cov-2 Infection in Human Airway Epithelial Cells. *Nat Commun* (2020) 11(1):3910. doi: 10.1038/s41467-020-17796-z
14. Vidarsson G, Dekkers G, Rispens T. Igg Subclasses and Allotypes: From Structure to Effector Functions. *Front Immunol* (2014) 5:520. doi: 10.3389/fimmu.2014.00520
15. Khoury DS, Cromer D, Reynaldi A, Schlub TE, Wheatley AK, Juno JA, et al. Neutralizing Antibody Levels Are Highly Predictive of Immune Protection From Symptomatic Sars-Cov-2 Infection. *Nat Med* (2021) 27(7):1205–11. doi: 10.1038/s41591-021-01377-8
16. Wang Z, Lorenzi JCC, Muecksch F, Finkin S, Viant C, Gaebler C, et al. Enhanced Sars-Cov-2 Neutralization by Dimeric Iga. *Sci Transl Med* (2021) 13 (577):eabf1555. doi: 10.1126/scitranslmed.abf1555
17. Klingler J, Weiss S, Itri V, Liu X, Oguntuyo KY, Stevens C, et al. Role of Igm and Iga Antibodies in the Neutralization of Sars-Cov-2. *medRxiv* (2020). doi: 10.1101/2020.08.18.20177303
18. Maeda K, Higashi-Kuwata N, Kinoshita N, Kutsuna S, Tsuchiya K, Hattori SI, et al. Neutralization of Sars-Cov-2 With Igg From Covid-19-Convalescent Plasma. *Sci Rep* (2021) 11(1):5563. doi: 10.1038/s41598-021-84733-5
19. Salazar E, Kuchipudi SV, Christensen PA, Eagar T, Yi X, Zhao P, et al. Convalescent Plasma Anti-Sars-Cov-2 Spike Protein Ectodomain and Receptor-Binding Domain Igg Correlate With Virus Neutralization. *J Clin Invest* (2020) 130(12):6728–38. doi: 10.1172/JCI141206
20. Terauchi Y, Sano K, Ainai A, Saito S, Taga Y, Ogawa-Goto K, et al. Iga Polymerization Contributes to Efficient Virus Neutralization on Human Upper Respiratory Mucosa After Intranasal Inactivated Influenza Vaccine Administration. *Hum Vaccin Immunother* (2018) 14(6):1351–61. doi: 10.1080/21645515.2018.1438791
21. Ding Q, Lu P, Fan Y, Xia Y, Liu M. The Clinical Characteristics of Pneumonia Patients Coinfected With 2019 Novel Coronavirus and Influenza Virus in Wuhan, China. *J Med Virol* (2020) 92(9):1549–55. doi: 10.1002/jmv.25781
22. Pan Y, Guan H, Zhou S, Wang Y, Li Q, Zhu T, et al. Initial Ct Findings and Temporal Changes in Patients With the Novel Coronavirus Pneumonia (2019-Ncov): A Study of 63 Patients in Wuhan, China. *Eur Radiol* (2020) 30(6):3306–9. doi: 10.1007/s00330-020-06731-x
23. Zhu N, Zhang D, Wang W, Li X, Yang B, Song J, et al. A Novel Coronavirus From Patients With Pneumonia in China, 2019. *N Engl J Med* (2020) 382 (8):727–33. doi: 10.1056/NEJMoa2001017
24. Muramatsu M, Yoshida R, Yokoyama A, Miyamoto H, Kajihara M, Maruyama J, et al. Comparison of Antiviral Activity Between Iga and Igg Specific to Influenza Virus Hemagglutinin: Increased Potential of Iga for Heterosubtypic Immunity. *PLoS One* (2014) 9(1):e85582. doi: 10.1371/journal.pone.0085582
25. Sterlin D, Mathian A, Miyara M, Mohr A, Anna F, Claer L, et al. Iga Dominates the Early Neutralizing Antibody Response to Sars-Cov-2. *Sci Transl Med* (2021) 13(577):eabd2223. doi: 10.1126/scitranslmed.abd2223
26. Self WH, Tenforde MW, Rhoads JP, Gaglani M, Ginde AA, Douin DJ, et al. Comparative Effectiveness of Moderna, Pfizer-Biontech, and Janssen (Johnson & Johnson) Vaccines in Preventing Covid-19 Hospitalizations Among Adults Without Immunocompromising Conditions - United States, March-August 2021. *MMWR Morb Mortal Wkly Rep* (2021) 70(38):1337–43. doi: 10.15585/mmwr.mm7038e1
27. Cazzola M, Rogliani P, Mazzeo F, Matera MG. Controversy Surrounding the Sputnik V Vaccine. *Respir Med* (2021) 187:106569. doi: 10.1016/j.rmed.2021.106569
28. Barrett JR, Belij-Rammerstorfer S, Dold C, Ewer KJ, Folegatti PM, Gilbride C, et al. Author Correction: Phase 1/2 Trial of Sars-Cov-2 Vaccine Chadox1 Ncov-19 With a Booster Dose Induces Multifunctional Antibody Responses. *Nat Med* (2021) 27(6):1113. doi: 10.1038/s41591-021-01372-z
29. Barrett JR, Belij-Rammerstorfer S, Dold C, Ewer KJ, Folegatti PM, Gilbride C, et al. Phase 1/2 Trial of Sars-Cov-2 Vaccine Chadox1 Ncov-19 With a Booster Dose Induces Multifunctional Antibody Responses. *Nat Med* (2021) 27 (2):279–88. doi: 10.1038/s41591-020-01179-4
30. FDA. *Coronavirus (Covid-19) Update: Fda Takes Additional Actions on the Use of a Booster Dose for Covid-19 Vaccines* (2021). Available at: https://www.fda.gov/news-events/press-announcements/coronavirus-covid-19-update-fda-takes-additional-actions-use-booster-dose-covid-19-vaccines.
31. Jahromi M, Al Sheikh MH. Partial Protection of Sinopharm Vaccine Against Sars Cov2 During Recent Outbreak in Bahrain. *Microb Pathog* (2021) 158:105086. doi: 10.1016/j.micpath.2021.105086

32. Saeed U, Uppal SR, Piracha ZZ, Uppal R. Sars-Cov-2 Spike Antibody Levels Trend Among Sinopharm Vaccinated People. *Iran J Public Health* (2021) 50 (7):1486–7. doi: 10.18502/ijph.v50i7.6640
33. Wang H, Zhang Y, Huang B, Deng W, Quan Y, Wang W, et al. Development of an Inactivated Vaccine Candidate, Bbibp-Corv, With Potent Protection Against Sars-Cov-2. *Cell* (2020) 182(3):713–21.e9. doi: 10.1016/j.cell.2020.06.008
34. Saeed BQ, Al-Shahrabi R, Alhaj SS, Alkokhardi ZM, Adrees AO. Side Effects and Perceptions Following Sinopharm Covid-19 Vaccination. *Int J Infect Dis* (2021) 111:219–26. doi: 10.1016/j.ijid.2021.08.013
35. Ferenci T, Sarkadi B. Rbd-Specific Antibody Responses After Two Doses of Bbibp-Corv (Sinopharm, Beijing Cnbg) Vaccine. *BMC Infect Dis* (2022) 22 (1):87. doi: 10.1186/s12879-022-07069-z
36. Lang PO, Govind S, Bokum AT, Kenny N, Matas E, Pitts D, et al. Immune Senescence and Vaccination in the Elderly. *Curr Top Med Chem* (2013) 13 (20):2541–50. doi: 10.2174/15680266113136660181
37. Coe CL, Lubach GR, Kinnard J. Immune Senescence in Old and Very Old Rhesus Monkeys: Reduced Antibody Response to Influenza Vaccination. *Age (Dordr)* (2012) 34(5):1169–77. doi: 10.1007/s11357-011-9356-8
38. Frasca D, Diaz A, Romero M, Blomberg BB. The Generation of Memory B Cells Is Maintained, But the Antibody Response Is Not, in the Elderly After Repeated Influenza Immunizations. *Vaccine* (2016) 34(25):2834–40. doi: 10.1016/j.vaccine.2016.04.023
39. Jacob-Dolan C, Barouch DH. Covid-19 Vaccines: Adenoviral Vectors. *Annu Rev Med* (2022) 73:41–54. doi: 10.1146/annurev-med-012621-102252
40. Sadoff J, Gray G, Vandebosch A, Cardenas V, Shukarev G, Grinsztejn B, et al. Safety and Efficacy of Single-Dose Ad26.Cov2.S Vaccine Against Covid-19. *N Engl J Med* (2021) 384(23):2187–201. doi: 10.1056/NEJMoa2101544
41. Voysey M, Clemens SAC, Madhi SA, Weckx LY, Folegatti PM, Aley PK, et al. Safety and Efficacy of the Chadox1 Ncov-19 Vaccine (Azd1222) Against Sars-Cov-2: An Interim Analysis of Four Randomised Controlled Trials in Brazil, South Africa, and the Uk. *Lancet* (2021) 397(10269):99–111. doi: 10.1016/S0140-6736(20)32661-1
42. Logunov DY, Dolzhikova IV, Zubkova OV, Tukhvatullin AI, Shcheblyakov DV, Dzharullaeva AS, et al. Safety and Immunogenicity of an Rad26 and Rad5 Vector-Based Heterologous Prime-Boost Covid-19 Vaccine in Two Formulations: Two Open, Non-Randomised Phase 1/2 Studies From Russia. *Lancet* (2020) 396(10255):887–97. doi: 10.1016/S0140-6736(20)31866-3
43. Graham F. Daily Briefing: European Regulator Links Astrazeneca Vaccine to Rare Blood Clots. *Nature* (2021). doi: 10.1038/d41586-021-00932-0
44. Wise J. Covid-19: European Countries Suspend Use of Oxford-Astrazeneca Vaccine After Reports of Blood Clots. *BMJ* (2021) 372:n699. doi: 10.1136/bmj.n699
45. Callaway E. Mix-And-Match Covid Vaccines Trigger Potent Immune Response. *Nature* (2021) 593(7860):491. doi: 10.1038/d41586-021-01359-3
46. Supasa P, Zhou D, Dejnirattisai W, Liu C, Mentzer AJ, Ginn HM, et al. Reduced Neutralization of Sars-Cov-2 B.1.1.7 Variant by Convalescent and Vaccine Sera. *Cell* (2021) 184(8):2201–11.e7. doi: 10.1016/j.cell.2021.02.033
47. Ho D, Wang P, Liu L, Iketani S, Luo Y, Guo Y, et al. Increased Resistance of Sars-Cov-2 Variants B.1.351 and B.1.1.7 to Antibody Neutralization. *Res Sq* (2021). doi: 10.21203/rs.3.rs-155394/v1
48. Wang P, Nair MS, Liu L, Iketani S, Luo Y, Guo Y, et al. Antibody Resistance of Sars-Cov-2 Variants B.1.351 and B.1.1.7. *Nature* (2021) 593(7857):130–5. doi: 10.1038/s41586-021-03398-2
49. Perez-Alos L, Armenteros JJA, Madsen JR, Hansen CB, Jarlhelt I, Hamm SR, et al. Modeling of Waning Immunity After Sars-Cov-2 Vaccination and Influencing Factors. *Nat Commun* (2022) 13(1):1614. doi: 10.1038/s41467-022-29225-4
50. Peng Q, Zhou R, Wang Y, Zhao M, Liu N, Li S, et al. Waning Immune Responses Against Sars-Cov-2 Variants of Concern Among Vaccinees in Hong Kong. *EBioMedicine* (2022) 77:103904. doi: 10.1016/j.ebiom.2022.103904


**Conflict of Interest:** The authors declare that the research was conducted in the absence of any commercial or financial relationships that could be construed as a potential conflict of interest.

frontiers | Frontiers in Immunology

TYPE Review
PUBLISHED 13 September 2022
DOI 10.3389/fimmu.2022.905867



OPEN ACCESS

EDITED BY
Eui Ho Kim,
Institut Pasteur Korea, South Korea

REVIEWED BY
Fabian Salazar,
University of Exeter, United Kingdom
Na Cui,
Peking Union Medical College Hospital (CAMS), China

*CORRESPONDENCE
Som Gowda Nanjappa
nanjappa@illinois.edu

†These authors have contributed equally to this work

SPECIALTY SECTION
This article was submitted to Immunological Memory, a section of the journal Frontiers in Immunology

RECEIVED 28 March 2022
ACCEPTED 22 August 2022
PUBLISHED 13 September 2022

CITATION
Sharma J, Mudalagiriyappa S and Nanjappa SG (2022) T cell responses to control fungal infection in an immunological memory lens. *Front. Immunol.* 13:905867. doi: 10.3389/fimmu.2022.905867



# T cell responses to control fungal infection in an immunological memory lens

Jaishree Sharma†, Srinivasu Mudalagiriyappa† and Som Gowda Nanjappa*

Department of Pathobiology, College of Veterinary Medicine, University of Illinois at Urbana-Champaign, Urbana, IL, United States

In recent years, fungal vaccine research emanated significant findings in the field of antifungal T-cell immunity. The generation of effector T cells is essential to combat many mucosal and systemic fungal infections. The development of antifungal memory T cells is integral for controlling or preventing fungal infections, and understanding the factors, regulators, and modifiers that dictate the generation of such T cells is necessary. Despite the deficiency in the clear understanding of antifungal memory T-cell longevity and attributes, in this review, we will compile some of the existing literature on antifungal T-cell immunity in the context of memory T-cell development against fungal infections.

KEYWORDS

CD4+ T cells, CD8+ T cells, memory, fungal, vaccination, infection, immunity

## Introduction

An increasing global burden of fungal diseases due to increasing immunocompromised individuals has heightened the need for effective preventive and therapeutic strategies. Fungi are one of the large biome classes, but only a handful of them are pathogenic to humans, causing a significant case fatality of up to 90%. More than 150 million severe cases and over 1.5 million succumb to fungal infections annually, despite the use of antifungal drugs (1–3). Some existing antifungals are effective but cause serious side effects and are liable to the growing drug-resistant fungal pathogens. With expanding knowledge on host–fungal pathogen interactions, there is a tremendous leap in the thrust to develop fungal vaccines. The pan-fungal vaccine is highly desirable, but the features of different fungal pathogenesis and elicitation of distinct immune responses require a clear understanding of the fungus–immune system interface, i.e., vaccine immunity and the potential to develop immunological memory. This review gives an overview of antifungal memory T cells.

Although there is a good amount of evidence of antibody-mediated immunity (4), adaptive immune cell responses against pathogenic fungi are mainly mediated by T cells, and

genetic or acquired T-cell deficiency leads to a higher incidence of opportunistic infections (1, 5, 6). Antifungal defense mechanisms by $CD4^+$ T cells, a major class of T cells, involve the secretion of proinflammatory cytokines and cell–cell interactions to activate innate immune cells, help $CD8^+$ T cells, and provide help for the generation of antibodies from B cells (7). The antifungal $CD4^+$ T-cell immunity involves the expression of IFNγ, TNFα, GM-CSF, and IL-17A cytokines, which are differentially produced in a fungus- and tissue-specific manner. For example, IFNγ, TNFα, and GM-CSF are predominantly induced during histoplasmosis, aspergillosis, cryptococcosis, paracoccidioidomycosis, pneumocystosis, and talaromycosis, whereas type 17 cytokines, IL-17A/F, and IL-22 are mainly induced during candidiasis, coccidioidomycosis, blastomycosis, and mucormycosis (reviewed here). Nonetheless, it is common to see both types of responses with variable degrees in most fungal infections. These secreted cytokines generate an inflammatory milieu and act on other cells for innate cell recruitment, activation, secretion of antimicrobial peptides, and killing of fungi (8–10). In contrast, the antifungal T cell-mediated immunity is compromised if their cytokine signature yields regulatory or unprotective cytokines that can lead to severe disseminated infections (11, 12). Despite the need for $CD4^+$ T-cell help for $CD8^+$ T-cell activation and memory maintenance in viral and bacterial infection scenarios, using mouse models of fungal infections against *Pneumocystis*, *Histoplasma*, and *Blastomyces*, the studies have shown that antifungal $CD8^+$ T cells can be induced, retained as long-lasting memory, and recalled upon the challenge to provide immunity independent of the T-cell help during mouse models of *Pneumocystis*, *Histoplasma*, and *Blastomyces* infections (8, 13–16). Antifungal activity of $CD8^+$ T cells involves cell cytotoxicity (17) and secretion of proinflammatory cytokines; the latter often mimics $CD4^+$ T-cell antifungal cytokine functions.

The host's first response to fungal invasion starts with innate immunity, which then engages the adaptive immune arm to mount antigen-specific responses to control or clear fungal infection (18). The pattern recognition receptors (PRRs) are critical for innate immune responses for initial fungal control, and their mutations are associated with higher susceptibility (6, 19–21). The activation of innate immune cells and generation of apt inflammatory milieu facilitate dendritic cell priming of naïve T cells to become effectors, which eventually differentiate to form antifungal memory T cells (22). Thus, the innate immunity dictated by fungal recognition shapes adaptive T-cell immunity and immunological memory.

## Fungal recognition by the immune system: Bridging innate to adaptive immunity

Among innate cells, dendritic cells are essential for priming naïve T cells (23). The activated dendritic cells process and present the antigens to $CD4^+$ and $CD8^+$ T cells through MHC-II and MHC-I molecules, respectively. Along with antigen presentation, dendritic cells provide costimulatory signals for T-cell responses (24). Thus, the functions of dendritic cell maturation and activation are a critical step toward bridging innate with adaptive immunity, and such events are mainly mediated by PRR signals. PRRs are a category of host cell receptors that sense specific molecules/patterns, the pathogen-associated molecular patterns (PAMPs) such as β-glucans and mannans of pathogenic fungi, and this recognition is key for innate immune cell activation to provide a primary antifungal defense. The PRRs are mainly classified as Toll-like receptors (TLRs), C-type lectin receptors (CLRs), retinoic acid-inducible gene I-like receptors (RLRs), and NOD-like receptors (NLRs), which can directly bind to the PAMPs of fungi, whereas damage-associated molecular patterns (DAMPs) can bind to PRRs and their canonical DAMP-sensing receptors such as P2X purinoceptor 7 (P2XR7), triggering receptor expressed on myeloid cells 1/2 (TREM1/2), and receptor for advanced glycation end products (RAGE) (25–28). Several of PAMPs of fungi, including β-glucans, mannans, glycoprotein A, and glyceroglycolipids, have been identified for their functions using their PRRs in the host (29–32). There are excellent reviews on PRRs and fungal immunity elsewhere. Here, we highlight how PRRs can influence the innate immune cells to guide adaptive T-cell immunity.

Although negative signaling is noted with few PRRs, many are associated with their positive signaling to promote activation, phagocytosis, and antigen presentation by dendritic cells to T cells. The activated innate immune cells generate an inflammatory micro milieu conducive to the recruitment, activation, differentiation, and expansion of fungal-specific T cells by secreting cytokines and chemokines. Among PRRs, fungal-recognizing CLRs are instrumental in driving innate immune cell responses. Due to structural differences, different fungi show differential CLR binding properties leading to diverse host cell responses. The prototypic member of this family, the Dectin-1 receptor, expressed on innate immune cells including macrophages, neutrophils, and dendritic cells (DCs), recognizes β1-3-glucans of the fungal cell wall. The interference of Dectin-1 interaction with β-glucans by a soluble dectin-Fc fusion protein dampened the expression of inflammatory cytokines, TNFα, IL-1, IL-6, MIP-2, CCL3, G-CSF, and GM-CSF, expression *in vivo*, and increased fungal burden during aspergillosis (33). Ablation of Dectin-1 resulted in decreased reactive oxygen species (ROS) production by neutrophils and the ability to kill *Aspergillus in vitro*. Additionally, alveolar macrophages of Dectin-$1^{-/-}$ mice had defective production of proinflammatory cytokines and chemokines, including IL-1α, IL-1β, and TNFα. The Dectin-1 recognition of *Aspergillus* seems important for IL-17A production, and neutralization of IL-17A led to impaired *Aspergillus fumigatus* clearance and higher mortality of infected mice (34). Dectin-1 promoted the survival of antigen-specific $CD4^+$ T cells, not the $CD8^+$ T cells, specifically in GI-associated lymphoid

tissues following systemic *Candida* infection, and ablation of Dectin-1 reduced the tissue-specific dendritic cells and increased activation of $CD4^+$ T cells leading to higher susceptibility to *Candida*-induced colitis (35). During systemic *Candida* infection, the protective role of Dectin-1 was fungal strain-specific, possibly due to variable adaptation of *Candida albicans* strains *in vivo*, including the changes in the microbiota of mice due to different mouse facilities, with changes in the cell wall components and high chitin in the cell wall masks the dependability on Dectin-1 recognition (36). Further, pathogenic fungi can avoid host Dectin-1 recognition of β-(1,3)-glucan by masking with α-(1,3)-glucan, phosphatidylserine, capsule, rodlet layer/melanin, and mannans or trimming to reduce the exposure in the cell wall, thus increasing immune evasion *in vivo* (37–40). However, Dectin-1 was dispensable for controlling infections from *Blastomyces*, *Cryptococcus*, certain strains or species of *Candida*, or *Candida* colonization (36, 41–45), suggesting the differential requirement of CLRs for fungal immunity.

Unlike the Dectin-1 receptor, cytoplasmic domains of Dectin-2 and Mincle receptors lack their own ITAM motifs and associate with FcRγ immunoreceptor harboring cytoplasmic ITAM motif for signaling (46, 47). Dectin-2 and Mincle have been shown to be important for immunity against blastomycosis (48), aspergillosis (49), histoplasmosis (44), chromoblastomycosis (50), disseminated candidiasis (51, 52), and species-specific candidiasis (45). Dectin-2 signals through the Syk-CARD9 pathway and promote Th17 cell responses (51) by inducing the expression of IL-1 and IL-23 cytokines (53). Despite that Dectin-2 and Mincle share their signaling through FcRγ immunoreceptors, their role in activation, expansion, and differentiation of antigen-specific $CD4^+$ T-cell responses may differ. While Dectin-2 was essential for enhancing Th17 cell differentiation, Mincle recognition suppressed Th17 polarization during chromoblastomycosis (50).

In addition to CLRs, TLRs expressed by innate cells are involved in the control of fungal infection. Myeloid differentiation primary response protein 88 (MyD88), an adaptor molecule for many TLRs signaling, has been shown to play a role in antifungal immunity against *Blastomyces dermatitidis*, *Paracoccidioides brasiliensis*, *A. fumigatus*, *Cryptococcus neoformans*, and *C. albicans* (54–56). TLR2 plays a significant role in conferring protective immunity against *Candida* infection at mucosal sites, including gastrointestinal and reproductive tracts by inducing Th17 differentiation through MyD88 signaling (57, 58). However, the role of TLR2 in controlling systemic candidiasis seems to be fungal strain specific (59, 60). Additionally, IL-1R/MyD88 signaling pathway is necessary for host resistance against *Candida*, and TLR4/MyD88 pathways mediate protection against *Aspergillus* infection by regulating Th1 and Th2 response (54, 61). TLR3 in DCs senses fungal RNA derived from dying cells and potentiates the cross-presentation to activate $CD8^+$ T cells during aspergillosis (62). Nevertheless, compared to those of CLRs, the functions of many TLRs in the context of antifungal immunity seem to be modest or redundant.

NLRs function against fungal defense mainly involved the activation of inflammasomes, which leads to caspase-dependent production of functional IL-1β and IL-18 cytokines. Both of these cytokines have been shown to exert antifungal host defense in an NLRP3-dependent manner (63). NLRC4 negatively regulates NLRP3 inflammasome activity, suppressing early IL-1β and late IL-18-mediated antifungal $CD8^+$ T-cell responses during pneumocystosis (64). Thus, some PRRs of the non-CLR class play a role in immunity against fungal infections (26).

Genetic polymorphisms are associated with susceptibility or resistance to infections. The genetic TLR polymorphisms related to fungal disease susceptibility in humans undergoing allogenic stem cell transplants seem to be modest or minimal (65, 66). The genetic predisposition due to PRR polymorphisms to fungal infections is variable and depends on the pathogen or the degree of inflammation. For example, TLR4 polymorphism D299G is associated with increased susceptibility to *Candida* bloodstream infection, possibly due to higher immunosuppressive cytokine IL-10 production. However, such susceptibility was not seen in urogenital *Candida* infection (67). Similarly, the TLR4 polymorphisms (D299G/T399I), despite the normal colonization of the fungus, are associated with mitigating the hyperinflammation and tissue damage during aspergillosis (66). Similarly, genetic polymorphisms of CLRs have been associated with susceptibility to fungal infections. Dectin-1 single-nucleotide polymorphisms (SNPs), rs3901533 and rs7309123, enhanced the susceptibility to invasive pulmonary aspergillosis (68). Dectin-1 polymorphism of Y238X led to decreased receptor signaling and increased susceptibility to invasive aspergillosis and recurrent vulvovaginitis caused by *Candida* (69, 70). Alternative splicing leading to truncated Dectin-1 seen in the C57BL/6 strain, compared to the DBA/2 mouse strain, increased the susceptibility to coccidioidomycosis (71). Thus, it is essential to decipher gene polymorphisms in humans to understand the susceptibility to fungal infections.

T cells can also express several PRRs to respond to PAMPs during fungal infections. Engagement of the cell-intrinsic PRR pathway is one of the non-classical T-cell signaling routes to enhance the activation, effector function, and memory formation of T cells as proposed originally by Janeway (72). Important PRRs on T cells that detect fungal PAMPs are TLRs, NLRs, and damage-associated molecular pattern-sensing receptors. TLRs can function as co-stimulatory receptors that complement TCR-induced signals to enhance effector T-cell proliferation, survival, and cytokine production (73). T cells expressing TLRs, including TLR2 and TLR4, can directly sense pathogens and modulate T-cell responses. Naïve $CD4^+$ T cells do not express significant levels of TLR2/TLR4 mRNA and proteins, but activated and memory T cells express high levels of membrane-bound TLR2 and TLR4 (74, 75). TLR2 signaling

in T cells can be modulated by TCR and IL-2-induced mTOR signals (76). Intrinsic MyD88 signaling can modulate the T-cell functions during fungal infections. MyD88 signaling, both extrinsic, non-$CD4^+$ T cell-mediated (77) and intrinsic, $CD8^+$ T cell-mediated (78), fosters fungal vaccine immunity by T cells by regulating the survival and proliferation of effector T cells. MyD88 promoted the sustained Tc17 cell proliferation by activating mTOR *via* Akt1, and cell-intrinsic IL-1R and TLR2 signaling, but not IL-18R, were required for MyD88-dependent Tc17 responses (78). MyD88 deletion in $FoxP3^+$ regulatory T cells increased the fungal burden and immunopathology during oral *C. albicans* infection in mice, coinciding with reduced IL-17A expressing $FoxP3^+$ T cells ($T_{reg}17$) and increased dysfunctional $IFN\gamma^+/FoxP3^+$ cells ($IFN\gamma^+$ $T_{reg}$). This dysregulated IL-1β-mTOR-Treg17 axis contributes to overt inflammation during mucosal infections in elderly individuals in a model of oral candidiasis (79). NLRP3, a member of the NLR family, can indirectly sense danger signals. In a murine model of disseminated talaromycosis, compared to wild-type mice, Casp-1 and Nlrp3 global KO mice displayed higher mortality rates and fungal load, which correlated with impaired $CD4^+$ T-cell recruitment into granulomas (80). Although this study did not look into T-cell intrinsic effect, NLRP3 signaling in $CD4^+$ T cells has been shown to augment Th1 immunity (81). Further studies are needed to dissect the T-cell intrinsic PRR functions against fungal infections. Interestingly, PRR has been used to generate modified TCR of T cells. Dectin-1-chimeric antigen receptor (D-CAR) was bioengineered using the extracellular domain of Dectin-1 to redirect T-cell specificity toward fungal β-glucan moieties for immunity (82). D-CAR+ T cells could inhibit *A. fumigatus* hyphae formation *in vitro* and reduce pulmonary fungal burden *in vivo*. In this study, chimeric $CD8^+$ T cells kill the fungi directly by pumping out cytolysins onto yeast/hyphae of *Aspergillus* and indirectly by secreting IFNγ that can potentiate the killing of yeasts by neutrophils (83).

# Antifungal T cells

$CD4^+$ T cells, also called helper T cells, are instrumental in controlling fungal infections, and their deficiency leads to severe disseminated infections by opportunistic fungal pathogens. As the name suggests, the helper cells bolster innate immune cell functions, aid in the generation of productive B-cell responses, help $CD8^+$ T-cell responses, and control autoimmunity. Based on their cytokine secretion and functions during fungal infections (84, 85), T cells are classified into Th1 (IFNγ, GM-CSF, and TNFα), Th17 (IL-17A/F), Th22 (IL-22), Th2 (IL-4 and IL-13), Th9 (IL-9 and IL-10), Treg (IL-10 and TGFβ), and Tr1 (IL-10). The cytokines produced by T cells have a multifaceted role in controlling or regulating the pathogenesis during infections, including fungal infections (86). Although a mixture of different cytokine-producing T cells is often found during fungal infections, the predominant subset of T-cell responses is associated with the type of pathogen, infection, or tissue location (Table 1). Here, we will highlight some of the roles of these T cells for immunity against different pathogenic fungi with a focus on memory phenotypic cells.

# Pathogen-specific antifungal T cells

## *Candida*

Anti-*Candida* memory T-cell responses are studied in the context of mucosal infections, vaccine-induced responses, and commensal-specific/pre-exposed T cells in healthy donors. *Candida* is a commensal but opportunistic fungal pathogen that causes disseminated infection under compromised immunity. In a mouse model of oropharyngeal candidiasis (OPC), after resting for 6 weeks following primary infection, the memory $CD4^+$ conferred immunity to secondary infection by producing antigen-specific IL-17A responses (91). However,

TABLE 1 Major T-cell subsets elicited and shown to be protective against fungal pathogens.

| Pathogenic fungi | Mechanism(s) of protection | | | References |
|---|---|---|---|---|
| ***Aspergillus* spp.** | Th1 (circulation), Th17 (lungs) | Tc1 | | (87–89) |
| ***Blastomyces* spp.** | Th1, Th17 | Tc1, Tc17 | Tc1 ($_{EM/CM}$)<br>Tc17 ($_{EM}$) | (56, 90) |
| ***Candida* spp.** | Th1, Th17 | Tc1, Tc17 | $T_{RM}$ | (91–94) |
| ***Cryptococcus* spp.** | Th1, Th17? | Tc1 | $T_{RM}$ | (95, 96) |
| ***Coccidioides* spp.** | Th1, Th17, Th2 | Tc1 | $T_{EM}$ | (97–99) |
| ***Histoplasma* spp.** | Th1, Th17 | Tc1 | | (100) |
| ***Paracoccidioides* spp.** | Th1, Th17 | Tc1 | | (101) |
| ***Pneumocystis* spp.** | Th1? | Tc1 | | (102) |
| ***Talaromyces* spp.** | Th1, Th17 | | | (103, 104) |

Different subsets of $CD4^+$ T helper cells and $CD8^+$ T cells have been shown to participate in immunity against different pathogenic fungi. In some of the pathogenic fungi, different types of memory T-cell development have been documented.

depletion of $CD4^+$ T cells did not cause OPC, possibly compensated by developed residual IL-17A expressing memory $CD8^+$ T cells and $CD3^+CD4^-CD8^-$ cells. In a mouse model of *C. albicans* skin infection, IL-$17^+$ $CD4^+$ T cells were enriched in the skin, which transitioned into sessile $CD69^+$/$CD103^+$ tissue-resident memory T cells ($T_{RM}$) within 90 days. This suggests that the long-lasting antifungal memory Th17 cells are generated in the non-lymphoid organ, such as the skin (105). Importantly, these $T_{RM}$ cells provided better immunity than migratory Th17 cells following infectious challenges. In a mouse model of vulvovaginal candidiasis, Th17 cells persisted even after the clearance of the yeast but in low numbers by day 30 (106). The vaginal washes showed the presence of IL-17A, IL-23, and β-defensins. Nevertheless, this study did not examine the long-term maintenance of effector/memory $CD4^+$ T cells.

The *C. albicans* hypha-specific surface protein antigen, agglutinin-like sequence (Als3)-based NDV-3A vaccine was used for active immunization in a mouse model that prevented *Candida* colonization at vein catheterization site (107), and the mechanisms involve the induction of high levels of anti-rAls3p-N antibodies. Here, the antibody titers persisted 15 days post-boost, interfered with *Candida* colonization at the catheter site, and reduced the fungal burdens in the kidneys. Although the elicitation of $CD4^+$ T-cell responses or their persistence was not evaluated in this study, the blocking/inhibitory ability of the antibodies may suggest their potential. In another study, where the NDV-3 vaccine was used in a mouse model of vaccine immunity to vulvovaginal candidiasis, robust antibody responses and immunity were dependent on both T and B cells (108). However, the immunity was assessed 2 weeks following the boost, which may not give a clear understanding of long-lasting memory $CD4^+$ T-cell development. Nevertheless, in a human study, intramuscular NDV-3 vaccination of the volunteers induced the durable serum and cervicovaginal antibody titer (anti-Als3) for up to 1 year and provided significant immunity against recurrent vulvovaginal candidiasis (109). This study found significantly higher numbers of Als3-specific cytokine (IFNγ and IL-17A) secreting peripheral blood mononuclear cells (PBMCs) even after day 90 of vaccination. Although this trial evaluated an immunotherapeutic vaccine, whether the vaccination induces the antigen-free (*Candida* reexposure-free) persistence of long-lasting "memory adaptive (T and B) cells" needs to be assessed.

*Candida*-specific memory $CD4^+$ T cells in healthy blood donors produced IL-17A and IFNγ, but not IL-10, following restimulation (110). The human *Candida*-specific memory Th17 cells preferentially expressed phenotypic markers, CCR6 and CCR4 (92), which suggests the generation of long-lived anti-*Candida* memory T cells in humans, possibly due to stimulations from commensal microorganisms. Notably, human *Candida*-specific memory $CD4^+$ T cells are heterogeneous, produce multiple cytokines, and have unique and shared clonotypes among memory subsets (111). *C. albicans*-specific $T_{RM}$ cells prevented the fungal overgrowth in human skin and oral mucosa by producing IL-17A (105, 112). Similarly, *Candida*-specific IL-9-producing $CD4^+$ T cells, Th9, were found enriched in the skin of healthy donors (suggesting their memory phenotype) and have the ability to amplify IFNγ, IL-9, IL-13, and IL-17 by skin-tropic T cells (113). However, gut Th9 cells protect against *Candida* reinfection and mitigate associated pathology (114). Another *Candida*-specific subset of $CD4^+$ T cells expressing IL-22 (Th22) is found in humans as memory cells and is increased following infection (115). Further, Th22 seems to provide defense against recurrent vulvovaginitis caused by *Candida* in humans (116), suggesting the formation of mucosal memory Th22 cells. In this line, defective Th22 responses are associated with chronic mucocutaneous candidiasis (117). Although little is known about the fate of pre-existing antifungal memory T cells during co-infection, a recent study suggests the impaired T-cell responses to *Candida* following COVID-19 infection that was associated with diminished inflammatory cytokines release (118).

In the mouse models of mucosal candidiasis, studies have shown that Tc17 cells play a role in both oral and vaginal infections (91, 119). Oral immunization of mice with *C. albicans* under B-cell deficiency induced systemic memory of $CD8^+$ T cells and provided protection following the challenge (120). The screening of *Candida*-specific memory $CD8^+$ T cells in healthy human blood donors showed a non-classical cytotoxic molecules expression profile, i.e., secretion of granulysin and granzyme K rather than perforin/granzyme B (121). The $CD8^+$ T cells were reactive to *C. albicans*, *Candida glabrata*, and *Sporothrix* and expressed lysosomal degranulation markers, CD107a/b, and secreted IFNγ and TNFα, following *ex vivo* stimulation with yeast-loaded dendritic cells.

In one study, the various phylogenetically closer and distant yeast-specific T-cell responses were assessed using PBMCs of humans and found a predominant presence of IFNγ-expressing effector memory $CD8^+$ T cells (122). Interestingly, in this study, enriched $CD8^+$ T cells were more reactive to filamentous form than the unicellular form of *Candida*. In $HIV^+$ patients, the *Candida*-specific activated memory $CD8^+$ T cells were accumulated within the oropharyngeal candidiasis (OPC) lesions at the lamina propria–epithelium interface (123). Similarly, *C. albicans*-specific $CD8^+$ T cells were found in the blood and nasal mucosa of chronic rhinosinusitis patients, suggesting a possible persistent T cell-mediated mucosal inflammation (124), which may be due to repeated exposure to the antigen.

## *Aspergillus*

*Aspergillus*, a globally prevalent opportunistic fungal pathogen, causes pulmonary and invasive mycoses following inhalation of spores. Immunity to aspergillosis is primarily

associated with the development of memory Th1 cells, while biased Th2 or regulatory responses are linked to exacerbated disease (125–127). Experimental vaccination of mice with conidia, hyphae, crude culture filtrate antigens, or adjuvanted (CpG ODN1862) cell wall glucanase Crf1 protein strongly induced Th1 (IFNγ and IL-2) responses, formed effector or memory T cells, and conferred immunity following the challenge (87, 128–131). In line with the protective role of Th1 responses, IL-4 seems to play a negative role following *A. fumigatus* challenge (127). In chronic rhinosinusitis with nasal polyposis patients, the mycology culture showed the presence of *Aspergillus flavus*, and PBMCs stimulated with aspergillus antigens showed an increased ratio of aspergillus-specific Th17 cells over Tregs, suggesting prior sensitization (132). Further, stimulated PBMC culture supernatant showed elevated levels of IL-17 and IL-10 with reduced TGFβ levels, suggesting the possible associated pathology in these patients. Prior work has shown the negative effect of IL-10 for control of experimental lethal systemic aspergillosis (133), and its overexpression, due to genetic polymorphisms, predisposes to invasive aspergillosis possibly by inhibiting TNFα secretion in hematopoietic stem cell recipients or hematological patients (134, 135). However, IL-10 seems to be protective in regulating exaggerated immune responses and inflammation in allergic bronchopulmonary aspergillosis (136), suggesting that the regulatory role of IL-10 depends on the disease context. In many healthy individuals (10%–30%), multi-*Aspergillus*-specific T cells were found, suggesting their memory potential and feasibility to expand, store, and be used for self-adoptive transfers following hematopoietic stem cell transplantation (137–139). Hematopoietic stem cell transplant patients undergo a period of immunocompromised state, enhancing vulnerability to many opportunistic fungal infections, including aspergillosis. Thus, rapid preventive or therapeutic reconstitution of the functional adaptive immune system is beneficial. Adoptive immunotherapy using either donor-derived (139) or partially HLA-matched antigen-specific T cells can be used to prevent or treat opportunistic fungal infections (140). In a preclinical study, *in vitro* expanded yeast-specific cytokine-producing Th cells have been used to reduce the severity of pulmonary and cerebral forms of aspergillus infections in mice (141).

Although the role of Th17 cells in pulmonary aspergillosis is debated, a recent study suggests the presence of aspergillus-specific Th17 cells that correlated with protective immunity (88), and possible mechanisms may include the formation of inducible bronchus-associated lymphoid tissue (iBALT) structures and development of $T_{RM}$ cells (142). With the use of recombinant aspergillus proteins (Asp f proteins), a study investigated the presence of yeast-specific $CD4^+$ and $CD8^+$ T cells in healthy non-atopic donors (143). In these individuals, the cytokine production signature suggested the presence of aspergillus-specific memory T cells expressing IFNγ, IL-17A, and to some extent IL-4, possibly due to prior exposure. Importantly, this study showed the presence of *Aspergillus*-reactive $IFN\gamma^+$ T cells for up to 6 months of follow-up observations. However, the persistence of diverse cytokine-expressing T cells as memory in humans needs to be evaluated for their role in immunity or immunopathology following infection.

## *Pneumocystis*

*Pneumocystis* is another opportunistic fungus that causes infection under immunodeficiency, especially of $CD4^+$ T cells and B cells. It is believed that *Pneumocystis* may persist in individuals upon early age exposure without any apparent symptoms, akin to toxoplasma. The reactivation occurs when an individual becomes immunodeficient or severely immunosuppressed, suggesting an active role of memory or effector adaptive immunity to keep the fungus at bay. However, recent studies suggest the possibility of reinfection in immunocompromised individuals (144). Murine models have been valuable in understanding the host–*Pneumocystis* interface for adaptive immunity and recapitulating human primary immune disorders (145). Increasing evidence suggests that B-cell responses are important in the control of *Pneumocystis*. Anti-CD20 mAb therapy in humans enhanced the susceptibility to pneumocystosis, suggesting a critical role of B cells (146). Of note, the CD20 mAb therapy does not deplete mature plasma cells (147), raising questions on mature long-lived plasma cell generation against *Pneumocystis*. It is possible that anti-CD20 mAb therapy leads to functional impairment of antibody-secreting cells. However, in a murine model of pneumocystosis, neither the memory $CD4^+$ T cells nor B cells are required for clearance of infection (146). Here, convalescent *Pneumocystis*-specific IgGs were enough to provide immunity. Interestingly, B cells are required for elicitation of antigen-specific $CD4^+$ T-cell responses to *Pneumocystis* (148, 149), suggesting a potential cross-talk between these two subsets for immunity against pneumocystosis. Notably, in the simian model of vaccination with *Pneumocystis jirovecii* protease kexin (KEX1), once the B cells are primed, induction of $CD4^+$ T-cell deficiency with SHIV infection did not prevent antibody-dependent control of infection, suggesting the persistence of "memory" plasma cells or threshold levels of Ab titers (150). In a murine model, memory $CD4^+$ T cells were dispensable for pneumocystosis control, whereas memory $CD8^+$ T cells, alveolar macrophages, and *Pneumocystis*-specific IgG contributed to secondary immunity (102). Here, the IgG antibody enhanced the macrophage killing of yeast, while macrophages helped $CD8^+$ T-cell recall responses in IFNγ production. IFNγ-stimulated $CD8^+$ T cells, in turn, can be potent antifungal cytotoxic cells (13). However, interestingly, $CD8^+$ T cells seem to help $CD4^+$ T cells with their IFNγ responses. Memory $CD4^+$ T cells can indirectly potentiate NK

cell functions against infection caused by *Pneumocystis murina*, and depletion of $CD4^+$ T cells significantly reduced the accumulation of NK cells and NK-cell mediated immunity (151). In a mouse model of vaccine immunity, immunization with a recombinant fusion protein containing N-terminal 544-aa *Pneumocystis* cross-reactive antigen-1 and trigger factor (TF) induced protective and cross-reactive antibody responses that provided immunity even after memory $CD4^+$ T cells were depleted at the time of challenge infection (152). Thus, $CD4^+$ T cells seem to have functional duality against *Pneumocystis* infection, first by helping B cells and $CD8^+$ T cells to become protective differentiated memory cells and second by secreting proinflammatory cytokines to control the primary infection.

## *Cryptococcus*

*C. neoformans* is a facultative intracellular opportunistic pathogen commonly associated with AIDS patients due to severe $CD4^+$ T-cell deficiency. The $CD4^+$ T-cell immunity to cryptococcosis is mainly dependent on Th1 cytokines. Models of vaccination and infection suggested the role of $CD4^+$ T cells and their Th1 cytokine profile. *Cryptococcus*-activated $CD4^+$ T cells recruited other immune cells, enhanced the phagocytosis, and killed infected cells by $CD8^+$ T cells, akin to intracellular bacterial infections (153). Striking effects of Th1-derived cytokines for immunity against cryptococcosis are noticed when genetically engineered *C. neoformans* strain H99 expressing IFNγ (H99-γ) was experimentally used in mice (154). Here, the "vaccinated" mice cleared the infection that was associated with a large influx of leukocytes, enhanced T-cell recruitment, and increased Th1 and decreased Th2-type cytokines following challenge infection. The use of a recombinant strain of *C. neoformans* (H99-γ) as a vaccine strain induced memory $CD8^+$ T cells to mediate immunity under $CD4^+$ T-cell deficiency, suggesting that antifungal $CD8^+$ T cells can compensate $CD4^+$ T cells (155). Notably, there was the development of memory T cells and enhanced secondary responses following the challenge. *C. neoformans* chitin deacetylase 2 peptide (Cda2-Pep1) delivered in glucan particle (GP)-based vaccination robustly protected the mice following the challenge, and the immunity was correlated with their MHC-II binding affinity (156). Similarly, multi-epitope vaccine/s may be useful in controlling cryptococcosis (157). In an experimental model, immunization with either cell wall or cytoplasmic protein preparation from *Cryptococcus gattii* induced vaccine immunity after challenge and protection that was associated with enhanced Th1 responses and antigen-specific serum IgG (158). Nevertheless, in such vaccination platforms, the development of memory T cells is not clear. However, *Cryptococcus* antigen-pulsed dendritic cell-based systemic vaccination elicited long-lived memory Th17 cells in the lungs (95). Interestingly, these cells were lung resident $T_{RM}$ cells, produced IL-17A but not IFNγ, and mediated protection against *C. gattii* challenge. Pulmonary infection with *C. neoformans* elicited strong $CD8^+$ T-cell responses to control the infection independent of $CD4^+$ T cells (15). In this line, immunization with the genetically mutant *Cryptococcus* strain (Δsgl1) that accumulates steryl glucosides led to induction of protective immunity that required either $CD8^+$ or $CD4^+$ T cells (159). However, these studies did not show memory T-cell development or persistence. In HIV-associated *Cryptococcus* meningitis patients, the clearance of infection was strongly correlated with Th1, not Th2 or Th17, cytokines (IFNγ or TNFα). In contrast, their defective expression led to higher mortality (160), suggesting an importance of type I immunity. Lower frequency of cytokine-producing memory $CD8^+$ and $CD4^+$ T cells was found in HIV-infected patients with *Cryptococcus* meningitis (CM), but their numbers were increased with more polyfunctional $IL\text{-}2^+/IL\text{-}17^+$ $CD4^+$ T cells and $IL\text{-}2^+$ $CD8^+$ T cells following antiretroviral therapy (ART) in CM-associated immune reconstitution inflammatory syndrome (CM-IRIS) (161) patients, suggesting the pathological role of cryptococcal memory T cells under certain conditions.

## *Blastomyces*

Mouse models of immunity to blastomycosis suggest that $CD4^+$ T cells are essential for controlling primary pulmonary infections. An experimental mouse model of vaccination suggested that Th17 cells expressing IL-17A are the main driver for immunity against pulmonary blastomycosis by activating macrophages and neutrophils (56). A *Blastomyces*-specific fungal antigen, Calnexin, was found to be conserved among multiple fungal pathogens, and vaccination with Adjuplex adjuvant or encapsulated glucan mannan particles seems to induce robust $CD4^+$ T-cell responses and immunity (162, 163). Identification of such conserved antigens may help the design of pan-fungal vaccines (164). Although homeostasis of memory $CD4^+$ T cells was not studied, the fungal-specific $CD4^+$ T cells persisted for 8 weeks and the adoptive transfer of vaccine-induced effector $CD4^+$ T cells mediated the immunity following the lethal challenge even after 10 weeks of rest (162), suggesting their potential to become memory. Interestingly, intranasal delivery of vaccine-candidate *Blastomyces* endonuclease-2 (Bl-Eng2) induced $T_{RM}$ cells in the lungs but failed to provide proactive immunity, unlike systemic vaccine-induced migratory $CD4^+$ T cells (165). Importantly, Bl-Eng2 is a glycoprotein antigen that has mannose residues that bind to Dectin-2 and a protein backbone with protective CD4 T-cell epitope/peptide (165, 166), thus a vaccine candidate with intrinsic adjuvanticity property. Admixing adjuvants, especially TLR9 (CpG55.2) and Aldeltin (formulation with alum OH) with fungal antigen (Bl-Eng2 peptide) potentiated the vaccine immunity against blastomycosis, which was dependent on type

1 and type 17 cytokine-producing migratory and lung-resident T cells (167). In the mouse model of vaccination under $CD4^+$ T-cell deficiency, $CD8^+$ T cells could mount sterilizing immunity to lethal pulmonary infection. Immunity was predominantly mediated by IL-$17A^+$ $CD8^+$ (Tc17) cells (90) with disparate dependency on the type I cytokines (by Tc1 cells), IFNγ, TNFα, and GM-CSF (168); i.e., deficiency of one Tc1 cytokine was compensated by other Tc1 cytokines. Notably, antifungal memory $CD8^+$ T cells were long-lasting and persisted stably without plasticity in the absence of vaccine antigen or $CD4^+$ T-cell help (16, 169). These memory $CD8^+$ T-cell precursors portrayed stem cell-like phenotype and can be fine-tuned by MyD88-Akt-mTOR signaling (78). Additionally, targeting the negative regulator of the TCR signaling molecule, Cblb, could enhance memory $CD8^+$ T-cell responses of both Tc1 and Tc17 responses to inactivated vaccine and potentiate immunity following lethal pulmonary challenge (170). Memory Tc17 cells predominantly expressed GM-CSF, and these co-expressing cells potentiated the fungal vaccine immunity without precipitating pathology (171).

## Histoplasma

*Histoplasma* is an opportunistic fungal pathogen and causes disseminated infection in severely immunocompromised patients. Incidentally, most people living in the Ohio-Mississippi river valley endemic regions were reactive to *Histoplasma* (172), suggesting memory T-cell persistence. Memory $CD4^+$ T cells contributed to immunity following the secondary infection, and depletion of both $CD4^+$ and $CD8^+$ T-cell subsets enhanced the infection and decreased survivability (173). The deficiency of IL-10 conferred salutary effects on memory T cell-mediated protection to secondary histoplasmosis (174). The immunity was dependent on T cell-derived TNFα or IFNγ, and the protection conferred by T cells generated under IL-10 deficiency was robust. Although memory responses of IL-$17^+$ T cells are not clear, induction of their effector type and immunity has been noticed following vaccination or infection with *Histoplasma* (56, 90, 170, 175). In a model of histoplasmosis, $CD8^+$ T cells could compensate for the loss of $CD4^+$ T cells for vaccine immunity (176), and the depletion of $CD8^+$ T cells compromised the primary immune responses (177). Immunity to histoplasmosis was perforin-dependent and perforin-independent, which included cytokine-mediated (IFNγ or TNα) mechanisms (178). The antigen cross-presentation by dendritic cells seems to be critical for the elicitation of protective antifungal $CD8^+$ T-cell responses (14). Although the above studies do not evaluate memory homeostasis, memory responses to histoplasmosis were bolstered by IL-10 neutralization, where fewer $CD8^+$ T cells were enough to mediate immunity (174).

## Coccidioides

Coccidioidomycosis or Valley Fever is caused by species of dimorphic fungus, *Coccidioides*, a major cause of mycosis endemic to the southwestern United States. Immunity to Valley Fever is primarily associated with T cells expressing both type 1 and type 17 cytokines (Th1/Th17) (179, 180). The regulatory T cells were associated with persistent coccidioidomycosis in the pediatric population that was recapitulated in resistant vs. susceptible mice (181, 182). Cytokine IL-10 plays a negative role in memory Th1 and Th17 recall responses and immunity following *Coccidioides* infection, but not for the development of memory T cells. Coccidioidomycosis immune donors had polyfunctional T cells composed of both effector and central memory phenotypic cells (183), suggesting their long-term immune role. In a human vaccine study using formaldehyde-killed sperules of *Coccidioides immitis*, no statistical differences in susceptibility to infection were found between placebo and vaccination groups (184). However, the memory T-cell development or their functions between these groups were not clear. Nevertheless, there is an active attempt to improve the vaccine efficacy using a multivalent vaccine against *Coccidioides* infection that required mixed Th1 and Th17 cell-mediated immunity (185, 186). In a mouse model of vaccine immunity using a temperature-sensitive, auxotrophic mutant of *C. immitis*, the adoptive transfers of either $CD4^+$ or $CD8^+$ T cells from vaccinated mice to recipient mice infected with lethal strain conferred protection, and the immunity was mediated through TNFα (97). In this study, although effector $CD8^+$ T cells (2 weeks post-immunization) were used to show protective immunity, the mice were monitored for 50 days following the challenge, suggesting the effector cells' persistence and possible conversion into memory cells.

## Paracoccidioides

Immunity to paracoccidioidomycosis depends on the $CD4^+$ T cells expressing Th1 cytokines, IFNγ, TNFα, and IL-2 (187). The type of T-cell response determines the nature of the disease or the susceptibility, with Th2-dominant responses being non-protective and a mix of Th17/Th22 and Th1/Th2 providing the intermediate protection (188). Experimental vaccination with P10 antigen (of gp43 protein) in Montanide ISA 720, CFA, flagellin, and DODAB adjuvants induced Th1 response and protected against intratracheal challenge infection (189, 190). Here, both effector and central memory phenotypic cells were found to be successfully recalled into the lungs after infection. Similarly, fungal-specific memory $CD4^+$ and $CD8^+$ T cells were seen in the patients, and low numbers of memory $CD4^+$ T cells were associated with relapse of the disease (191). In the model of pulmonary paracoccidioidomycosis, $CD8^+$ T cells were induced to control the fungi in the absence of $CD4^+$ T cells by secretion of type 1 cytokines (IFNγ and IL-2), and the

depletion of $CD8^+$ T cells increased the fungal burden with a concomitant increase of non-protective IL-4 and IL-5 cytokines (101). Nitric oxide helps control *Paracoccidioides* infection, and deficiency of NO and $CD8^+$ T cells seems to be detrimental to immunity. Interestingly, $CD8^+$ T cells enhance the recruitment of TNFα/IFNγ-producing $CD4^+$ T cells and the influx of inflammatory cells (192). However, the maintenance of such a response as memory is unclear.

## Cross-reactive antifungal T cells

Cross-reactivity, the recognition of two or more peptides by the same TCR, of T cells has been documented. Cross-reactive antifungal T cells are useful, and identifying the antigens helps in the generation of a pan-fungal T-cell vaccine (193). *C. albicans* existence as a commensal microbe induces memory $CD4^+$ T cells. Incidentally, these *C. albicans*-specific cells can cross-react with airborne fungi, like *Aspergillus*, and exacerbate acute inflammatory lung pathologies (194, 195). Similarly, *A. fumigatus* antigen-induced memory Th1 cells were cross-reactive to *C. albicans* (130). T cells specific to *A. fumigatus* were cross-reacted to induce protective immune responses against *Aspergillus* and *Mucorales* sp. infections (138). *A. fumigatus*-specific T cells, in culture, exhibited cross-reactivity with lysates derived from other fungi, including non-fumigatus *Aspergillus*, *C. albicans*, *Penicillium* spp., and *Scedosporium apiospermum* but not with *Aspergillus terreus*, *C. glabrata*, *Fusarium* spp., and *Mucor* spp. (196). Although such distantly related fungi have cross-reactive T cells, high cross-reactivity of T cells was noticed between phylogenetically related *Scedosporium* and *Lomentospora* species, but not with *A. fumigatus* (197). The cross-reactivity by adaptive immunity across kingdoms, i.e., fungus and bacteria, is noticed and exploited for vaccination against *Candida* and *Staphylococcus aureus* (198), including emerging multidrug-resistant *Candida auris* infection (199). Similarly, pan-fungal vaccines can be developed and used against different pathogenic fungi if the shared antigen is identified (163). Although the mechanism of cross-reactivity of fungal T cells is mainly due to shared epitope sequence (163), the broad cross-reactivity of the $CD4^+$ T cells may be due to the nature of TCR binding with peptide-MHC class II that allows multiple anchor residues with greater flexibility of amino acid variation (200, 201). The bystander activation *via* TCR-independent mechanisms (202) may also be involved.

## Mechanisms of T cell-mediated fungal control

T cell-mediated control of fungal infections involves mechanisms that are chiefly mediated through the effectual functions of the cytokines they secrete. Additionally, cytotoxic functions, independent of cytokines, of $CD8^+$ T have been documented during fungal infections. Here we highlight some of the actions of cytokines/cytotoxic molecules for fungal control.

IL-17A and GM-CSF cytokines at the site of infection protected against fungal pathogens in part by enhancing the neutrophil recruitment to the site of infection (9). Further, these cytokines can activate recruited neutrophils and macrophages to bolster their ability to kill fungal cells. Activated neutrophils and macrophages may exert direct fungicidal activity *via* phagocytosis, degranulation, ROS production, and neutrophil extracellular trap (NET) formation (203). Different granules (primary azurophilic, secondary specific, and tertiary gelatinase) in neutrophils contain different cytolytic molecules (17). The role of the IL-17 axis and neutrophils during dimorphic fungal infections has been reviewed elsewhere (204). IL-17 and IL-22 act on cells to promote STAT3 activation, upregulate Reg proteins, and secrete antimicrobial peptides (AMPs), S100 proteins, and β-defensins from epithelial cells and keratinocytes that destroy the fungal pathogen (205). Further, IL-22 signaling helps in the regeneration of oral epithelial cells and "licenses" IL-17 signaling for resistance against oral mucosal candidiasis (206). AMPs secreted by epithelial cells induce cell wall permeabilization, mitochondrial dysfunction, and osmotic dysregulation in fungi to elicit fungicidal and fungistatic activity (207). Conversely, IL-17A may drive allergic outcomes by enhancing eosinophil recruitment following repeated exposure to *A. fumigatus* conidia (208).

IFNγ, GM-CSF, and TNFα enhance macrophage functions by promoting phagocyte maturation, polarization of macrophages to M1 type, and fungus-killing ability. IFNγ is known to strongly activate phagocytes and their functions against fungi (209). Both IFNγ and TNF induce ROS production from macrophages, which is fungistatic to intracellular fungal pathogens *Histoplasma capsulatum* and *C. immitis* (210, 211). Furthermore, IFNγ promotes rapid acidification of phagolysosomes in macrophages (212), upregulation of MHC-II molecules, and antigen presentation by APCs to elicit T-cell immunity (213). GM-CSF enhances macrophage ROS production and limits intracellular yeast growth by sequestration of zinc (214). GM-CSF deficiency impairs the production of TNFα and IFNγ (215), which are important for the control of intracellular fungal infections. Similarly, TNFα signaling enhances the activation, phagocytosis, and ROS-producing ability of innate immune cells for antifungal functions. Interestingly, early TNFα expression during *C. neoformans* infection increased the fungal burden, reduced mature dendritic cells, and increased Th2 responses (216). TNFα was needed for the maturation and recruitment of DC and the production of IL-12 and IFNγ. However, TNFα prevented biofilm development by *C. albicans* (217), and TNF blockade can enhance opportunistic infections.

Cytotoxic functions of T cells are well documented for $CD8^+$ T cells. Antifungal $CD8^+$ T cells deploy several antimicrobial granules (mainly granulysin and granzyme K) (121) for direct cytotoxic activity against the fungal pathogen or fungus-infected cells (218, 219). Granzymes can mediate cell death by induction of active caspases, generation of ROS, and mitochondrial damage, while perforin may facilitate their release from the endosomes (220). Although this review focuses on T cells and their memory, antifungal NK cell development is not well documented. NK cells, like $CD8^+$ T cells, can produce cytotoxic molecules to kill fungi. The binding of NK cell receptors NKp46 and NCR1 to surface glycans of *Candida* led to degranulation and death of the yeast (221). Similar observations were made with human NK activating receptor NKp30 for the direct killing of *Cryptococcus* and *Candida* (222). Interestingly, "cytotoxic" $CD4^+$ T cells can also produce granulysin to mediate the killing of *C. neoformans* (223), and this function was dysregulated in HIV-infected patients.

## $CD4^+$ T-cell help for antifungal $CD8^+$ T cells

Most fungal infections are caused by opportunistic fungal pathogens under compromised $CD4^+$ T cells or their functions. Unlike viral or bacterial models, effector and memory $CD8^+$ T-cell homeostasis in fungal infections is poorly understood, and the studies have been done using animal models of fungal vaccine immunity. Attempts have been made to understand the role of antifungal $CD8^+$ T cells in the absence of $CD4^+$ T cells, a potential avenue to exploit residual immunity for preventive and therapeutic purposes for individuals with $CD4^+$ T-cell lymphopenia. Because optimal programming leads to the generation of long-lasting memory $CD8^+$ T cells (224, 225) and contributes to fungal vaccine immunity (8), we reason that a potent fungal vaccination can "license" dendritic cells for $CD8^+$ T-cell priming independent of $CD4^+$ T-cell help. Fungi are decorated, including some secretory, with several potential PAMPs that can bolster the dendritic cell activation and functions (226–228). Therefore, the $CD8^+$ T-cell memory imprinting and memory homeostasis following fungal vaccination can be independent of $CD4^+$ T-cell help (16, 169). However, evidence from viral and bacterial infections suggests that $CD4^+$ T-cell help is essential for eliciting $CD8^+$ T-cell responses (229). The mechanisms of $CD4^+$ T cells help $CD8^+$ T cells involve optimal activation of dendritic cells, enhancement of their phagocytosis, potentiation of antigen processing and presentation, upregulation of costimulatory ligands, and generation of an apt inflammatory *micro milieu* by dendritic cells for naïve $CD8^+$ T-cell priming and programming (230, 231). The direct mechanisms of $CD4^+$ T cells help involve providing IL-2 for the proliferation of differentiating $CD8^+$ T cells and lending co-stimulation through CD40L-CD40 (7). Further, $CD4^+$ T cells may help recruit memory $CD8^+$ T cells into mucosal surfaces (232). Well-primed $CD8^+$ T cells can produce IL-2 (169) and get help in an autocrine manner (233). We also found chemokine receptor-mediated recruitment of effector $CD8^+$ T cells into the lungs, which was independent of $CD4^+$ T cells following pulmonary challenge in a mouse model of vaccine immunity to pulmonary blastomycosis (90). Recent evidence suggests that the requirement of help from $CD4^+$ T cells to $CD8^+$ T cells largely depends on their distinct interactions with the dendritic cells during their activation (230, 234). Thus, well-programmed $CD8^+$ T cells, endowed with intrinsic memory capacity, can independently bestow their recall responses and immunity (235, 236). Further studies are needed to understand the fungal antigens and the role of dendritic cells in $CD8^+$ T-cell priming.

## Memory T cells: An overview

The development of immunological memory is the hallmark of vaccination. Following infection or vaccination, the first responders, innate immune cells, exert broadly specific immunity to limit pathogen growth and initiate adaptive T-cell immunity. T-cell recognition is highly antigen-specific and binds to processed antigens/epitopes loaded onto MHC molecules, resulting in their activation, differentiation, and proliferation during the first phase of T-cell response, which is the expansion phase (237). In the ensuing contraction phase, mostly coinciding with the elimination of pathogen or antigen, ~90%–95% of effector T cells [short-lived effector cells (SLECs)] undergo attrition by apoptosis, and the remaining 5%–10% of cells [memory precursor effector cells (MPECs)] differentiate to become long-lived, quickly and robustly responding, memory cells (238) in the memory phase (Figure 1). The central paradigm of vaccination is to generate qualitatively superior threshold numbers of memory T cells (237, 239, 240).

Memory T cells are unique and often behave like stem cells in their homeostasis and longevity. Many models of memory T-cell generation are proposed, and one of them suggests that memory programming or imprinting can happen as early as the first antigen encounter (241, 242). Others suggested dynamic and progressive imprinting of memory from a subset of effector cells. In the absence of cognate antigen, memory T cells are quiescent and slow dividing and share many features with naïve T cells (243, 244). However, they are uniquely programmed for stem cell potential and balanced cell apoptosis and proliferation for their steady homeostasis (240, 245), chiefly controlled by cytokines IL-7 and IL-15 (246). Naïve, effector, and memory T cells are differentiated based on their expression of surface and intracellular markers (241, 247–249), which endorse their homing and functional attributes. Memory T cells are a heterogeneous pool of cells derived from multiple clones and fates of polarization and differentiation based on the "one cell

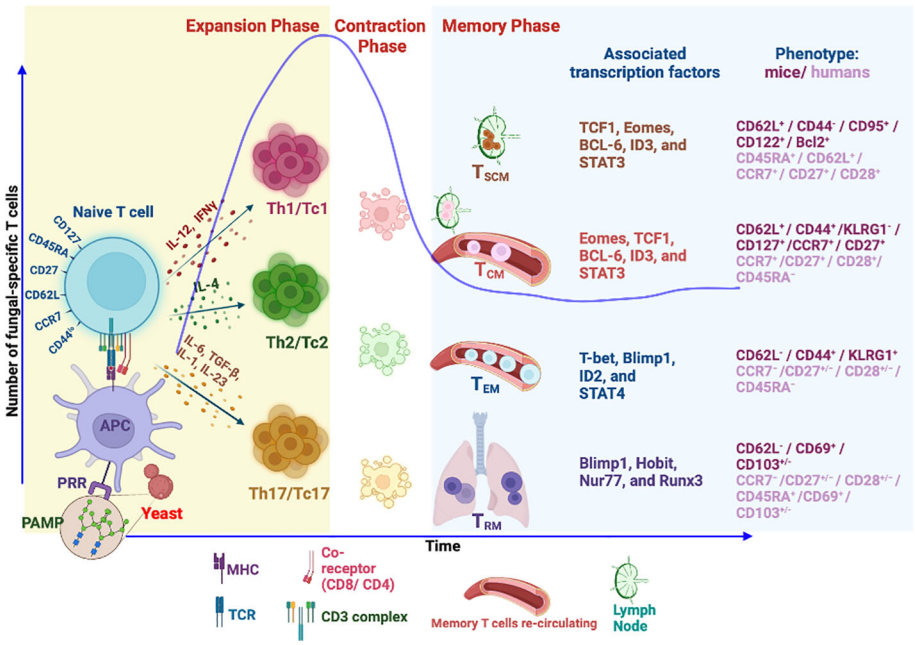


FIGURE 1
Differentiation and generation of memory T-cell subsets. Following recognition of fungal PAMPs by PRRs, activated antigen-presenting cells (APCs) process the antigen from phagocytosed fungus to load onto MHC molecule. MHC–peptide complex is recognized by cognate TCR of naïve T cells leading to TCR signaling, activation, and differentiation of T cells into different subsets directed by different cytokine milieus. The differentiated T cells accompanied by proliferation during expansion phase secrete inflammatory cytokines to aid in fungal killing. Fungal clearance usually coincides with initiation of T-cell contraction phase where 90% of effector cells die by apoptosis. The remaining cells differentiate to become long-lived memory cells. Memory T cells express unique phenotypic attributes and transcription factors, some of which dictate homing to lymphoid organs (CCR7/CD62L). Tissue-resident memory T cells ($T_{RM}$) continue to reside in tissue of responses. The effector memory T cells ($T_{EM}$) continue to invigilate the pathogen by recirculation between peripheral tissues and blood. Self-renewing central memory ($T_{CM}$) and central memory stem T cells ($T_{SCM}$) are preferentially home to secondary lymphoid organs and serve as "seeders" of secondary effector and memory T cells when needed. PAMPs, pathogen-associated molecular patterns; PRR, pattern recognition receptors; Th, helper T cell; Tc, cytotoxic T cell ($CD8^+$ T cell); $T_{SCM}$, stem memory T cells; $T_{CM}$, central memory T cell; $T_{EM}$, effector memory T cell.

multiple fate theory" (250, 251). Hence, these features are imprinted in memory T-cell heterogeneity in homeostatic turnover, effector function, location, and trafficking properties (111, 248, 252).

Classically, memory T cells were divided into two groups, $T_{EM}$ and $T_{CM}$, based on their lymph node homing properties with distinct proliferative renewal and functional properties (240, 241). With the advancement of our understanding and discovery of new markers, memory cells are classified into many groups in both humans and mice. Based on the markers, memory cells are broadly classified as central memory T ($T_{CM}$), effector memory T ($T_{EM}$), tissue-resident memory T ($T_{RM}$), and stem cell memory T ($T_{SCM}$) cells (241, 253–255). Effector memory T cells ($T_{EM}$), $CD45RA^-CD127^+CD122^+CD27^{-/+}CD62L^-/CCR7^-$, can migrate into peripheral tissues and exhibit immediate higher effector function with limited proliferation potential during the reinfection. $T_{CM}$ cells, $CD45RA^-CD127^+CD122^+CD27^+CD62L^+/CCR7^+$, are housed in secondary lymphoid organs with high proliferative potential but weaker effector properties as compared to $T_{EM}$ cells (255, 256). The dogma is that $T_{CM}$ cells are reservoirs or seeders of $T_{EM}$ cells in need. The property of $CD62L^{lo}/CCR7^{lo}$ defines the $T_{EM}$ cell exclusion from lymph nodes and migration to peripheral tissues to rapidly exude effector molecules upon antigen encounter. In contrast, $T_{CM}$ cells are $CD62L^{hi}/CCR7^{hi}$, allowing them to be preferentially home to lymph nodes (257). Both types of memory cells endow memory homeostasis properties where $T_{CM}$ mediates secondary immune responses for long-term protection and $T_{EM}$ offers instant protection (258). Nevertheless, as alluded earlier, the homeostatic proliferative potential of $T_{EM}$ and $T_{CM}$ cells varies (259).

A newly emerging T-cell memory subset, tissue-resident memory ($T_{RM}$), is restricted to a particular tissue and is identified based on the expression of $CD103^{+/-}$, CD49a, and CD69 (260). The main feature of $T_{RM}$ is their restriction to the tissue (261), possibly due to the expression of CD69 that suppresses the S1P receptor function for lymph node homing (262). Further, TGFβ signaling in these T cells augments the CD103 expression that facilitates latching onto epithelial cells (263, 264). Given the strategic position, $T_{RM}$ cells offer immediate local tissue immunity against invading pathogens (265).

The memory stem T cell ($T_{SCM}$) subset, unique and often considered closest to naïve T cells, exhibits stem cell-like properties with higher self-renewal capacity. Unlike conventional memory T-cell subsets, the $T_{SCM}$ subset maintains a naïve cell phenotype with *multipotency* and serves as a reservoir of memory T cells for a lifetime (266, 267). However, the identity of such unique memory T cells that are fungal-specific is lacking despite the description of antifungal memory cells in humans (111). Further studies are required to reveal the existence of antifungal $T_{SCM}$ in mice and humans.

With our understanding of memory T-cell differentiation and function, the memory cells can be classified in many ways, may depend on the infection or model system, and may be largely due to graded responses during the early programming of effector cells (254, 268–270). Unlike an acute viral infection, in chronic viral infection, the central memory phenotypic T cells poorly develop (271), and high antigen levels induce an exhausted phenotype (272). It should be noted that antifungal memory T-cell homeostasis is poorly defined and not well understood.

## Factors influencing generation of antifungal memory T cells

Our understanding of memory T-cell generation suggests that their attributes are bestowed by early programming during the expansion phase. However, the inflammatory milieu and the antigen persistence can affect their fate. The graded imprinting and epigenetic changes during the effector phase determine the memory T cell fate and the type. Naïve T cells must recognize cognate antigens portrayed on MHC molecules (Signal 1) of dendritic cells. Studies have shown that degree of antigen recognition by naïve or effector cells and antigen persistence (chronic and persistent infections) has a greater impact (273–275). However, this feature can be valuable during vaccine formulations where the antigen is delivered to the site of T-cell activation gradually to enhance the magnitude of their differentiation and expansion. Not surprisingly, booster doses are often given to augment adaptive immune responses, especially with subunit or inactivated vaccines. The costimulatory signal/s (Signal 2) is essential to break the TCR signaling threshold or tolerance to activate the T cells. The role of the classical costimulatory molecule, CD28, in recognizing B7 ligands on antigen-presenting cells is well defined, including during fungal vaccine immunity (276). However, other costimulatory molecules may influence memory T cells' qualitative and quantitative traits (277), including fungal immunity (278–282). Interestingly, CD28 may play a negative role in Th17 subset differentiation (283), but in the absence of CD28, the differentiation required proinflammatory cytokine signaling (284). Nevertheless, for subunit or less potent vaccine antigen formulations, engaging multiple costimulatory molecules may help potentiate the T-cell responses and eventual memory formation (167, 226). The inflammatory milieu generated by proinflammatory cytokines (Signal 3) is instrumental for effector T-cell differentiation and memory feature imprinting (285). Immunity to different fungal infections needs distinct cytokines produced by T-cell subsets (4), and the deviation from protective T-cell subsets may lead to enhanced pathology and disseminated infections (286–289). Immunity to different fungal pathogens predominantly requires either T cell-derived type I cytokines (IFNγ, GM-CSF, and TNFα) or type 17 (IL-17A/F) responses (80, 290) mainly at systemic and mucosal surfaces, respectively. Nevertheless, following fungal vaccination or infections, both types of subsets are induced at different magnitudes and found to contribute to immunity at variable degrees (8, 22, 168, 291–294). Future studies are necessary to understand the elements of memory T-cell differentiation, homeostasis, and their recall responses for immunity following infection or vaccination.

## Co-stimulatory and coinhibitory molecules influencing antifungal potential memory T cells

Co-stimulatory and coinhibitory receptor molecules present in T cells can fine-tune immune responses to fungal vaccines and infections. While co-stimulation leads to the potentiation of cell signaling, inhibitory signals deliver opposite effects during T-cell activation, thus inhibiting T-cell responses (295). Similarly, coinhibitory receptors present on memory T cells restrict recall responses but preserve memory cells by inhibiting terminal differentiation (296). Interestingly, the expression of coinhibitory molecules on resident memory $CD8^+$ T cells (Trm) is an intrinsic property present in their core gene signature (297, 298). Compared to circulatory memory T cells, resident memory T cells expressing high amounts of coinhibitory receptors (2B4, CTLA-4, LAG3, PD-1, and Tim-3) were able to undergo local proliferation following secondary rechallenge (299). Here, we highlight a few studies where the co-stimulatory or inhibitory molecules modulate antifungal T-cell responses.

PD-1 is a coinhibitory molecule expressed in T cells associated with dysfunction, and blocking PD-1 enhances the T-cell functions. Hence, anti-PD-1 mAb administration improved the fungal clearance in a model of persistent cryptococcosis (297). Interestingly, the effect was independent of effector cell numbers and myeloid cell activation, but reduced expression of IL-5 and IL-10 by lung leukocytes and enhanced sustained expression of OX40, a costimulatory molecule, on T cells. Similarly, the blockade of PD-1 and CTLA-4 improves survival during primary and secondary fungal sepsis (300) associated with improved T-cell functions. Signaling

lymphocyte activation molecule (SLAM) family members act as co-receptors for T cells fine-tuning immune homeostasis during infections (301). Mutation in SLAM-associated protein (SAP), required for SLAM signaling, results in X-linked lymphoproliferative disease (XLP). A recent study showed that SLAMF1, a member of the SLAM family, was dispensable for T-cell activation and expansion following fungal vaccination, but the fungal immunity was severely compromised (302). This study of vaccine immunity against lethal fungal pneumonia implied that SLAMF1 is mainly important for innate host control of lung fungal overgrowth as well as inflammation, recruitment, or expansion of fungal-specific effector $CD4^+$ T cells. Another molecule, CD43, also called sialophorin, is a membrane-bound receptor that exists in two forms with one highly glycosylated on T cells (303, 304). CD43 can be co-stimulatory and inhibitory, and depending on the context, it is known to promote T-cell contraction and reduced memory (305). In the context of cell-to-cell interactions, studies showed that CD43 deficiency led to enhanced homotypic binding of T cells through ligands such as ICAM-1 and fibronectin while augmenting the T-cell proliferation (306, 307). In other studies, pre-activation of CD43 with a mAb reduced the TCR signaling threshold, enhanced the degradation of Cbl, prolonged the TCR signaling, and augmented the T-cell response (308). Our recent study showed the indispensable role of CD43 for Tc17 responses and vaccine immunity to pulmonary fungal infection (309).

T cells typically express one or more co-stimulatory receptors. Thus, understanding the role of their signaling helps design vaccines to bolster qualitatively superior antifungal memory T cells and potentiate their functions for immunotherapeutics. Further, formulations of vaccines for fungal infections should account for the type of T-cell responses desired. Nevertheless, additional studies are warranted to delineate the role of co-stimulatory molecules during fungal infections. Adjuvants in vaccines act to enhance the T-cell stimulatory signals and proinflammatory cytokine production that polarize the T-cell responses (310). Different adjuvants have different characteristics in biasing T-cell response/s. For example, Alum potentiates Th2 responses, while Monophosphoryl lipid A (MPL)/CpG1018 bolsters Th1 responses. For controlling some fungal infections, especially those that are dependent on IL-17 responses, novel adjuvants are necessary.

## Conclusions and future directions

Immunological memory of fungal infections is poorly defined, but their existence and longevity are documented in preclinical and clinical studies. Most studies on T-cell memory came from preclinical model systems of fungal vaccine immunity. It is increasingly evident that T cells play a dominant role in fungal immunity, although other immune elements, including B cells and antibodies, cannot be overlooked. Although the innate cell inflammatory *micro milieu* is key for defining T-cell lineages and their functions for fungal immunity, the direct costimulatory signals or blockade of inhibitory signals delivered to T cells can regulate their effectors and memory cells. Non-canonical T cells such as natural T helper, MAIT, and NKT cell's role in some fungal infections have been documented, but their persistence as memory cells is not clear (32). Harnessing non-canonical T cells for vaccine immunity can be a new avenue for controlling fungal infections.

The mechanisms of the generation of antifungal memory T cells are not well understood and need in-depth investigations. The studies will be particularly relevant for the development and application of vaccine platforms. As with many different bacterial and viral defense mechanisms, the protective T-cell effectors vary depending on the pathogenic fungi, so the memory T-cell development mechanisms. Further, fungal co-infections and the disease outcomes need thorough studies, such as mucormycosis in COVID-19 patients. Novel findings on the use of fungal PAMPs as adjuvants for vaccines call for an understanding of adjuvanticity properties and their role in the programming of immunological memory. The new concept-based emergence of chimeric antigen receptor T (CAR-T) cells for immunotherapy to treat fungal infections is attractive, and its efficiency or utility needs attention. The plasticity of antifungal T cells has not been clearly understood, and its bases for immunopathology during recall responses and immunity need further evaluation. Further, the identification of phenotypic and functional markers of protective immunological memory T cells would be useful in designing and assessing the potency and efficacy of fungal vaccines.

## Author contributions

JS, SM, and SN conceived, wrote, and edited the manuscript. All authors contributed to the article and approved the submitted version.

## Funding

This study was funded by NIAID-NIH 5R01AI153522 (SN).

## Acknowledgment

Wee used biorender 2022 for genereation of a figure.

## Conflict of interest

The authors declare that the research was conducted in the absence of any commercial or financial relationships that could be construed as a potential conflict of interest.

## Publisher's note



## References

1. Brown GD, Denning DW, Gow N, Levitz SM, Netea MG, White TC. Hidden killers: Human fungal infections. *Sci Transl Med* (2012) 4:165rv113–165rv113. doi: 10.1126/scitranslmed.3004404

2. Bongomin F, Gago S, Oladele RO, Denning DW. Global and multi-national prevalence of fungal diseases-estimate precision. *J Fungi (Basel)* (2017) 3(4):57. doi: 10.3390/jof3040057

3. Kainz K, Bauer MA, Madeo F, Carmona-Gutierrez D. Fungal infections in humans: the silent crisis. *Microb Cell* (2020) 7:143–5. doi: 10.15698/mic2020.06.718

4. Verma A, Wuthrich M, Deepe G, Klein B. Adaptive immunity to fungi. *Cold Spring Harb Perspect Med* (2014) 5:a019612. doi: 10.1101/cshperspect.a019612.

5. Wuthrich M, Deepe GSJr., Klein B. Adaptive immunity to fungi. *Annu Rev Immunol* (2012) 30:115–48. doi: 10.1146/annurev-immunol-020711-074958

6. Lionakis MS, Netea MG, Holland SM. Mendelian genetics of human susceptibility to fungal infection. *Cold Spring Harb Perspect Med* (2014) 4(6): a019638. doi: 10.1101/cshperspect.a019638.

7. Castellino F, Germain RN. Cooperation between CD4+ and CD8+ T cells: When, where, and how. *Annu Rev Immunol* (2006) 24:519–40. doi: 10.1146/annurev.immunol.23.021704.115825

8. Nanjappa SG, Klein BS. Vaccine immunity against fungal infections. *Curr Opin Immunol* (2014) 28:27–33. doi: 10.1016/j.coi.2014.01.014

9. Conti HR, Gaffen SL. IL-17-Mediated immunity to the opportunistic fungal pathogen candida albicans. *J Immunol* (2015) 195:780–8. doi: 10.4049/jimmunol.1500909

10. Lionakis MS, Iliev ID, Hohl TM. Immunity against fungi. *JCI Insight* (2017) 2(11):e93156. doi: 10.1172/jci.insight.93156

11. Van De Veerdonk FL, Netea MG. T-Cell subsets and antifungal host defenses. *Curr Fungal Infect Rep* (2010) 4:238–43. doi: 10.1007/s12281-010-0034-6

12. Bacher P, Kniemeyer O, Schonbrunn A, Sawitzki B, Assenmacher M, Rietschel E, et al. Antigen-specific expansion of human regulatory T cells as a major tolerance mechanism against mucosal fungi. *Mucosal Immunol* (2014) 7:916–28. doi: 10.1038/mi.2013.107

13. Mcallister F, Steele C, Zheng M, Young E, Shellito JE, Marrero L, et al. T Cytotoxic-1 CD8+ T cells are effector cells against pneumocystis in mice. *J Immunol* (2004) 172:1132–8. doi: 10.4049/jimmunol.172.2.1132

14. Lin JS, Yang CW, Wang DW, Wu-Hsieh BA. Dendritic cells cross-present exogenous fungal antigens to stimulate a protective CD8 T cell response in infection by histoplasma capsulatum. *J Immunol* (2005) 174:6282–91. doi: 10.4049/jimmunol.174.10.6282

15. Lindell DM, Moore TA, Mcdonald RA, Toews GB, Huffnagle GB. Generation of antifungal effector CD8+ T cells in the absence of CD4+ T cells during cryptococcus neoformans infection. *J Immunol* (2005) 174:7920–8. doi: 10.4049/jimmunol.174.12.7920

16. Nanjappa SG, Mcdermott AJ, Fites JS, Galles K, Wuthrich M, Deepe GSJr., et al. Antifungal Tc17 cells are durable and stable, persisting as long-lasting vaccine memory without plasticity towards IFNgamma cells. *PloS Pathog* (2017) 13: e1006356. doi: 10.1371/journal.ppat.1006356

17. Mok AC, Mody CH, Li SS. Immune cell degranulation in fungal host defence. *J Fungi* (2021) 7:484. doi: 10.3390/jof7060484

18. Cutler JE, Deepe GSJr., Klein BS. Advances in combating fungal diseases: Vaccines on the threshold. *Nat Rev Microbiol* (2007) 5:13–28. doi: 10.1038/nrmicro1537

19. Jaeger M, Stappers MH, Joosten LA, Gyssens IC, Netea MG. Genetic variation in pattern recognition receptors: Functional consequences and susceptibility to infectious disease. *Future Microbiol* (2015) 10:989–1008. doi: 10.2217/fmb.15.37

20. Merkhofer RM, Klein BS. Advances in understanding human genetic variations that influence innate immunity to fungi. *Front Cell Infect Microbiol* (2020) 10:69. doi: 10.3389/fcimb.2020.00069

21. Naik B, Ahmed SMQ, Laha S, Das SP. Genetic susceptibility to fungal infections and links to human ancestry. *Front Genet* (2021) 12:709315. doi: 10.3389/fgene.2021.709315

22. Verma A, Wüthrich M, Deepe G, Klein B. Adaptive immunity to fungi *Cold Spring Harb Perspect Med* (2015) 5(3):a019612. doi: 10.1101/cshperspect.a019612

23. Banchereau J, Steinman RM. Dendritic cells and the control of immunity. *Nature* (1998) 392:245–52. doi: 10.1038/32588

24. Steinman RM. Dendritic cells and the control of immunity: Enhancing the efficiency of antigen presentation. *Mt Sinai J Med* (2001) 68:160–6.

25. Takeuchi O, Akira S. Pattern recognition receptors and inflammation. *Cell* (2010) 140:805–20. doi: 10.1016/j.cell.2010.01.022

26. Plato A, Hardison SE, Brown GD. Pattern recognition receptors in antifungal immunity. *Semin Immunopathol* (2015) 37:97–106. doi: 10.1007/s00281-014-0462-4

27. Patin EC, Thompson A, Orr SJ. Pattern recognition receptors in fungal immunity. *Semin Cell Dev Biol* (2019) 89:24–33. doi: 10.1016/j.semcdb.2018.03.003

28. Gong T, Liu L, Jiang W, Zhou R. DAMP-sensing receptors in sterile inflammation and inflammatory diseases. *Nat Rev Immunol* (2020) 20:95–112. doi: 10.1038/s41577-019-0215-7

29. Brown GD. Innate antifungal immunity: The key role of phagocytes. *Annu Rev Immunol* (2011) 29:1–21. doi: 10.1146/annurev-immunol-030409-101229

30. Lionakis MS, Levitz SM. Host control of fungal infections: Lessons from basic studies and human cohorts. *Annu Rev Immunol* (2018) 36:157–91. doi: 10.1146/annurev-immunol-042617-053318

31. Salazar F, Brown GD. Antifungal innate immunity: A perspective from the last 10 years. *J Innate Immun* (2018) 10:373–97. doi: 10.1159/000488539

32. Dunne MR, Wagener J, Loeffler J, Doherty DG, Rogers TR. Unconventional T cells - new players in antifungal immunity. *Clin Immunol* (2021) 227:108734. doi: 10.1016/j.clim.2021.108734

33. Steele C, Rapaka RR, Metz A, Pop SM, Williams DL, Gordon S, et al. The beta-glucan receptor dectin-1 recognizes specific morphologies of aspergillus fumigatus. *PloS Pathog* (2005) 1:0323–34. doi: 10.1371/journal.ppat.0010042

34. Werner JL, Metz AE, Horn D, Schoeb TR, Hewitt MM, Schwiebert LM, et al. Requisite role for the dectin-1 β-glucan receptor in pulmonary defense against aspergillus fumigatus. *J Immunol* (2009) 182:4938–46. doi: 10.4049/jimmunol.0804250

35. Drummond RA, Dambuza IM, Vautier S, Taylor JA, Reid DM, Bain CC, et al. CD4+ T-cell survival in the GI tract requires dectin-1 during fungal infection. *Mucosal Immunol* (2015) 9:492–502. doi: 10.1038/mi.2015.79

36. Marakalala MJ, Vautier S, Potrykus J, Walker LA, Shepardson KM, Hopke A, et al. Differential adaptation of candida albicans *in vivo* modulates immune recognition by dectin-1. *PloS Pathog* (2013) 9:e1003315. doi: 10.1371/journal.ppat.1003315

37. Rappleye CA, Eissenberg LG, Goldman WE. Histoplasma capsulatum alpha-(1,3)-glucan blocks innate immune recognition by the beta-glucan receptor. *Proc Natl Acad Sci U.S.A.* (2007) 104:1366–70. doi: 10.1073/pnas.0609848104

38. Davis SE, Hopke A, Minkin SCJr., Montedonico AE, Wheeler RT, Reynolds TB. Masking of beta(1-3)-glucan in the cell wall of candida albicans from detection by innate immune cells depends on phosphatidylserine. *Infect Immun* (2014) 82:4405–13. doi: 10.1128/IAI.01612-14

39. Hopke A, Brown AJP, Hall RA, Wheeler RT. Dynamic fungal cell wall architecture in stress adaptation and immune evasion. *Trends Microbiol* (2018) 26:284–95. doi: 10.1016/j.tim.2018.01.007

40. Yang M, Solis NV, Marshall M, Garleb R, Zhou T, Wang D, et al. Control of beta-glucan exposure by the endo-1,3-glucanase Eng1 in candida albicans modulates virulence. *PloS Pathog* (2022) 18:e1010192. doi: 10.1371/journal.ppat.1010192

41. Nakamura K, Kinjo T, Saijo S, Miyazato A, Adachi Y, Ohno N, et al. Dectin-1 is not required for the host defense to cryptococcus neoformans. *Microbiol Immunol* (2007) 51:1115–9. doi: 10.1111/j.1348-0421.2007.tb04007.x

42. Saijo S, Fujikado N, Furuta T, Chung S-H, Kotaki H, Seki K, et al. Dectin-1 is required for host defense against pneumocystis carinii but not against candida albicans. *Nat Immunol* (2007) 8:39–46. doi: 10.1038/ni1425

43. Vautier S, Drummond RA, Redelinghuys P, Murray GI, Maccallum DM, Brown GD. Dectin-1 is not required for controlling candida albicans colonization of the gastrointestinal tract. *Infect Immun* (2012) 80:4216–22. doi: 10.1128/IAI.00559-12

44. Wang H, Lebert V, Hung CY, Galles K, Saijo S, Lin X, et al. C-type lectin receptors differentially induce th17 cells and vaccine immunity to the endemic mycosis of north America. *J Immunol* (2014) 192:1107–19. doi: 10.4049/jimmunol.1302314

45. Thompson A, Da Fonseca DM, Walker L, Griffiths JS, Taylor PR, Gow N, et al. Dependence on mincle and dectin-2 varies with multiple candida species during systemic infection. *Front Microbiol* (2021) 12:633229. doi: 10.3389/fmicb.2021.633229

46. Sato K, Yang XL, Yudate T, Chung JS, Wu J, Luby-Phelps K, et al. Dectin-2 is a pattern recognition receptor for fungi that couples with the fc receptor gamma chain to induce innate immune responses. *J Biol Chem* (2006) 281:38854–66. doi: 10.1074/jbc.M606542200

47. Graham LM, Brown GD. The dectin-2 family of c-type lectins in immunity and homeostasis. *Cytokine* (2009) 48:148–55. doi: 10.1016/j.cyto.2009.07.010

48. Wang H, Lee TJ, Fites SJ, Merkhofer R, Zarnowski R, Brandhorst T, et al. Ligation of dectin-2 with a novel microbial ligand promotes adjuvant activity for vaccination. *PloS Pathog* (2017) 13:e1006568. doi: 10.1371/journal.ppat.1006568

49. Loures FV, Rohm M, Lee CK, Santos E, Wang JP, Specht CA, et al. Recognition of aspergillus fumigatus hyphae by human plasmacytoid dendritic cells is mediated by dectin-2 and results in formation of extracellular traps. *PloS Pathog* (2015) 11:e1004643. doi: 10.1371/journal.ppat.1004643

50. Wuthrich M, Wang H, Li M, Lerksuthirat T, Hardison SE, Brown GD, et al. Fonsecaea pedrosoi-induced Th17-cell differentiation in mice is fostered by dectin-2 and suppressed by mincle recognition. *Eur J Immunol* (2015) 45:2542–52. doi: 10.1002/eji.201545591

51. Saijo S, Ikeda S, Yamabe K, Kakuta S, Ishigame H, Akitsu A, et al. Dectin-2 recognition of alpha-mannans and induction of Th17 cell differentiation is essential for host defense against candida albicans. *Immunity* (2010) 32:681–91. doi: 10.1016/j.immuni.2010.05.001

52. Ifrim DC, Quintin J, Courjol F, Verschueren I, Van Krieken JH, Koentgen F, et al. The role of dectin-2 for host defense against disseminated candidiasis. *J Interferon Cytokine Res* (2016) 36:267–76. doi: 10.1089/jir.2015.0040

53. Saijo S, Iwakura Y. Dectin-1 and dectin-2 in innate immunity against fungi. *Int Immunol* (2011) 23:467–72. doi: 10.1093/intimm/dxr046

54. Bellocchio S, Montagnoli C, Bozza S, Gaziano R, Rossi G, Mambula SS, et al. The contribution of the toll-like/IL-1 receptor superfamily to innate and adaptive immunity to fungal pathogens *in vivo*. *J Immunol* (2004) 172:3059–69. doi: 10.4049/jimmunol.172.5.3059

55. Calich VLG, Pina A, Felonato M, Bernardino S, Costa TA, Loures FV. Toll-like receptors and fungal infections: the role of TLR2, TLR4 and MyD88 in paracoccidioidomycosis. *FEMS Immunol Med Microbiol* (2008) 53:1–7. doi: 10.1111/j.1574-695X.2008.00378.x

56. Wuthrich M, Gern B, Hung CY, Ersland K, Rocco N, Pick-Jacobs J, et al. Vaccine-induced protection against 3 systemic mycoses endemic to north America requires Th17 cells in mice. *J Clin Invest* (2011) 121:554–68. doi: 10.1172/JCI43984

57. Prieto D, Carpena N, Maneu V, Gil ML, Pla J, Gozalbo D. TLR2 modulates gut colonization and dissemination of candida albicans in a murine model. *Microbes Infect* (2016) 18:656–60. doi: 10.1016/j.micinf.2016.05.005

58. Miró MS, Rodríguez E, Vigezzi C, Icely PA, García LN, Painetti N, et al. Contribution of TLR2 pathway in the pathogenesis of vulvovaginal candidiasis. *Pathog Dis* (2017) 75(7). doi: 10.1093/femspd/ftx096

59. Netea MG, Sutmuller R, Hermann C, van der Graaf CA, van der Meer JW, Van Krieken JH, et al. Toll-like receptor 2 suppresses immunity against candida albicans through induction of IL-10 and regulatory T cells. *J Immunol* (2004) 172:3712–8. doi: 10.4049/jimmunol.172.6.3712

60. Villamon E, Gozalbo D, Roig P, O'connor JE, Fradelizi D, Gil ML. Toll-like receptor-2 is essential in murine defenses against candida albicans infections. *Microbes Infect* (2004) 6:1–7. doi: 10.1016/j.micinf.2003.09.020

61. Dubourdeau M, Athman R, Balloy V, Huerre M, Chignard M, Philpott DJ, et al. Aspergillus fumigatus induces innate immune responses in alveolar macrophages through the MAPK pathway independently of TLR2 and TLR4. *J Immunol* (2006) 177:3994–4001. doi: 10.4049/jimmunol.177.6.3994

62. Carvalho A, De Luca A, Bozza S, Cunha C, D'angelo C, Moretti S, et al. TLR3 essentially promotes protective class I–restricted memory CD8+ T-cell responses to aspergillus fumigatus in hematopoietic transplanted patients. *Blood* (2012) 119:967–77. doi: 10.1182/blood-2011-06-362582

63. Van De Veerdonk FL, Joosten LA, Netea MG. The interplay between inflammasome activation and antifungal host defense. *Immunol Rev* (2015) 265:172–80. doi: 10.1111/imr.12280

64. Souza COS, Ketelut-Carneiro N, Milanezi CM, Faccioli LH, Gardinassi LG, Silva JS. NLRC4 inhibits NLRP3 inflammasome and abrogates effective antifungal CD8+ T cell responses. *iScience* (2021) 24:102548. doi: 10.1016/j.isci.2021.102548

65. Bochud PY, Chien JW, Marr KA, Leisenring WM, Upton A, Janer M, et al. Toll-like receptor 4 polymorphisms and aspergillosis in stem-cell transplantation. *N Engl J Med* (2008) 359:1766–77. doi: 10.1056/NEJMoa0802629

66. Carvalho A, Cunha C, Carotti A, Aloisi T, Guarrera O, Di Ianni M, et al. Polymorphisms in toll-like receptor genes and susceptibility to infections in allogeneic stem cell transplantation. *Exp Hematol* (2009) 37:1022–9. doi: 10.1016/j.exphem.2009.06.004

67. Morre SA, Murillo LS, Spaargaren J, Fennema HS, Pena AS. Role of the toll-like receptor 4 Asp299Gly polymorphism in susceptibility to candida albicans infection. *J Infect Dis* (2002) 186:1377–1379; author reply 1379. doi: 10.1086/344328

68. Sainz J, Perez E, Hassan L, Moratalla A, Romero A, Collado MD, et al. Variable number of tandem repeats of TNF receptor type 2 promoter as genetic biomarker of susceptibility to develop invasive pulmonary aspergillosis. *Hum Immunol* (2007) 68:41–50. doi: 10.1016/j.humimm.2006.10.011

69. Plantinga TS, van der Velden WJ, Ferwerda B, Van Spriel AB, Adema G, Feuth T, et al. Early stop polymorphism in human DECTIN-1 is associated with increased candida colonization in hematopoietic stem cell transplant recipients. *Clin Infect Dis* (2009) 49:724–32. doi: 10.1086/604714

70. Cunha C, Di Ianni M, Bozza S, Giovannini G, Zagarella S, Zelante T, et al. Dectin-1 Y238X polymorphism associates with susceptibility to invasive aspergillosis in hematopoietic transplantation through impairment of both recipient- and donor-dependent mechanisms of antifungal immunity. *Blood* (2010) 116:5394–402. doi: 10.1182/blood-2010-04-279307

71. Del Pilar Jimenez AM, Viriyakosol S, Walls L, Datta SK, Kirkland T, Heinsbroek SE, et al. Susceptibility to coccidioides species in C57BL/6 mice is associated with expression of a truncated splice variant of dectin-1 (Clec7a). *Genes Immun* (2008) 9:338–48. doi: 10.1038/gene.2008.23

72. Janeway CAJr. Approaching the asymptote? Evolution and revolution in immunology. *Cold Spring Harb Symp Quant Biol* (1989) 54 Pt 1:1–13. doi: 10.1101/SQB.1989.054.01.003

73. Rahman AH, Taylor DK, Turka LA. The contribution of direct TLR signaling to T cell responses. *Immunol Res* (2009) 45:25–36. doi: 10.1007/s12026-009-8113-x

74. Komai-Koma M, Jones L, Ogg GS, Xu D, Liew FY. TLR2 is expressed on activated T cells as a costimulatory receptor. *Proc Natl Acad Sci* (2004) 101:3029–34. doi: 10.1073/pnas.0400171101

75. Imanishi T, Hara H, Suzuki S, Suzuki N, Akira S, Saito T. Cutting edge: TLR2 directly triggers Th1 effector functions. *J Immunol* (2007) 178:6715–9. doi: 10.4049/jimmunol.178.11.6715

76. Imanishi T, Unno M, Kobayashi W, Yoneda N, Akira S, Saito T. mTORC1 signaling controls TLR2-mediated T-cell activation by inducing TIRAP expression. *Cell Rep* (2020) 32:107911. doi: 10.1016/j.celrep.2020.107911

77. Wang H, Li M, Hung CY, Sinha M, Lee LM, Wiesner DL, et al. MyD88 shapes vaccine immunity by extrinsically regulating survival of CD4+ T cells during the contraction phase. *PloS Pathog* (2016) 12:e1005787. doi: 10.1371/journal.ppat.1005787

78. Nanjappa SG, Hernandez-Santos N, Galles K, Wuthrich M, Suresh M, Klein BS. Intrinsic MyD88-Akt1-mTOR signaling coordinates disparate Tc17 and Tc1 responses during vaccine immunity against fungal pneumonia. *PloS Pathog* (2015) 11:e1005161. doi: 10.1371/journal.ppat.1005161

79. Bhaskaran N, Faddoul F, Paes Da Silva A, Jayaraman S, Schneider E, Mamileti P, et al. Il-1β-Myd88-Mtor axis promotes immune-protective IL-17a+ Foxp3+ cells during mucosal infection and is dysregulated with aging. *Front Immunol* (2020) 11:2818. doi: 10.3389/fimmu.2020.595936

80. Ma H, Chan JFW, Tan YP, Kui L, Tsang CC, Pei SLC, et al. NLRP3 inflammasome contributes to host defense against talaromyces marneffei infection. *Front Immunol* (2021) 12:760095. doi: 10.3389/fimmu.2021.760095

81. Arbore G, West EE, Spolski R, Robertson A, Klos A, Rheinheimer C, et al. T Helper 1 immunity requires complement-driven NLRP3 inflammasome activity in CD4(+) T cells. *Science* (2016) 352:aad1210. doi: 10.1126/science.aad1210

82. Kumaresan PR, Manuri PR, Albert ND, Maiti S, Singh H, Mi T, et al. Bioengineering T cells to target carbohydrate to treat opportunistic fungal infection. *Proc Natl Acad Sci U.S.A.* (2014) 111:10660–5. doi: 10.1073/pnas.1312789111

83. Roilides E, Uhlig K, Venzon D, Pizzo PA, Walsh TJ. Enhancement of oxidative response and damage caused by human neutrophils to aspergillus fumigatus hyphae by granulocyte colony-stimulating factor and gamma interferon. *Infect Immun* (1993) 61:1185–93. doi: 10.1128/iai.61.4.1185-1193.1993

84. Borghi M, Renga G, Puccetti M, Oikonomou V, Palmieri M, Galosi C, et al. Antifungal Th immunity: Growing up in family. *Front Immunol* (2014) 5:506. doi: 10.3389/fimmu.2014.00506

85. Mcdermott AJ, Klein BS. Helper T-cell responses and pulmonary fungal infections. *Immunology* (2018) 155:155–63. doi: 10.1111/imm.12953

86. Gray JI, Westerhof LM, Macleod MKL. The roles of resident, central and effector memory CD4 T-cells in protective immunity following infection or vaccination. *Immunology* (2018) 154(4):574–581. doi: 10.1111/imm.12929

87. Cenci E, Mencacci A, Bacci A, Bistoni F, Kurup VP, Romani L. T Cell vaccination in mice with invasive pulmonary aspergillosis. *J Immunol* (2000) 165:381–8. doi: 10.4049/jimmunol.165.1.381

88. Jolink H, De Boer R, Hombrink P, Jonkers RE, Van Dissel JT, Falkenburg JH, et al. Pulmonary immune responses against aspergillus fumigatus are characterized by high frequencies of IL-17 producing T-cells. *J Infect* (2017) 74:81–8. doi: 10.1016/j.jinf.2016.10.010

89. Jolink H, Hagedoorn RS, Lagendijk EL, Drijfhout JW, Van Dissel JT, Falkenburg JH, et al. Induction of a. Fumigatus-specific CD4-positive T cells in patients recovering from invasive aspergillosis. *Haematologica* (2014) 99:1255–63. doi: 10.3324/haematol.2013.098830

90. Nanjappa SG, Heninger E, Wuthrich M, Gasper DJ, Klein BS. Tc17 cells mediate vaccine immunity against lethal fungal pneumonia in immune deficient hosts lacking CD4+ T cells. *PloS Pathog* (2012) 8:e1002771. doi: 10.1371/journal.ppat.1002771

91. Hernandez-Santos N, Huppler AR, Peterson AC, Khader SA, Mckenna KC, Gaffen SL. Th17 cells confer long-term adaptive immunity to oral mucosal candida albicans infections. *Mucosal Immunol* (2013) 6:900–10. doi: 10.1038/mi.2012.128

92. Acosta-Rodriguez EV, Rivino L, Geginat J, Jarrossay D, Gattorno M, Lanzavecchia A, et al. Surface phenotype and antigenic specificity of human interleukin 17-producing T helper memory cells. *Nat Immunol* (2007) 8:639–46. doi: 10.1038/ni1467

93. Iannitti RG, Carvalho A, Romani L. From memory to antifungal vaccine design. *Trends Immunol* (2012) 33:467–74. doi: 10.1016/j.it.2012.04.008

94. Kirchner FR, Leibundgut-Landmann S. Tissue-resident memory Th17 cells maintain stable fungal commensalism in the oral mucosa. *Mucosal Immunol* (2021) 14:455–67. doi: 10.1038/s41385-020-0327-1

95. Ueno K, Urai M, Sadamoto S, Shinozaki M, Takatsuka S, Abe M, et al. A dendritic cell-based systemic vaccine induces long-lived lung-resident memory Th17 cells and ameliorates pulmonary mycosis. *Mucosal Immunol* (2019) 12:265–76. doi: 10.1038/s41385-018-0094-4

96. Ueno K, Kinjo Y, Okubo Y, Aki K, Urai M, Kaneko Y, et al. Dendritic cell-based immunization ameliorates pulmonary infection with highly virulent cryptococcus gattii. *Infect Immun* (2015) 83:1577–86. doi: 10.1128/IAI.02827-14

97. Fierer J, Waters C, Walls L. Both CD4+ and CD8+ T cells can mediate vaccine-induced protection against coccidioides immitis infection in mice. *J Infect Dis* (2006) 193:1323–31. doi: 10.1086/502972

98. Hung CY, Castro-Lopez N, Cole GT. Vaccinated C57BL/6 mice develop protective and memory T cell responses to coccidioides posadasii infection in the absence of interleukin-10. *Infect Immun* (2014) 82:903–13. doi: 10.1128/IAI.01148-13

99. Diep AL, Hoyer KK. Host response to coccidioides infection: Fungal immunity. *Front Cell Infect Microbiol* (2020) 10:581101. doi: 10.3389/fcimb.2020.581101

100. Deepe JGS, Buesing WR, Ostroff GR, Abraham A, Specht CA, Huang H, et al. Vaccination with an alkaline extract of histoplasma capsulatum packaged in glucan particles confers protective immunity in mice. *Vaccine* (2018) 36:3359–67. doi: 10.1016/j.vaccine.2018.04.047

101. Chiarella AP, Arruda C, Pina A, Costa TA, Ferreira RC, Calich VL. The relative importance of CD4+ and CD8+T cells in immunity to pulmonary paracoccidioidomycosis. *Microbes Infect* (2007) 9:1078–88. doi: 10.1016/j.micinf.2007.04.016

102. De La Rua NM, Samuelson DR, Charles TP, Welsh DA, Shellito JE. CD4+ T-cell-independent secondary immune responses to pneumocystis pneumonia. *Front Immunol* (2016) 7:178.

103. Galdino N, Loures FV, De Araújo EF, Da Costa TA, Preite NW, Calich VLG. Depletion of regulatory T cells in ongoing paracoccidioidomycosis rescues protective Th1/Th17 immunity and prevents fatal disease outcome. *Sci Rep* (2018) 8(1):16544. doi: 10.1038/s41598-018-35037-8

104. Pruksaphon K, Nosanchuk JD, Ratanabanangkoon K, Youngchim S. Talaromyces marneffei infection: Virulence, intracellular lifestyle and host defense mechanisms. *J Fungi* (2022) 8:200. doi: 10.3390/jof8020200

105. Park CO, Fu X, Jiang X, Pan Y, Teague JE, Collins N, et al. Staged development of long-lived T-cell receptor αβ TH17 resident memory T-cell population to candida albicans after skin infection. *J Allergy Clin Immunol* (2018) 142:647–62. doi: 10.1016/j.jaci.2017.09.042

106. Pietrella D, Rachini A, Pines M, Pandey N, Mosci P, Bistoni F, et al. Th17 cells and IL-17 in protective immunity to vaginal candidiasis. *PloS One* (2011) 6: e22770. doi: 10.1371/journal.pone.0022770

107. Alqarihi A, Singh S, Edwards JEJr., Ibrahim AS, Uppuluri P. NDV-3A vaccination prevents c. albicans colonization of jugular vein catheters in mice. *Sci Rep* (2019) 9:6194. doi: 10.1038/s41598-019-42517-y

108. Ibrahim AS, Luo G, Gebremariam T, Lee H, Schmidt CS, Hennessey JPJr., et al. NDV-3 protects mice from vulvovaginal candidiasis through T- and b-cell immune response. *Vaccine* (2013) 31:5549–56. doi: 10.1016/j.vaccine.2013.09.016

109. Edwards JEJr., Schwartz MM, Schmidt CS, Sobel JD, Nyirjesy P, Schodel F, et al. A fungal immunotherapeutic vaccine (NDV-3A) for treatment of recurrent vulvovaginal candidiasis-a phase 2 randomized, double-blind, placebo-controlled trial. *Clin Infect Dis* (2018) 66:1928–36. doi: 10.1093/cid/ciy185

110. Zielinski CE, Mele F, Aschenbrenner D, Jarrossay D, Ronchi F, Gattorno M, et al. Pathogen-induced human TH17 cells produce IFN-gamma or IL-10 and are regulated by IL-1beta. *Nature* (2012) 484:514–8. doi: 10.1038/nature10957

111. Becattini S, Latorre D, Mele F, Foglierini M, De Gregorio C, Cassotta A, et al. T Cell immunity. functional heterogeneity of human memory CD4(+) T cell clones primed by pathogens or vaccines. *Science* (2015) 347:400–6. doi: 10.1126/science.1260668

112. Kirchner FR, Leibundgut-Landmann S. Tissue-resident memory Th17 cells maintain stable fungal commensalism in the oral mucosa. *Mucosal Immunol* (2020) 14:455–67. doi: 10.1038/s41385-020-0327-1

113. Schlapbach C, Gehad A, Yang C, Watanabe R, Guenova E, Teague JE, et al. Human TH9 cells are skin-tropic and have autocrine and paracrine proinflammatory capacity. *Sci Transl Med* (2014) 6:219ra218. doi: 10.1126/scitranslmed.3007828

114. Renga G, Moretti S, Oikonomou V, Borghi M, Zelante T, Paolicelli G, et al. IL-9 and mast cells are key players of candida albicans commensalism and pathogenesis in the gut. *Cell Rep* (2018) 23:1767–78. doi: 10.1016/j.celrep.2018.04.034

115. Liu Y, Yang B, Zhou M, Li L, Zhou H, Zhang J, et al. Memory IL-22-producing CD4+ T cells specific for candida albicans are present in humans. *Eur J Immunol* (2009) 39:1472–9. doi: 10.1002/eji.200838811

116. De Luca A, Carvalho A, Cunha C, Iannitti RG, Pitzurra L, Giovannini G, et al. IL-22 and IDO1 affect immunity and tolerance to murine and human vaginal candidiasis. *PloS Pathog* (2013) 9:e1003486. doi: 10.1371/journal.ppat.1003486

117. Zelante T, Iannitti R, De Luca A, Romani L. IL-22 in antifungal immunity. *Eur J Immunol* (2011) 41:270–5. doi: 10.1002/eji.201041246

118. Moser D, Biere K, Han B, Hoerl M, Schelling G, Chouker A, et al. COVID-19 impairs immune response to candida albicans. *Front Immunol* (2021) 12:640644. doi: 10.3389/fimmu.2021.640644

119. Ghaleb M, Hamad M, Abu-Elteen KH. Vaginal T lymphocyte population kinetics during experimental vaginal candidosis: evidence for a possible role of CD8 + T cells in protection against vaginal candidosis. *Clin Exp Immunol* (2003) 131:26–33. doi: 10.1046/j.1365-2249.2003.02032.x

120. Jones-Carson J, Vazquez-Torres FA, Balish E. B cell-independent selection of memory T cells after mucosal immunization with candida albicans. *J Immunol* (1997) 158:4328–35.

121. Breinig T, Scheller N, Glombitza B, Breinig F, Meyerhans A. Human yeast-specific CD8 T lymphocytes show a nonclassical effector molecule profile. *Med Microbiol Immunol* (2012) 201:127–36. doi: 10.1007/s00430-011-0213-2

122. Heintel T, Breinig F, Schmitt MJ, Meyerhans A. Extensive MHC class I-restricted CD8 T lymphocyte responses against various yeast genera in humans. *FEMS Immunol Med Microbiol* (2003) 39:279–86. doi: 10.1016/S0928-8244(03)00294-3

123. Myers TA, Leigh JE, Arribas AR, Hager S, Clark R, Lilly E, et al. Immunohistochemical evaluation of T cells in oral lesions from human immunodeficiency virus-positive persons with oropharyngeal candidiasis. *Infect Immun* (2003) 71:956–63. doi: 10.1128/IAI.71.2.956-963.2003

124. Ickrath P, Sprugel L, Beyersdorf N, Scherzad A, Hagen R, Hackenberg S. Detection of candida albicans-specific CD4+ and CD8+ T cells in the blood and nasal mucosa of patients with chronic rhinosinusitis. *J Fungi (Basel)* (2021) 7(6):403. doi: 10.3390/jof7060403

125. Roilides E, Dimitriadou A, Kadiltsoglou I, Sein T, Karpouzas J, Pizzo PA, et al. IL-10 exerts suppressive and enhancing effects on antifungal activity of mononuclear phagocytes against aspergillus fumigatus. *J Immunol* (1997) 158:322–9.

126. Cenci E, Mencacci A, Fe D'ostiani C, Del Sero G, Mosci P, Montagnoli C, et al. Cytokine- and T helper-dependent lung mucosal immunity in mice with invasive pulmonary aspergillosis. *J Infect Dis* (1998) 178:1750–60. doi: 10.1086/314493

127. Cenci E, Mencacci A, Del Sero G, Bacci A, Montagnoli C, D'ostiani CF, et al. Interleukin-4 causes susceptibility to invasive pulmonary aspergillosis through suppression of protective type I responses. *J Infect Dis* (1999) 180:1957–68. doi: 10.1086/315142

128. Bozza S, Gaziano R, Lipford GB, Montagnoli C, Bacci A, Di Francesco P, et al. Vaccination of mice against invasive aspergillosis with recombinant

aspergillus proteins and CpG oligodeoxynucleotides as adjuvants. *Microbes Infect* (2002) 4:1281–90. doi: 10.1016/S1286-4579(02)00007-2

129. Ito JI, Lyons JM. Vaccination of corticosteroid immunosuppressed mice against invasive pulmonary aspergillosis. *J Infect Dis* (2002) 186:869–71. doi: 10.1086/342509

130. Stuehler C, Khanna N, Bozza S, Zelante T, Moretti S, Kruhm M, et al. Cross-protective TH1 immunity against aspergillus fumigatus and candida albicans. *Blood* (2011) 117:5881–91. doi: 10.1182/blood-2010-12-325084

131. Levitz SM. Aspergillus vaccines: Hardly worth studying or worthy of hard study? *Med Mycol* (2017) 55:103–8. doi: 10.1093/mmy/myw081

132. Rai G, Das S, Ansari MA, Singh PK, Dar SA, Haque S, et al. TLR-2 expression and dysregulated human Treg/Th17 phenotype in aspergillus flavus infected patients of chronic rhinosinusitis with nasal polyposis. *Microb Cell Fact* (2020) 19:215. doi: 10.1186/s12934-020-01481-3

133. Clemons KV, Grunig G, Sobel RA, Mirels LF, Rennick DM, Stevens DA. Role of IL-10 in invasive aspergillosis: increased resistance of IL-10 gene knockout mice to lethal systemic aspergillosis. *Clin Exp Immunol* (2000) 122:186–91. doi: 10.1046/j.1365-2249.2000.01382.x

134. Sainz J, Hassan L, Perez E, Romero A, Moratalla A, Lopez-Fernandez E, et al. Interleukin-10 promoter polymorphism as risk factor to develop invasive pulmonary aspergillosis. *Immunol Lett* (2007) 109:76–82. doi: 10.1016/j.imlet.2007.01.005

135. Cunha C, Goncalves SM, Duarte-Oliveira C, Leite L, Lagrou K, Marques A, et al. IL-10 overexpression predisposes to invasive aspergillosis by suppressing antifungal immunity. *J Allergy Clin Immunol* (2017) 140:867–870 e869. doi: 10.1016/j.jaci.2017.02.034

136. Grunig G, Corry DB, Leach MW, Seymour BW, Kurup VP, Rennick DM. Interleukin-10 is a natural suppressor of cytokine production and inflammation in a murine model of allergic bronchopulmonary aspergillosis. *J Exp Med* (1997) 185:1089–99. doi: 10.1084/jem.185.6.1089

137. Bacher P, Schink C, Teutschbein J, Kniemeyer O, Assenmacher M, Brakhage AA, et al. Antigen-reactive T cell enrichment for direct, high-resolution analysis of the human naive and memory Th cell repertoire. *J Immunol* (2013) 190:3967–76. doi: 10.4049/jimmunol.1202221

138. Stuehler C, Nowakowska J, Bernardini C, Topp MS, Battegay M, Passweg J, et al. Multispecific aspergillus T cells selected by CD137 or CD154 induce protective immune responses against the most relevant mold infections. *J Infect Dis* (2015) 211:1251–61. doi: 10.1093/infdis/jiu607

139. Gottlieb DJ, Clancy LE, Withers B, Mcguire HM, Luciani F, Singh M, et al. Prophylactic antigen-specific T-cells targeting seven viral and fungal pathogens after allogeneic haemopoietic stem cell transplant. *Clin Transl Immunol* (2021) 10:e1249. doi: 10.1002/cti2.1249

140. Inam SS,G, Avdic S, Street J, Atkins E, Clany LE, Gottlieb DJ. Third-party partially HLA matched fungus-specific T-cells (FSTs) used to treat invasive fungal infection (IFI) with scedosporium aurantiacum after allogeneic hemopoietic stem cell transplant (aHSCT). *Blood* (2021) 138(1):2825. doi: 10.1182/blood-2021-152384

141. Castellano-Gonzalez G, Mcguire HM, Luciani F, Clancy LE, Li Z, Avdic S, et al. Rapidly expanded partially HLA DRB1-matched fungus-specific T cells mediate *in vitro* and *in vivo* antifungal activity. *Blood Adv* (2020) 4:3443–56. doi: 10.1182/bloodadvances.2020001565

142. Hirahara K, Kokubo K, Aoki A, Kiuchi M, Nakayama T. The role of CD4 (+) resident memory T cells in local immunity in the mucosal tissue - protection versus pathology. *Front Immunol* (2021) 12:616309. doi: 10.3389/fimmu.2021.616309

143. Chaudhary N, Staab JF, Marr KA. Healthy human T-cell responses to aspergillus fumigatus antigens. *PloS One* (2010) 5:e9036. doi: 10.1371/journal.pone.0009036

144. Ma L, Cisse OH, Kovacs JA. A molecular window into the biology and epidemiology of pneumocystis spp. *Clin Microbiol Rev* (2018) 31(3):e00009-18. doi: 10.1128/CMR.00009-18

145. Elsegeiny W, Zheng M, Eddens T, Gallo RL, Dai G, Trevejo-Nunez G, et al. Murine models of pneumocystis infection recapitulate human primary immune disorders. *JCI Insight* (2018) 3(12):e91894. doi: 10.1172/jci.insight.91894

146. Elsegeiny W, Eddens T, Chen K, Kolls JK. Anti-CD20 antibody therapy and susceptibility to pneumocystis pneumonia. *Infect Immun* (2015) 83:2043–52. doi: 10.1128/IAI.03099-14

147. Hofmann K, Clauder AK, Manz RA. Targeting b cells and plasma cells in autoimmune diseases. *Front Immunol* (2018) 9. doi: 10.3389/fimmu.2018.00835

148. Lund FE, Hollifield M, Schuer K, Lines JL, Randall TD, Garvy BA. B cells are required for generation of protective effector and memory CD4 cells in response to pneumocystis lung infection. *J Immunol* (2006) 176:6147–54. doi: 10.4049/jimmunol.176.10.6147

149. Opata MM, Hollifield ML, Lund FE, Randall TD, Dunn R, Garvy BA, et al. B lymphocytes are required during the early priming of CD4(+) T cells for clearance of pneumocystis infection in mice. *J Immunol* (2015) 195:611–20. doi: 10.4049/jimmunol.1500112

150. Kling HM, Norris KA. Vaccine-induced immunogenicity and protection against pneumocystis pneumonia in a nonhuman primate model of HIV and pneumocystis coinfection. *J Infect Dis* (2016) 213:1586–95. doi: 10.1093/infdis/jiw032

151. Kelly MN, Zheng M, Ruan S, Kolls J, D'souza A, Shellito JE. Memory CD4+ T cells are required for optimal NK cell effector functions against the opportunistic fungal pathogen pneumocystis murina. *J Immunol* (2013) 190:285–95. doi: 10.4049/jimmunol.1200861

152. Tesini BL, Wright TW, Malone JE, Haidaris CG, Harber M, Sant AJ, et al. Immunization with pneumocystis cross-reactive antigen 1 (Pca1) protects mice against pneumocystis pneumonia and generates antibody to pneumocystis jirovecii. *Infect Immun* (2017) 85(4):e00850-16. doi: 10.1128/IAI.00850-16

153. Huffnagle GB, Yates JL, Lipscomb MF. Immunity to a pulmonary cryptococcus neoformans infection requires both CD4+ and CD8+ T cells. *J Exp Med* (1991) 173:793–800. doi: 10.1084/jem.173.4.793

154. Wormley FLJr., Perfect JR, Steele C, Cox GM. Protection against cryptococcosis by using a murine gamma interferon-producing cryptococcus neoformans strain. *Infect Immun* (2007) 75:1453–62. doi: 10.1128/IAI.00274-06

155. Wozniak KL, Young ML, Wormley FLJr. Protective immunity against experimental pulmonary cryptococcosis in T cell-depleted mice. *Clin Vaccine Immunol* (2011) 18:717–23. doi: 10.1128/CVI.00036-11

156. Specht CA, Homan EJ, Lee CK, Mou Z, Gomez CL, Hester MM, et al. Protection of mice against experimental cryptococcosis by synthesized peptides delivered in glucan particles. *mBio* (2022) 13(1):e0336721. doi: 10.1128/mbio.03367-21

157. Hester MM, Lee CK, Abraham A, Khoshkenar P, Ostroff GR, Levitz SM, et al. Protection of mice against experimental cryptococcosis using glucan particle-based vaccines containing novel recombinant antigens. *Vaccine* (2020) 38:620–6. doi: 10.1016/j.vaccine.2019.10.051

158. Chaturvedi AK, Hameed RS, Wozniak KL, Hole CR, Leopold Wager CM, Weintraub ST, et al. Vaccine-mediated immune responses to experimental pulmonary cryptococcus gattii infection in mice. *PloS One* (2014) 9:e104316. doi: 10.1371/journal.pone.0104316

159. Normile TG, Rella A, Del Poeta M. Cryptococcus neoformans Deltasgl1 vaccination requires either CD4(+) or CD8(+) T cells for complete host protection. *Front Cell Infect Microbiol* (2021) 11:739027. doi: 10.3389/fcimb.2021.739027

160. Jarvis JN, Casazza JP, Stone HH, Meintjes G, Lawn SD, Levitz SM, et al. The phenotype of the cryptococcus-specific CD4+ memory T-cell response is associated with disease severity and outcome in HIV-associated cryptococcal meningitis. *J Infect Dis* (2013) 207:1817–28. doi: 10.1093/infdis/jit099

161. Meya DB, Okurut S, Zziwa G, Cose S, Boulware DR, Janoff EN. HIV-Associated cryptococcal immune reconstitution inflammatory syndrome is associated with aberrant T cell function and increased cytokine responses. *J Fungi (Basel)* (2019) 5(2):42. doi: 10.20944/preprints201904.0086.v1

162. Wuthrich M, Hung CY, Gern BH, Pick-Jacobs JC, Galles KJ, Filutowicz HI, et al. A TCR transgenic mouse reactive with multiple systemic dimorphic fungi. *J Immunol* (2011) 187:1421–31. doi: 10.4049/jimmunol.1100921

163. Wuthrich M, Brandhorst TT, Sullivan TD, Filutowicz H, Sterkel A, Stewart D, et al. Calnexin induces expansion of antigen-specific CD4(+) T cells that confer immunity to fungal ascomycetes *via* conserved epitopes. *Cell Host Microbe* (2015) 17:452–65. doi: 10.1016/j.chom.2015.02.009

164. Rivera A, Hohl TM. Calnexin bridges the gap toward a pan-fungal vaccine. *Cell Host Microbe* (2015) 17:421–3. doi: 10.1016/j.chom.2015.03.012

165. Dobson HE, Dias LDS, Kohn EM, Fites S, Wiesner DL, Dileepan T, et al. Antigen discovery unveils resident memory and migratory cell roles in antifungal resistance. *Mucosal Immunol* (2020) 13:518–29. doi: 10.1038/s41385-019-0244-3

166. Dos Santos Dias L, Dobson HE, Bakke BK, Kujoth GC, Huang J, Kohn EM, et al. Structural basis of blastomyces endoglucanase-2 adjuvancy in anti-fungal and -viral immunity. *PloS Pathog* (2021) 17:e1009324. doi: 10.1371/journal.ppat.1009324

167. Wuthrich M, Dobson HE, Ledesma Taira C, Okaa UJ, Dos Santos Dias L, Isidoro-Ayza M, et al. Combination adjuvants enhance recombinant protein vaccine protection against fungal infection. *mBio* (2021) 12:e0201821. doi: 10.1128/mBio.02018-21

168. Wuthrich M, Filutowicz HI, Warner T, Deepe GSJr., Klein BS. Vaccine immunity to pathogenic fungi overcomes the requirement for CD4 help in exogenous antigen presentation to CD8+ T cells: implications for vaccine development in immune-deficient hosts. *J Exp Med* (2003) 197:1405–16. doi: 10.1084/jem.20030109

169. Nanjappa SG, Heninger E, Wuthrich M, Sullivan T, Klein B. Protective antifungal memory CD8(+) T cells are maintained in the absence of CD4(+) T cell help and cognate antigen in mice. *J Clin Invest* (2012) 122:987–99. doi: 10.1172/JCI58762

170. Nanjappa SG, Mudalagiriyappa S, Fites JS, Suresh M, Klein BS. CBLB constrains inactivated vaccine-induced CD8(+) T cell responses and immunity against lethal fungal pneumonia. *J Immunol* (2018) 201:1717–26. doi: 10.4049/jimmunol.1701241

171. Mudalagiriyappa SS,J, Vieson M, Klein BS, Nanjappa SG. GM-CSF + Tc17 cells are required to bolster vaccine immunity against lethal fungal pneumonia without causing overt pathology. *SSRN* (2022). doi: 10.2139/ssrn.4099074

172. Edwards LB, Acquaviva FA, Livesay VT, Cross FW, Palmer CE. An atlas of sensitivity to tuberculin, PPD-b, and histoplasmin in the united states. *Am Rev Respir Dis* (1969) 99:Suppl:1–132.

173. Allendorfer R, Brunner GD, Deepe GSJr. Complex requirements for nascent and memory immunity in pulmonary histoplasmosis. *J Immunol* (1999) 162:7389–96.

174. Deepe GSJr., Gibbons RS. Protective and memory immunity to histoplasma capsulatum in the absence of IL-10. *J Immunol* (2003) 171:5353–62. doi: 10.4049/jimmunol.171.10.5353

175. Deepe GSJr., Gibbons RS. Interleukins 17 and 23 influence the host response to histoplasma capsulatum. *J Infect Dis* (2009) 200:142–51. doi: 10.1086/599333

176. Deepe GSJr., Gibbons RS. Cellular and molecular regulation of vaccination with heat shock protein 60 from histoplasma capsulatum. *Infect Immun* (2002) 70:3759–67. doi: 10.1128/IAI.70.7.3759-3767.2002

177. Deepe GS. Role of Cd8(+) T-cells in host-resistance to systemic infection with histoplasma-capsulatum in mice. *J Immunol* (1994) 152:3491–500.

178. Zhou P, Freidag BL, Caldwell CC, Seder RA. Perforin is required for primary immunity to histoplasma capsulatum. *J Immunol* (2001) 166:1968–74. doi: 10.4049/jimmunol.166.3.1968

179. Hung CY, Hsu AP, Holland SM, Fierer J. A review of innate and adaptive immunity to coccidioidomycosis. *Med Mycol* (2019) 57:S85–92. doi: 10.1093/mmy/myy146

180. Ward RA, Thompson GR3rd, Villani AC, Li B, Mansour MK, Wuethrich M, et al. The known unknowns of the immune response to coccidioides. *J Fungi (Basel)* (2021) 7(5):377. doi: 10.3390/jof7050377

181. Fierer J, Walls L, Eckmann L, Yamamoto T, Kirkland TN. Importance of interleukin-10 in genetic susceptibility of mice to coccidioides immitis. *Infect Immun* (1998) 66:4397–402. doi: 10.1128/IAI.66.9.4397-4402.1998

182. Davini D, Naeem F, Phong A, Al-Kuhlani M, Valentine KM, Mccarty J, et al. Elevated regulatory T cells at diagnosis of coccidioides infection associates with chronicity in pediatric patients. *J Allergy Clin Immunol* (2018) 142:1971–1974 e1977. doi: 10.1016/j.jaci.2018.10.022

183. Nesbit L, Johnson SM, Pappagianis D, Ampel NM. Polyfunctional T lymphocytes are in the peripheral blood of donors naturally immune to coccidioidomycosis and are not induced by dendritic cells. *Infect Immun* (2010) 78:309–15. doi: 10.1128/IAI.00953-09

184. Pappagianis D. Evaluation of the protective efficacy of the killed coccidioides immitis spherule vaccine in humans. the valley fever vaccine study group. *Am Rev Respir Dis* (1993) 148:656–60. doi: 10.1164/ajrccm/148.3.656

185. Tarcha EJ, Basrur V, Hung CY, Gardner MJ, Cole GT. Multivalent recombinant protein vaccine against coccidioidomycosis. *Infect Immun* (2006) 74:5802–13. doi: 10.1128/IAI.00961-06

186. Campuzano AP, Komali Devi P, Liao Y, Zhang H, Wiederhold N, Ostroff G, et al. A recombinant multivalent vaccine (rCpa1) induces protection for C57BL/6 and HLA transgenic mice against pulmonary infection with both species of coccidioides. *bioRxiv* (2021). doi: 10.1101/2021.10.20.465232

187. Burger E. Paracoccidioidomycosis protective immunity. *J Fungi (Basel)* (2021) 7(2):137. doi: 10.3390/jof7020137

188. De Castro LF, Ferreira MC, Da Silva RM, Blotta MH, Longhi LN, Mamoni RL. Characterization of the immune response in human paracoccidioidomycosis. *J Infect* (2013) 67:470–85. doi: 10.1016/j.jinf.2013.07.019

189. Mayorga O, Munoz JE, Lincopan N, Teixeira AF, Ferreira LC, Travassos LR, et al. The role of adjuvants in therapeutic protection against paracoccidioidomycosis after immunization with the P10 peptide. *Front Microbiol* (2012) 3:154. doi: 10.3389/fmicb.2012.00154

190. Holanda RA, Munoz JE, Dias LS, Silva LBR, Santos JRA, Pagliari S, et al. Recombinant vaccines of a CD4+ T-cell epitope promote efficient control of paracoccidioides brasiliensis burden by restraining primary organ infection. *PloS Negl Trop Dis* (2017) 11:e0005927. doi: 10.1371/journal.pntd.0005927

191. Bozzi A, Reis BS, Goulart MI, Pereira MC, Pedroso EP, Goes AM. Analysis of memory T cells in the human paracoccidioidomycosis before and during chemotherapy treatment. *Immunol Lett* (2007) 114:23–30. doi: 10.1016/j.imlet.2007.08.004

192. Bernardino S, Pina A, Felonato M, Costa TA, Frank De Araujo E, Feriotti C, et al. TNF-alpha and CD8+ T cells mediate the beneficial effects of nitric oxide synthase-2 deficiency in pulmonary paracoccidioidomycosis. *PloS Negl Trop Dis* (2013) 7:e2325.

193. Deo SS, Virassamy B, Halliday C, Clancy L, Chen S, Meyer W, et al. Stimulation with lysates of aspergillus terreus, candida krusei and rhizopus oryzae maximizes cross-reactivity of anti-fungal T cells. *Cytotherapy* (2016) 18:65–79. doi: 10.1016/j.jcyt.2015.09.013

194. Aggor FEY, Way SS, Gaffen SL. Fungus among us: The frenemies within. *Trends Immunol* (2019) 40:469–71. doi: 10.1016/j.it.2019.04.007

195. Bacher P, Hohnstein T, Beerbaum E, Röcker M, Blango MG, Kaufmann S, et al. Human anti-fungal Th17 immunity and pathology rely on cross-reactivity against candida albicans. *Cell* (2019) 176:1340–55:e1315. doi: 10.1016/j.cell.2019.01.041

196. Gaundar SS, Clancy L, Blyth E, Meyer W, Gottlieb DJ. Robust polyfunctional T-helper 1 responses to multiple fungal antigens from a cell population generated using an environmental strain of aspergillus fumigatus. *Cytotherapy* (2012) 14:1119–30. doi: 10.3109/14653249.2012.704013

197. Buldain I, Pellon A, Zaldibar B, Antoran A, Martin-Souto L, Aparicio-Fernandez L, et al. Study of humoral responses against Lomentospora/Scedosporium spp. and aspergillus fumigatus to identify l. prolificans antigens of interest for diagnosis and treatment. *Vaccines* (2019) 7:212. doi: 10.3390/vaccines7040212

198. Lin L, Ibrahim AS, Xu X, Farber JM, Avanesian V, Baquir B, et al. Th1-Th17 cells mediate protective adaptive immunity against staphylococcus aureus and candida albicans infection in mice. *PloS Pathog* (2009) 5:e1000703. doi: 10.1371/journal.ppat.1000703

199. Singh S, Uppuluri P, Mamouei Z, Alqarihi A, Elhassan H, French S, et al. The NDV-3A vaccine protects mice from multidrug resistant candida auris infection. *PloS Pathog* (2019) 15:e1007460. doi: 10.1371/journal.ppat.1007460

200. Su LF, Kidd BA, Han A, Kotzin JJ, Davis MM. Virus-specific CD4+ memory-phenotype T cells are abundant in unexposed adults. *Immunity* (2013) 38:373–83. doi: 10.1016/j.immuni.2012.10.021

201. Birnbaum ME, Mendoza JL, Sethi DK, Dong S, Glanville J, Dobbins J, et al. Deconstructing the peptide-MHC specificity of T cell recognition. *Cell* (2014) 157:1073–87. doi: 10.1016/j.cell.2014.03.047

202. Lee H-G, Lee J-U, Kim D-H, Lim S, Kang I, Choi J-M. Pathogenic function of bystander-activated memory-like CD4+ T cells in autoimmune encephalomyelitis. *Nat Commun* (2019) 10:1–14. doi: 10.1038/s41467-019-08482-w

203. Thompson-Souza GA, Santos GMP, Silva JC, Muniz VS, Braga Y, Figueiredo RT, et al. Histoplasma capsulatum-induced extracellular DNA trap release in human neutrophils. *Cell Microbiol* (2020) 22:e13195. doi: 10.1111/cmi.13195

204. Puerta-Arias JD, Mejia SP, Gonzalez A. The role of the interleukin-17 axis and neutrophils in the pathogenesis of endemic and systemic mycoses. *Front Cell Infect Microbiol* (2020) 10:595301. doi: 10.3389/fcimb.2020.595301

205. De Luca A, Zelante T, D'angelo C, Zagarella S, Fallarino F, Spreca A, et al. IL-22 defines a novel immune pathway of antifungal resistance. *Mucosal Immunol* (2010) 3:361–73. doi: 10.1038/mi.2010.22

206. Aggor FEY, Break TJ, Trevejo-Nunez G, Whibley N, Coleman BM, Bailey RD, et al. Oral epithelial IL-22/STAT3 signaling licenses IL-17-mediated immunity to oral mucosal candidiasis. *Sci Immunol* (2020) 5(48):eaba0570. doi: 10.1126/sciimmunol.aba0570

207. Swidergall M, Ernst JF. Interplay between candida albicans and the antimicrobial peptide armory. *Eukaryot Cell* (2014) 13:950–7. doi: 10.1128/EC.00093-14

208. Murdock BJ, Falkowski NR, Shreiner AB, Sadighi Akha AA, Mcdonald RA, White ES, et al. Interleukin-17 drives pulmonary eosinophilia following repeated exposure to aspergillus fumigatus conidia. *Infect Immun* (2012) 80:1424–36. doi: 10.1128/IAI.05529-11

209. Netea MG, Joosten L, van der Meer JWM, Kullberg B-J, Van De Veerdonk FL. Immune defence against candida fungal infections. *Nat Rev Immunol* (2015) 15:630–42. doi: 10.1038/nri3897

210. Kroetz DN, Deepe GS. The role of cytokines and chemokines in histoplasma capsulatum infection. *Cytokine* (2012) 58:112–7. doi: 10.1016/j.cyto.2011.07.430

211. Castro-Lopez N, Hung CY. Immune response to coccidioidomycosis and the development of a vaccine. *Microorganisms* (2017) 5:13. doi: 10.3390/microorganisms5010013

212. Kak G, Raza M, Tiwari BK. Interferon-gamma (IFN-γ): Exploring its implications in infectious diseases. *Biomol Concepts* (2018) 9:64–79. doi: 10.1515/bmc-2018-0007

213. Speakman EA, Dambuza IM, Salazar F, Brown GD. T Cell antifungal immunity and the role of c-type lectin receptors. *Trends Immunol* (2020) 41:61–76. doi: 10.1016/j.it.2019.11.007

214. Vignesh KS, Figueroa J, Porollo A, Caruso JA, Deepe JGS. Granulocyte macrophage-colony stimulating factor induced zn sequestration enhances macrophage superoxide and limits intracellular pathogen survival. *Immunity* (2013) 39:697–710. doi: 10.1016/j.immuni.2013.09.006

215. Deepe GS, Gibbons R, Woodward E. Neutralization of endogenous granulocyte-macrophage colony-stimulating factor subverts the protective immune response to histoplasma capsulatum. *J Immunol* (1999) 163:4985–93.

216. Herring AC, Falkowski NR, Chen G-H, Mcdonald RA, Toews GB, Huffnagle GB. Transient neutralization of tumor necrosis factor alpha can produce a chronic fungal infection in an immunocompetent host: potential role of immature dendritic cells. *Infect Immun* (2005) 73:39–49. doi: 10.1128/IAI.73.1.39-49.2005

217. Rocha F, Alves A, Rocha MFG, Cordeiro RA, Brilhante RSN, Pinto A, et al. Tumor necrosis factor prevents candida albicans biofilm formation. *Sci Rep* (2017) 7:1206. doi: 10.1038/s41598-017-01400-4

218. Ma LL, Spurrell JC, Wang JF, Neely GG, Epelman S, Krensky AM, et al. CD8 T cell-mediated killing of cryptococcus neoformans requires granulysin and is dependent on CD4 T cells and IL-15. *J Immunol* (2002) 169:5787–95. doi: 10.4049/jimmunol.169.10.5787

219. Dotiwala F, Lieberman J. Granulysin: killer lymphocyte safeguard against microbes. *Curr Opin Immunol* (2019) 60:19–29. doi: 10.1016/j.coi.2019.04.013

220. Voskoboinik I, Whisstock JC, Trapani JA. Perforin and granzymes: function, dysfunction and human pathology. *Nat Rev Immunol* (2015) 15:388–400. doi: 10.1038/nri3839

221. Vitenshtein A, Charpak-Amikam Y, Yamin R, Bauman Y, Isaacson B, Stein N, et al. NK cell recognition of candida glabrata through binding of NKp46 and NCR1 to fungal ligands Epa1, Epa6, and Epa7. *Cell Host Microbe* (2016) 20:527–34. doi: 10.1016/j.chom.2016.09.008

222. Li SS, Ogbomo H, Mansour MK, Xiang RF, Szabo L, Munro F, et al. Identification of the fungal ligand triggering cytotoxic PRR-mediated NK cell killing of cryptococcus and candida. *Nat Commun* (2018) 9:751. doi: 10.1038/s41467-018-03014-4

223. Zheng CF, Ma LL, Jones GJ, Gill MJ, Krensky AM, Kubes P, et al. Cytotoxic CD4+ T cells use granulysin to kill cryptococcus neoformans, and activation of this pathway is defective in HIV patients. *Blood* (2007) 109:2049–57. doi: 10.1182/blood-2006-03-009720

224. Kaech SM, Ahmed R. Memory CD8+ T cell differentiation: initial antigen encounter triggers a developmental program in naive cells. *Nat Immunol* (2001) 2:415–22. doi: 10.1038/87720

225. Chung HK, Mcdonald B, Kaech SM. The architectural design of CD8+ T cell responses in acute and chronic infection: Parallel structures with divergent fates. *J Exp Med* (2021) 218(4):e20201730. doi: 10.1084/jem.20201730

226. Portuondo DL, Ferreira LS, Urbaczek AC, Batista-Duharte A, Carlos IZ. Adjuvants and delivery systems for antifungal vaccines: current state and future developments. *Med Mycol* (2015) 53:69–89. doi: 10.1093/mmy/myu045

227. Oliveira LVN, Wang R, Specht CA, Levitz SM. Vaccines for human fungal diseases: close but still a long way to go. *NPJ Vaccines* (2021) 6:33. doi: 10.1038/s41541-021-00294-8

228. Borriello F, Poli V, Shrock E, Spreafico R, Liu X, Pishesha N, et al. An adjuvant strategy enabled by modulation of the physical properties of microbial ligands expands antigen immunogenicity. *Cell* (2022) 185:614–629 e621. doi: 10.1016/j.cell.2022.01.009

229. Sun JC, Bevan MJ. Defective CD8 T cell memory following acute infection without CD4 T cell help. *Science* (2003) 300:339–42. doi: 10.1126/science.1083317

230. Hor JL, Whitney PG, Zaid A, Brooks AG, Heath WR, Mueller SN. Spatiotemporally distinct interactions with dendritic cell subsets facilitates CD4+ and CD8+ T cell activation to localized viral infection. *Immunity* (2015) 43:554–65. doi: 10.1016/j.immuni.2015.07.020

231. Ahrends T, Spanjaard A, Pilzecker B, Babala N, Bovens A, Xiao Y, et al. CD4(+) T cell help confers a cytotoxic T cell effector program including coinhibitory receptor downregulation and increased tissue invasiveness. *Immunity* (2017) 47:848–861 e845. doi: 10.1016/j.immuni.2017.10.009

232. Nakanishi Y, Lu B, Gerard C, Iwasaki A. CD8(+) T lymphocyte mobilization to virus-infected tissue requires CD4(+) T-cell help. *Nature* (2009) 462:510–3. doi: 10.1038/nature08511

233. Redeker A, Welten SP, Baert MR, Vloemans SA, Tiemessen MM, Staal FJ, et al. The quantity of autocrine IL-2 governs the expansion potential of CD8+ T cells. *J Immunol* (2015) 195:4792–801. doi: 10.4049/jimmunol.1501083

234. Eickhoff S, Brewitz A, Gerner MY, Klauschen F, Komander K, Hemmi H, et al. Robust anti-viral immunity requires multiple distinct T cell-dendritic cell interactions. *Cell* (2015) 162:1322–37. doi: 10.1016/j.cell.2015.08.004

235. Kaech SM, Tan JT, Wherry EJ, Konieczny BT, Surh CD, Ahmed R. Selective expression of the interleukin 7 receptor identifies effector CD8 T cells that give rise to long-lived memory cells. *Nat Immunol* (2003) 4:1191–8. doi: 10.1038/ni1009

236. Ahrends T, Busselaar J, Severson TM, Babala N, De Vries E, Bovens A, et al. CD4(+) T cell help creates memory CD8(+) T cells with innate and help-independent recall capacities. *Nat Commun* (2019) 10:5531. doi: 10.1038/s41467-019-13438-1

237. Woodland DL, Kohlmeier JE. Migration, maintenance and recall of memory T cells in peripheral tissues. *Nat Rev Immunol* (2009) 9:153–61. doi: 10.1038/nri2496

238. Kaech SM, Wherry EJ. Heterogeneity and cell-fate decisions in effector and memory CD8+ T cell differentiation during viral infection. *Immunity* (2007) 27:393–405. doi: 10.1016/j.immuni.2007.08.007

239. Seder RA, Ahmed R. Similarities and differences in CD4+ and CD8+ effector and memory T cell generation. *Nat Immunol* (2003) 4:835–42. doi: 10.1038/ni969

240. Sallusto F, Geginat J, Lanzavecchia A. Central memory and effector memory T cell subsets: function, generation, and maintenance. *Annu Rev Immunol* (2004) 22:745–63. doi: 10.1146/annurev.immunol.22.012703.104702

241. Kaech SM, Wherry EJ, Ahmed R. Effector and memory T-cell differentiation: implications for vaccine development. *Nat Rev Immunol* (2002) 2:251–62. doi: 10.1038/nri778

242. Chang JT, Palanivel VR, Kinjyo I, Schambach F, Intlekofer AM, Banerjee A, et al. Asymmetric T lymphocyte division in the initiation of adaptive immune responses. *Science* (2007) 315:1687–91. doi: 10.1126/science.1139393

243. Stemberger C, Neuenhahn M, Gebhardt FE, Schiemann M, Buchholz VR, Busch DH. Stem cell-like plasticity of naive and distinct memory CD8+ T cell subsets. *Semin Immunol* (2009) 21:62–8. doi: 10.1016/j.smim.2009.02.004

244. Fuertes Marraco SA, Soneson C, Cagnon L, Gannon PO, Allard M, Abed Maillard S, et al. Long-lasting stem cell-like memory CD8+ T cells with a naive-like profile upon yellow fever vaccination. *Sci Transl Med* (2015) 7:282ra248. doi: 10.1126/scitranslmed.aaa3700

245. Surh CD, Sprent J. Homeostasis of naive and memory T cells. *Immunity* (2008) 29:848–62. doi: 10.1016/j.immuni.2008.11.002

246. Raeber ME, Zurbuchen Y, Impellizzieri D, Boyman O. The role of cytokines in T-cell memory in health and disease. *Immunol Rev* (2018) 283:176–93. doi: 10.1111/imr.12644

247. Masopust D, Kaech SM, Wherry EJ, Ahmed R. The role of programming in memory T-cell development. *Curr Opin Immunol* (2004) 16:217–25. doi: 10.1016/j.coi.2004.02.005

248. Martin MD, Badovinac VP. Defining memory CD8 T cell. *Front Immunol* (2018) 9:2692. doi: 10.3389/fimmu.2018.02692

249. Muroyama Y, Wherry EJ. Memory T-cell heterogeneity and terminology. *Cold Spring Harb Perspect Biol* (2021) 13(10):a037929. doi: 10.1101/cshperspect.a037929

250. Reiner SL, Sallusto F, Lanzavecchia A. Division of labor with a workforce of one: Challenges in specifying effector and memory T cell fate. *Science* (2007) 317:622–5. doi: 10.1126/science.1143775

251. Gerlach C, Van Heijst JWJ, Swart E, Sie D, Armstrong N, Kerkhoven RM, et al. One naive T cell, multiple fates in CD8+ T cell differentiation. *J Exp Med* (2010) 207:1235–46. doi: 10.1084/jem.20091175

252. Bresser K, Kok L, Swain AC, King LA, Jacobs L, Weber TS, et al. Replicative history marks transcriptional and functional disparity in the CD8(+) T cell memory pool. *Nat Immunol* (2022) 23(5):791–801. doi: 10.1038/s41590-022-01171-9

253. Ahmed R, Bevan MJ, Reiner SL, Fearon DT. The precursors of memory: models and controversies. *Nat Rev Immunol* (2009) 9:662–8. doi: 10.1038/nri2619

254. Kaech SM, Cui W. Transcriptional control of effector and memory CD8+ T cell differentiation. *Nat Rev Immunol* (2012) 12:749–61. doi: 10.1038/nri3307

255. Chang JT, Wherry EJ, Goldrath AW. Molecular regulation of effector and memory T cell differentiation. *Nat Immunol* (2014) 15:1104–15. doi: 10.1038/ni.3031

256. Hope JL, Stairiker CJ, Bae EA, Otero DC, Bradley LM. Striking a balance-cellular and molecular drivers of memory T cell development and responses to chronic stimulation. *Front Immunol* (2019) 10:1595. doi: 10.3389/fimmu.2019.01595

257. Sallusto F, Lenig D, Förster R, Lipp M, Lanzavecchia A. Two subsets of memory T lymphocytes with distinct homing potentials and effector functions. *Nature* (1999) 401:708–12. doi: 10.1038/44385

258. Lanzavecchia A, Sallusto F. Understanding the generation and function of memory T cell subsets. *Curr Opin Immunol* (2005) 17:326–32. doi: 10.1016/j.coi.2005.04.010

259. Geginat J, Lanzavecchia A, Sallusto F. Proliferation and differentiation potential of human CD8+ memory T-cell subsets in response to antigen or homeostatic cytokines. *Blood* (2003) 101:4260–6. doi: 10.1182/blood-2002-11-3577

260. Leibundgut-Landmann S. Tissue-resident memory T cells in antifungal immunity. *Front Immunol* (2021) 0:1976. doi: 10.3389/fimmu.2021.693055

261. Szabo PA, Miron M, Farber DL. Location, location, location: Tissue resident memory T cells in mice and humans. *Sci Immunol* (2019) 4(34): eaas9673. doi: 10.1126/sciimmunol.aas9673

262. Mackay LK, Braun A, Macleod BL, Collins N, Tebartz C, Bedoui S, et al. Cutting edge: CD69 interference with sphingosine-1-phosphate receptor function regulates peripheral T cell retention. *J Immunol* (2015) 194:2059–63. doi: 10.4049/jimmunol.1402256

263. Casey KA, Fraser KA, Schenkel JM, Moran A, Abt MC, Beura LK, et al. Antigen-independent differentiation and maintenance of effector-like resident memory T cells in tissues. *J Immunol* (2012) 188:4866–75. doi: 10.4049/jimmunol.1200402

264. Hirai T, Yang Y, Zenke Y, Li H, Chaudhri VK, de la Cruz Diaz JS, et al. Competition for active TGFbeta cytokine allows for selective retention of antigen-specific tissue- resident memory T cells in the epidermal niche. *Immunity* (2021) 54:84–98 e85. doi: 10.1016/j.immuni.2020.10.022

265. Sasson SC, Gordon CL, Christo SN, Klenerman P, Mackay LK. Local heroes or villains: tissue-resident memory T cells in human health and disease. *Cell Mol Immunol* (2020) 17:113–22. doi: 10.1038/s41423-019-0359-1

266. Lugli E, Dominguez MH, Gattinoni L, Chattopadhyay PK, Bolton DL, Song K, et al. Superior T memory stem cell persistence supports long-lived T cell memory. *J Clin Invest* (2013) 123:594. doi: 10.1172/JCI66327

267. Graef P, Buchholz VR, Stemberger C, Flossdorf M, Henkel L, Schiemann M, et al. Serial transfer of single-Cell-Derived immunocompetence reveals stemness of CD8+ central memory T cells. *Immunity* (2014) 41:116–26. doi: 10.1016/j.immuni.2014.05.018

268. Joshi NS, Cui W, Chandele A, Lee HK, Urso DR, Hagman J, et al. Inflammation directs memory precursor and short-lived effector CD8(+) T cell fates *via* the graded expression of T-bet transcription factor. *Immunity* (2007) 27:281–95. doi: 10.1016/j.immuni.2007.07.010

269. Nayar R, Schutten E, Bautista B, Daniels K, Prince AL, Enos M, et al. Graded levels of IRF4 regulate CD8+ T cell differentiation and expansion, but not attrition, in response to acute virus infection. *J Immunol* (2014) 192:5881–93. doi: 10.4049/jimmunol.1303187

270. Jameson SC, Masopust D. Understanding subset diversity in T cell memory. *Immunity* (2018) 48:214–26. doi: 10.1016/j.immuni.2018.02.010

271. Wherry EJ, Barber DL, Kaech SM, Blattman JN, Ahmed R. Antigen-independent memory CD8 T cells do not develop during chronic viral infection. *Proc Natl Acad Sci U.S.A.* (2004) 101:16004–9.

272. Utzschneider DT, Alfei F, Roelli P, Barras D, Chennupati V, Darbre S, et al. High antigen levels induce an exhausted phenotype in a chronic infection without impairing T cell expansion and survival. *J Exp Med* (2016) 213:1819–34. doi: 10.1084/jem.20150598

273. Wirth TC, Xue HH, Rai D, Sabel JT, Bair T, Harty JT, et al. Repetitive antigen stimulation induces stepwise transcriptome diversification but preserves a core signature of memory CD8(+) T cell differentiation. *Immunity* (2010) 33:128–40. doi: 10.1016/j.immuni.2010.06.014

274. Angelosanto JM, Blackburn SD, Crawford A, Wherry EJ. Progressive loss of memory T cell potential and commitment to exhaustion during chronic viral infection. *J Virol* (2012) 86:8161–70. doi: 10.1128/JVI.00889-12

275. Daniels MA, Teixeiro E. TCR signaling in T cell memory. *Front Immunol* (2015) 6:617. doi: 10.3389/fimmu.2015.00617

276. Wuthrich M, Warner T, Klein BS. CD28 is required for optimal induction, but not maintenance, of vaccine-induced immunity to blastomyces dermatitidis. *Infect Immun* (2005) 73:7436–41. doi: 10.1128/IAI.73.11.7436-7441.2005

277. Chen L, Flies DB. Molecular mechanisms of T cell co-stimulation and co-inhibition. *Nat Rev Immunol* (2013) 13:227–42. doi: 10.1038/nri3405

278. Humphreys IR, Edwards L, Walzl G, Rae AJ, Dougan G, Hill S, et al. OX40 ligation on activated T cells enhances the control of cryptococcus neoformans and reduces pulmonary eosinophilia. *J Immunol* (2003) 170:6125–32. doi: 10.4049/jimmunol.170.12.6125

279. Wuthrich M, Fisette PL, Filutowicz HI, Klein BS. Differential requirements of T cell subsets for CD40 costimulation in immunity to blastomyces dermatitidis. *J Immunol* (2006) 176:5538–47. doi: 10.4049/jimmunol.176.9.5538

280. Zhou Q, Gault RA, Kozel TR, Murphy WJ. Immunomodulation with CD40 stimulation and interleukin-2 protects mice from disseminated cryptococcosis. *Infect Immun* (2006) 74:2161–8. doi: 10.1128/IAI.74.4.2161-2168.2006

281. Chen GH, Osterholzer JJ, Choe MY, Mcdonald RA, Olszewski MA, Huffnagle GB, et al. Dual roles of CD40 on microbial containment and the development of immunopathology in response to persistent fungal infection in the lung. *Am J Pathol* (2010) 177:2459–71. doi: 10.2353/ajpath.2010.100141

282. Felonato M, Pina A, Bernardino S, Loures FV, De Araujo EF, Calich VL. CD28 exerts protective and detrimental effects in a pulmonary model of paracoccidioidomycosis. *Infect Immun* (2010) 78:4922–35. doi: 10.1128/IAI.00297-10

283. Bouguermouh S, Fortin G, Baba N, Rubio M, Sarfati M. CD28 co-stimulation down regulates Th17 development. *PloS One* (2009) 4:e5087. doi: 10.1371/journal.pone.0005087

284. Revu S, Wu J, Henkel M, Rittenhouse N, Menk A, Delgoffe GM, et al. IL-23 and IL-1beta drive human Th17 cell differentiation and metabolic reprogramming in absence of CD28 costimulation. *Cell Rep* (2018) 22:2642–53. doi: 10.1016/j.celrep.2018.02.044

285. Dong C. Cytokine regulation and function in T cells. *Annu Rev Immunol* (2021) 39:51–76. doi: 10.1146/annurev-immunol-061020-053702

286. Cavassani KA, Campanelli AP, Moreira AP, Vancim JO, Vitali LH, Mamede RC, et al. Systemic and local characterization of regulatory T cells in a chronic fungal infection in humans. *J Immunol* (2006) 177:5811–8. doi: 10.4049/jimmunol.177.9.5811

287. Romani L. Immunity to fungal infections. *Nat Rev Immunol* (2011) 11:275–88. doi: 10.1038/nri2939

288. Murdock BJ, Teitz-Tennenbaum S, Chen GH, Dils AJ, Malachowski AN, Curtis JL, et al. Early or late IL-10 blockade enhances Th1 and Th17 effector responses and promotes fungal clearance in mice with cryptococcal lung infection. *J Immunol* (2014) 193:4107–16. doi: 10.4049/jimmunol.1400650

289. Break TJ, Oikonomou V, Dutzan N, Desai JV, Swidergall M, Freiwald T, et al. Aberrant type 1 immunity drives susceptibility to mucosal fungal infections. *Science* (2021) 371(6526):eaay5731. doi: 10.1126/science.aay5731

290. Montano DE, Voigt K. Host immune defense upon fungal infections with mucorales: Pathogen-immune cell interactions as drivers of inflammatory responses. *J Fungi* (2020) 6(3):173. doi: 10.3390/jof6030173

291. Deepe GSJr., Gibbons RS. T Cells require tumor necrosis factor-alpha to provide protective immunity in mice infected with histoplasma capsulatum. *J Infect Dis* (2006) 193:322–30. doi: 10.1086/498981

292. Romani L. Innate and acquired cellular immunity to fungi. *Mol Principles Fungal Pathogene* (2006), 471–86. doi: 10.1128/9781555815776.ch32

293. Romani L. Cell mediated immunity to fungi: a reassessment. *Med Mycol* (2008) 46:515–29. doi: 10.1080/13693780801971450

294. Leibundgut-Landmann S, Wuthrich M, Hohl TM. Immunity to fungi. *Curr Opin Immunol* (2012) 24:449–58. doi: 10.1016/j.coi.2012.04.007

295. Azuma M. Co-Signal molecules in T-cell activation: Historical overview and perspective. *Adv Exp Med Biol* (2019) 1189:3–23. doi: 10.1007/978-981-32-9717-3_1

296. Morris AB, Adams LE, Ford ML. Influence of T cell coinhibitory molecules on CD8+ recall responses. *Front Immunol* (2018) 1810. doi: 10.3389/fimmu.2018.01810

297. Roussey JA, Viglianti SP, Teitz-Tennenbaum S, Olszewski MA, Osterholzer JJ. Anti–PD-1 antibody treatment promotes clearance of persistent cryptococcal lung infection in mice. *J Immunol* (2017) 199:3535–46. doi: 10.4049/jimmunol.1700840

298. Shwetank, Abdelsamed HA, Frost EL, Schmitz HM, Mockus TE, Youngblood BA, et al. Maintenance of PD-1 on brain-resident memory CD8 T cells is antigen independent. *Immunol Cell Biol* (2017) 95:953–9. doi: 10.1038/icb.2017.62

299. Park SL, Zaid A, Hor JL, Christo SN, Prier JE, Davies B, et al. Local proliferation maintains a stable pool of tissue-resident memory T cells after antiviral recall responses. *Nat Immunol* (2018) 19:183–91. doi: 10.1038/s41590-017-0027-5

300. Chang KC, Burnham CA, Compton SM, Rasche DP, Mazuski RJ, Mcdonough JS, et al. Blockade of the negative co-stimulatory molecules PD-1 and CTLA-4 improves survival in primary and secondary fungal sepsis. *Crit Care* (2013) 17:R85. doi: 10.1186/cc12711

301. Gartshteyn Y, Askanase AD, Mor A. SLAM associated protein signaling in T cells: Tilting the balance toward autoimmunity. *Front Immunol* (2021) 12:654839. doi: 10.3389/fimmu.2021.654839

302. Kohn EM, Dos Santos Dias L, Dobson HE, He X, Wang H, Klein BS, et al. SLAMF1 is dispensable for vaccine-induced T cell development but required for resistance to fungal infection. *J Immunol* (2022) 208:1417–23. doi: 10.4049/jimmunol.2100819

303. Cyster JG, Shotton DM, Williams AF. The dimensions of the T lymphocyte glycoprotein leukosialin and identification of linear protein epitopes that can be modified by glycosylation. *EMBO J* (1991) 10:893–902. doi: 10.1002/j.1460-2075.1991.tb08022.x

304. Ostberg JR, Barth RK, Frelinger JG. The Roman god janus: A paradigm for the function of CD43. *Immunol Today* (1998) 19:546–50. doi: 10.1016/S0167-5699(98)01343-7

305. Onami TM, Harrington LE, Williams MA, Galvan M, Larsen CP, Pearson TC, et al. Dynamic regulation of T cell immunity by CD43. *J Immunol* (2002) 168:6022–31. doi: 10.4049/jimmunol.168.12.6022

306. Manjunath N, Johnson RS, Staunton DE, Pasqualini R, Ardman B. Targeted disruption of CD43 gene enhances T lymphocyte adhesion. *J Immunol* (1993) 151:1528–34.

307. Manjunath N, Correa M, Ardman M, Ardman B. Negative regulation of T-cell adhesion and activation by CD43. *Nature* (1995) 377:535–8. doi: 10.1038/377535a0

308. Pedraza-Alva G, Merida LB, Del Rio R, Fierro NA, Cruz-Munoz ME, Olivares N, et al. CD43 regulates the threshold for T cell activation by targeting cbl functions. *IUBMB Life* (2011) 63:940–8. doi: 10.1002/iub.554

309. Mudalagiriyappa SD, George S DJr, Nanjappa SG. Sialophorin is an essential host element for vaccine immunity against pulmonary fungal infections. *bioRxiv* (2022). doi: 10.1101/2022.03.31.486552

310. Pulendran B, Arunachalam PS, O'hagan DT. Emerging concepts in the science of vaccine adjuvants. *Nat Rev Drug Discov* (2021) 20:454–75. doi: 10.1038/s41573-021-00163-y

frontiers | Frontiers in Immunology

TYPE Original Research
PUBLISHED 21 December 2022
DOI 10.3389/fimmu.2022.859598



OPEN ACCESS

EDITED BY
Kihyuck Kwak,
Yonsei University, South Korea

REVIEWED BY
Thierry Fest,
University of Rennes 1, France
Paolo Casali,
The University of Texas Health Science Center at San Antonio, United States

*CORRESPONDENCE
Meinrad Busslinger
busslinger@imp.ac.at

†PRESENT ADDRESS
Peter Bönelt,
Takeda Pharma Ges.m.b.H.,
Vienna, Austria
Johannes Stadlmann,
Institute of Biochemistry, University of Natural Resource and Life Sciences,
Vienna, Austria

‡These authors have contributed equally to this work and share first authorship

SPECIALTY SECTION
This article was submitted to B Cell Biology, a section of the journal Frontiers in Immunology

RECEIVED 21 January 2022
ACCEPTED 15 November 2022
PUBLISHED 21 December 2022

CITATION
Wöhner M, Pinter T, Bönelt P, Hagelkruys A, Kostanova-Poliakova D, Stadlmann J, Konieczny SF, Fischer M, Jaritz M and Busslinger M (2022) The Xbp1-regulated transcription factor Mist1 restricts antibody secretion by restraining Blimp1 expression in plasma cells.
*Front. Immunol.* 13:859598.
doi: 10.3389/fimmu.2022.859598



# The Xbp1-regulated transcription factor Mist1 restricts antibody secretion by restraining Blimp1 expression in plasma cells

Miriam Wöhner[1‡], Theresa Pinter[1‡], Peter Bönelt[1†], Astrid Hagelkruys[2], Daniela Kostanova-Poliakova[1], Johannes Stadlmann[2†], Stephen F. Konieczny[3], Maria Fischer[1], Markus Jaritz[1] and Meinrad Busslinger[1*]

[1]Research Institute of Molecular Pathology (IMP), Vienna Biocenter (VBC), Vienna, Austria, [2]Institute of Molecular Biotechnology of the Austrian Academy of Sciences (IMBA), Vienna Biocenter (VBC), Vienna, Austria, [3]Department of Biological Science, Purdue University, West Lafayette, IN, United States

Antibody secretion by plasma cells provides acute and long-term protection against pathogens. The high secretion potential of plasma cells depends on the unfolded protein response, which is controlled by the transcription factor Xbp1. Here, we analyzed the Xbp1-dependent gene expression program of plasma cells and identified *Bhlha15* (Mist1) as the most strongly activated Xbp1 target gene. As Mist1 plays an important role in other secretory cell types, we analyzed in detail the phenotype of Mist1-deficient plasma cells in *Cd23*-Cre *Bhlha15*$^{fl/fl}$ mice under steady-state condition or upon NP-KLH immunization. Under both conditions, Mist1-deficient plasma cells were 1.4-fold reduced in number and exhibited increased IgM production and antibody secretion compared to control plasma cells. At the molecular level, Mist1 regulated a largely different set of target genes compared with Xbp1. Notably, expression of the Blimp1 protein, which is known to activate immunoglobulin gene expression and to contribute to antibody secretion, was 1.3-fold upregulated in Mist1-deficient plasma cells, which led to a moderate downregulation of most Blimp1-repressed target genes in the absence of Mist1. Importantly, a 2-fold reduction of Blimp1 (*Prdm1*) expression was sufficient to restore the cell number and antibody expression of plasma cells in *Prdm1*$^{Gfp/+}$ *Cd23*-Cre *Bhlha15*$^{fl/fl}$ mice to the same level seen in control mice. Together, these data indicate that Mist1 restricts antibody secretion by restraining Blimp1 expression, which likely contributes to the viability of plasma cells.

KEYWORDS

**Mist1 (Bhlha15), Blimp1 (Prdm1), XBP1, plasma cell differentiation, antibody secretion, unfolded protein response (UPR), gene regulation**

# Introduction

Plasma cells (PCs) provide protection of the host against infection by secreting high-affinity antibodies that recognize an almost unlimited number of pathogens (1). Activation of mature B cells in peripheral lymphoid organs leads to the differentiation of short-lived, antibody-secreting plasmablasts (PBs) and PCs, which can subsequently develop into quiescent long-lived PCs upon migration to survival niches in the bone marrow (1). The differentiation of mature B cells to PBs is associated with substantial changes in gene expression and cell morphology (1, 2). While the expression of B cell-specific regulators, like Pax5 and Ebf1, which maintain the B cell gene expression program, is downregulated during PB formation (2, 3), the increased expression of Irf4 and Blimp1 (*Prdm1*) promotes PB differentiation by activating PC-specific genes and repressing the B cell gene expression program (4–6). During the process of PB differentiation, the rearranged antigen receptor loci encoding the immunoglobulin heavy chain (*Igh*) and light chain (*Igk* and *Igl*) genes are strongly activated, and the *Igh* gene transcripts furthermore undergo a posttranscriptional expression switch from the membrane-bound form to the secreted form of the Ig heavy chain, which results in the production and secretion of large amounts of antibodies (1, 3). The PBs and PCs thereby undergo a massive change in morphology by enlarging their endoplasmic reticulum (ER), which promotes efficient antibody secretion and ensures their cell survival (1, 7).

The morphological change of PBs and PCs is a direct consequence of the unfolded protein response (UPR), which is induced by protein overloading of the ER and restores the folding, processing and export of proteins that pass through the ER (8). The essential UPR pathway of PBs and PCs is under the control of the ER-resident transmembrane protein Ire1α (*Ern1*), which is normally inactivated by the inhibitory Hsp70-type chaperone BiP (*Hsp5*) inside of the ER (8). Upon accumulation of unfolded proteins in the ER, BiP dissociates from Ire1α, which in turn activates the endoribonuclease activity of Ire1α that splices out 26 nucleotides from the cytoplasmic *Xbp1* mRNA, thus leading to a frameshift mediating translation of the transcriptionally active regulator Xbp1s (9, 10). Xbp1s activates the UPR gene expression program, thus resulting in a massive expansion of the ER and secretory protein apparatus (7). Consequently, antibody secretion is severely impaired upon inactivation of *Xbp1* in PBs and PCs (11–13). Xbp1 is, however, not essential for the generation of PBs and PCs (12), and its gene-regulatory function in these antibody-secreting cells has not yet been fully explored.

Our investigation of the Xbp1-dependent gene expression program in PBs by ChIP- and RNA-seq analyses revealed that the most strongly activated Xbp1 target gene is *Bhlha15* coding for the transcription factor Mist1 (14). Mist1 was previously shown to play an important role in other secretory cell types by inducing and maintaining their secretory cell architecture (14–18). Here, we used conditional gene inactivation combined with RNA- and ChIP-seq analyses to systematically investigate the role of Mist1 in PCs. Mist1-deficient PCs were decreased in the spleen and bone marrow under steady-state condition and upon immunization. Moreover, the antibody secretion was increased in Mist1-deficient PCs, in marked contrast to Xbp1-deficient PCs, as previously shown (12, 13). At the molecular level, Xbp1 and Mist1 regulated a largely different set of target genes. Notably, the PC-specific regulator Blimp1 was upregulated in Mist1-deficient PCs, which resulted in a moderate downregulation of most Blimp1-repressed target genes. Importantly, a two-fold reduction of Blimp1 expression in Mist1-deficient PCs rescued PC numbers and reduced antibody secretion to the same level observed in control PCs. Hence, these data indicate that Mist1 largely mediates its effects on plasma cells by restricting antibody secretion through restraining Blimp1 expression, which likely imparts PC viability.

# Results

## Analysis of the Xbp1-regulated gene expression program in plasmablasts

To identify regulated Xbp1 target genes contributing to antibody secretion in PBs and PCs, we performed RNA-seq and ChIP-seq analyses with *in vitro* generated PBs. To this end, we cultured splenic $CD43^-$ B cells for 8 days in the iGB system on 40LB feeder cells (19). In this system, which mimics T cell help, naïve B cells are initially stimulated with BAFF, CD40 ligand and IL-4 for 4 days, followed by 4 days of stimulation with BAFF, CD40 ligand and IL-21, which promotes PB differentiation (19).

For conditional inactivation of the floxed (fl) *Xbp1* allele (20), we used the *Cd23*-Cre line, which initiates Cre-mediated deletion in immature B cells and leads to efficient deletion in mature B cells of the spleen (21). B cells from the spleen of *Cd23*-Cre $Xbp1^{fl/fl}$ and control $Xbp1^{fl/fl}$ mice were differentiated in the iGB system to PBs, which were sorted as $CD19^+CD138^+CD23^-$ cells for RNA-seq analysis (Supplementary Figures 1A, B). We identified 197 Xbp1-activated and 29 Xbp1-repressed genes, which were selected for an expression difference of > 3-fold, an adjusted *P* value of < 0.05 and an expression value of > 5 transcripts per million (TPM) in $Xbp1^{fl/fl}$ PBs (activated genes) or *Cd23*-Cre $Xbp1^{fl/fl}$ PBs (repressed genes), respectively (Figure 1A and Supplementary Table 1). The 197 Xbp1-activated genes were annotated and grouped according to their function. The two largest functional groups consisted of 46 genes involved in UPR or ER function and 33 genes implicated in metabolism (Figures 1B, C), which is consistent with a critical role of Xbp1 in orchestrating antibody synthesis, modification and secretion as well as metabolic reprogramming of PBs (7). We next compared the identified Xbp1-activated genes by gene set enrichment analysis (GSEA) with a published dataset

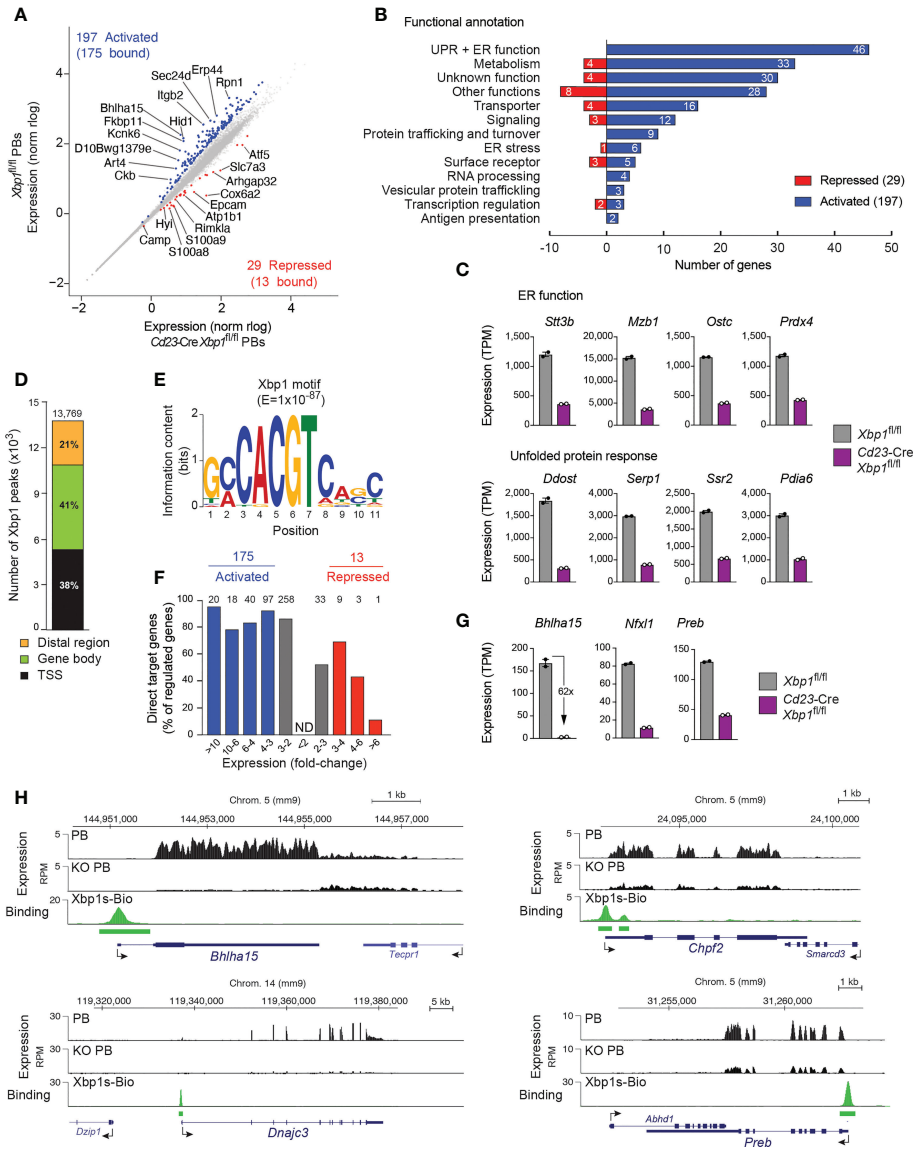


FIGURE 1
Xbp1-dependent gene expression program in plasmablasts. **(A)** Scatter plot of gene expression differences between *Cd23*-Cre *Xbp1*$^{fl/fl}$ and *Xbp1*$^{fl/fl}$ PBs that were sorted as CD19$^{+}$CD138$^{+}$CD23$^{-}$cells after stimulation in the iGB system for 4 days with IL-4 followed by 4 days with IL-21. Two independent RNA-seq experiments were performed with PBs of each genotype. Each dot corresponds to one gene, whose expression is plotted as normalized $\log_{10}$ (norm rlog) expression value. Genes with an expression difference of > 3-fold, an adjusted *P* value of < 0.05, a transcripts per million (TPM) expression value of > 5 (at least in one sample) are colored in blue or red corresponding to activation or repression by Xbp1, respectively. **(B)** Functional classification and quantification (number) of proteins encoded by Xbp1-activated and Xbp1-repressed genes. **(C)** Expression of genes involved in UPR or ER function, shown as mean TPM values of two RNA-seq experiments of *Cd23*-Cre *Xbp1*$^{fl/fl}$ or *Xbp1*$^{fl/fl}$ PBs, respectively. **(D)** Presence of Xbp1 peaks in distal regions, gene bodies and promoter (TSS) regions. Splenic B cells from *Xbp1*$^{Bio/Bio}$ *Rosa26*$^{BirA/+}$ mice were stimulated for 4 days with LPS followed by Bio-ChIP-seq analysis. The Xbp1 peaks were assigned to genes as described (22). **(E)** Consensus Xbp1-binding motif identified with an E-value of 1 x 10$^{-87}$ by the *de novo* motif-discovery program MEME-Chip. **(F)** The number of regulated target genes is shown for the indicated fold-change of gene expression between *Cd23*-Cre *Xbp1*$^{fl/fl}$ and *Xbp1*$^{fl/fl}$ PBs. Grey bars indicated activated or repressed genes with less than a 3-fold expression change. **(G)** Expression of Xbp1-activated transcription factor genes in *Cd23*-Cre *Xbp1*$^{fl/fl}$ and *Xbp1*$^{fl/fl}$ PBs, shown as mean TPM values of two RNA-seq experiments per genotype. **(H)** Xbp1 binding and RNA-seq expression at selected activated Xbp1 target loci. Horizontal bars indicate Xbp1s-Bio peaks identified by MACS peak calling.

obtained with *ex vivo* sorted Xbp1-deficient plasma cells (13). Notably, the Xbp1-activated genes, which were downregulated upon loss of Xbp1 in *in vivo* plasma cells, were also downregulated in our dataset (Supplementary Figure 1C). Moreover, we also observed a strong correlation of expression between known UPR genes (13) and the Xbp1-regulated genes of our dataset (Supplementary Figure 1C), in agreement with the fact that many UPR genes are regulated by Xbp1 (8).

As the development and function of PBs and PCs is critically dependent on the transcription factors Irf4 (23), Blimp1 (*Prdm1*) (24), Ikaros (*Ikzf1*) (25), Aiolos (*Ikzf3*) (26), E2A (*Tcf3*) and E2-2 (*Tcf4*) (27), we next analyzed the expression of these genes in Xbp1-deficient PBs. All 6 genes were expressed at a moderately elevated level in the *Cd23*-Cre $Xbp1^{fl/fl}$ PBs compared with control $Xbp1^{fl/fl}$ PBs (Supplementary Figure 1D). *Pax5*, which is downregulated in the transition from mature B cells to PCs (28), was expressed at an equally low level in Xbp1-deficient and control PBs. Hence, Xbp1 does not play a crucial role in the regulation of key transcription factors that control plasma cell development and function.

To be able to analyze the genome-wide pattern of Xbp1 binding by ChIP-seq, we generated a $Xbp1s^{Bio}$ allele by inserting a biotin acceptor sequence at the last codon of *Xbp1s* (Supplementary Figure 1E). To facilitate *in vivo* biotinylation of the biotin acceptor sequence by the *E.coli* BirA ligase, we generated $Xbp1s^{Bio/Bio}$ $Rosa26^{BirA/BirA}$ mice, which exhibited normal B cell development and only a small increase in bone marrow PCs (Supplementary Figure 1F). Importantly, the Mist1 protein, encoded by an activated Xbp1 target gene (see below), was similarly expressed in PCs from the bone marrow of $Xbp1s^{Bio/Bio}$ $Rosa26^{BirA/BirA}$ and control $Rosa26^{BirA/BirA}$ mice, indicating that the C-terminal addition of the biotin acceptor sequence did not interfere with the transcriptional activity of Xbp1s-Bio (Supplementary Figure 1G). Moreover, enzyme-linked immunospot (ELISPOT) assays furthermore revealed similar numbers of IgM and IgG antibody-secreting cells (ASC) in the bone marrow, indicating that the plasma cells of $Xbp1s^{Bio/Bio}$ $Rosa26^{BirA/BirA}$ mice were functional (Supplementary Figure 1H). We next stimulated splenic $Xbp1s^{Bio/Bio}$ $Rosa26^{BirA/+}$ B cells with lipopolysaccharide (LPS) for 4 days and performed streptavidin-mediated pulldown of the Xbp1s-Bio protein from nuclear extracts of these LPS-stimulated cells followed by Bio-ChIP-seq analysis (22). Peak calling with a stringent *P* value of $< 10^{-10}$ identified 13,769 Xbp1 peaks, which were primarily located in promoter regions (38%) and gene bodies (41%) (Figure 1D). Analysis of the Xbp1 peak sequences with a *de novo* motif discovery program identified a consensus Xbp1-binding motif (Figure 1E), which resembles a published Xbp1 recognition sequence (29) (Supplementary Figure 1I). Peak-to-gene assignment defined 9,210 Xbp1-bound genes. By determining the overlap between these Xbp1-bound genes and the Xbp1-regulated genes (Figure 1A), we identified 175 potentially directly activated Xbp1 target genes (corresponding to 89% of all activated genes) and 13 potentially directly repressed target genes (44%, Figures 1A, F and Supplementary Table 1). Consistent with this finding, gene activation clearly correlated with Xbp1 binding in marked contrast to the inverse correlation of Xbp1 binding with increasing gene repression (Figure 1F). These data strongly suggest that Xbp1s is a dedicated transcriptional activator.

Xbp1 directly activated the 3 transcription factor genes *Bhlha15*, *Nfxl1* and *Preb* in PBs (Figures 1G, H). Other examples of directly and strongly regulated Xbp1 targets include the metabolic gene *Chpf2* (30) and UPR gene *Dnajc3* (31) (Figure 1H). Notably, *Bhlha15* was 62-fold activated by Xbp1 in PBs and was thus the most strongly activated Xbp1 target gene, showing prominent Xbp1 binding at its promoter (Figures 1G, H). This finding is consistent with previous reports, demonstrating that Xbp1 binds to and regulates *Bhlha15* in gastric cells and fibroblasts (16, 32). The *Bhlha15* gene, which codes for the transcription factor Mist1 (14), was strongly activated during *in vitro* differentiation in the iGB system from the activated B cell stage to pre-PBs and PBs as well as *in vivo* during the developmental transition from mature and germinal center (GC) B cells to plasma cells (Supplementary Figure 2A). Despite its prominent PC-specific expression pattern, Mist1 was previously reported to play only a minimal role in *in vitro* differentiated PBs (33) and *in vivo* splenic PCs (34). We therefore decided to reinvestigate in a systematic manner the function of Mist1 *in vivo* in PCs under steady-state conditions and upon immunization.

## Moderate plasma cell reduction and increased antibody secretion upon loss of Mist1

To study the function of Mist1 in PCs, we crossed $Bhlha15^{fl/fl}$ mice (35) with *Cd23*-Cre mice. In addition, we employed *Cd23*-Cre $Xbp1^{fl/fl}$ mice as reference mice with strongly impaired antibody secretion and used $Bhlha15^{fl/fl}$ and $Xbp1^{fl/fl}$ mice as controls. Consistent with the specific expression of *Bhlha15* in terminally differentiated PCs (Supplementary Figure 2A), B cell development was normal in *Cd23*-Cre $Bhlha15^{fl/fl}$ mice, as indicated by a similar frequency of mature B cells in the spleen of both experimental and control mice (Supplementary Figure 2B). However, flow cytometric analysis of PCs ($TACI^{+}CD138^{+}$) in unimmunized *Cd23*-Cre $Bhlha15^{fl/fl}$ mice revealed that the frequencies of PCs in the bone marrow and spleen were moderately (1.4-fold) reduced compared with those of control mice in three independent experiments (Figures 2A, B). In contrast, PCs in the spleen, but not in the bone marrow, were 2.3-fold increased in *Cd23*-Cre $Xbp1^{fl/fl}$ mice compared with control mice (Figures 2A, B). Intracellular staining combined with flow-cytometric analysis confirmed that Mist1 was lost in PCs from the bone marrow of both *Cd23*-Cre $Bhlha15^{fl/fl}$ and *Cd23*-Cre $Xbp1^{fl/fl}$

10.3389/fimmu.2022.859598

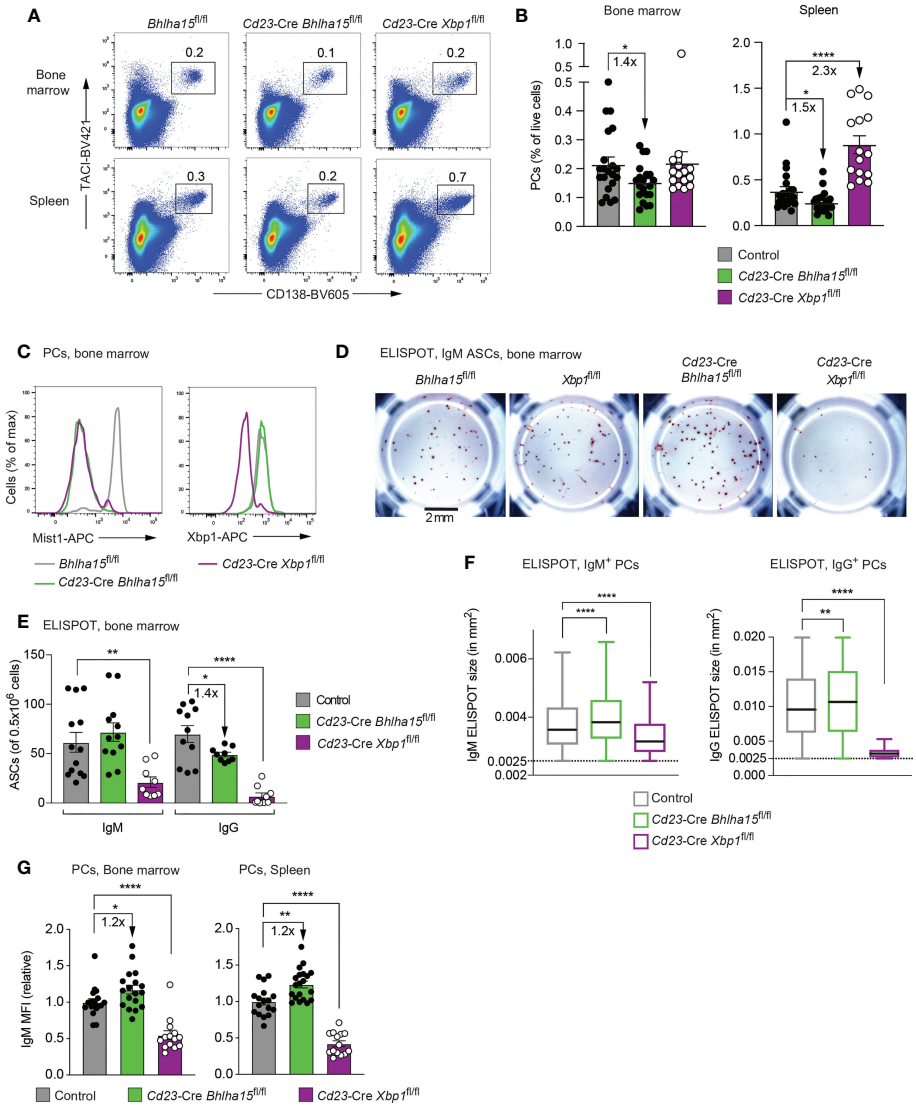


FIGURE 2
Reduced plasma cell numbers and increased antibody secretion in unimmunized *Cd23*-Cre *Bhlha15*$^{fl/fl}$ mice. **(A)** Flow-cytometric analysis of PCs (TACI$^+$CD138$^+$) in the spleen and bone marrow of 13-23-week-old mice of the indicated genotypes. The percentage of cells in the indicated gate is shown. One of 3 independent experiments with similar results is displayed. **(B)** The relative frequency of PCs in the bone marrow and spleen of 13-23-week-old mice of the indicated genotypes is shown for 3 independent experiments ($n > 18$ mice) per genotype. *Bhlha15*$^{fl/fl}$ and *Xbp1*$^{fl/fl}$ mice served as controls. **(C)** Expression of Mist1 and Xbp1 in PCs from the bone marrow of age-matched mice of the indicated genotypes, as determined by intracellular staining. One of two experiments is shown. **(D–F)** ELISPOT analysis of IgM and IgG antibody-secreting cells (ASC) from the bone marrow of age-matched mice of the indicated genotypes (see Methods). **(D)** Representative wells of an anti-IgM ELISPOT experiment. The scale bar indicates 2 mm. **(E)** Quantification of the number of IgM and IgG ASCs per 500,000 plated bone marrow cells. The combined data of two independent experiments are shown. **(F)** Size distribution of the antibody-containing dots, which were produced by the IgM and IgG ASCs shown in **(E)**. The dot sizes were automatically quantified by using the Fiji software (see Methods). Black lines indicate the median, and boxes represent the middle 50% of the data. Whiskers denote all values of the 1.5x interquartile range. Dots with a size of > 0.0025 mm$^2$ are analyzed. The results of one of 2 independent experiments are shown. **(G)** Quantification of the mean fluorescence intensity (MFI) of intracellular IgM staining in plasma cells (TACI$^+$CD138$^+$) from the bone marrow (left) and spleen (right) of 13-23-week-old mice of the indicated genotypes. The MFI values of 3 independent experiments were normalized relative to those of the control mice (mean value set to 1). Statistical data are shown as mean values with SEM and were analyzed with the unpaired Student's *t* test **(B–G)** or Mann-Whitney test **(F)**; *$P < 0.05$, **$P < 0.01$, ****$P < 0.0001$. Each dot **(B–G)** represents one mouse.

mice (Figure 2C). In the spleen, the Mist1 protein was also absent in *Cd23*-Cre *Bhlha15*$^{fl/fl}$ PCs, but was still lowly expressed in *Cd23*-Cre *Xbp1*$^{fl/fl}$ PCs (Supplementary Figure 2C). While the Xbp1 protein was lost in *Cd23*-Cre *Xbp1*$^{fl/fl}$ PCs in the bone marrow and spleen, it was similarly expressed in *Cd23*-Cre *Bhlha15*$^{fl/fl}$ and control PCs (Figure 2C and Supplementary Figure 2C). Hence, we conclude that Mist1 does not control *Xbp1* expression, while Xbp1 activates *Bhlha15* expression also in PCs. Notably, *Cd23*-Cre *Xbp1*$^{fl/fl}$ PCs were smaller in size than *Cd23*-Cre *Bhlha15*$^{fl/fl}$ and control PCs (Supplementary Figure 2D), which is likely caused by the low amount of ER in Xbp1-deficient PCs (12).

We next studied the antibody secretion of mutant PCs by performing ELISPOT analysis with bone marrow cells and found a small but significant decrease in IgG ASCs in *Cd23*-Cre *Bhlha15*$^{fl/fl}$ mice, while the number of IgM ASCs was comparable with that of control mice (Figures 2D, E and Supplementary Figure 2E). In contrast, IgG ASCs were almost lost, and IgM ASCs were significantly reduced in the bone marrow of *Cd23*-Cre *Xbp1*$^{fl/fl}$ mice (Figure 2D, E), consistent with the known role of Xbp1 in controlling antibody secretion (11, 12). Notably, the ELISPOT size of individual IgM or IgG ASCs was increased in *Cd23*-Cre *Bhlha15*$^{fl/fl}$ mice, suggesting that the antibody secretion was higher per mutant PC compared with a control PC (Figure 2F). To corroborate this result, we measured the IgM levels per plasma cell by intracellular flow-cytometric analysis and quantification of the mean fluorescence intensity (MFI), indicating that the expression of IgM was 1.2-fold increased in Bhlha15-deficient PCs compared with control PCs both in the spleen and bone marrow (Figure 2G). In this context, it is important to note that a 1.2-fold increase in IgM expression corresponds to a relatively strong transcriptional increase, as immunoglobulin transcripts account for up to 60% of all mRNAs in PCs (2, 3). Enzyme-linked immunosorbent assay (ELISA) revealed, however, normal titers of different antibody isoforms in the sera of *Cd23*-Cre *Bhlha15*$^{fl/fl}$ mice compared with control *Bhlha15*$^{fl/fl}$ mice (Supplementary Figure 2F). The normal antibody titers in *Cd23*-Cre *Bhlha15*$^{fl/fl}$ mice may be explained by the increased antibody secretion per PC (Figures 2F, G) that could compensate for the reduced PC numbers in these mice (Figures 2A, B). In contrast, *Cd23*-Cre *Xbp1*$^{fl/fl}$ mice had strongly reduced titers of all antibody isoforms compared with *Xbp1*$^{fl/fl}$ littermates (Supplementary Figure 2F). Together, these data indicate that the loss of *Bhlha15* leads to increased antibody secretion but lower numbers of plasma cells in the spleen and bone marrow.

## Mist1-dependent control of the plasma cell response to NP-KLH immunization

To study the function of Mist1 in response to a defined antigen, we immunized mice with the T cell-dependent antigen NP-KLH (in alum) and analyzed the frequency of splenic PCs and immunoglobulin secretion at day 7 after immunization. The frequency of PCs (TACI$^{+}$CD138$^{+}$) was 1.4-fold reduced in the spleen of the *Cd23*-Cre *Bhlha15*$^{fl/fl}$ mice relative to control mice (Figures 3A, B). In contrast, the percentage of splenic PCs was 2-fold increased in *Cd23*-Cre *Xbp1*$^{fl/fl}$ mice compared with control mice (Figures 3A, B). As shown by intracellular staining at day 7 after immunization, the Mist1 protein was completely lost in *Cd23*-Cre *Bhlha15*$^{fl/fl}$ PCs and was only lowly expressed in *Cd23*-Cre *Xbp1*$^{fl/fl}$ PCs (Figure 3C). We next investigated the expression of the PC regulators Xbp1, Blimp1 and Irf4 by intracellular staining and MFI quantification. The Xbp1 protein was expressed at a similar level in *Cd23*-Cre *Bhlha15*$^{fl/fl}$ and control PCs (Figures 3C, D). In contrast, the expression of Blimp1 and Irf4 was 1.3-fold increased in *Cd23*-Cre *Bhlha15*$^{fl/fl}$ PCs relative to control PCs (Figures 3C, E, F).

ELISPOT analysis of splenocytes at day 7 after immunization revealed a decrease of NP-specific IgG1 ASCs in *Cd23*-Cre *Bhlha15*$^{fl/fl}$ and *Cd23*-Cre *Xbp1*$^{fl/fl}$ mice relative to control mice (Figure 3G). The ELISPOT size of NP-IgG1 ASCs was again increased in *Cd23*-Cre *Bhlha15*$^{fl/fl}$ mice and strongly decreased in *Cd23*-Cre *Xbp1*$^{fl/fl}$ compared with control mice (Figure 3H). The serum titers of NP-IgG1 and NP-IgG2b antibodies were also similar in *Cd23*-Cre *Bhlha15*$^{fl/fl}$ and control mice, possibly reflecting compensation between increased secretion and reduced frequency of the Mist1-deficient PCs, while the titers of both antibodies were strongly reduced in *Cd23*-Cre *Xbp1*$^{fl/fl}$ mice (Figure 3I), as expected (12, 13).

In summary, our analysis of PCs *in vivo* in unimmunized or NP-KLH-immunized mice demonstrated that the loss of Mist1 resulted in decreased PC numbers but increased antibody secretion per PC.

## Normal *in vitro* differentiation and antibody secretion of plasmablasts lacking *Bhlha15*

As the *in vivo* phenotype of the *Bhlha15* mutant PCs is at odds with the reported absence of phenotypic differences between LPS-stimulated PBs derived from wild-type and *Bhlha15*$^{-/-}$ B cells (33), we reinvestigated a possible role of Mist1 in *in vitro* differentiated PBs. To this end, we analyzed PBs after 4 days of treatment with LPS and IL-4 (Supplementary Figures 3A–C) or after 8 days of stimulation in the iGB system (Supplementary Figures 3D, E). LPS plus IL-4 stimulation of B cells from *Cd23*-Cre *Bhlha15*$^{fl/fl}$ and control mice resulted in the generation of similar numbers of PBs and IgM ASCs, which were furthermore characterized by a similar ELISPOT size (Supplementary Figures 3A–C). Likewise, *Cd23*-Cre *Bhlha15*$^{fl/fl}$ and control B cells gave rise to similar numbers of IgE ASCs with a similar ELISPOT size after 8 days in the iGB system (Supplementary Figures 3D, E). While *Cd23*-Cre *Xbp1*$^{fl/fl}$ PBs were generated in similar numbers as control PBs upon

10.3389/fimmu.2022.859598

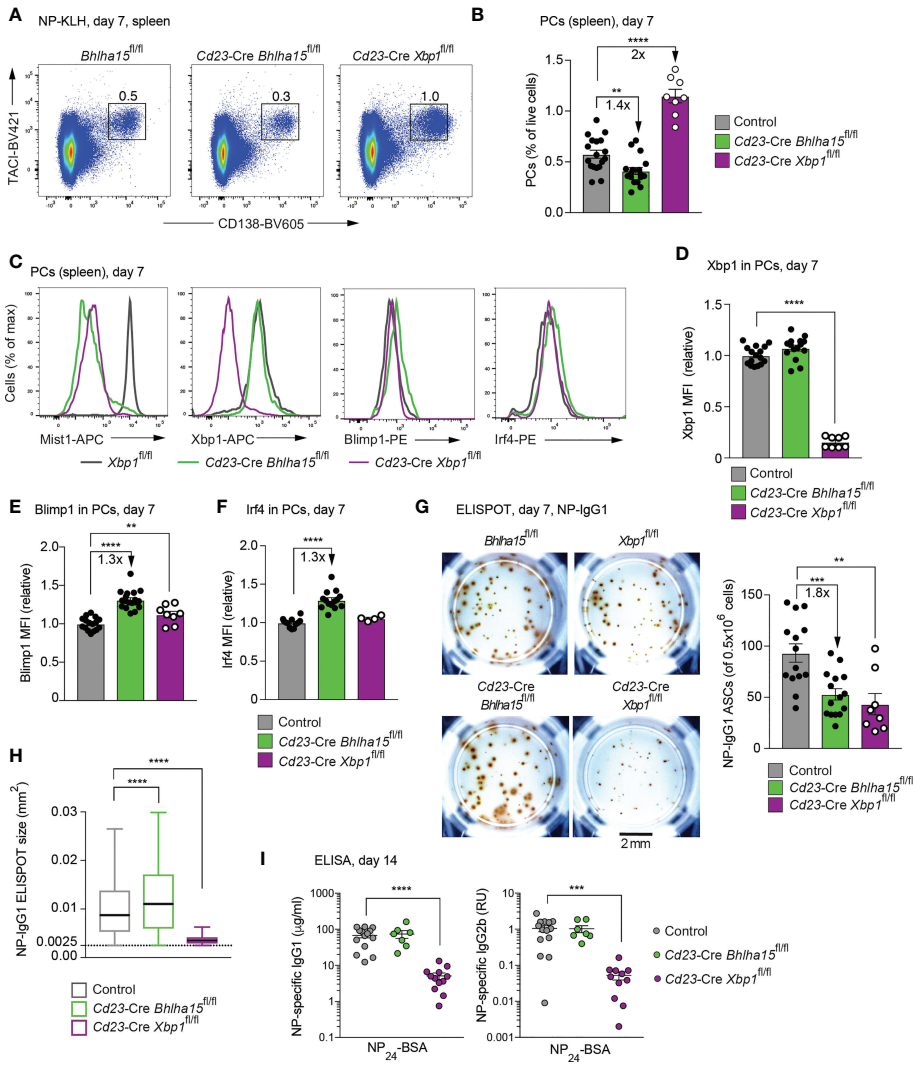


FIGURE 3
Reduced plasma cell numbers and increased antibody secretion in NP-KLH-immunized *Cd23*-Cre *Bhlha15*$^{fl/fl}$ mice. **(A)** Flow-cytometric analysis of PCs (TACI$^{+}$CD138$^{+}$) in the spleen of the indicated genotypes at day 7 after NP-KLH immunization (in alum). The percentage of cells in the indicated gate is shown. One of 2 (*Cd23*-Cre *Xbp1*$^{fl/fl}$) or 3 (*Cd23*-Cre *Bhlha15*$^{fl/fl}$ and control) independent experiments with similar results is displayed. **(B)** The relative frequency of PCs in the spleen of age-matched mice of the indicated genotypes at day 7 after NP-KLH immunization is shown for 2 or 3 independent experiments (see **A**). *Bhlha15*$^{fl/fl}$ and *Xbp1*$^{fl/fl}$ mice served as controls. **(C)** Expression of Mist1, Xbp1, Blimp1 and Irf4 in splenic PCs from mice of the indicated genotypes, as determined by intracellular staining at day 7 after NP-KLH immunization. **(D–F)** Quantification of the mean fluorescence intensity (MFI) of Xbp1 **(D)**, Blimp1 **(E)** and Irf4 **(F)** intracellular staining in PCs shown in **(C)**. The MFI values were normalized relative to those of the control mice (mean value set to 1). The results of 3 independent experiments are shown for the control and *Cd23*-Cre *Bhlha15*$^{fl/fl}$ genotypes and the results of 2 experiments are displayed for *Cd23*-Cre *Xbp1*$^{fl/fl}$ genotype. **(G)** ELISPOT analysis of NP-IgG1 ASCs from the spleen of the indicated genotypes at day 7 after NP-KLH immunization. Plates were coated with $NP_{24}$-BSA and developed using anti-IgG1 antibodies. Left: Representative ELISPOT wells with the scale bar indicating 2 mm. Right: Quantification of the number of NP-IgG1 ASCs per 500,000 plated cells. The combined data of two experiments are shown. **(H)** Size distribution of the antibody-containing dots, which were produced by the NP-IgG1 ASCs shown in **(G)**. The dot sizes were automatically quantified by using the Fiji software (see Methods). Black lines indicate the median, and boxes represent the middle 50% of the data. Whiskers denote all values of the 1.5× interquartile range. Dots with a size of > 0.0025 mm$^2$ are analyzed. The results of one of 2 experiments are shown. **(I)** Serum titers of NP-specific IgG1 or IgG2b antibodies at day 14 after NP-KLH immunization. Plates were coated with $NP_{24}$-BSA and then developed with anti-IgG1 or anti-IgG2b. The NP-IgG1 concentration was determined relative to a NP-IgG1 standard (hybridoma line SSX2.1). RU; relative units. The data of 3 independent experiments are shown. Statistical data **(B, D-I)** are indicated as mean values with SEM and were analyzed with the unpaired Student's *t* test **(B, D–G, I)** or Mann-Whitney test **(H)**; $^{**}P < 0.01$; $^{***}P < 0.001$; $^{****}$, $P < 0.0001$. Each dot **(B, D–G, I)** represents one mouse.

stimulation with LPS and IL-4 (Figure 4A), they exhibited a severe defect in antibody secretion in both differentiation systems, as shown by the reduced numbers of ASCs and their smaller ELISPOT size, consistent with published data (12). We conclude therefore that *in vitro* PB differentiation did not recapitulate the *in vivo* phenotype of *Cd23*-Cre *Bhlha15*$^{fl/fl}$ PCs, as the respective *in vitro* differentiated PBs were generated in normal numbers and exhibited normal antibody secretion.

## Normal cellular morphology of Mist1-deficient plasma cells *in vivo*

We next analyzed the cellular architecture of *in vivo* PCs by electron microscopy (EM). For this, we sorted PCs as Lin$^-$ B220$^{int}$CD138$^{hi}$CD28$^+$ cells from the bone marrow of unimmunized mice by flow cytometry prior to EM analysis. The cytoplasm of *Cd23*-Cre *Xbp1*$^{fl/fl}$ PCs contained little ER, which was thin and disorganized (Figures 4A, B and Supplementary Figure 4A). By measuring the ER mass per section, we confirmed a significant reduction of the ER in the *Cd23*-Cre *Xbp1*$^{fl/fl}$ PCs relative to *Xbp1*$^{fl/fl}$ PCs (Figure 4B), which is consistent with the observed small size of Xbp1-deficient PCs (Supplementary Figure 2D). A previous EM analysis of *Cd19*-Cre *Xbp1*$^{fl/fl}$ PCs demonstrated that, in addition to the low ER content, the Xbp1-deficient plasma cells also contained large vesicular structures (12) that we did, however, not detect in our analysis. The *Cd23*-Cre *Bhlha15*$^{fl/fl}$ and control PCs had the same large size and a similarly extended network of well-stacked ER, whose cytosolic surfaces were densely occupied with ribosomes (Figure 4A and Supplementary Figure 4A). As shown by quantification of the ER mass, the *Cd23*-Cre *Bhlha15*$^{fl/fl}$ and control PCs had a similar content of ER (Figure 4B). Moreover, at day 7 after NP-KLH immunization, splenic PCs of *Cd23*-Cre *Bhlha15*$^{fl/fl}$ and control mice were equally stained with a Golgi-Tracker or ER-Tracker

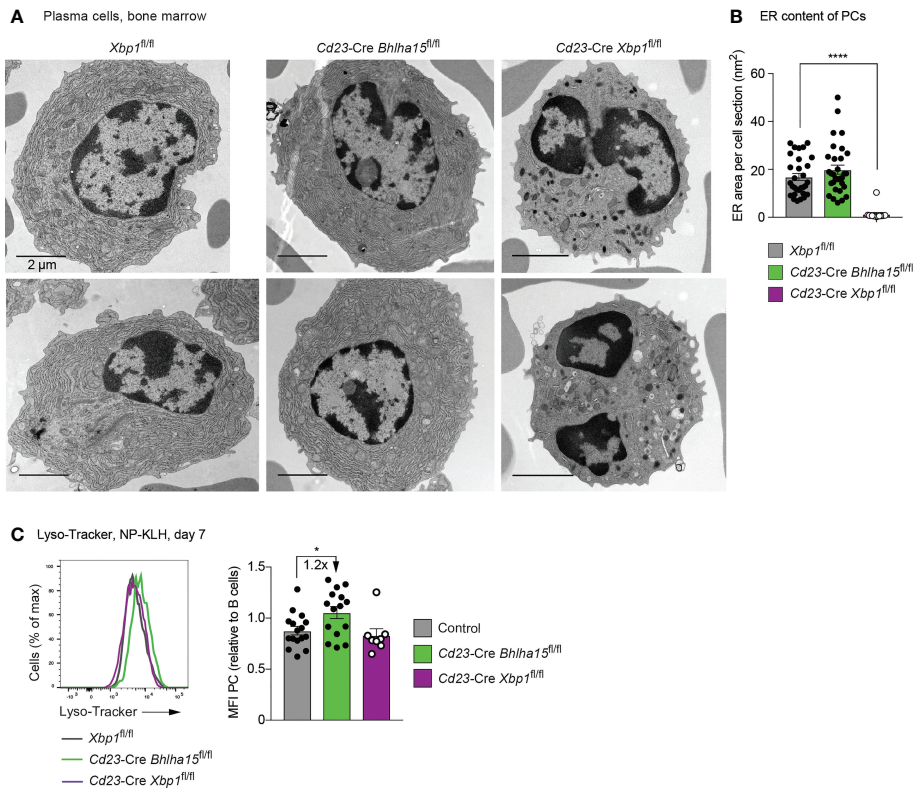


FIGURE 4
Normal morphological structure of *Cd23*-Cre *Bhlha15*$^{fl/fl}$ plasma cells. **(A)** Electron microscopic analysis of bone marrow PCs of the indicated genotypes, which were sorted as B220$^{int}$CD138$^+$CD138$^+$Lin$^-$ cells, fixed and processed as described in Methods. The scale bars indicate 2 µm. The cells surrounding the PCs are erythrocytes. **(B)** Quantification of the content of endoplasmic reticulum (ER) in PCs of the different genotypes. The ER content was manually determined by using the Fiji software. Each dot represents one PC. In total, 33 *Xbp1*$^{fl/fl}$ PCs, 14 *Cd23*-Cre *Xbp1*$^{fl/fl}$ PCs, and 31 *Cd23*-Cre *Bhlha15*$^{fl/fl}$ PCs were analyzed. **(C)** Staining of splenic PCs (TACI$^+$CD138$^+$) of the indicated genotypes with Lyso-Tracker at day 7 after NP-KLH immunization (left). The MFI values of the Lyso-Tracker staining (right) are shown for all PCs analyzed in 3 independent experiments. Each dot represents one mouse. Statistical data **(B, C)** are shown as mean values with SEM and were analyzed with the unpaired Student's *t* test; *$P < 0.05$; ****$P < 0.0001$.

fluorescent dye (Supplementary Figures 4B, C). Based on these data, we conclude that the *Cd23*-Cre *Bhlha15*$^{fl/fl}$ and control PCs have a similar ultrastructure. Upon staining with the Lyso-Tracker fluorescent dye, the *Cd23*-Cre *Bhlha15*$^{fl/fl}$ PCs exhibited a 1.2-fold increase in staining intensity compared to control PCs (Figure 4C), which indicates an increase of acidic compartments in the absence of Mist1. The *Cd23*-Cre *Xbp1*$^{fl/fl}$ PCs in contrast displayed significantly reduced Golgi-Tracker and ER-Tracker staining (Supplementary Figures 4B, C), while the Lyso-Tracker staining was comparable to that of control cells (Figure 4C).

As changes in ER and Golgi structures can lead to altered glycosylation patterns of antibodies (36), we analyzed the glycoprofiles by assessing the relative abundance of IgG3-specific glycopeptide glycoforms purified from mouse serum by liquid chromatography electrospray ionization mass spectrometry (LC-ESI-MS). IgG3 peptides from *Cd23*-Cre *Xbp1*$^{fl/fl}$ mice exhibited altered glycoprofiles defined by reduced fucosylation (GnGnF) and increased sialylation (NgAF, NgNgF), when compared to IgG3 peptides from *Cd23*-Cre *Bhlha15*$^{fl/fl}$ and control mice (Supplementary Figure 2G). Additionally, the sera of *Cd23*-Cre *Xbp1*$^{fl/fl}$ mice contained non-fucosylated GnGn and AGn glycoforms, which were absent in the sera of *Cd23*-Cre *Bhlha15*$^{fl/fl}$ and control mice (Supplementary Figure 2G). Hence, the glycosylation of antibodies is altered in *Cd23*-Cre *Xbp1*$^{fl/fl}$ PCs consistent with the observed defect in ER structure. The similar glycosylation pattern of IgG3 in *Cd23*-Cre *Bhlha15*$^{fl/fl}$ and control PCs further demonstrates that the ER and Golgi structures are functional in the absence of Mist1.

## Mist1-binding regions overlap with E2A peaks in plasmablasts

We next performed RNA- and ChIP-seq experiments to investigate the role of Mist1 in PCs. For ChIP-seq analysis, we took advantage of the fact that the floxed *Bhlha15* allele contains an N-terminal insertion of a biotin acceptor sequence (35). Splenic B cells from *Bhlha15*$^{fl/fl}$ *Rosa26*$^{BirA/BirA}$ mice were stimulated with LPS for 4 days and then enriched for CD138$^{+}$ PBs by immunomagnetic sorting (Supplementary Figure 5A), followed by Bio-ChIP-seq analysis (22). Peak calling of the data of two Bio-ChIP-seq experiments with a $P$ value of $< 10^{-10}$ identified 35,342 and 36,634 Mist1 peaks, resulting in an overlap of 30,212 common peaks that were used for subsequent analysis (Figure 5A). A large fraction of the Mist1 peaks was located in gene bodies (49%; Figure 5B), indicating that Mist1 binds less frequently to TSS regions (21%) relative to Xbp1 (38%) (Figure 1D). *De novo* motif discovery analysis of the Mist1 peak sequences identified a consensus Mist1-binding motif (Figure 5C) that resembles the consensus binding motif of the bHLH transcription factor E2A (Supplementary Figure 5B) (27).

We next overlapped the Mist1 peaks with the 11,872 E2A peaks that we previously identified in LPS-differentiated PBs (27). Notably, 94% of all E2A peaks overlapped with Mist1 peaks (Supplementary Figure 5C), suggesting that the Mist1 homodimers may bind to the same recognition sequences as E2A homodimers or E2A-E2-2 heterodimers in PBs. Alternatively, it is conceivable that Mist1 forms heterodimers with E2A in PBs, as previously shown in a myoblast cell line (37). Streptavidin pulldown of biotinylated Mist1 from nuclear extracts of LPS-differentiated *Bhlha15*$^{fl/fl}$ *Rosa26*$^{BirA/BirA}$ PBs revealed that E2A was co-precipitated with Mist1, indicating that both bHLH proteins can form heterodimers also in PBs (Supplementary Figure 5D). Consistent with this finding, co-binding of Mist1 and E2A was observed in PBs at many previously identified elements (27) of the *Prdm1* (Blimp1) locus (Supplementary Figure 5G). Together, these data suggest that Mist1 and E2A can bind their genomic recognition sequences as heterodimers in PBs.

## Mist1 and Xbp1 regulate largely distinct gene expression programs in plasma cells

We next performed RNA-seq analysis with *ex vivo* sorted TACI$^{+}$CD138$^{+}$ PCs from the spleen of *Bhlha15*$^{fl/fl}$ and *Cd23*-Cre *Bhlha15*$^{fl/fl}$ mice 7 days after NP-KLH immunization. Comparison of the two RNA-seq datasets identified 87 Mist1-activated and 11 Mist1-repressed genes, which were selected for an expression difference of > 3-fold, an adjusted $P$ value of < 0.05 and an expression value of > 5 TPM in *Bhlha15*$^{fl/fl}$ PCs (activated genes) or *Cd23*-Cre *Bhlha15*$^{fl/fl}$ PCs (repressed genes), respectively (Figure 5D and Supplementary Figure 5E, Supplementary Table 2). Interestingly, 81 of the 87 activated genes were bound by Mist1 in contrast to only 1 of the 11 repressed genes, indicating that Mist1 mainly functions a transcriptional activator in PCs. The most prominent functional classes of Mist1-activated genes code for 12 metabolic proteins, 12 transporters and 10 signaling molecules, while genes implicated in UPR and ER function were not regulated by Mist1 (Figure 5E). Seven activated Mist1 target genes code for transcriptional (Zfp667, Cited4, Creb3l1, Hdac1) and translational (Rps27l, Eed1akmt3) regulators as well as for the autophagy-controlling Asah2 protein (Figure 5F). Similar to the observed increase of Blimp1 and Irf4 protein expression (Figures 3E, F), the *Prdm1* and *Irf4* mRNA expression was also moderately upregulated in Mist1-deficient PCs (Figure 5G), consistent with Mist1 binding at both genes (Supplementary Figures 5F, G). Moreover, only 8 genes were deregulated more than 3-fold in both Mist1-deficient PCs and Xbp1-deficient PBs (Supplementary Figure 5H), indicating that both factors largely regulate distinct gene expression programs in PBs.

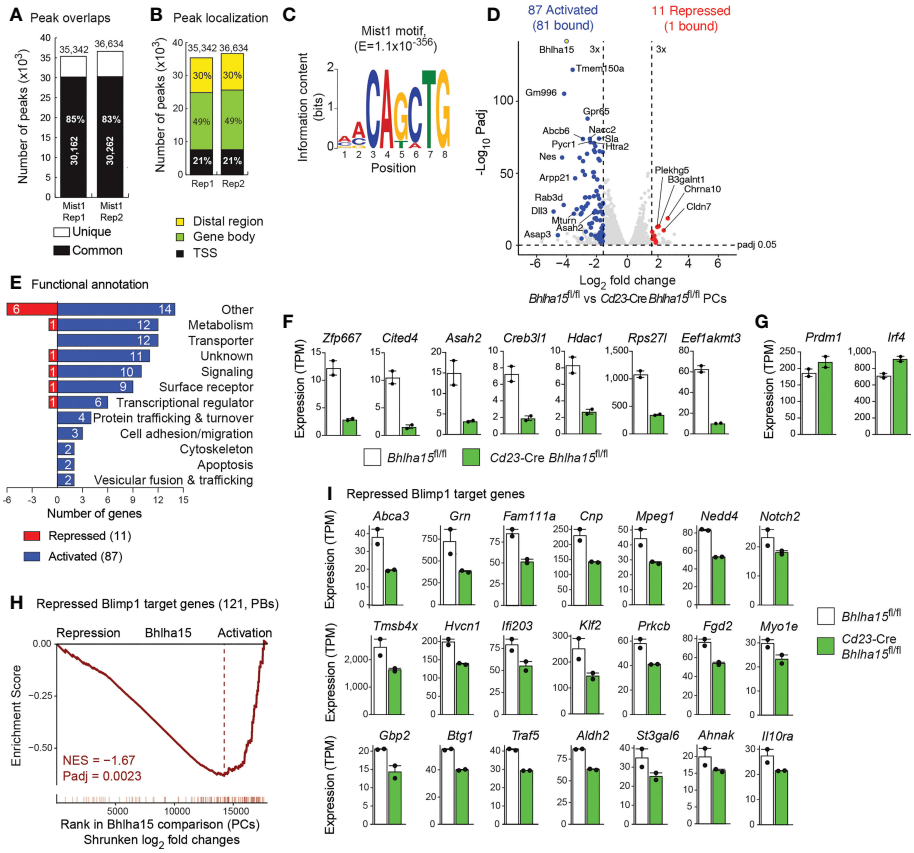


FIGURE 5
Mist1-dependent gene expression program in plasma cells. **(A–C)** Genome-wide Mist1 binding in PBs that were *in vitro* differentiated for 4 days by LPS stimulation of CD43$^-$ B cells from the spleen of *Bhlha15*$^{fl/fl}$ *Rosa26*$^{BirA/BirA}$ mice. CD138$^+$ PBs, which were purified by immunomagnetic enrichment with CD138-MicroBeads, were used for Bio-ChIP-seq analysis (22), and Mist1 peaks were identified by MACS peak calling with a stringent *P* value of < $10^{-10}$. **(A)** Overlap and number of Mist1 peaks identified in two Bio-ChIP-seq replica (Rep) experiments. **(B)** Presence of Mist1 peaks in distal regions, gene bodies and promoter (TSS) regions. Mist1 peaks were assigned to genes, as described (22). **(C)** Consensus Mist1-binding motif identified with an E-value of 1 x $10^{-356}$ by the *de novo* motif-discovery program MEME-Chip. **(D)** Volcano plot of gene expression differences between *Cd23*-Cre *Bhlha15*$^{fl/fl}$ and control *Bhlha15*$^{fl/fl}$ PCs that were sorted as TACI$^+$CD138$^+$ cells from the spleen at day 7 after NP-KLH immunization. Two independent RNA-seq experiments were performed with PCs of each genotype. Each dot corresponds to one gene, whose expression is plotted as $\log_2$-fold change against the -$\log_{10}$ adjusted *P* value. Genes with an expression difference of > 3-fold, an adjusted *P* value of < 0.05 and an expression value of > 5 TPM (at least in one sample) are colored in blue or red corresponding to activation or repression by Mist1, respectively. **(E)** Functional classification and quantification (number) of proteins encoded by Mist1-activated and Mist1-repressed genes. **(F)** Expression of selected activated Mist1 target genes in *Cd23*-Cre *Bhlha15*$^{fl/fl}$ and *Bhlha15*$^{fl/fl}$ PCs. **(G)** Expression of *Prdm1* and *Irf4* in *Cd23*-Cre *Bhlha15*$^{fl/fl}$ and *Bhlha15*$^{fl/fl}$ PCs. **(H)** GSEA analysis of 121 repressed Blimp1 target genes (3), as compared to their ranked shrunken $\log_2$-fold gene expression changes in *Cd23*-Cre *Bhlha15*$^{fl/fl}$ PCs versus *Bhlha15*$^{fl/fl}$ PCs. NES, normalized enrichment score. **(I)** Expression of repressed Blimp1 target genes in *Bhlha15*$^{fl/fl}$ and *Cd23*-Cre *Bhlha15*$^{fl/fl}$ PCs, as determined by RNA-seq. All depicted genes are significantly deregulated with an adjusted *P* value of < 0.05.

As Blimp1 (*Prdm1*) expression was increased in Mist1-deficient PCs (Figures 3E, 5G), we next used the previously identified 121 repressed Blimp1 target genes (3) for gene set enrichment analysis (GSEA) of the RNA-seq data of control and Mist1-deficient PCs. Interestingly, there was a strong correlation between repressed Blimp1 target genes and Mist1-activated genes (Figure 5H). Importantly however, there was no overlap between the published repressed Blimp1 target genes (> 3-fold) (3) and the Mist1-activated genes (> 3-fold; Figure 5D and Supplementary Table 2). In contrast, the expression of most Blimp1-repressed target genes (3) was modestly (≤ 2-fold) reduced in *Cd23*-Cre *Bhlha15*$^{fl/fl}$ PCs compared with control *Bhlha15*$^{fl/fl}$ PCs (Figure 5I). This repression is likely caused by the increased expression of Blimp1 in *Cd23*-Cre *Bhlha15*$^{fl/fl}$ PCs and may thus not reflect direct activation by Mist1. In summary, we conclude that Mist1 regulates a largely different gene expression program than Xbp1 and further represses Blimp1 target genes by activating *Prdm1* expression in PCs.

## Reduced Blimp1 expression rescues the cell number and antibody secretion of Mist1-deficient plasma cells

Blimp1 is known to contribute to antibody secretion by strongly activating the transcription of the *Igh* and *Igk* genes and by regulating the posttranscriptional expression switch from the membrane-bound form to the secreted form of the Ig heavy chain (3). Hence, it is conceivable that the increased Blimp1 expression in *Cd23*-Cre *Bhlha15*$^{fl/fl}$ PCs may be responsible for the observed increase in antibody secretion in addition to the moderate repression of its target genes. To test this hypothesis, we took advantage of the *Prdm1*$^{Gfp}$ null allele (38) to reduce the expression of Blimp1 by a factor of two in bone marrow PCs of unimmunized *Prdm1*$^{Gfp/+}$ *Cd23*-Cre *Bhlha15*$^{fl/fl}$ mice. While the frequency of PCs was 1.8-fold reduced in *Cd23*-Cre *Bhlha15*$^{fl/fl}$ mice compared to control *Bhlha15*$^{fl/fl}$ mice, it was 1.5-fold increased in *Prdm1*$^{Gfp/+}$ *Cd23*-Cre *Bhlha15*$^{fl/fl}$ mice relative to *Cd23*-Cre *Bhlha15*$^{fl/fl}$ mice and thus reached a similar level observed in control *Bhlha15*$^{fl/fl}$ and *Prdm1*$^{Gfp/+}$ *Bhlha15*$^{fl/fl}$ mice (Figures 6A, B). Moreover, the frequencies of both the less mature GFP(Blimp1)$^{lo}$ and more mature GFP(Blimp1)$^{hi}$ PCs (38) were equally but only moderately reduced in *Prdm1*$^{Gfp/+}$ *Cd23*-Cre *Bhlha15*$^{fl/fl}$ compared to control *Prdm1*$^{Gfp/+}$ *Bhlha15*$^{fl/fl}$ mice (Figures 6C, D). Importantly, the expression of IgM was 1.4-fold increased only in PCs of *Cd23*-Cre *Bhlha15*$^{fl/fl}$ PCs but not in PCs of *Prdm1*$^{Gfp/+}$ *Cd23*-Cre *Bhlha15*$^{fl/fl}$ mice or the control *Prdm1*$^{Gfp/+}$ *Bhlha15*$^{fl/fl}$ and *Bhlha15*$^{fl/fl}$ mice, as shown by intracellular staining (Figure 6E). Hence, a 2-fold reduction of Blimp1 expression restored both PC numbers and IgM expression in *Prdm1*$^{Gfp/+}$ *Cd23*-Cre *Bhlha15*$^{fl/fl}$ mice. These data therefore indicate that Mist1 largely mediates its effects on plasma cells by restraining Blimp1 expression.

# Discussion

An essential function of the transcription factor Xbp1 is to activate the UPR gene expression program upon induced ER

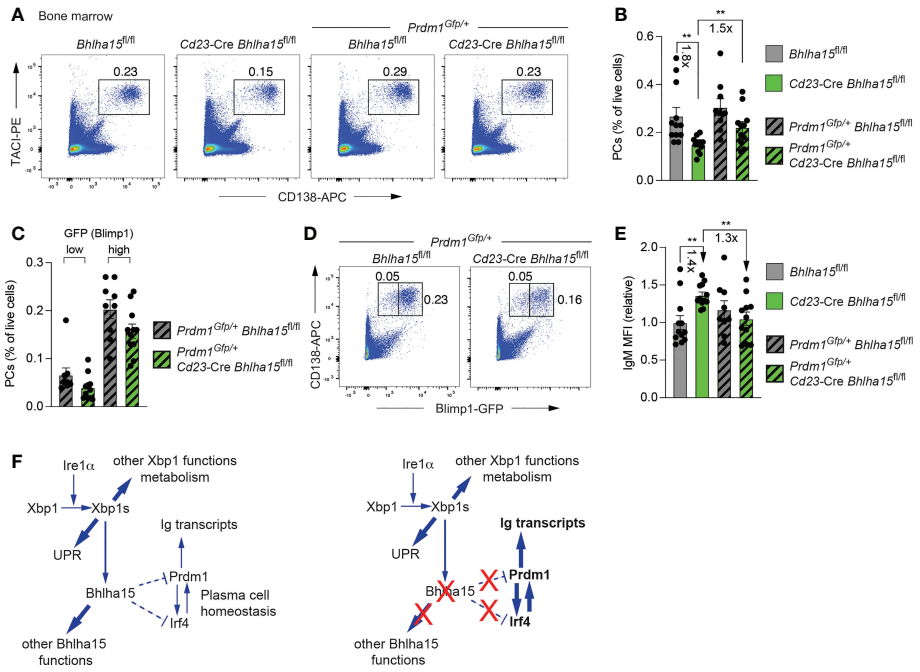


FIGURE 6
Reduced Blimp1 expression rescues the cell number and antibody secretion of Mist1-deficient plasma cells. **(A)** Flow-cytometric analysis of PCs (TACI$^+$CD138$^+$) in the bone marrow of unimmunized 10-13-week-old mice of the indicated genotypes. The percentage of cells in the gate is indicated. One of two independent experiments is shown. **(B)** Frequency of bone marrow PCs in unimmunized mice of the indicated genotypes. The frequencies were calculated based on the data of two independent experiments performed with *Bhlha15*$^{fl/fl}$ ($n$ = 12), *Cd23*-Cre *Bhlha15*$^{fl/fl}$ ($n$ = 12), *Prdm1*$^{Gfp/+}$ *Bhlha15*$^{fl/fl}$ ($n$ = 9) and *Prdm1*$^{Gfp/+}$ *Cd23*-Cre *Bhlha15*$^{fl/fl}$ ($n$ = 11) mice. **(C, D)** Flow cytometric analysis of GFP (Blimp1) expression in PCs (GFP$^+$CD138$^+$) from the bone marrow of *Prdm1*$^{Gfp/+}$ *Cd23*-Cre *Bhlha15*$^{fl/fl}$ and control *Prdm1*$^{Gfp/+}$ *Bhlha15*$^{fl/fl}$ mice **(D)**. Frequency of GFP$^{hi}$ and GFP$^{lo}$ PCs in the bone marrow of *Prdm1*$^{Gfp/+}$ *Cd23*-Cre *Bhlha15*$^{fl/fl}$ and *Prdm1*$^{Gfp/+}$ *Bhlha15*$^{fl/fl}$ mice **(C)**. **(E)** Quantification of the mean fluorescence intensity (MFI) of intracellular IgM staining in bone marrow PCs (TACI$^+$CD138$^+$) of unimmunized mice with the genotypes and mouse numbers described in **(B)**. The MFI data are shown relative to the mean value of the *Bhlha15*$^{fl/fl}$ PCs (set to 1). **(F)** Model explaining how the loss of *Bhlha15* (Mist1) influences the regulatory networks controlling PC homeostasis and antibody secretion. Statistical data are shown as mean values with SEM and were analyzed with the unpaired Student's $t$ test (**B**, **C**, **E**); $^{**}P < 0.01$. Each dot **(B, C, E)** represents one mouse.

stress in most cell types (39) and to promote antibody secretion at a high rate in PBs and PCs of the B cell lineage (7, 11, 12). By analyzing the Xbp1-dependent gene expression program in PBs, we identified the *Bhlha15* (Mist1) gene as the most strongly activated direct target gene of Xbp1. Mist1 was previously shown to play an important role in other secretory cell types by inducing and maintaining their secretory cell architecture (15–18). By systematically investigating the phenotype of Mist1-deficient PCs *in vivo* in unimmunized and NP-KLH-immunized mice, we realized that antibody secretion was moderately increased in Mist1-deficient PCs, in marked contrast to the strong reduction of antibody secretion in Xbp1-deficient PCs (12, 13). Although Mist1 is also not expressed in the absence of Xbp1, the loss of immunoglobulin secretion in Xbp1-deficient PCs interferes with the manifestation of the Mist1-deficient phenotype, which appears to be largely caused by increased immunoglobulin secretion. Molecular analyses revealed that Mist1 and Xbp1 regulate largely different sets of target genes, as Xbp1 regulates UPR genes involved in ER expansion and antibody secretion, while Mist1 restrains the expression of Blimp1 and Irf4 in PCs.

A previous study investigating the role of Mist1 in LPS-stimulated *Bhlha15*$^{-/-}$ PBs (33) did not report any differences in the formation and function of mutant and wild-type PBs, which is consistent with our finding that *Cd23*-Cre *Bhlha15*$^{fl/fl}$ and control B cells differentiated *in vitro* to PBs at equal frequency in response to LPS stimulation or treatment with IL-21 in the iGB system. A second study also did not find significant differences in the generation and function of splenic PCs *in vivo* by analyzing few immunized *Bhlha15*$^{-/-}$ and wild-type mice (34). In our comprehensive study, we performed multiple experiments to analyze *in vivo* PCs in the spleen and bone marrow of *Cd23*-Cre *Bhlha15*$^{fl/fl}$ and control mice under steady-state condition and upon immunization, which allowed us to detect a significant decrease in PCs and a significant increase in antibody secretion in the *Bhlha15* mutant mice.

In the absence of Mist1, PCs were not only reduced in number but also secreted more antibodies per cell, based on their increased immunoglobulin protein expression and larger ELISPOT size. Consistent with efficient antibody secretion, Mist1-deficient PCs had a similar cell size and content of well-stacked rough ER as control PCs. While a previous study reported subtle difference in the ER structure of two analyzed Mist1-deficient PCs in the small intestine (33), we provide now statistically relevant data for our observation that Mist1-deficient PCs in the bone marrow have a normal ER ultrastructure.

The enhanced antibody production and secretion in Mist1-deficient PCs likely increases the ER stress, which may impair cell survival, thus explaining the reduced PC numbers in *Cd23*-Cre *Bhlha15*$^{fl/fl}$ mice. In this context, it is important to mention that autophagy is known to restrain antibody secretion in PCs, thereby promoting homeostasis and survival of PCs (40). Autophagy-deficient PBs show increased antibody secretion, Blimp1 expression and apoptosis, similar to the Mist1-deficient PCs. Interestingly, Lyso-Tracker staining of Mist1-deficient PCs revealed an increase in acidic compartments consisting of lysosomes or autophagosomes. The Mist1-activated gene *Asah2* (nCDase) has been implicated in the control of autophagy, as its inactivation in mouse embryonic fibroblasts results in increased autophagy (41). The downregulation of this gene in Mist1-deficient PCs (Figure 5F) may explain the observed increase in acidic compartments, which likely indicates enhanced autophagy. This observation therefore suggests that enhanced autophagy is not able to correct the Blimp1-induced increase of antibody secretion in Mist1-deficient PCs.

The elevated expression of the PC-specific transcription factor Blimp1 is likely responsible for the increased antibody secretion by Mist1-deficient PCs, as Blimp1 is known to strongly activate the transcription of the *Igh* and *Igk* genes *via* their 3' enhancer and to regulate the posttranscriptional expression switch from the membrane-bound form to the secreted form of the Ig heavy chain (3) (Figure 6F). In addition to Blimp1, the expression of Irf4, another essential PC regulator, is also increased in Mist1-deficient PCs. Irf4 and Blimp1 appear to cross-regulate each other, as Irf4 activates *Prdm1* (Blimp1) expression at the onset of PB differentiation (5, 6), while Blimp1 further induces *Irf4* expression in PBs (3) (Figure 6F). Both *Irf4* and *Prdm1* are bound by Mist1 and thus qualify as potentially repressed Mist1 target genes, although DNA-binding data alone can only suggest, but not prove, a direct role of Mist1 in the repression of *Prdm1*, *Irf4* or both genes (Figure 6F). Importantly, a 2-fold reduction of Blimp1 expression was sufficient to restore both PC numbers and antibody expression in *Prdm1*$^{Gfp/+}$ *Cd23*-Cre *Bhlha15*$^{fl/fl}$ mice. These genetic data therefore demonstrate that Mist1 largely mediates its effects on plasma cells by restraining Blimp1 expression (Figure 6F).

Mist1 lacks a transactivation domain (14), and its homodimer is therefore considered to act as a transcriptional repressor (37). However, Mist1 predominantly functions as a transcriptional activator in PCs, as shown by our transcriptomic analysis. Here, we demonstrate that Mist1 can heterodimerize with the E-protein E2A in PBs, as it was previously shown in a myoblast cell line (37). Moreover, the majority of all E2A-binding sites in PBs (27) were also bound by Mist1, suggesting that Mist1 may bind DNA as an Mist1-E2A heterodimer in PBs. As E2A contains two strong transactivation domains (42, 43), it is likely that Mist1 can activate gene expression in PCs primarily by recruiting E2A as a Mist1-E2A heterodimer to the activated Mist1 target genes.

In summary, our study has identified Mist1 as a critical regulator that restrains Blimp1 expression and thus reduces

antibody secretion to promote PC viability similar to the role of autophagy in PCs (40).

## Data availability statement

The RNA-seq and ChIP-seq data, which were generated for this study (Supplementary Table 3), are available at the Gene Expression Omnibus (GEO) repository under the accession numbers GSE190591.

## Ethics statement

The animal study was reviewed and approved by the Magistratsabteilung 58, Amt der Wiener Landesregierung, City of Vienna.

## Author contributions

MW performed most experiments, TP performed the flow-cytometric analyses of unimmunized PCs, the intracellular staining of IgM expression and the Blimp1 rescue experiments, PB performed the Xbp1 ChIP-seq experiment, AH and JS performed the glycosylation analysis, DK-P generated the *Xbp1*$^{Bio/+}$ mouse, SK generated the *Bhlh15*$^{fl/fl}$ mouse, MJ and MF performed the bioinformatic analysis of the RNA-seq and ChIP-seq data, respectively, MB and MW planned the project and wrote the manuscript. All authors contributed to the article and approved the submitted version.

## Funding

The authors declare that this study received funding from Boehringer Ingelheim. The funder was not involved in the study design, collection, analysis, interpretation of data, the writing of this article, or the decision to submit it for publication. This research was also supported by the European Research Council (ERC) under the European Union's Horizon 2020 research and innovation program (grant agreement No 740349-PlasmaCellControl), the Austrian Research Promotion Agency (Early Stage Grant 'Molecular Control' FFG-878286) and a PhD fellowship of the Boehringer Ingelheim Fonds (to TP).

## Acknowledgments

We thank L.H. Glimcher for providing *Xbp1*$^{fl/fl}$ mice, S.L. Nutt for *Prdm1*$^{Gfp/+}$ mice, J. Tellier and S.L. Nutt for discussion of Xbp1-regulated genes identified in LPS-stimulated PBs, G. Schmauß, M. Nezhyba and M. Weninger for FACS sorting, T. Lendl for writing the program script for ELISPOT size analysis, A. Sommer and his team at the Vienna BioCenter Core Facilities (VBCF) for Illumina sequencing and N. Drexler at VBCF for electron microscopy.

## Conflict of interest

The authors declare that the research was conducted in the absence of any commercial or financial relationships that could be construed as a potential conflict of interest.

## Publisher's note



## Supplementary material

The Supplementary Material for this article can be found online at: https://www.frontiersin.org/articles/10.3389/fimmu.2022.859598/full#supplementary-material

## References

1. Nutt SL, Hodgkin PD, Tarlinton DM, Corcoran LM. The generation of antibody-secreting plasma cells. *Nat Rev Immunol* (2015) 15:160–71. doi: 10.1038/nri3795

2. Shi W, Liao Y, Willis SN, Taubenheim N, Inouye M, Tarlinton DM, et al. Transcriptional profiling of mouse B cell terminal differentiation defines a signature for antibody-secreting plasma cells. *Nat Immunol* (2015) 16:663–73. doi: 10.1038/ni.3154

3. Minnich M, Tagoh H, Bönelt P, Axelsson E, Fischer M, Cebolla B, et al. Multifunctional role of the transcription factor Blimp-1 in coordinating plasma cell differentiation. *Nat Immunol* (2016) 17:331–43. doi: 10.1038/ni.3349

4. Shaffer AL, Lin KI, Kuo TC, Yu X, Hurt EM, Rosenwald A, et al. Blimp-1 orchestrates plasma cell differentiation by extinguishing the mature B cell gene expression program. *Immunity* (2002) 17:51–62. doi: 10.1016/S1074-7613(02)00335-7

5. Kwon H, Thierry-Mieg D, Thierry-Mieg J, Kim HP, Oh J, Tunyaplin C, et al. Analysis of interleukin-21-induced *Prdm1* gene regulation reveals functional cooperation of STAT3 and IRF4 transcription factors. *Immunity* (2009) 31:941–52. doi: 10.1016/j.immuni.2009.10.008

6. Sciammas R, Shaffer AL, Schatz JH, Zhao H, Staudt LM, Singh H. Graded expression of interferon regulatory factor-4 coordinates isotype switching with

plasma cell differentiation. *Immunity* (2006) 25:225–36. doi: 10.1016/j.immuni.2006.07.009

7. Shaffer AL, Shapiro-Shelef M, Iwakoshi NN, Lee AH, Qian SB, Zhao H, et al. XBP1, downstream of Blimp-1, expands the secretory apparatus and other organelles, and increases protein synthesis in plasma cell differentiation. *Immunity* (2004) 21:81–93. doi: 10.1016/j.immuni.2004.06.010

8. Bettigole SE, Glimcher LH. Endoplasmic reticulum stress in immunity. *Annu Rev Immunol* (2015) 33:107–38. doi: 10.1146/annurev-immunol-032414-112116

9. Yoshida H, Matsui T, Yamamoto A, Okada T, Mori K. XBP1 mRNA is induced by ATF6 and spliced by IRE1 in reponse to ER stress to produce a highly active transcription factor. *Cell* (2001) 107:881–91. doi: 10.1016/S0092-8674(01)00611-0

10. Calfon M, Zeng H, Urano F, Till JH, Hubbard SR, Harding HP, et al. IRE1 couples endoplasmic reticulum load to secretory capacity by processing the *XBP-1* mRNA. *Nature* (2002) 415:92–6. doi: 10.1038/415092a

11. Reimold AM, Iwakoshi NN, Manis J, Vallabhajosyula P, Szomolanyl-Tsuda E, Gravallese EM, et al. Plasma cell differentiation requires the transcription factor XBP-1. *Nature* (2001) 412:300–7. doi: 10.1038/35085509

12. Taubenheim N, Tarlinton DM, Crawford S, Corcoran LM, Hodgkin PD, Nutt SL. High rate of antibody secretion is not integral to plasma cell differentiation as revealed by XBP-1 deficiency. *J Immunol* (2012) 189:3328–38. doi: 10.4049/jimmunol.1201042

13. Tellier J, Shi W, Minnich M, Liao Y, Crawford S, Smyth GK, et al. Blimp-1 controls plasma cell function through the regulation of immunoglobulin secretion and the unfolded protein response. *Nat Immunol* (2016) 17:323–30. doi: 10.1038/ni.3348

14. Lemercier C, To RQ, Swanson BJ, Lyons GE, Konieczny SF. Mist1: A novel basic helix-loop-helix transcription factor exhibits a developmentally regulated expression pattern. *Dev Biol* (1997) 182:101–13. doi: 10.1006/dbio.1996.8454

15. Pin CL, Rukstalis JM, Johnson C, Konieczny SF. The bHLH transcription factor Mist1 is required to maintain exocrine pancreas cell organization and acinar cell identity. *J Cell Biol* (2001) 155:519–30. doi: 10.1083/jcb.200105060

16. Huh WJ, Esen E, Geahlen JH, Bredemeyer AJ, Lee AH, Shi G, et al. XBP1 controls maturation of gastric zymogenic cells by induction of MIST1 and expansion of the rough endoplasmic reticulum. *Gastroenterology* (2010) 139:2038–49. doi: 10.1053/j.gastro.2010.08.050

17. Direnzo D, Hess DA, Damsz B, Hallett JE, Marshall B, Goswami C, et al. Induced Mist1 expression promotes remodeling of mouse pancreatic acinar cells. *Gastroenterology* (2012) 143:469–80. doi: 10.1053/j.gastro.2012.04.011

18. Lo HG, Jin RU, Sibbel G, Liu D, Karki A, Joens MS, et al. A single transcription factor is sufficient to induce and maintain secretory cell architecture. *Genes Dev* (2017) 31:154–71. doi: 10.1101/gad.285684.116

19. Nojima T, Haniuda K, Moutai T, Matsudaira M, Mizokawa S, Shiratori I, et al. *In-vitro* derived germinal centre B cells differentially generate memory B or plasma cells *in vivo*. *Nat Commun* (2011) 2:465. doi: 10.1038/ncomms1475

20. Hetz C, Lee AH, Gonzalez-Romero D, Thielen P, Castilla J, Soto C, et al. Unfolded protein response transcription factor XBP-1 does not influence prion replication or pathogenesis. *Proc Natl Acad Sci USA* (2008) 105:757–62. doi: 10.1073/pnas.0711094105

21. Kwon K, Hutter C, Sun Q, Bilic I, Cobaleda C, Malin S. Instructive role of the transcription factor E2A in early B lymphopoiesis and germinal center B cell development. *Immunity* (2008) 28:751–62. doi: 10.1016/j.immuni.2008.04.014

22. Revilla-i-Domingo R, Bilic I, Vilagos B, Tagoh H, Ebert A, Tamir IM, et al. The B-cell identity factor Pax5 regulates distinct transcriptional programmes in early and late B lymphopoiesis. *EMBO J* (2012) 31:3130–46. doi: 10.1038/emboj.2012.155

23. Mittrücker H-W, Matsuyama T, Grossman A, Kündig TM, Potter J, Shahinian A, et al. Requirement for the transcription factor LSIRF/IRF4 for mature B and T lymphocyte function. *Science* (1997) 275:540–3. doi: 10.1126/science.275.5299.540

24. Shapiro-Shelef M, Lin KI, McHeyzer-Williams LJ, Liao J, McHeyzer-Williams MG, Calame K. Blimp-1 is required for the formation of immunoglobulin secreting plasma cells and pre-plasma memory B cells. *Immunity* (2003) 19:607–20. doi: 10.1016/S1074-7613(03)00267-X

25. Schwickert TA, Tagoh H, Schindler K, Fischer M, Jaritz M, Busslinger M. Ikaros prevents autoimmunity by controlling anergy and toll-like receptor signaling in B cells. *Nat Immunol* (2019) 20:1517–29. doi: 10.1038/s41590-019-0490-2

26. Cortés M, Georgopoulos K. Aiolos is required for the generation of high affinity bone marrow plasma cells responsible for long-term immunity. *J Exp Med* (2004) 199:209–19. doi: 10.1084/jem.20031571

27. Wöhner M, Tagoh H, Bilic I, Jaritz M, Kostanova-Poliakova D, Fischer M, et al. Molecular functions of the transcription factors E2A and E2-2 in controlling germinal center B cell and plasma cell development. *J Exp Med* (2016) 213:1201–21. doi: 10.1084/jem.20152002

28. Fuxa M, Busslinger M. Reporter gene insertions reveal a strictly B lymphoid-specific expression pattern of Pax5 in support of its B cell identity function. *J Immunol* (2007) 178:3031–7. doi: 10.4049/jimmunol.178.5.3031

29. Jolma A, Yan J, Whitington T, Toivonen J, Nitta KR, Rastas P, et al. DNA-Binding specificities of human transcription factors. *Cell* (2013) 152:327–39. doi: 10.1016/j.cell.2012.12.009

30. Gotoh M, Sato T, Akashima T, Iwasaki H, Kameyama A, Mochizuki H, et al. Enzymatic synthesis of chondroitin with a novel chondroitin sulfate N-acetylgalactosaminyltransferase that transfers N-acetylgalactosamine to glucuronic acid in initiation and elongation of chondroitin sulfate synthesis. *J Biol Chem* (2002) 277:38189–96. doi: 10.1074/jbc.M203619200

31. Polyak SJ, Tang N, Wambach M, Barber GN, Katze MG. The P58 cellular inhibitor complexes with the interferon-induced, double-stranded RNA-dependent protein kinase, PKR, to regulate its autophosphorylation and activity. *J Biol Chem* (1996) 271:1702–7. doi: 10.1074/jbc.271.3.1702

32. Hess DA, Strelau KM, Karki A, Jiang M, Azevedo-Pouly AC, Lee AH, et al. MIST1 links secretion and stress as both target and regulator of the unfolded protein response. *Mol Cell Biol* (2016) 36:2931–44. doi: 10.1128/MCB.00366-16

33. Capoccia BJ, Lennerz JK, Bredemeyer AJ, Klco JM, Frater JL, Mills JC. Transcription factor MIST1 in terminal differentiation of mouse and human plasma cells. *Physiol Genomics* (2011) 43:174–86. doi: 10.1152/physiolgenomics.00084.2010

34. Bhattacharya D, Cheah MT, Franco CB, Hosen N, Pin CL, Sha WC, et al. Transcriptional profiling of antigen-dependent murine B cell differentiation and memory formation. *J Immunol* (2007) 179:6808–19. doi: 10.4049/jimmunol.179.10.6808

35. Karki A, Humphrey SE, Steele RE, Hess DA, Taparowsky EJ, Konieczny SF, et al. Silencing Mist1 gene expression is essential for recovery from acute pancreatitis. *PloS One* (2015) 10:e0145724. doi: 10.1371/journal.pone.0145724

36. Hagelkruys A, Wirnsberger G, Stadlmann J, Wöhner M, Horrer M, Vilagos B, et al. A crucial role for Jagunal homolog 1 in humoral immunity and antibody glycosylation in mice and humans. *J Exp Med* (2021) 218:e20200559. doi: 10.1084/jem.20200559

37. Lemercier C, To RQ, Carrasco RA, Konieczny SF. The basic helix-loop-helix transcription factor Mist1 functions as a transcriptional repressor of MyoD. *EMBO J* (1998) 17:1412–22. doi: 10.1093/emboj/17.5.1412

38. Kallies A, Hasbold J, Tarlinton DM, Dietrich W, Corcoran LM, Hodgkin PD, et al. Plasma cell ontogeny defined by quantitative changes in Blimp-1 expression. *J Exp Med* (2004) 200:967–77. doi: 10.1084/jem.20040973

39. Moore KA, Hollien J. The unfolded protein response in secretory cell function. *Annu Rev Genet* (2012) 46:165–83. doi: 10.1146/annurev-genet-110711-155644

40. Pengo N, Scolari M, Oliva L, Milan E, Mainoldi F, Raimondi A, et al. Plasma cells require autophagy for sustainable immunoglobulin production. *Nat Immunol* (2013) 14:298–305. doi: 10.1038/ni.2524

41. Sundaram K, Mather AR, Marimuthu S, Shah PP, Snider AJ, Obeid LM, et al. Loss of neutral ceramidase protects cells from nutrient- and energy-deprivation-induced cell death. *Biochem J* (2016) 473:743–55. doi: 10.1042/BJ20150586

42. Aronheim A, Shiran R, Rosen A, Walker MD. The E2A gene product contains two separable and functionally distinct transcription activation domains. *Proc Natl Acad Sci USA* (1993) 90:8063–7. doi: 10.1073/pnas.90.17.8063

43. Quong MW, Massari ME, Zwart R, Murre C. A new transcriptional-activation motif restricted to a class of helix-loop-helix proteins is functionally conserved in both yeast and mammalian cells. *Mol Cell Biol* (1993) 13:792–800. doi: 10.1128/mcb.13.2.792-800.1993

# Frontiers in Immunology

**Explores novel approaches and diagnoses to treat immune disorders.**

The official journal of the International Union of Immunological Societies (IUIS) and the most cited in its field, leading the way for research across basic, translational and clinical immunology.

## Discover the latest Research Topics

See more →


**Frontiers**

Avenue du Tribunal-Fédéral 34
1005 Lausanne, Switzerland
frontiersin.org

**Contact us**

+41 (0)21 510 17 00
frontiersin.org/about/contact